ISBN 0-315-61814-0

A CONTINENTAL VOLCANIC ARC OF EARLY PROTEROZOIC AGE AT GREAT BEAR LAKE NORTHWEST TERRITORIES

ROBERT S. HILDEBRAND

NOTICE

The quality of this microform is heavily dependent upon the quality of the original thesis submitted for microfilming. Every effort has been made to ensure the highest quality of reproduction possible.

If pages are missing, contact the university which granted the degree.

Some pages may have indistinct print especially if the original pages were typed with a poor typewriter ribbon or if the university sent us an inferior photocopy.

AVIS

La qualité de cette microforme dépend grandement de la qualité de la thèse soumise au microfilmage. Nous avons tout fait pour assurer une qualité supérieure de reproduction.

S'il manque des pages, veuillez communiquer avec l'université qui a conféré le grade.

La qualité d'impression de certaines pages peut laisser à désirer, surtout si les pages originales ont été dactylographiées à l'aide d'un ruban usé ou si l'université nous a fait parvenir une photocopie de qualité inférieure.

A CONTINENTAL VOLCANIC ARC OF EARLY PROTEROZOIC AGE AT GREAT BEAR LAKE, NORTHWEST TERRITORIES

by

© Robert S. Hildebrand, B.A.

A Dissertation submitted in partial fulfillment

of the requirements for the degree of

Doctor of Philosophy

Department of Geology

Memorial University of Newfoundland

April 1982

St. John's Newfoundland

ISBN 0-315-61814-0

"A leading question is concerned with
the amount of reaction between Sial
and Sima and the resulting diversity
among eruptive species."
(R.A. Daly, 1933)

Oblique aerial photograph of part of the study area taken from over Great Bear Lake. Most of the visible outcrops are Echo Bay Formation.

ABSTRACT

The 1.875 Ga LaBine Group, which comprises mostly volcanic rocks, outcrops along the western margin of Wopmay Orogen at Great Bear Lake and rests on a deformed and metamorphosed 1.920 Ga sialic basement complex. It is overlain by rocks of the mainly rhyodacitic Sloan Group. Syn- to post-volcanic plutons of the Great Bear batholith intrude both groups.

Facies relations and the overall evolution of the Group are closely comparable to Cenozoic volcanic fields believed related to subduction. Rocks of the LaBine field were hydrothermally altered by high-level geothermal processes but on the basis of SiO_2, TiO_2, REE, and phenocryst mineralogy they can be classified as calc-alkaline. Therefore, it is concluded that the LaBine Group represents an early Proterozoic volcanic arc developed upon continental crust. Laccoliths in Athapuscow Aulacogen together with recent geochronological and field data suggest that the LaBine Group postdates continent-microcontinent collision in Wopmay Orogen and was probably generated above an eastward-dipping Benioff zone which was either segmented or became shallower with time.

Geochemical data and petrological considerations indicate that the magmatic rocks of the belt were generated by partial melting of lower continental crust and perhaps mixing of those magmas with slab-derived basaltic andesite. Preservation of high-level volcanic and plutonic rocks suggest that the region was never topographically high-standing. Therefore, the zone may be an early Proterozoic analog of

the Longitudinal Depression of Chile and other intra-arc synclinal basins which seem to be the loci for major pyroclastic eruptions. The calculated volume of vitric ash removed from the basins by high-level atmospheric transport approximates the estimated volume of basaltic andesite intruded and extruded in island arcs. This may explain why the basins remain in isostatic equilibrium close to sea level. Because the volume of magma erupted and intruded in continental arcs is equal to, or exceeds, the volume of mafic magma rising out of the mantle, batholiths cannot be derived directly from the mantle--they are products of processes occurring in the continental crust.

RÉSUMÉ

Le groupe de Labine, qui date de 1.875 Ga, affleure le long de la marge ouest de l'orogène de Wopmay, dans la région du Grand lac de l'Ours, et repose sur un complexe rocheux de caractère sialique, déformé et métamorphisé, âgé de 1.920 Ga. Il est recouvert par les roches principalement rhyodacitiques du groupe de Sloan. Des plutons synvolcaniques à postvolcaniques du batholite du Grand lac de l'Ours traversent les deux groupes.

Les relations de faciès et l'évolution globale du terrain, d'abord soumis à des éruptions andésitiques pauvres en émanations gazeuses, puis aux éruptions gazeuses de tufs répandus en coulées de cendres rappellent fortement les secteurs volcaniques oligocènes des Etats-Unis, que l'on estime associés aux phénomènes de subduction. Les roches du secteur de Labine ont été altérées par des réactions hydrothermales intenses, mais en raison de leur teneur en SiO_2, en TiO_2 et REE et de la minéralogie des phénocristaux, on peut les classer dans les roches calcoalcalines. On en conclut donc que le groupe de Labine correspond à un arc volcanique d'âge protérozoïque inférieur, formé audessus de la croûte continental.

Dans l'aulacogène d'Athapuscow, l'existence de laccolites et les récentes données géochronologiques et données obtenues sur le terrain semblent indiquer que le groupe de Labine est ultérieur à la collision entre continent et microcontinent qui a eu lieu lors de l'orogène de Wopmay, et a probablement été formé au-dessus d'une zone de Benioff plongeant vers l'est, qui s'est fragmentée ou est devenue moins profonde au cours des temps.

Les donnés geochimiques et les observations pétrographiques montrent que les roches magmatiques de la ceinture sont derivées du mélange de fragments d'andésite basaltique avec le liquide produit par la réfusion partielle de la partie inférieure de la croûte. La conservation des roches volcaniques et plutoniques de la partie supérieure suggère que la région n'a pas été topographiquement élevée. Donc la zone peut être un analogue Protérozoique de la dépression longitudinale de Chile et de bassins synformes associés aux zones d'îles en arc, qui semblent être des sites d'éruptions pyroclastiques majeures. Le volume calculé de cendres de verre volcanique deplacé des bassins par des conditions atmosphériques intenses, est à peu près équivalent au volume estimé d'andésite basaltique qui a été mis en place dans les îles en arc de façon intrusive et extrusive. Ceci peut expliquer pourquoi les bassins sont restés en equilibre isostatique près du niveau de la mer. Comme le volume de magma introduit de façon intrusive ou extrusive dans les arcs continentaux est égale ou excède de volume de magma provenant du manteau, les batholites sont des produits de la croûte continentale; ne peuvant dériver directement du manteau.

TABLE OF CONTENTS

Page

Page

LIST OF TABLES

TABLE Page

LIST OF FIGURES

FIGURE | Page

FIGURE Page

FIGURE		Page

FIGURE Page

GEOLOGICAL MAPS

MAP

INTRODUCTION

The controversy regarding the origin of granites is nearly as old as the science of geology itself and no lesser giants of the science than Hutton, Werner, Michel-Levy, Eskola, Barrell, Sederholm, Buddington, Grout, Bucher, Lawson, Daly, and Shand to mention but a few, have been drawn into it. The controversy reached a climax during the late 1940's and early 1950's (see for example: Gilluly, 1948) when granitization was the main issue of debate and now most geologists are comfortable with the notion that granites are derived by partial melting. Yet the granite controversy rages on, with only a change in emphasis. For example, today's geologists argue whether granitic melts of continental arcs are derived from the crust or from the mantle.

Another classic problem in geology concerns the relationship of volcanic rocks to plutonic rocks. On a grand scale, are the giant batholiths of continental arcs related to the volcanic rocks which form their roofs? If so, then what are the compositional and temporal relationships? On a smaller scale, geologists are concerned with the nature of plutons beneath stratovolcanoes and cauldrons (see for example: Thorpe and Francis, 1979; Lipman and others, 1981). Are they, in fact, comagmatic? Do ring complexes, such as those of Peru (Bussell and others, 1976) represent subcauldron plutonic complexes?

Yet another matter of contention which interests geologists is the nature of tectonic processes during the Precambrian. Was there "plate tectonics" and if so do precise actualistic models apply?

This dissertation reports the results of a detailed mapping, petrographic, and geochemical study of parts of the Great Bear Magmatic

Belt, an early Proterozoic volcano-plutonic terrane located along the east shore of Great Bear Lake. Rocks of the belt are folded and sections thousands of metres thick are exposed on individual fold limbs. This coupled with greater than 60 percent outcrop, superb lakeshore exposures, and only minor surficial weathering since deglaciation combine to make the area an excellent place to study the 3-dimensional make-up of a continental volcano-plutonic complex and address some of the above questions and controversies.

Specifically, work in the area was expected to yield data that would: (1) contribute to the understanding of the 3-dimensional relationships, processes, and petrogenesis of continental intermediate to siliceous terranes; (2) disprove or prove earlier hypotheses that the area was an ancient magmatic arc related to subduction, and by doing so elucidate tectonic and petrologic processes during the early Proterozoic; and (3) aid in constraining models concerned with the evolution of the early Proterozoic Wopmay Orogen.

Mapping, petrographical, and geochemical work were focused on the LaBine Group and associated plutons (Figure 1) because the group is compositionally heterogeneous and because the east shore of Great Bear Lake is more accessible than other areas of the belt. Along the east shore of the lake the LaBine Group is mainly exposed in two areas: one (Echo Bay-MacAlpine Channel area) covered by the MacAlpine Channel (86K/5), Echo Bay (86K/4), and Port Radium (86L/1) sheets and the other (Camsell River-Conjuror Bay area) by the White Eagle Falls (86F/12) and Rainy Lake (86E/9) sheets (Figure 2).

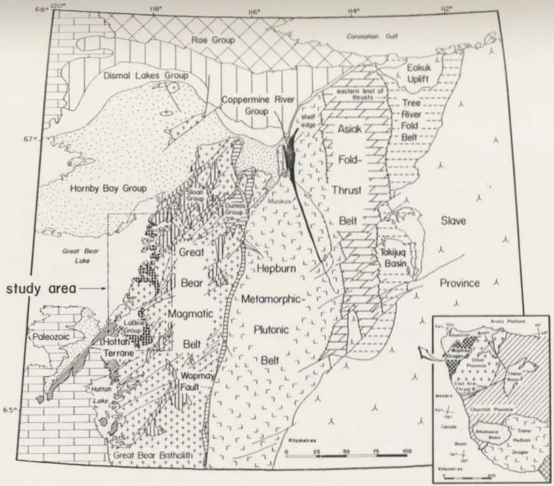

Figure 1. Maps showing location of study area in relation to Wopmay Orogen and northwestern parts of the Canadian Shield.

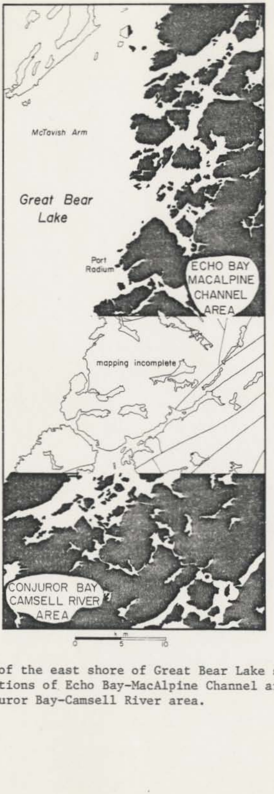

Figure 2. Map of the east shore of Great Bear Lake showing locations of Echo Bay-MacAlpine Channel area and Conjuror Bay-Camsell River area.

PRESENT INVESTIGATION

This report summarizes the results of eight months field work in the Conjuror Bay-Camsell River area during the summers of 1978 through 1980 and follow-up laboratory studies on rocks collected during 1977, 1978, 1979, and 1980 from the entire LaBine Group. Geological mapping of the entire White Eagle Falls (86F/12), Rainy Lake (86E/9) 1:50,000 sheets was done on 1:62,000 black and white aerial photographs except for the area of the LaBine Group which was mapped at 1:16,000 scale on colour aerial photographs or on 1:16,000 enlargements made from the standard 1:62,000 black and white aerial photographs. This work was compiled on 1:50,000 topographic maps.

In general, terminology of ash-flow tuffs is that of R.L. Smith (Smith, 1960a, b; Ross and Smith, 1961). Volcanic stratigraphic nomenclature is that of Fisher (1966a; unpublished manuscript). Modal analyses of intrusive rocks were estimated in the field and terminology follows that recommended by Streckeisen (1967, 1973). The volcanic rocks have been divided on the basis of their SiO_2 contents as follows:

basalt	≤ 52% SiO_2
andesite	53–63% SiO_2
dacite	64–70% SiO_2
rhyolite	> 70% SiO_2

This classification agrees reasonably well with the classification used in the field (Streckeisen, 1967) which suggests that in most rocks there have been only minor changes in SiO_2 contents during alteration.

All of the major oxide analyses reported here were made at Memorial University of Newfoundland using standard atomic absorption techniques, except P_2O_5 which was determined colorimetrically. Precision and accuracy for major element chemical data are given in Appendix 5a.

All of the minor element determinations were made by standard in-house x-ray flourescence techniques on fully automated Phillips 1450 AHP X-ray Flourescence Spectrometer using a rhodium tube. Standards were included with each run to check working curves and precision-accuracy are as given in Appendix 5b. Values below detection limits are reported as 0 while elements not determined are given the abbreviation nd.

Rare earth element analyses reported here were determined by the thin film XRF technique of Fryer (1977). These data were then normalized to the chondritic values of Taylor and Gorton (1977). Accuracy and precision for all reported elements are 10 percent or less.

Samples used for Rb-Sr whole rock study were assumed to be representative on the basis of field selection, petrography, and preliminary Rb-Sr values determined by x-ray flourescence. All samples were pulverized to -400 mesh in a tungsten-carbide shatterbox, and splits of .25 grams were treated with HCl, HF, and $HClO_4$ in Teflon beakers. Sr was separated by standard ion exchange techniques using Fisher strong cation exchange resin and loaded as a phosphate on a single tantalum filament. Rb and Sr absolute abundances were determined by a minimum of 10 replicate analyses on a Phillips 1450 x-ray spectrometer by in-house x-ray techniques. The estimated errors for Rb and Sr concentrations and for Rb/Sr ratios are given by Taylor (1981). Mass ratios for Sr isotopes were determined on a Micromass 30B mass spectrometer using a Faraday collector and on-line data processing (HP 2114A). Regression of the data was by the weighted least squares method of Fryer (unpublished) using a value of 1.42×10^{-11} $year^{-1}$ for the decay constant of ^{87}Rb.

Analyses of individual minerals were made on a JOEL JXA-50A electron probe microanalyzer using Kriesel Control Probe System V6A-J6PI with Alpha corrections. Analyzed natural and synthetic minerals were used as standards. Ferrous-Ferric ratios of amphiboles were determined by the method of Papike and others (1974) while amphibole nomenclature follows Leake (1978).

ACKNOWLEDGEMENTS

First and foremost I would like to thank P.F. Hoffman, not only for suggesting the study and helping to see it through, but also for contributing to a life style that would not have been possible without the wizardry of modern air transport. B.J. Fryer, R.K. Stevens, and D.F. Strong were a constant source of guidance, rapport, encouragement, and discussion. W.A. Padgham and his staff at DIAND, Yellowknife assisted the project in many ways. Superb assistance in the field was provided by Karen S. Pelletier and Bradford J. Johnson in both 1979 and 1980, Tracey Cooke and Lisa Campbell during 1979, Joseph Conway and X.Y. Zhang, 1980.

Fruitful discussions both in and out of the field were had with S. Bowring, G.R. Osburn, T.A. Steven, S. Roscoe, B.D. Marsh, J.G. McGlynn, P.F. Hoffman, R. Flood, R.M. Easton and H. Sanche. Thanks also to D. Press for assisting with the trace element analyses; G. Andrews for performing most of the major element analyses; J. Vaahtra for x-ray diffraction work; H. Longerich for assistance with microprobe analyses; W. Marsh for darkroom assistance; Tim Horton's for coffee; and V.S. Services for superior indigestion. DIAND, Yellowknife supported the fieldwork while laboratory work was carried out under NSERC and DIAND grants to B.J. Fryer and a Memorial University of Newfoundland graduate fellowship to the author.

R.K. Stevens, B.J. Fryer, and S. Bowring critically read the manuscript.

PREVIOUS WORK

Bell (1901) first investigated the geology in the region of Great Bear Lake as part of a lengthy canoe reconnaissance for the Geological Survey of Canada in 1899. He noted "cobalt bloom and copper stain" along the east shore of the lake but was unable to investigate his discovery as he was under great pressure to reach civilization before freezeup.

The area received only minor attention from prospectors and trappers until 1930 when Gilbert LaBine, then president of Eldorado Mining Company, discovered high grade silver-pitchblende veins at the present townsite of Port Radium. The veins were mined for radium and silver until 1940 when the mine was shut down due to World War II and the resulting disruption of the radium market.

Kidd (1932) examined the mineral deposit for the Geological Survey of Canada in 1931. Kidd subsequently mapped much of the region at a scale of 1:250,000 (1933) and also made a broad reconnaissance of a 20 mile wide strip from Great Bear Lake to Great Slave Lake (1936). Smaller areas near Port Radium were mapped by Robinson (1933), Riley (1935), and Furnival (1939).

In 1941 Eldorado gave Enrico Fermi and associates at Columbia University 5 tons of uranium oxide for their experiments to generate a chain reaction and the mine was reopened to supply the strategic metal uranium to the United States Government. In 1944 the Canadian Government obtained ownership of the property and a program of 1 inch to 400 foot mapping in the vicinity of Port Radium was initiated by the Geological Survey of Canada (Joliffe and Bateman, 1944; Thurber, 1946; Feniak, 1947; Fortier, 1948). Later, Feniak (1952) mapped the MacAlpine Channel area at a scale of 1:50,000 while Lord and Parsons (1947) mapped the Camsell River region.

During the next 25 years geological work was mainly confined to detailed studies of the mineral deposits at Port Radium (Campbell, 1955, 1957; Jory, 1964; Robinson, 1971; Robinson and Morton, 1972; Robinson and Badham, 1974) and in the Conjuror Bay-Camsell River region (Badham, 1972, 1973a, b, 1975; Badham and others, 1972; Shegelski, 1973; Badham and Morton, 1976; Ghandi, 1978; Shegelski and Scott, 1975; Thorpe, 1974; Withers, 1979) but some maps were made (Shegelski and Murphy, 1973; Padgham and others, 1974). Mursky (1973) compiled much of the previously restricted data collected in the Echo Bay area by the Geological Survey of Canada.

Hoffman, who was mapping a narrow strip across the northern part of Wopmay Orogen, was the first to propose a subduction-related origin for the entire Great Bear Volcano-Plutonic Belt (Hoffman, 1972, 1973; Fraser and others, 1972). Shortly thereafter, Badham (1973a) reached a similar conclusion based on 18 chemical analyses from rocks in the Conjuror Bay-Camsell River area.

Hoffman and others (1976) and McGlynn (1974, 1975, 1976) mapped the area and were the first to undertake a comprehensive treatment of the regional stratigraphy and structural relationships (Hoffman and McGlynn, 1977). However, the geological space-time relationships were not known in enough detail to work out the evolution and genesis of the various magmas. So the author undertook, in 1977, a more detailed mapping project of the LaBine Group as the initial phase of a larger study aimed at understanding the tectonic setting and petrogenesis of the area.

REGIONAL GEOLOGY

The LaBine Group is widely exposed in the western part of Wopmay Orogen (Figure 1), an early Proterozoic north-south trending, orogen which developed on the western margin of the Archean Slave Craton between 2.1 and 1.8 Ga (Hoffman, 1973, 1980a). The orogen is one of the best-exposed early Proterozoic orogenic belts in the world and it appears to contain many of the features found in Cenozoic orogens. For this reason Hoffman (1973, 1980a) has suggested that plate tectonic models for the Cenozoic Earth are applicable to the early Proterozoic. Hoffman and others (in press) divided the orogen into three major zones whose boundaries parallel the trend of the belt as a whole. From east to west they are: Asiak fold and thrust belt, Great Bear magmatic zone, and the Hottah Terrane (Figure 1).

Asiak fold and thrust belt is a zone 140 km wide where easterly derived, passive continental margin sedimentary and volcanic rocks along with overlying exogeoclinal, or foredeep, deposits of northwesterly provenance were thrust eastward toward the craton, then in the west metamorphosed and intruded by numerous S-type plutons (Hepburn plutonic-metamorphic belt). The plutons for a continuous series in which the oldest are protomylonitic granites and the youngest are relatively undeformed diorites and gabbros (Hoffman and others, 1980; Hoffman and St. Onge, 1981). U-Pb ages of the plutons fall between 1.800-1.895 Ga (Van Schmus and Bowring, 1980, personal communication).

The Great Bear Magmatic zone (Figure 3) comprises a multitude of gregarious plutons, mostly massive I-types, which intrude their own volcanic cover. It is separated from Asiak Fold and Thrust belt by the poorly understood Wopmay fault zone (Figure 3) but locally, rocks of the Great Bear Magmatic zone overstep this zone and lie unconformably on deformed rocks of the internal zone. Rocks in the extreme western part of the zone unconformably overlie polydeformed and metamorphosed rocks of the Hottah Terrane (Hildebrand, 1981).

All of the non-plutonic rocks in the zone were termed the McTavish Supergroup by Hoffman (1976a) while the plutonic rocks have been referred to as the Great Bear batholith (Hildebrand, 1981). The McTavish Supergroup is divided into three groups separated by unconformities: the LaBine Group, Sloan Group and Dumas Group in ascending order (Hoffman, 1978).

The LaBine Group, which forms the principal subject of this paper, is a diverse aggregation, up to 7 km thick, of siliceous to intermediate lava flows and pyroclastic rocks, plus associated sedimentary and high-level porphyritic intrusive rocks (Hoffman and McGlynn, 1977). This group outcrops only along the western margin of the volcano-plutonic zone (Figure 3) where it unconformably overlies the Hottah Terrane (McGlynn, 1976; Hildebrand, 1981).

The stratigraphy of the LaBine Group in the Echo Bay-MacAlpine Channel area (Figure 2) was described in detail by Hildebrand (1981) and for lithostratigraphic descriptions the interested reader is referred to that paper. The pertinent points to be extracted from that work are as follows: the oldest rocks are mainly andesitic lavas, breccias, and pyroclastic rocks at least 3,000 m thick, interpreted to be the

Figure 3. Major tectonic and geologic subdivisions of Wopmay Orogen and adjacent area.

remains of a number of large stratovolcanoes. Overlying, and in part interfingering with the stratovolcanoes are seven major ash-flow tuff sheets which are locally intercalated with andesite, dacite, rhyolite flows and domes, and a diverse assemblage of fluvial and lacustrine sedimentary rocks. At least 3, and perhaps as many as 5, cauldrons have been identified and can be related to specific ash-flow tuff sheets. The LaBine Group is disconformably overlain by the Sloan Group, which consists mostly of thick sequences of densely-welded intermediate ash-flow tuff and intermediate and mafic lava flows (Hoffman and McGlynn, 1977; Bowring, personal communication, 1981). Outcrops of the Sloan Group are confined to the central portion of the Great Bear zone (Figure 3). To the west (Figure 3), the Sloan Group is unconformably overlain by the Dumas Group. This group, which also unconformably lies on the internal parts of Asiak Fold and Thrust Belt, is a sequence of mudstone, intermediate to siliceous ash-flow tuff and intermediate to mafic lava flows.

Plutonic rocks of the Great Bear magmatic zone are mainly hornblende and biotite-bearing. They have been roughly divided into four age groups (Hoffman and McGlynn, 1977; Hoffman, 1978), each with similar compositions. The oldest are sheets and laccoliths of quartz diorite and quartz monzonite (G1) here informally termed the "early intermediate intrusive suite." They intrude piles of andesite occurring in the LaBine Group. These plutons were generally followed by emplacement of dome-shaped biotite-hornblende quartz monzonite plutons (G2), some of which can be shown to occupy the cores of cauldrons (Hildebrand, 1981). Large discordant biotite granites (G3), without known extrusive equivalents, were intruded after eruption of the Dumas Group and after the belt was folded. The final plutons to be emplaced were a suite of small, ovoid tonalite to diorite bodies (G4), found sporadically throughout the eastern Great Bear zone. U-Pb zircon ages in the belt range from 1.876 Ga to 1.840 Ga (Van Schmus and Bowring, 1980, personal communication).

The entire Great Bear Magmatic zone, except the G3 and G4 plutons, is folded about shallowly plunging axes which trend northwest-southeast except near the Wopmay fault-flexure where they trend east-west. The folds are <u>en echelon</u> which led Hildebrand (1981) to suggest that they were the product of oblique convergence.

The folds, and even the youngest plutons (G4) of the Great Bear zone, are cut by a swarm of northeast-southwest trending transcurrent faults (used in the sense of Freund, 1974). Most of these faults are steeply dipping and have right-lateral separation on the order of kilometres. They are part of a larger set of conjugate transcurrent faults found throughout Wopmay Orogen (Hoffman, 1980b). Freund (1970, 1974) has pointed out that in regions undergoing transcurrent faulting, each fault plane rotates about a vertical axis away from the axes of principal compressive stress. In the Great Bear Zone such rotations are counter-clockwise. Thus, as pointed out by Hoffman (1980b), all studies of directional properties such as paleomagnetism or paleocurrent studies, as well as all pre-fault reconstructions, require a clockwise correction.

The Hottah Terrane (Figure 3) forms the basement for the western part of the Great Bear magmatic zone as it is unconformably overlain by the LaBine Group. The terrane comprises deformed and metamorphosed sedimentary and volcanic rocks which are cut by a variety of pre-tectonic intrusions. One of the deformed intrusions, a granite at Hottah Lake, has yielded a U-Pb zircon age of 1.915 Ga (Van Schmus and Bowring, personal communication, 1982). Thus the deformation of the terrane is younger than 1.915 Ga.

The supracrustal rocks (Holly Lake metamorphic suite) are of unknown age and provenance. Their metamorphic grade appears to range up to the amphibolite facies (McGlynn, 1976) but the terrane has not been mapped in detail and to date only one petrographic study has been undertaken (Violette, 1978).

GEOLOGY OF THE CAMSELL RIVER-CONJUROR BAY AREA

The geology of the area is complex and varied, resulting from a long history of volcanism, plutonism, and sedimentation followed by folding and transcurrent faulting. The distribution of the LaBine Group and nomenclature of plutonic rocks in the area are illustrated in Figure 4 and a table of formations occurring in the area is shown in Table 1. Geographic names used in this section are shown in Figure 5.

The purpose of this section is to describe the major geological units of the area, emphasizing those aspects which are necessary to give the reader a feel for the complexity and variability of the rocks so that he may fully comprehend the complex interplay between volcanism, plutonism, sedimentation, and hydrothermal alteration. In most cases a brief interpretation follows the lithological descriptions. The interpretations are purposely succinct as it is not the purpose of this report to examine all the nooks and crannies of the stratigraphy but merely to provide an overview of the geologic history and development of the area, partly to provide a basis for later geochemical arguments and partly for comparison with younger volcano-plutonic terranes. For convenience, the overall geologic history is brought together and summarized at the end.

Hottah Terrane

Holly Lake metamorphic suite

The oldest rocks of the study area are deformed and metamorphosed impure quartzite and semi-pelites of the Holly Lake metamorphic suite. The term Holly Lake metamorphic suite is an informal one proposed by

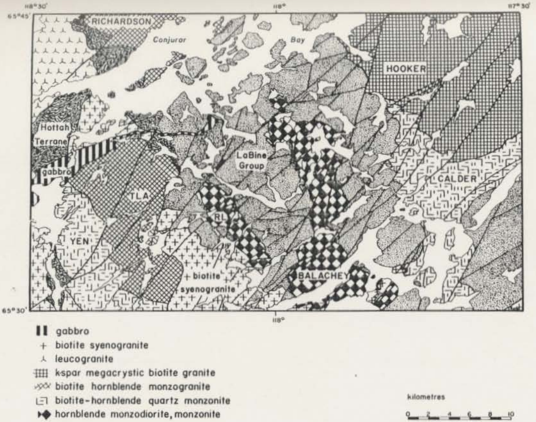

Figure 4. Distribution of Hottah Terrane, LaBine Group, and major plutons in the area of the Rainy Lake and White Eagle Falls 1:50,000 sheets. Nomenclature and dominant rock types of major plutons are also shown, RL=Rainy Lake Intrusive Complex.

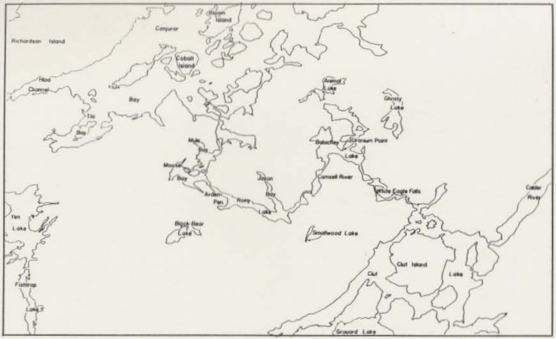

Figure 5. Geographic names in the Camsell River-Conjuror Bay area used in this report.

TABLE 1

TABLE OF FORMATIONS

Age	Domain	Group	FORMATION	Member	LITHOLOGY
			Gunbarrel Gabbro		Coarse-grained gabbro
			Intrusive Contact		
			Cleaver Diabase		East-west trending altered diabase dikes
			Intrusive Contact		
Early Proterozoic	GREAT BEAR MAGMATIC ZONE		Hooker Megacrystic Granite		Biotite, K-spar megacrystic syenogranite
			Intrusive Contact		
			Grouard Dikes		Plagioclase-hornblende-quartz-biotite-Kspar porphyritic dikes
			Intrusive Contact		
			Calder Quartz Monzonite		Hornblende-biotite quartz monzonite
			Intrusive Contact		
		LaBine Group	"younger ash-flow tuffs"		Simple cooling units of dacite to rhyolite ash-flow tuff
			Animal Andesite		Pyroxene and amphibole bearing andesite flows and breccia
			Uranium Point Formation		Sandstone, conglomerate, lapilli tuff, mudstone, ashstone
			White Eagle Tuff		Lithic and crystal-rich dacite ash-flow tuff
				mesobreccia member	Breccia
			Unconformity		
			Early Intermediate Intrusive Suite	Dalachey Intrusive Complex	Mainly quartz monzonite
				Rainy Lake Intrusive Complex	Monzodiorite, monzonite pseudosyenite
			Intrusive Contact		
			Camsell River Formation		Andesitic lavas, breccias, ash-flow tuff, sandstone, mudstone, conglomerate
			Arden Formation		Mudstone, sandstone, limestone, breccia, rhyolite flows, ashstone typically strongly altered
			Moose Bay Tuff	ash-flow tuff member	Rhyolitic ash-flow tuff, andesite, sandstone
				lower member	Sandstone, mudstone, breccia, andesite, limey argillite
			Unconformity		
			unnamed sills		Gabbro, diabase, plagioclase porphyritic dikes
			Intrusive Contact		
			unnamed dikes		Plagioclase, quartz, K-spar porphyritic dikes
			Intrusive Contact		
			Bloom Basalt		Pillow basalt, breccia, tuff
			Conjuror Bay Formation	upper member	Mudstone, ashstone, tuff, breccia
				lower member	Quartz arenite, conglomerate
			Unconformity		
	HOTTAH TERRANE		unnamed mafic intrusions		Deformed gabbro and diabase
			Intrusive Contact		
			unnamed granitoid intrusions		Deformed diorite, granodiorite, quartz monzonite
			Intrusive Contact		
			Holly Lake Metamorphic Suite		Deformed metasedimentary rocks

Hildebrand (1981) to include all non-granitoid rocks of the Hottah Terrane. In the map area the Holly Lake metamorphic suite is exposed only in the Conjuror Bay area and at Fishtrap Lake.

In the Conjuror Bay area rocks of the Holly Lake metamorphic suite typically have a steeply-dipping NNE-SSW cleavage and are folded about axes which trend nearly north-south. Locally the cleavage is spaced several centimetres apart and is therefore probably of pressure solution origin (Beach, 1979). In places the spaced cleavage is kinked.

Myriads of quartz veins (25 cm wide) form en echelon groups that parallel fold axes (Figure 6), while numerous smaller veins (1-2 cm) are oriented either parallel to bedding or randomly. In most places the small veins are folded (Figure 7) and/or broken by faults. On the mainland south of Conjuror Bay zones of intense mylonitization up to 20 m wide and striking NNE-SSW are cut by metre-wide quartz veins whose trends parallel the shear zones.

Where the rocks are not intensely sheared, such as on Bloom Island, abundant sedimentary structures such as ripple laminations, load features and graded bedding are common (Figure 8). Thickness of beds ranges from thin laminations to 30 cm and individual beds are generally continuous over outcrop length of 20 or 30 m.

Intrusions

Prior to deformation the sedimentary rocks of the Holly Lake metamorphic suite were intruded by quartz diorite-quartz monzonite plutons. Remnants of the plutons occur south of Hloo Channel, on Richardson Island, and on islands in western Conjuror Bay (Map 1). They are variably foliated and often contain aligned potassium feldspar megacrysts and enclaves of country rock (Figure 9). In several places

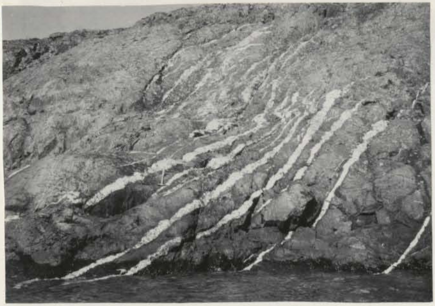

Figure 6. En echelon quartz veins cutting folded metasedimentary rocks of the Holly Lake metamorphic suite, southern Bloom Island.

Figure 7. Detail of Figure 6 showing folded quartz veins.

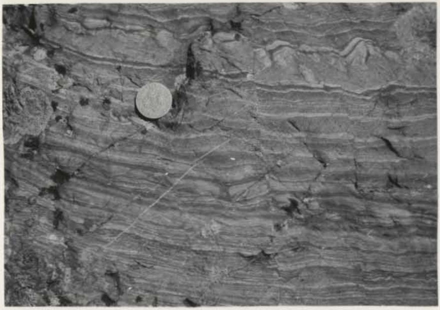

Figure 8. Deformed metasedimentary rocks, Holly Lake metamorphic suite, showing well-preserved sedimentary structures. Photo taken south end Bloom Island.

Figure 9. Enclaves of metavolcanic rocks in granitoid of the Hottah Terrane. Pen in the top center for scale. Photo taken south side of Hloo Channel.

potassium feldspar megacrysts were observed to cut across aplite dike margins. They are also commonly found in enclaves and xenoliths within the plutons. These relations suggest a subsolidus metasomatic origin for the megacrysts (Pitcher and Berger, 1972).

In most places the fabric of the deformed granitoids is abruptly truncated by non-foliated granitoid plutons of the Great Bear batholith. For example, on Richardson Island foliated granitoid forms the roof for two younger undeformed plutons (Map 1). The youngest rocks of the Hottah Terrane appear to be gabbro and diabases. These intrusive bodies, which are always strongly foliated, occur as boudins in the most deformed granitoids and as dikes in the lesser deformed granitoids. A complete gradation exists between the two. Therefore they postdate emplacement of the Hottah Terrane granitoid rocks and predate the deformation.

Conjuror Bay Formation

Unconformably overlying the Hottah Terrane in the Conjuror Bay area is a complex succession of sedimentary and pyroclastic rocks about 150 m thick, here termed the Conjuror Bay Formation. The formation is conformably overlain by several kilometres of basaltic lavas and breccia of the Bloom Island Formation.

The Conjuror Bay Formation is exposed on several islands in Conjuror Bay, on the mainland east of Tla Bay, and south of Rainy Lake (Map 1). The best exposures and most complete sections occur on the islands in Conjuror Bay and east of the bay but there is nowhere a completely exposed section. However, the section exposed on Bloom Island is nearly complete with only the unconformity and basal few metres of section inferred.

The formation is divided into two members: a lower member of mature crossbedded quartz arenite and an upper member comprising concretionary mudstone, ashstone, lapilli tuff, sandstone, conglomerate, and breccia.

Basal unconformity

The unconformity between the Hottah Terrane and the Conjuror Bay Formation is well exposed on the small island south of Cobalt Island and less well exposed, due to younger intrusions, on the mainland south of Conjuror Bay (Map 1). On Bloom Island the unconformity is not actually exposed but sedimentary rocks of the Conjuror Bay Formation are separated from the Hottah Terrane by a valley 20 metres wide.

On the small island south of Cobalt Island vertically dipping and foliated metasedimentary rocks of the Hottah Terrane are overlain by gently northward-dipping quartz arenite (Figure 10). There is about 20 m of relief on the unconformity at this locale and rounded hills of Hottah Terrane appear to be preserved beneath the quartz arenite.

A peculiar feature found above the unconformity is a breccia 3 to 4 m thick comprised of semi-rounded, phaccoidal blocks of the overlying quartz arenite with ferrodolomite void filling and replacement (Figure 11). The breccia grades upwards into unbrecciated quartz arenite. At the margins of the fragments are darkened zones of unknown composition. Locally within the breccia anomalous uranium values are encountered. The breccia is interpreted to be a solution feature which developed when water percolated along the unconformity. The darkened zones rimming fragments may be insoluble residues.

Figure 10. Unconformity between Hottah Terrane and Conjuror Bay Formation, small island south of Cobalt Island. Tree in left centre is 3 m high.

Figure 11. Detail of possible solution breccia at base of Conjuror Bay Formation.

Lower member

The lower quartz arenite member of the Conjuror Bay Formation is generally well-bedded (4 cm to 1 m); medium to fine-grained, and trough crossbedded with laminations rich in heavy minerals (Figure 12). Paleocurrents indicate south-southwest transport direction. In some areas herringbone crossbedding occurs (Figure 13), but outcrops are not sufficient to determine whether or not crossbedding is bipolar. Coarse sand lenses are locally present and these often contain doiomite concretions.

Near the top of the sandstone are lenses of vein-quartz pebble conglomerate (Figure 14) up to 10 m thick with irregular, probably scoured, basal contacts and sharp planar upper contacts. Pebbles are clast supported with minor mudstone matrix. Clasts contained within the lenses are dominantly rounded to subrounded vein quartz pebbles along with minor subangular to angular clasts of mudstone, quartz arenite, quartzite granulestone, and rounded vesicular basalt cobbles.

Upper member

Conformably overlying the lower member is an assemblage, of variable thickness from 40 m to 100 m, comprising intercalated fine sandstone, basaltic ashstone, siltstone, chert, lapilli tuff, conglomerate and breccia. The thickest preserved sections are east of Tla Bay and the unit thins rapidly to less than 50 m on the islands in Conjuror Bay.

Bedding ranges from fine laminations to about 1 m thick and is generally planar. However, some low-angle crossbedding, load features, and scoured channels are present in the sedimentary rocks.

Figure 12. Crossbedded quartz arenite of Conjuror Bay Formation. Pen in top centre for scale.

Figure 13. Herringbone crossbedding of Conjuror Bay Formation.

Figure 14. Quartz pebble conglomerate in upper part of Conjuror Bay Formation.

Many tuffaceous units only 4 to 10 cm thick, contain abundant flattened fragments of pumice, devitrified shards, and about 20 percent broken phenocrysts of plagioclase. They do not appear to be welded and therefore flattening of the pumice is attributed to compaction.

Sandstones of this member are typically immature pebbly arkoses containing a variety of volcanic and sedimentary fragments. They are commonly crossbedded or graded and are generally less than 1 metre thick. Clast supported polymictic conglomerates often appear to fill channels and are sometimes graded.

Interpretation

The uniform lithology, substantial thickness, sedimentary structures, and mineralogically mature nature of the formation suggest that deposition was subaqueous. The presence of herringbone crossbedding suggests tidal dominance and therefore relatively shallow marine water. The formation is therefore interpreted as marginal marine. The general fining-upward nature of the formation from sandstones to mudstones is interpreted as reflecting either a change in the size of material being transported into the area or deepening of the water.

Bloom Basalt

Two to three kilometres of pillow basalt, associated breccia and aquagene tuff, along with intercalated oolitic and stromatolitic dolomite is exposed in the Conjuror Bay area (Map 1). It is here named Bloom Basalt after its exposures on Bloom Island.

The contact with the underlying Conjuror Bay Formation is placed at the base of the lowest lava flow. The original top of the formation is not exposed in the mapped area. However, the formation is overlain along an angular unconformity by Moose Bay Tuff and in a few places by the "younger ash-flow tuffs." Bloom Basalt occupies a similar stratigraphic position as pillow basalts found at Hottah Lake and the two units were correlated by Hoffman and McGlynn (1976).

The formation is dominantly composed of pillow lavas. The pillows range in size from 0.3 m up to 3 m across. Most have well-developed vesicular selvages and contain abundant chlorite-carbonate amygdules in their central parts. Amygdules are commonly concentrated near the tops of the pillows. All are intensely altered and carbonate-epidote-chlorite veins and replacement are ubiquitous (Figure 15). For this reason no samples were analyzed for chemical composition but similar, less altered, rocks from the Hottah Lake area, in a similar stratigraphic position, were analyzed by Wilson (1979) and are high aluminum, low titanium basalts. By analogy the pillow lavas in the Conjuror Bay area may be of similar composition.

Lenses of pillow breccia are locally present in the formation. They comprise variably-sized pillow fragments in a fragmental mafic matrix. Sparse aquagene tuff also occurs as lenses in the pillow basalt piles but were not studied in detail due to the intense alteration and consequent obliteration of all original mineralogy and most textures.

Oolitic and stromatolitic dolomite (Figure 16), up to 30 m thick, occurs locally in the formation. The best exposures are on Cobalt Island where the dolomite units consist of crossbedded and rippled oolitic grainstone overlain by the distinctive branching stromatolite Jacutophyton (identification by P.F. Hoffman, 1981).

In thin section the pillow lavas contain completely saussuritized plagioclase microphenocrysts up to 1 mm long in an altered

Figure 15. Altered pillow basalts, Bloom Basalt.

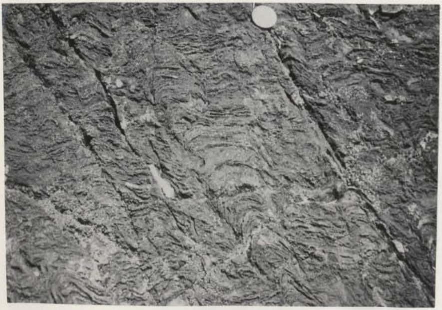

Figure 16. Stromatolitic dolomite of Bloom Basalt.

groundmass of epidote, chlorites, carbonate, tremolite-actinolite, sphene, and opaque Fe-Ti oxides. Much of the tremolite-actinolite appears to replace original pyroxenes. The texture of the rocks is best described as intersertal.

Interpretation

The thick sections of pillow basalt in the Bloom Basalt indicate deposition under water. The presence of intercalated Jacutophyton-bearing and oolitic dolomite, most easily interpreted as patch reefs suggest that the environment was shallow marine as Jacutophyton are known only from environments interpreted to be marine. The common occurrence of the stromatolite Jacutophyton stratigraphically above the oolitic dolomite indicates a slight deepening of water depth with time (Hoffman, 1976).

Because Bloom Basalt is over 2 km thick in the Conjuror Bay area and absent in sections south of Rainy Lake there may have been a period of normal faulting during eruption of the basalt. This would explain the presence of Conjuror Bay Formation and lack of Bloom Basalt in the eastern section. Another possibility may be uplift and erosion after eruption of Bloom Basalt. This would require considerable uplift, perhaps several kilometres. As the overlying Moose Bay Tuff is interpreted to be subaerial this is certainly a good possibility but there is no stratigraphic record of considerable erosion (i.e., conglomerates, talus) preserved.

Porphyritic Dikes and Sills

Quartz-feldspar porphyritic dikes and sills intrude the Holly Lake metamorphic suite, Conjuror Bay Formation, and Bloom Basalt but are themselves cut by mafic sills that lie unconformably beneath Moose Bay Tuff. Therefore, the porphyries were emplaced prior to the eruption and deposition of the Moose Bay Tuff.

The porphyritic intrusions are common on the mainland south of Conjuror Bay where most form sills intruded into intensely sheared rocks of the Holly Lake metamorphic suite. The sills are not sheared. A few intrusions occur on the islands in Conjuror Bay. There they form dikes up to 10 m across.

The intrusions are spectacularly porphyritic with centimetre-size phenocrysts of cryptoperthite, plagioclase, and quartz in a fleshy-red or gray coloured aphanitic matrix. The relative proportions of the various phenocrystic phases varies from body to body but K-feldspar always constitutes the majority.

Tabular plagioclase, to 1 cm long, are generally saussuritized but occasionally are replaced by chessboard albite. Locally they form glomeroporphyritic clots. Cryptoperthite after sanadine, often occurring as Carlsbad twins, range in size up to 2 cm long. In some of the intrusions they are not tabular but are ovoid to rounded in form. Both tabular and "golfball" types occur together in the same bodies. The perthites are often charged with inclusions which are found to be axiolitic intergrowths of plagioclase, quartz, chlorite, and carbonate. Quartz (4 mm) mostly occurs as bipyramids rounded and embayed by resorption, but in a few dikes clots up to 1 cm across occur. Less than 1 percent partially chloritized biotite occurs as small (<2 mm) flakes while original pyroxenes (<4 percent) now replaced by chlorites, opaques, and uralitic amphibole, form prisms up 3 mm long. Less than 1 percent accessory zircon and apatite also occur. The matrix is a microfelsitic intergrowth of quartz and feldspar, commonly dusted with hematite.

Mafic Sills

Rocks included under this section comprise mafic sills, up to 70 metres thick, that intrude the porphyries and older units but are unconformably overlain by Moose Bay Tuff. There are two basic varieties: fine-grained diabase sheets without phenocrysts and, diabases which contain plagioclase phenocrysts up to 2 centimetres across (Figure 17). All the sills of both types are considerably altered.

In thin section they are holocrystalline with subophitic texture comprising slender saussuritized plagioclase laths in a matrix of subhedral uralitized pyroxene and skeletal grains of opaque oxides. Where present, the large plagioclase phenocrysts are rounded, intensely fractured, and completely saussuritized.

Moose Bay Tuff

Rocks under this heading comprise a sequence, in ascending order, of sedimentary rocks, andesite, and densely-welded, lithic-rich rhyolite ash-flow tuff intercalated with minor intermediate lavas, tuffs and arkosic sandstone. The units beneath the ash-flow tuff are here designated as the lower member while the overlying ash-flows, and intercalated rocks, are termed the ash-flow tuff member. The Moose Bay Tuff is named for its excellent exposures around Moose Bay where it obtains its maximum exposed thickness of nearly 3 km.

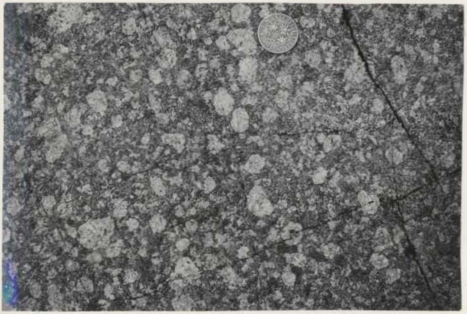

Figure 17. Plagioclase porphyritic sill.

Exposures of the Moose Bay Tuff occur in a broad, broken band on the southwest side of Norex syncline from 3 miles south of Arden Peninsula to the large point which juts out into Conjuror Bay west of the mouth of the Camsell River (Map 1). A few scattered exposures occur on islands in Conjuror Bay.

Relationships with older rocks at the base of the lower member are unknown because the unit is everywhere intruded by younger rocks. West of the Camsell River the lower member is absent and the ash-flow tuff member lies unconformably on Bloom Basalt but the contact is obscured by a distinctive K-feldspar quartz porphyry. South and east of the Gunbarrel Gabbro the tuff is overlain by the Arden Formation but the contact is never seen due to younger intrusions. To the west the tuff is overlain by White Eagle Tuff.

Lower member

The lower member is a sequence of sedimentary rocks, minor dacite ash-flow tuff, and at least one andesitic lava flow which underlies the upper ash-flow tuff member of the Moose Bay Tuff. The lower 40 m of the unit consists of interbedded sandstone, siltstone, and ashstone. Beds of mudstone and siltstone are generally 1-10 cm thick and ashstone beds are typically between 5 and 10 cm in thickness. Sandstones are mostly well-bedded wackes comprising angular to sub-rounded sand grains in a silty or muddy matrix. They commonly contain abundant mudchips.

South of Moose Bay the sedimentary rocks interfinger with poly-mictic breccias containing angular to rounded fragments ranging from sand size to 30 m or more, across. Clast lithologies include rhyo-litic ash-flow tuff and porphyries, andesite, ashstones, mudstone, siltstone and sandstone. In some cases the breccia is matrix supported while elsewhere there is a paucity of matrix such that the breccia is clast-supported. Some of the larger blocks are themselves intensely brecciated. The matrix is typically a greenish, strongly-altered, siliceous ashstone which sometimes contains fragments identical to the fine-grained matrix.

The breccia normally passes up into arkosic sandstone but in one fault block south of Mule Bay it is overlain by a calcareous ashstone, that is in part brecciated and in part folded, containing occasional large blocks (2-5 m) of silicified sediment. Overlying this unit is 10 m of white-weathering green, siliceous ashstone which in turn is capped by several metres of finely laminated red and purple concretionary mudstone with a corrugated appearance on weathered surfaces.

In most other sections north of Black Bear Lake, there is a plagioclase porphyritic andesitic lava flow about 20 m thick with quartz-filled amygdules about 5 mm across and well developed trachytic texture above the sandstone. The flow weathers red and gray, and is platy jointed in its lower parts.

In exposures on the peninsula which juts out from the northwest side of Black Bear Lake the flow is overlain by 20 m of massive pebbly sandstone. Clasts are subrounded to rounded and consist of chert, mudstone, rhyolite and orthoquartzite.

Ash-flow tuff member

The predominant lithology of the ash-flow tuff member of the Moose Bay Tuff is densely-welded, lithic-rich, rhyolite ash-flow tuff which reaches a maximum thickness of nearly 1.5 km. Generally, the ash-flows were deposited so quickly that they welded together without visible partings. However, north of Mule Bay the tuff shows compound cooling unit characteristics such as interfingering relationships with sandstone and intermediate extrusive rocks.

The tuff directly overlies Bloom Basalt northwest of the transcurrent fault that passes from the west side of Moose Bay out into Conjuror Bay (Figure 19 and Map 1) and it thins rapidly until it pinches-out at the mainland point south of Cobalt Island. East of the fault the upper part of the tuff is intercalated with 0.5 km of intermediate lava flows, breccia, and lapilli tuff which thin rapidly to the east such that they are not present in sections east and south of the Camsell River. Beneath the lavas are a few hundred metres of interbedded airfall tuff, ash-flow tuff, and sandstone. The sandstones are very similar in composition to the ash-flow tuff and are therefore considered to be its reworked arkosic equivalents.

South of Black Bear Lake, at the base of the member, occur large blocks of dacite welded tuff. The blocks are up to 15 metres across and have no preferred orientation.

Lithic fragments in the tuff are very abundant, locally making up to 50 percent of the rock. They are generally porphyritic volcanic rocks of a siliceous nature but fragments of metamorphic rock are also common. In stratigraphically higher parts of the tuff most lithic fragments are pebble to granule size. Their average size increases downsection with cobbles becoming more abundant.

The upper parts of the tuff are characterized by small ($\lesssim$2 cm) flattened pumice fragments, often green to black in colour (Figure 18). In stratigraphically lower parts of the tuff they are not often preserved due to alteration and recrystallization.

Figure 18. Lithic-rich densely-welded rhyolite ash-flow tuff of ash-flow tuff member, Moose Bay Tuff. Note abundant, small, flattened pumice fragments.

The upper kilometre of the tuff also weathers red to flesh-coloured while the lower parts weather shades of white and green due to more intense alteration and silicification. Quartz veining is common in the areas where the tuff weathers white.

In thin section the ash-flow tuff member is seen to contain 4-10 percent broken and embayed quartz phenocrysts (to 3 mm) along with 10-15 percent shattered phenocrysts of turbid microperthite, probably after sanadine (1-2 mm), and tiny anhedral flakes of chloritized biotite in an ultrafine-grained groundmass of quartz, feldspar, and sericite.

Interpretation

The tremendous thickness of the Moose Bay Tuff indicates that the tuff ponded in a topographic depression. The dramatic thickness change of the tuff across the transcurrent fault which passes along the western side of Moose Bay suggests that the depression was fault-bounded on the west. The disparity in thickness of the tuff across the fault and the presence of coarse breccias in the lower member just southeast of the fault suggest that it was active just prior to, and during, eruption of the ash-flow tuff member. This interpretation implies that the fault, as a zone of weakness, was later reactivated during transcurrent faulting because the fault presently separates stratigraphic units younger than the Moose Bay Tuff.

Stratigraphic and structural relations such as the above are typical of those found in Cenozoic calderas (Steven and Lipman, 1976; Lambert, 1974; Lipman, 1976; Bailey, 1976; Bailey and Koeppen, 1977; Smith and others, 1970; Byers and others, 1976; Seager, 1973; Elston and others, 1976). Therefore, the possible synvolcanic fault may have been the main ring fault along which subsidence of the central block of a cauldron took place. The rapid thinning and pinchout of the tuff along the unconformity with the Bloom Basalt is a type of buttress unconformity which could represent the original topographic wall of a cauldron, created as material collapsed from the oversteepened cauldron wall, itself generated by subsidence along the ring fracture zone.

If the above interpretations are correct then all exposures of the Moose Bay Tuff south of Conjuror Bay are intracauldron deposits. The postulated cauldron is here informally named the Mule Bay cauldron after Mule Bay.

The trace of the eroded topographic margin appears to pass out into Conjuror Bay and is exposed on Cobalt Island, the island south of Cobalt Island, and on Bloom Island (Figure 19). In those exposures ash-flow tuffs younger than Moose Bay Tuff lie uncomformably on Bloom Basalt. The unconformity was intruded by a distinctive porphyry which also can be traced through the islands of Conjuror Bay. While the porphyry may appear to be a type of ring pluton it is considered to be unrelated to Mule Bay cauldron as it intrudes the "younger ash-flow tuffs" and is therefore much younger than the Moose Bay Tuff.

The small normal and reverse faults south of Moose Bay are possibly related to differential subsidence of the central block. Because the proposed ring fracture dips slightly inward the faults probably developed as the central block collapsed. It is interesting that at least one of the fault blocks appears to have remained as a high during the subsidence. This suggests that one mechanism for decreasing the size of the central block so that it is able to subside along a ring fault whose radius is decreasing downward, might be to leave large marginal blocks hanging in the cauldron fill deposits.

Figure 19. Sketch map of southern Conjuror Bay showing possible ring fracture of Mule Bay cauldron and trace of topographic margin.

Arden Formation

The Arden Formation, as defined here, comprises up to 200 m of sedimentary and volcanic rocks which lie between the Moose Bay Tuff and the first intermediate lava flow (Camsell River Formation). It is exposed only on the southwest limb of Norex syncline from Clut Lake to Conjuror Bay (Map 1) and is named for exposures on Arden Pininsula. The formation pinches out abruptly at the proposed cauldron margin fault of Mule Bay cauldron.

There are no complete sections of the formation because it is a locus for intrusions. Most exposures form the roof of the Rainy Lake Intrusive Complex and so are considerably altered. The remaining exposures are north of Arden Peninsula (Map 1), where the base of the formation is intruded by a biotite-quartz microporphyritic sill which also alters the formation but to a lesser degree than the Rainy Lake Intrusive Complex. In addition, half of the exposures above the Rainy Lake were intruded by a plagioclase porphyry and at least one diorite body (Map 1).

Rapid lateral facies changes are characteristic of the formation as a whole but lithic arkose generally dominates the upper half of the formation. The lower half is a more varied assemblage of mudstone, breccia, limey argillite and ashstone.

Lithology

Lithic arkose is the major lithology of the Arden Formation and dominates the upper parts of the formation northwest of the plagioclase porphyry. These sandstones are typically volcanogenic, immature, granular to pebbly, fine to coarse-grained and weather various shades of brown, purplish brown, rust brown and green-gray. Commonly there are interbedded purplish-brown mudstones (Figure 20). Many of the sandstones

Figure 20. Intercalated sandstone-mudstone of Arden Formation.

contain abundant mudstone rip-ups. Locally, foresets are draped with mudstone. Beds of sandstone are lenticular and nearly always less than 1 m thick, with 0.2-0.3 m being typical. Sedimentary structures are common and include trough and planar crossbedding, ripple lamination and where interbedded with mudstone, load features. In places these are channels filled with clast-supported conglomerate comprising rounded to subrounded pebbles and cobbles of chert, andesite, silicified mudstone, siliceous porphyry, and vein quartz in an arkosic matrix containing up to 5 percent hematite grains. Beds of lithic pebbly sandstone sometimes contain mostly rhyolitic fragments.

The lower part of the section just west of Clut Lake is composed of siltstone and fine sandstone with minor mud drapes. The sandstones are generally well-sorted, arkosic, crossbedded, and rippled with minor climbing ripples. These grade upwards into coarser-grained trough-crossbedded sandstones with linear carbonate concretions (1 m x 5 cm).

Elsewhere the lower half of the formation comprises varicoloured, laminated mudstones and ashstones. They are always strongly altered and recrystallized (Figure 21) as they form the roof of the Rainy Lake Intrusive Complex. Reds, greens, and black are the dominant colours. In thin section green and black rocks are found to be dominated by tremolite-actinolite and chlorite while reddish laminations generally consist predominantly of albite with finely disseminated hematite.

Pyroclastic units are also common in the Arden Formation. They are most commonly fine siliceous and intermediate ashstones ranging in thickness from a few centimetres to half a metre. They generally weather shades of pink but where strongly altered weather white. In thin section, these units are seen to contain broken microphenocrysts of quartz and postassium feldspar. Occasionally normal and reverse size-graded beds of lapilli tuff can be found.

About 20 m of interbedded carbonate and argillite occur in the middle of the formation north of Arden Peninsula west of the Camsell River. Laminations are crinkly, somewhat irregular, and average about 1 cm thick. Interbedded with these units are beds and lenses of pink weathering rhyolitic ashstone, up to 0.5 m thick (Figure 22). Near the top of this succession are 0.3 m thick beds of fine-grained sandstone and crystal tuff. Both are typically graded.

Lenticular beds of completely unsorted breccia occur in the middle parts of the formation. They are thickest (15 m) and most abundant in the northwest. Typically, they contain angular to sub-rounded fragments of carbonate-argillite and rhyolitic ashstone in a sparse black or dark-green silty matrix (Figure 23). The fragments, which range up to 4 m across, are identical to the above described limestone-argillite and rhyolite assemblage (Figure 24). Badham (1972) interpreted the breccias to have resulted from emplacement of the Rainy Lake Intrusive Complex but because they are everywhere concordant with beds above and below them the breccias are here interpreted to be of sedimentary origin.

A stubby, quartz-porphyritic rhyolite flow occurs in the Arden Formation about 5 km southeast of Arden Peninsula. It overlies mafic ashstone. The lower 3 or 4 metres of the flow weather white and grade up into 12 m of dark-gray to green massive rhyolite. Most of the flow (30 m) is flow-banded and brecciated. Individual flow bands (less than 15 cm) are either pink or gray with both sharp and diffuse, gradational contacts. They are folded and micro-faulted. Brecciation generally postdates the formation of the flow banding as most fragments consist of flow-banded rhyolite.

Figure 21. Altered and fractured mudstone and siltstone, Arden Formation.

Figure 22. Intercalated limey argillite and rhyolitic ashstone, Arden Formation. Pen in top centre for scale.

Figure 23. Sedimentary breccia of Arden Formation.

Figure 24. Large clast of interbedded dolomite and argillite in sedimentary breccia of Arden Formation.

Interpretation

The fine-grained and thinly-laminated nature of the lower part of the Arden Formation and interbedded limey argillite-rhyolitic ashstones without scours and current structures indicate that deposition was in relatively quiet, shallow water. The rapid lateral facies changes of the formation coupled with the presence of sub-aerial units both directly above and below the unit suggest that the formation is nonmarine. Therefore it is probably lacustrine. The upper lithic arkose with its abundant current-generated structures and conglomeratic lenses is interpreted to be of fluvial origin.

Because the Arden Formation directly overlies intracauldron facies Moose Bay tuff and pinches out abruptly at the possible cauldron-margin fault northwest of Mule Bay it is interpreted to have accumulated within the topographic depression of Mule Bay cauldron. Lakes have developed inside most calderas following collapse and some younger examples include the giant Toba caldera (van Bemmelen, 1949), Creede caldera (Steven and Ratté, 1965, 1973), the Kari Kari caldera (Francis and others, 1981), and Kutcharo caldera (Katsui and others, 1975).

The coarse, locally-derived breccias of limey argillite-rhyolite suggest that local areas were subject to syndepositional uplift and erosion. Whether this resulted from resurgence or local block faulting near the ring fracture system could not be determined because the formation is exposed in only two dimensions.

Camsell River Formation

The Camsell River Formation is named for its exposures along the Camsell River at Rainy Lake. It is an assemblage of intercalated andesitic lava flows, laharic breccia, explosion breccia, andesitic ash-flow tuff, sandstone, conglomerate, ashstone, lapilli tuff and mudstone about 2 km thick that conformably overlies the Arden Formation. The lower contact is placed at the base of the lowest andesite flow or breccia. The top of the formation is not exposed.

Most exposures are in a broad northwest-southeast band from Conjuror Bay to Clut Lake (Map 1) between the Balachey Pluton and Rainy Lake Intrusive Complex, but many also occur north of the Balachey Pluton, such as on Clut Island (Map 1). Like the Arden Formation it is not present in sections west of the proposed ring fracture zone of the Mule Bay cauldron.

Lava flows

Andesitic to dacitic lava flows (Table 2) of the Camsell River Formation are characterized by abundant large platy plagioclase phenocrysts (Figure 25) that often are flow-aligned (Figure 26). Individual flows are generally 10 to 30 m thick. They are often columnar jointed above platy-jointed bases, but many flows have autobrecciated margins. In cases where basal flow breccias overlie mudstone it is common to find blocks of lava up to 0.5 m across "floating" in a mudstone matrix.

The predominant colour of the lavas is dark gray. However, parts of many flows were oxidized to a brick-red colour and some are altered to white, pink, and green. Most flows are amygdaloidal with amygdule content varying from less than 10 percent to nearly 50 percent of the rock by volume. The amygdules commonly comprise quartz, calcite, epidote, and chlorite.

All lavas of the Camsell River Formation are altered because they were intruded by the Balachey Pluton and the Rainy Lake Intrusive Complex. A few flows have original mineralogy preserved while

TABLE 2: Major and trace element analyses of lava flows, Camsell River Formation.

Sample No:	H-79-134	H-80-112	H-80-12	H-80-7	H-79-179	H-79-161	H-79-160	J-79-128	P-79-97	P-79-96
SiO_2	58.2	60.7	56.8	54.6	60.8	56.9	56.3	55.8	57.1	65.2
TiO_2	0.43	0.45	0.70	0.61	0.55	0.67	0.66	0.80	0.72	0.34
Al_2O_3	15.1	17.3	15.2	18.7	17.5	14.8	15.4	15.6	14.7	14.3
Fe_2O_3**	7.39	7.14	8.55	5.70	4.80	7.98	7.61	8.02	9.60	6.81
MnO	0.19	0.09	0.19	0.15	0.19	0.20	0.40	0.27	0.18	0.16
MgO	4.37	3.14	3.92	2.58	1.47	2.96	3.86	5.54	3.48	2.35
CaO	3.52	1.46	5.37	6.54	3.47	6.20	4.67	6.28	3.77	0.80
Na_2O	3.61	3.31	2.61	4.13	3.77	2.53	2.08	2.78	3.07	2.91
K_2O	4.15	3.75	3.53	3.73	5.49	3.42	4.13	2.92	4.47	5.16
P_2O_5	0.25	0.16	0.17	0.31	0.22	0.15	0.20	0.19	0.16	0.06
LOI	2.23	2.40	1.68	1.70	1.69	4.69	3.66	1.44	2.70	2.69
Total	99.44	99.90	98.78	98.75	99.95	100.50	98.97	99.64	99.95	100.59
Nb	10	15	10	9	10	10	9	8	10	10
Zr	167	233	151	133	177	163	172	126	152	136
Y	30	34	27	25	25	25	25	26	30	23
Sr	233	168	343	430	392	196	288	357	288	77
U	7	2	11	0	0	3	6	4	0	9
Rb	95	197	124	108	127	63	205	102	125	105
Th	15	13	4	3	10	12	15	3	12	13
Pb	11	2	23	12	5	11	7	13	22	5
Ga	15	22	18	17		14	16	20		15
Zn	149	95	105	86	80	53	124	186	101	166
Cu	0	0	0	0	19	0	69	0	18	0
Ni	22	9	14	11		13	8	34		1
Cr	74	20	49	27	5	47	44	150	36	26
V	131	83	167	151	81	164	167	178	384	
La	49	64	42	41	38	44	37	56		38
Ce	44	68	41	48	78	58	62	58	15	11
Ba	1297	1100	1049	779	1676	367	1037	845	931	1923

**Total Fe as Fe_2O_3. Oxides in weight percent; trace elements in parts per million

Figure 25. Porphyritic andesite flow of Camsell River Formation.

Figure 26. Photomicrograph of flow-oriented plagioclase phenocrysts in andesitic lava flow of Camsell River Formation.

others are completely recrystallized to mixtures of albite, epidote, chlorite, tremolite-actinolite, sphene and magnetite. A brief description of the alteration related to the two intrusions is found with the descriptions of those bodies.

In some flows, where vestiges of original mineralogy are preserved, phenocrysts of calcic andesine, up to 1 cm long, and augite or salite to 5 mm (Figure 27), are engulfed in a dense pilotaxitic matrix made up of subparallel microlites of plagioclase, intergranular chlorite and magnetite and undetermined interstitial material. Plagioclase always dominates the modes (Table 3).

Ash-flow tuffs

Ash-flow tuffs of the Camsell River Formation are generally less than 10 m thick. They are found at many horizons in the formation; are very discontinuous along strike; and probably fill paleovalleys. The tuffs are most common in the southeast and often thin to the northwest.

Most are densely-welded simple cooling units containing variable proportions of lithic fragments, broken crystals of plagioclase and altered ferromagnesium minerals, pumice, shards, and impalpable dust. All are completely devitrified, and many have well-developed eutaxitic structure. However, a few cooling units do not contain pumice or shards but are an aggregation of broken crystals, andesitic fragments, and dust.

Plagioclase dominates the modes of most samples, and chemical analyses (Table 4) show that they are andesitic and strongly altered.

Laharic and explosion breccias

The term laharic breccia is used here for rocks composed of blocks of a wide variety of size and shape engulfed in a muddy or silty matrix. Such rocks are rare in the Camsell River Formation but where

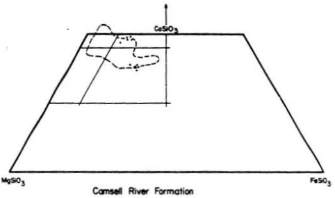

Figure 27. Composition of pyroxenes in andesite flows of Camsell River Formation. Field of clinopyroxenes from high-K andesites after Gill (1981).

TABLE 3: Modal analyses of Camsell River Formation andesite flows.

Sample No.	%groundmass	%plagioclase	%pyroxene	%oxide
H-79-296	59	41	1	—
P-79-97	72	15	11	2
H-79-135	55	44	1	--
H-79-124b	75	23	1	1
H-79-194	76	22	1	1
H-79-126	78	20	2	--
H-80-7	57	43	--	--

TABLE 4: Major and trace element analyses of ash-flow tuffs, Camsell River Formation.

Sample No.	H-79-83	H-79-86	H-79-91	H-79-96
SiO_2	58.1	58.1	57.4	58.9
TiO_2	0.68	0.64	0.44	0.44
Al_2O_3	16.2	15.6	17.4	15.6
Fe_2O_3**	8.28	10.0	5.02	5.17
MnO	0.08	0.14	0.10	0.07
MgO	3.49	2.40	1.08	1.38
CaO	0.79	0.96	1.92	4.75
Na_2O	2.34	3.38	3.00	4.00
K_2O	6.76	5.20	9.22	4.17
P_2O_5	0.18	0.17	0.17	0.18
LOI	2.24	2.34	2.46	4.97
Total	99.14	98.94	98.21	99.63
Nb	15	11	17	14
Zr	220	149	228	174
Y	27	23	30	25
Sr	142	83	106	96
U	7	1	7	4
Rb	232	97	212	133
Th	25	15	24	21
Pb	6	10	6	5
Ga	16	17	10	18
Zn	78	99	20	24
Cu	9	7	33	19
Ni	28	4	0	4
Cr	141	49	11	32
V	132	135	85	121
La	26	35	119	43
Ce	49	64	229	86
Ba	2313	1813	2421	1043

**Total Fe as Fe_2O_3
Oxides in weight percent; trace elements in parts/million.

found are generally dominated by andesitic fragments, many of which are larger than 1 m in diameter. The best and most accessible exposures of laharic breccia (Figure 28) in the Camsell River Formation occur on the north side of Arden Peninsula.

Another type of breccia found in the Camsell River Formation comprises angular andesitic fragments of various sizes in a fine-grained microbrecciated matrix of andesitic material (Figure 29). The matrix is identical to most of the fragments except that plagioclase crystals are broken and fractured in the matrix. Locally, a few foreign rock fragments can be found but at most they make up only a few percent of the rock. These breccias are interpreted to be explosion breccias created by Vulcanian-type eruptions.

Explosion breccias occur at several stratigraphic horizons in the Camsell River Formation but are most common near the top. One major unit of explosion breccia (Map 1) near the top of the formation thins to the northwest and as fragments decrease in size in this direction, it is considered to have been erupted from a source which lay to the east.

Ashstone-lapilli tuff-sandstone-conglomerate

The rock types under this heading occur throughout the Camsell River Formation. They are described together under one heading because they are intimately intercalated; grade into one another laterally; and because in many cases, due to alteration, it is difficult to determine whether or not a given bed of volcanic material has been reworked by sedimentary processes.

Ashstones of the formation are planar-bedded rocks comprised of whole and broken phenocrysts of plagioclase and pyroxene in a fine-grained

Figure 28. Laharic breccia, lower part of Camsell River Formation.

Figure 29. Explosion breccia, Camsell River Formation.

matrix of sphene, plagioclase, chlorites, tremolite-actinolite, and opaque oxides. Beds range from thin laminations to a few centimetres thick. They occur as normally and reversely-graded beds, some with razor-sharp contacts and others with gradational contacts. Most are strongly altered and contain abundant disseminated sulphides (up to 25 percent). Some beds contain sparse lapilli-size fragments of andesite.

Lapilli tuffs are thicker-bedded than the ashstones but a continuum exists between the two. Beds are typically greater than 5 cm, but less than 0.5 m thick. Some beds have closely packed subrounded lapilli of andesite but most contain sparse lapilli of andesite and plagioclase in an ashstone matrix. As with the ashstones, both normally and reversely graded beds occur.

Sandstones and conglomerates are more common in the Camsell River Formation than either ashstone or lapilli tuff. Most contain andesitic debris in beds ranging from thin laminations to several metres. The sandstones are commonly planar and trough crossbedded. Many individual beds have bouldery or cobbly zones near their bases interpreted to be lag deposits (Figure 30). The clasts in those zones are often imbricated. Many of the sandstones, particularly in the lower parts of the formation, comprise semispherical augite grains and imbricated tabular plagioclase crystals with abraided corners (Figure 31).

The uppermost unit of the Camsell River Formation, exposed only in the core of Norex syncline, is a bouldery conglomerate over 100 metres thick. It contains mostly well-rounded cobbles and boulders of andesite (Figures 32 and 33) in a sandy to muddy matrix. The unit is best exposed in outcrops along the shore east of the outlet of the Camsell River into Conjuror Bay.

Figure 30. Volcanic conglomerate of the Camsell River Formation. Note imbricated cobbles and abundant plagioclase crystals.

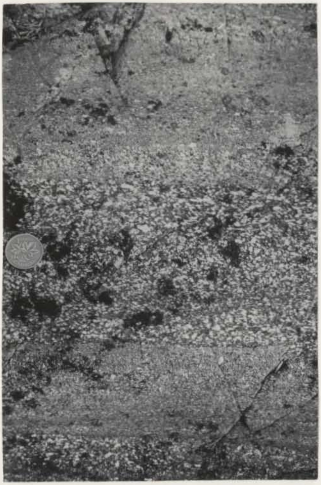

Figure 31. Plagioclase crystal sandstone, Camsell River Formation.

Figure 32. Interbedded sandstone and conglomerate of upper clastic member, Camsell River Formation.

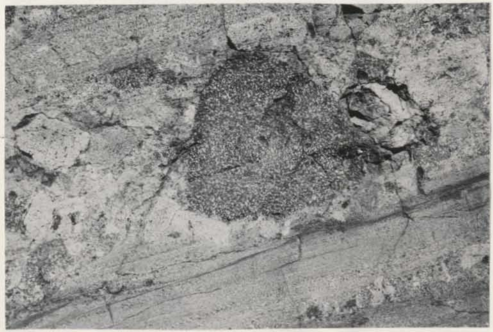

Figure 33. Detailed photograph of outcrop in Figure 32. The andesite boulder shown above is just to the left of the assistant's left knee in Figure 32. Note the mudstone drapes and imbricated cobbles.

Interpretation

The abundance of lava flows and explosion breccias in the Camsell River Formation is typical of near source facies of intermediate composition stratovolcanoes (Williams and McBirney, 1979). However, as no vent regions were observed and because there is a large amount of epiclastic material intercalated with the volcanic rocks it is most likely that the formation represents material deposited on the flanks of a volcano, perhaps in an environment similar to the large fluvio-volcanic fans of the Peusangan valley or Mt. Talang, Sumatra (Verstappen, 1973).

The occurrence of the formation above cauldron-fill deposits, along with its abrupt pinch-out at the proposed cauldron-margin fault, suggest that the formation accumulated within the Mule Bay cauldron after collapse. Post-collapse andesitic volcanism is known from several younger cauldrons. For example, post-collapse andesitic lavas and breccias fill both the Oligocene Platoro and Summitville calderas in the San Juan volcanic field of southwestern Colorado (Lipman, 1975); the andesitic stratovolcanoes Atosanupuri and Mashu formed after collapse of, and partially fill, the 7 million year old Kutcharo caldera, east Hokkaido (Katsui, 1955; Katsui and others, 1975); and four calderas of Kyushu, Japan (Aso, Aira, Ibusuki, and Kikai) each contain stratovolcanoes of pyroxene andesite (Matumoto, 1943).

In most of the cases cited above, there appears to be a compositional continuum between the ash-flow tuffs, which are mostly dacitic in composition, and the post-collapse andesites. For this reason Lipman (1975) suggested that post-collapse andesites might represent the lower parts of the same magma chambers from which the ash-flow tuffs were derived.

This is not a likely explanation for andesites of the Camsell River Formation because there is a large compositional gap between them and the rhyolitic ash-flow tuff of Mule Bay cauldron. Therefore, the andesites of the Camsell River Formation are thought to represent a different batch of magma than that which erupted the Moose Bay Tuff.

The thinning of explosion breccias to the northwest coupled with the decrease in ash-flow tuffs and thickening of epiclastic rocks in that direction suggest that the eruptive source lay to the southeast. Although the original extent of the Mule Bay cauldron is unknown, the lack of eruptive vents for the andesites and the probable non-genetic relationship between them and the tuff, suggest that the eruptive centre lay outside the cauldron and that the lavas spilled into the topographic depression remaining after collapse.

Augite Porphyritic Intrusions

Rocks under this heading are irregular-shaped augite porphyritic bodies common in the area around the eastern end of Rainy Lake. They typically contain uralitized euhedral to subhedral augite crystals up to 0.5 cm across (Figure 34) in a fine-grained matrix of altered plagioclase, sphene, amphibole, chlorites and epidote.

Badham (1972) and Withers (1979) mistook these intrusions for basalt flows. However, north of Smallwood Lake irregular fingers tens of metres long intrude breccias and andesite lava flows of the Camsell River Formation and have chilled margins. While locally a few vesicles are seen, most outcrops contain none of the features expected in basalt flows.

The bodies predate intrusion of the Balachey Intrusive Complex but whether they are related to volcanism of the Camsell River Formation

Figure 34. Detail of augite porphyritic intrusion.

is not known with any degree of certainty. Blocks of similar rocks in breccias of the formation do, however, suggest that some were exposed at the surface during that time and therefore may be genetically related to the andesites.

Balachey Pluton

This is a composite pluton comprising mainly seriate quartz monzonite, monzonite, and quartz monzodiorite, cut by granite, which outcrops continuously for over 20 km in a north-south trending belt, 1 to 6 km wide, in the central part of the study area (Map 1). The complex is named for its extensive polished and lichen-free outcrops on Balachey Lake.

General lithology

The major rock types of the complex are medium to coarse-grained hornblende quartz monzonite (Figure 35) in the north, and quartz monzodiorite in the south. Other rock types such as hornblende monzonite and hornblende monzodiorite are relatively minor phases. Locally, there is a plagioclase porphyritic phase adjacent to external contacts. Contacts between internal phases are everywhere gradational and moderate mineralogical variation were seen on scales ranging from kilometres down to the scale of a hand specimen.

Fine to coarse-grained biotite granite, with sharp contacts and associated aplite dikes, contains abundant partially consumed xenoliths of more intermediate members of the suite. However, the granite is not thought to be genetically related to the rest of the suite and is therefore not discussed here.

The Balachey Pluton contains a multitude of xenoliths and enclaves which are especially numerous in the northwest parts of the

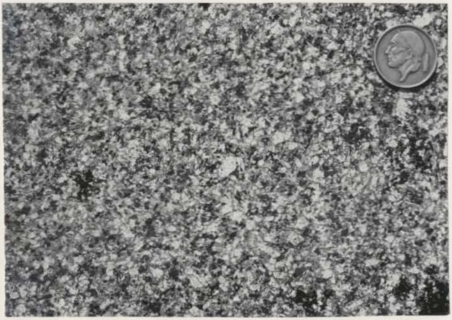

Figure 35. Detail of outcrop of Balachey Intrusive Complex. Note the wide variation in size of plagioclase phenocrysts characteristic of seriate texture.

TABLE 5: Major and trace element analyses, Balachey Pluton

Sample No:	J-79-93	H-79-40	J-79-62	J-79-92	J-79-66	J-79-61	H-80-26	H-80-24
SiO_2	65.4	65.5	60.5	64.3	65.7	62.5	64.0	63.0
TiO_2	0.33	0.34	0.59	0.45	0.45	0.44	0.58	0.63
Al_2O_3	15.4	15.9	14.1	15.5	15.5	14.4	14.1	14.4
Fe_2O_3**	4.86	4.12	6.49	4.54	3.65	5.59	5.80	6.74
MnO	0.10	0.04	0.36	0.09	0.11	0.11	0.10	0.15
MgO	1.94	1.51	3.33	1.53	1.56	2.98	2.24	2.80
CaO	1.02	3.71	4.76	2.11	2.09	3.32	3.74	3.80
Na_2O	3.00	3.25	2.45	2.98	3.43	3.08	2.61	2.61
K_2O	4.98	4.03	4.15	5.16	5.13	4.19	4.07	4.16
P_2O_5	0.08	0.10	0.14	0.09	0.08	0.09	0.07	0.11
LOI	2.41	0.64	2.88	2.30	1.90	2.17	1.33	1.55
Total	99.52	99.14	99.69	98.99	99.60	98.87	98.64	99.95
Nb	14	12	13	13	12	13	9	13
Zr	169	187	185	179	184	156	162	203
Y	30	36	25	38	32	31	31	31
Sr	134	280	264	199	214	229	222	271
U	9	5	4	7	1	6	2	1
Rb	184	142	160	177	132	148	155	155
Th	14	17	15	17	17	22	19	14
Pb	10	20	62	24	19	22	18	16
Ga	10	13		14	13	10	14	16
Zn	73	29	125	45	70	90	59	84
Cu	20	22	63	19	22	30	0	0
Ni	14	13		19	16	27	5	4
Cr	11	14	94	16	11	57	18	20
V	68	59	113	63	58	95	100	115
La	44	45	35	41	32	31	43	44
Ce	70	73	54	63	62	53	45	50
Ba	1145	973	834	1185	1131	979	1048	1077

**Total Fe as Fe_2O_3. Oxides in weight percent; trace elements in parts/million.

body and vary in size up to 7 m long. All of the xenoliths appear to be pieces of nearby wall rock and are intensely altered and more or less digested. Lithologies include andesite and epiclastic rocks with shapes ranging from angular to rounded. There is a general tendency for the smaller xenoliths to be more rounded than the larger ones. An interesting, and important feature, seen in many outcrops of the intrusion is the occurrence of abundant fractures along which amphiboles are concentrated (Figure 36). The amphiboles are similar to those seen elsewhere in the intrusion.

Numerous chalcopyrite-pyrite veins, up to 10 cm wide, are found to cut the intrusion as do smaller stringers of quartz and specular hematite (Figure 37). These veins and stringers trend approximately north-south, parallel to many small faults showing right-lateral separation. Both the faults and the veins are probably contemporaneous with, and related to, the post-Labine transcurrent faulting.

Contacts

Contacts of the Balachey Pluton with surrounding country rocks are always sharp and trend northwest-southeast (Map 1). Along the entire southwestern margin, and part of the northeastern, rocks of the complex intrude, and strongly alter, up to 2 km from the contact, lavas, tuffs, and sedimentary rocks of the Camsell River Formation, as well as earlier intrusions of monzonite and diorite. In these areas the contact dips away from the pluton at about the same inclination as the bedding of wall rocks.

From Uranium Point to Grouard Lake, a distance of 15 km, the northeastern margin of the intrusion is nearly always vertical but locally is roughly horizontal such that the contact is step-like in

Figure 36. Amphibole concentrations along fractures, Balachey Intrusive Complex.

Figure 37. Hematite veins cutting Balachey Intrusive Complex.

cross-section. Where the contact is flat, or nearly so, there occurs a peculiar breccia comprising angular fragments of the intrusion within a hematitic matrix. Overlying the breccia, and buttressed against the steeper portions of the contact nearly everywhere is another breccia, unaltered and characterized by a wide variety of fragments, 30 to 100 percent of which are identical to phases of the Balachey Pluton, sitting in a crudely-bedded muddy to sandy matrix. Quartz monzonite fragments, up to 1 m across, range from well-rounded to angular and some even appear to be bounded by original joint surfaces. Although a more detailed description of this unit and its genetic significance will be presented later, there is little doubt that this contact is an unconformity--an extremely important one because it tightly constrains the emplacement age of the Balachey Pluton.

Shape of the pluton

If the interpretation of relations along much of the northeastern margin as evidence of an unconformity is correct, then there are many stratigraphic units younger than the Balachey Pluton. Because the younger rocks are folded about similar axes as pre-Balachey rocks, then the Balachey must predate the folding and itself be folded. Furthermore, as there are northwesterly plunging synclines on both the northeast and southwest sides of the intrusion, and because the contacts of the pluton themselves, where intrusive, dip away from the intrusion, it appears that the pluton occupies the core of a northwesterly plunging anticline. If so, then the compositional change from quartz monzonite in the northwest to quartz monzodiorite in the southeast may be inferred to represent a vertical compositional zoning in the pluton with the quartz monzodiorite occupying deeper structural levels than the quartz monzonite. This interpretation is consistent with the observations that xenoliths become more numerous to the northwest and that the pluton itself becomes wider to the southeast.

Map 1 shows that not only do the intrusive contacts have similar dips as bedding in the country rocks, but they also have similar strikes. This implies that the roof of the intrusion is concordant with the country rocks and was rather flat prior to folding.

There are eight other intrusions which also intrude andesitic rocks of the LaBine Group and display striking similarities to the Balachey in texture, composition, and wall-rock alteration type. They are the seven plutons of the Mystery Island Intrusive Suite found in the Echo Bay area (Hildebrand, 1981) and the Rainy Lake Intrusive Complex (Tirrul, 1976) of the Camsell River area. All but one of these intrusions, the Tut pluton of the Echo Bay area which was itself deroofed early on, are exposed in cross-section and seen to be concordant, sheet-like bodies. Thus, it is reasonable to assume a similar sheet-like form for the Balachey Pluton.

Petrography

Thin section examination of the main body of the quartz monzonite shows it to be a massive rock consisting of euhedral, sericitized plagioclase phenocrysts, 1 to 4 mm long, in a matrix of quartz and microperthite, typically forming granophyric intergrowths. Concentric shells of sericite define original zoning in the plagioclase phenocrysts. Quartz always displays undulatory extinction. Both it and the microperthite locally appear to replace plagioclase. Fibrous green amphibole, probably tremolite-actinolite, is subhedral to anhedral, replaced by chlorite along cleavage planes, and form clots 2 to 4 mm across. A few small patches of amphibole are replaced by epidote. Anhedral grains of opaque iron-titanium oxides are concentrated in the amphibole clots but sparse hexagonal plates of hematite occur scattered throughout the rock. Hexagonal prisms of apatite less than 0.5 mm in diameter are a common accessory but total less than 1 percent of the rock, as do euhedral zircon crystals.

In thin sections made from samples collected closer to the roof of the pluton, plagioclase phenocrysts are seen to be replaced by an interlocking mosaic of quartz and albite. Vestiges of original plagioclase phenocrysts occur but most have been completely replaced by albite and are no longer euhedral. Instead, they have margins which grade into and interlock with the quartz and albite matrix. The few intensely sericitized cores of plagioclase that do remain are completely albitized around their margins. Amphibole is present in these rocks as felted mats and irregular clots of small crystals pseudomorphing earlier ferromagnesium minerals. The borders of the clots and aggregates are ragged and fuzzy. Opaque oxides are much sparser in these rocks than in the main body of the pluton; only a few tiny anhedral grains occur. Thousands of minute apatite grains are seen in individual thin sections but are so small that their total abundance is probably not much greater than 1 percent. As in the central parts of the intrusion all quartz grains display undulatory extinction.

The fact that even late replacement quartz has been strained might suggest that the deformation may not have taken place during emplacement of the pluton but instead occurred as the sheet-like body was folded. However, a block of the intrusion in the White Eagle Tuff, known to have been erupted prior to folding, also contains strained quartz, yet quartz phenocrysts in the tuff itself are not strained. Therefore, the deformation is ascribed to the latter stages of emplacement and not to folding.

Alteration of wall rocks

The Balachey Pluton strongly alters its wall rocks to a distance of at least 2 kilometres. At present a detailed study of the alteration and its relation to the intrusion is still under way. Accordingly, only a brief description will be given here.

Three zones of alteration were mapped in the field: an inner zone of intense bleaching and albitization; a central zone of magnetite-apatite-actinolite; and an outer zone of pyrite-chalcopyrite. The criteria used to delineate the zones were as follows: (1) the boundary between the inner and central zones was placed at the first appearance of the assemblage magnetite-apatite-actinolite; (2) the boundary between the central and outer zones was mapped as the disappearance of the magnetite-apatite-actinolite assemblage; and (3) the outer margin of the sulphide zone was placed at the disappearance of megascopically visible gossan. Mapped in this way albite is present in all three zones and sulphides occur in the outer part of the magnetite-apatite-actinolite zone.

The zones of alteration are widest in the northwest (Map 1) and pinch-out towards the southeast. They are truncated by the unconformity along the northeast side of the intrusion.

The inner zone is characterized by nearly complete albitization of the andesitic lavas and sedimentary rocks. Most original textures are obliterated and the rocks weather white to very pale pink. Nearly all bedded rocks are intensely brecciated but vestiges of bedding can still be seen within the fragments. A fine-grained, pre-Balachey, monzonitic intrusion located north of Jason Bay (Map 1) is completely albitized only adjacent to fractures which gives the rock a mottled pink and white appearance in outcrop. Andesite flows within this zone are often completely replaced by granoblastic-polygonal albite with only a few specks of chlorite and weather white in outcrop.

Analyses of andesitic lavas and volcanogenic sandstones from within this zone are presented in Table 6. The chemical modifications are large and include an increase in silicon, aluminum, and sodium. Elements lost appear to be all those incapable of being accommodated in the albite crystal lattice such as Ti, Fe, Ca, K, Nb, Y, U, Rb, Th, Pb, Cu, Ni, Cr, V, La, and Ce. Figure 38 shows the large increase in Na_2O and concomitant decrease of K_2O in andesites within the alteration halo.

The zone of magnetite-apatite-actinolite is characterized by the presence of those minerals as pods, veins, disseminations, and as rosettes with albite. Most commonly there are small veins a centimetre or two wide in which fibrous green amphibole grows perpendicular to the vein walls with interstitial, anhedral pink apatite and octahedra of magnetite or its non-magnetic equivalent, martite. Pods of magnetite-apatite-actinolite up to 2 m across also occur and those typically contain coarse blades of amphibole up to 30 cm long, magnetite octahedra to 5 or 6 cm, and patches of apatite of variable size up to 20 cm. Rosettes of bladed albite, up to 15 cm across, with interstitial chlorite, amphibole, and magnetite are commonly found as alteration products of andesite flows (Figure 39). Epidote is a common mineral within this zone and a few cavities within lava flows are lined with it and contain partially-filled cores of apatite.

TABLE 6: Major and trace element analyses, altered andesitic rocks.

Sample No.	H-79-131*	H-79-132**	H-79-133**	H-79-126*	H-79-124a*
SiO_2	59.1	71.3	65.0	59.4	61.5
TiO_2	0.28	tr	0.00	0.20	0.45
Al_2O_3	18.2	15.5	20.3	17.1	16.6
Fe_2O_3***	3.47	0.65	0.61	4.42	2.73
MnO	0.26	0.07	0.04	0.06	0.12
MgO	3.39	0.39	0.19	1.68	1.42
CaO	4.54	1.41	1.02	3.33	2.14
Na_2O	7.50	8.36	9.36	7.98	8.82
K_2O	1.12	0.37	1.46	0.88	0.88
P_2O_5	0.02	0.01	0.00	0.34	0.38
LOI	2.53	1.82	1.70	3.48	3.12
Total	100.41	99.88	98.68	98.87	98.16
Nb	7	0	0	22	35
Zr	175	35	171	206	203
Y	19	0	6	32	45
Sr	370	83	203	78	45
U	0	0	0	5	5
Rb	25	6	49	9	13
Th	0	0	0	14	12
Pb	6	15	0	3	1
Ga	20	20	20	20	21
Zn	147	24	20	55	15
Cu	8	15	6	13	38
Ni	0	0	0	0	0
Cr	0	0	0	0	0
V	31	6	0	0	122
La	11	5	17	50	64
Ce	11	1	17	72	122
Ba	1034	262	419	204	163

***Total Fe as Fe_2O_3. **Andesitic sandstones; *Andesitic lavas.
Oxides in weight percent; trace elements in parts/million.

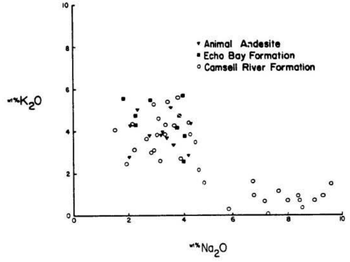

Figure 38. K_2O versus Na_2O plot for various andesites of the LaBine Group showing the effects of albitization within the alteration halo of the Balachey Pluton. Note the increase of Na_2O and concomitant decrease of K_2O in samples collected from within the alteration halo.

Figure 39. Albite rosettes in magnetite-apatite-actinolite zone of Balachey Intrusive Complex alteration halo.

The contact of the magnetite-apatite-actinolite zone with the sulphide zone is gradational but was mapped as the disappearance of magnetite-apatite-actinolite. Sulphides within this zone are mainly pyrite and chalcopyrite although secondary (?) pyrhotite is also commonly present. Typically the sulphides occur as patches of variable size, but generally tens of metres across, of 20-25 percent fine disseminations. They are easily recognizable in the field from great distances as gossans. It is this zone that contains polymetallic veins of native silver and bismuth and Ni-Co arsenides located along the north side of the Camsell River.

Interpretation

The late stage replacement of plagioclase phenocrysts in the Balachey Pluton by quartz and albite; the concentration of amphibole adjacent to fractures in the pluton; and the wide alteration halo, sometimes with fracture controlled albitization, attest to the activity of high-temperature hydrothermal fluids. At the present time, without oxygen isotope data, it is not possible to determine the relative role of magmatic versus ground water but the incredible volume of altered rock suggests large scale ground water:rock interactions.

The pinch-out of the alteration zones in a southeasterly direction suggests that the alteration is depth-controlled for, as argued earlier, deeper levels of the pluton are exposed in that direction.

As the Balachey Pluton is unconformably overlain by White Eagle Tuff but intrudes the Camsell River Formation its age of emplacement is tightly constrained. This may indicate that the hydrothermal cell was not especially long-lived for there are abundant fragments of the altered rocks in the breccia at the unconformity which indicate that alteration had already taken place prior to the deroofing of the pluton.

Although it is not possible to know how much Camsell River Formation was eroded prior to eruption of the White Eagle Tuff the upper conglomerate of the Camsell River Formation may mark the original top of the pile. If so, then the Balachey Pluton was intruded 2-3 km beneath the surface. Even if substantial volumes of andesite were stripped away, the pluton was nevertheless emplaced at only a few kilometres depth--a remarkable occurrence considering its size.

The close temporal, spatial, and chemical relationships of the Balachey Pluton to the Camsell River Formation suggests that the two are genetically related. Probably the intrusion represents the type of magma chamber which at deeper levels fed the surface volcanism of the Camsell River Formation. Eventually the body migrated upwards and invaded its own volcanic ejecta much in the manner envisioned by Hamilton and Myers (1967).

Rainy Lake Intrusive Complex

The Rainy Lake Intrusive Complex (Tirrul, 1976) is a compositionally and mineralogically zoned sheet-like pluton about 1,500 m thick and 10-11 km across. The pluton was folded after intrusion and is now exposed in cross section on the southwest limb of Norex Syncline (Map 1). Only a brief description of the pluton will be made here because work on this complex, but interesting, body is still in progress.

The intrusion has a flat roof that is roughly concordant with bedding of the roof rocks. However, down dip in the Terra Mine workings the upper contact is seen to cut up section. The floor of the body is convex downward with the thickest parts near the centre of the intrusion. Both the upper and lower contacts strike northwest-southeast and dip from 50-90° to the northeast. In the southeast the pluton was intruded by a younger syenogranite and the original lower contact of the Rainy Lake Intrusive Complex is therefore not exposed in that area.

Tirrul (1976) recognized that the pluton was compositionally zoned, parallel to its flat roof, and mapped five major lithologic units within the body. From top to bottom they are: upper border monzonite, fine-grained syenite, coarse-grained syenite, monzonite, and monzodiorite (Map 1). In addition, there is also a lower border monzonite.

Where the upper margin of the intrusion is exposed (Figure 40) there is typically a well-developed border phase, up to 20 metres thick, comprising 30-35 percent intensely sericitized plagioclase phenocrysts (Figure 41) up to 1 cm long and ragged mafic clots (3 mm) of chlorites, amphibole, carbonate, and opaque oxides sitting in a much finer groundmass of chlorites, carbonate, chessboard albite, sphene, epidote, and a trace of quartz. Concentric shells of sericite outline original zoning in some of the plagioclase phenocrysts. Under the microscope all original plagioclase seems altered but the microprobe revealed tiny domains of unaltered andesine. Most of the phenocrysts are rimmed with unaltered albite that intimately interlocks with the matrix.

Large numbers of slender needles of apatite, up to 2 mm long, are found throughout the matrix. Veins of magnetite-apatite-actinolite,

Figure 40. Upper contact of Rainy Lake Intrusive Complex.

Figure 41. Detail of upper border monzonite. Note the similarities of plagioclase phenocrysts to those of andesites of the Camsell River Formation.

up to 30 cm across, are found cutting the monzonite (Figure 42) and most trend normal to the outer contact, locally cutting across it. In the veins fibrous amphibole grows normal to the vein walls with central zones of coarse anhedral apatite and magnetite octahedra.

The lower border phase is similar to the upper border monzonite except that it does not contain mafic clots nor magnetite-apatite-actinolite veins. It generally weathers pink.

The lower half of the pluton is, in its lowest parts, a seriate monzodiorite (Figure 43) consisting of euhedral, sericitized plagioclase phenocrysts from 1 or 2 mm to 1 cm long with interstitial pale green amphibole, opaques, perthite, granophyre, and a few specks of chlorite. The plagioclase crystals occur as euhedral tablets of oscillatory zoned andesine. They are heavily sericitized and closely packed. Only locally have crystals grown together. Some of the phenocrysts have been replaced at their margins by unaltered albite. In the field the plagioclase crystals locally define a weak foliation. These features led Tirrul (1976) to suggest that the lower monzodiorite was a cumulate rock derived from gravitational settling of the plagioclase.

The pale green amphibole occurs as mostly interstitial clots (3 mm) consisting of fibrous material with random optical orientations but a few light brown to green actinolitic hornblendes show uniform crystallographic orientation. They are about 2-3 mm across and also fill interstices between plagioclase phenocrysts. Anhedral opaque oxides are ubiquitous in the clots but uncommon in the crystals with uniform optical orientation.

Anhedral perthite, about 4 mm across, also occurs as interstitial material and is often intimately intergrown with the amphibole.

Figure 42. Magnetite-apatite-actinolite vein cutting upper border monzonite.

Figure 43. Lower monzodiorite of Rainy Lake Intrusive Complex.

In places it appears to have replaced marginal portions of the plagioclase phenocrysts. Granophyric intergrowths of quartz and microperthite have a similar mode of occurrence as the perthite in that they are mainly interstitial, intergrown with amphibole, and appear to have replaced plagioclase. Locally, quartz occurs without alkali feldspar. Tiny hexagonal prisms of apatite are a common feature in the interstitial areas between plagioclase phenocrysts.

Upwards in the basal monzodiorite the following changes are seen: plagioclase phenocrysts become more heavily sericitized, have wider rims of albite, cores of finely disseminated zoisite or clinozoisite, and are replaced along cleavage traces by albite; the clots of amphibole become smaller and the amphiboles themselves become more ragged and felted; and quartz becomes sparser and locally absent.

The transition from monzodiorite to monzonite is gradational and takes place over a distance of several metres. Mineralogically, the change is characterized by an increase in the size of perthite to 7 mm and the appearance of minor amounts of chessboard albite. Quartz is absent. Apatite becomes especially common and nests of tiny needles occur throughout the matrix. Epidote clots become common and appear to be after amphibole. Chlorite and fine amphibole occur in the cores of plagioclase phenocrysts.

Texturally, both unaltered albite and perthite replace significant portions of the plagioclase phenocrysts such that only ovoid sericitized cores remain. Felted ferromagnesium minerals form ragged clots with abundant opaque oxides.

In general, the monzonite appears much less altered in thin section than the lower monzodiorite. This is mainly due to the destruction of altered plagioclase and replacement by rather fresh appearing albite and perthite, but there are fewer plagioclase phenocrysts in the monzonite than in the monzodiorite.

The upper contact of the monzonite is also gradational over several metres. The syenite is characterized by a sudden decrease in the size of perthite to 4 mm, the growth of abundant chessboard albite, and the development of abundant carbonate in the ferromagnesium clots. The clots are smaller and much sparser in this phase than in lower parts of the intrusion. The destruction of plagioclase is so great that only sparse elliptical relicts of intensely chloritized cores remain (Figure 44). Apatite is either very common or virtually absent and there does not appear to be a gradation between the two. Quartz makes up at most 2 percent of the rock but granophyre is completely absent. Opaque oxides are still concentrated in the ferromagnesium clots but like the clots they become finer and more disseminated upwards.

As higher levels of the intrusion are reached, perthite decreases in size until just below the upper border phase where it is absent altogether. Chessboard albite increases as perthite decreases. Tiny blebs of quartz become common where perthite is sparse or absent. By this level there is only one, or perhaps two, relict cores of plagioclase per thin section. They are always heavily chloritized and contain tiny wisps of amphibole.

The syenitic portions of the intrusion weather pink, probably due to the presence of finely disseminated hematite. Numerous dikes of fine-grained albitite, up to 30 cm across, and typically with gradational contacts, cut the body. They appear to be randomly oriented but were not systematically measured during mapping. Overall, the syenitic phases appear remarkably fresh in thin section except for the relict cores of plagioclase.

Figure 44. Upper syenite phase of Rainy Lake Intrusive Complex. Note sparse plagioclase phenocrysts.

A remarkable feature found in the top 10 metres of the syenite is the occurrence of pink apatite coating fracture surfaces. The fractures typically trend at high angles to the roof of the intrusion.

The contact of the syenitic phase with the upper border phase is sharp. Locally the syenite transgresses the border monzonite such that it is absent, or nearly so, and syenite occurs at the upper contact of the intrusive.

Microprobe analyses of amphiboles from the lowermost parts of the intrusion indicate that they are actinolitic hornblende. Upwards in the intrusion there is a change to ferroactinolite. Amphibole is mostly absent in the upper portions of the intrusion but amphibole in the magnetite-apatite-actinolite veins cutting the upper border phase are silicic ferroactinolite. The compositional changes of the amphiboles with respect to level within the intrusion are shown in Figure 45.

All of the amphiboles, with perhaps the exception of the actinolitic hornblendes which may be low temperature hypersolidus phases (de Albuquerque, 1974), are relatively low temperature phases, stable at oxygen fugacities around the FMQ buffer, only at subsolidus temperatures in rocks of the composition of the Rainy Lake Intrusive Complex (Ernst, 1968; Bookstrom, 1977). This suggests that they have a hydrothermal origin.

In melt-crystal systems of intermediate to mafic composition at temperatures below about 825°C the amount of tetrahedrally-coordinated aluminum in amphiboles decreases steadily with falling temperature and there is a positive correlation beween Al (IV) and the number of cations in the A-site (Helz, 1973). A constant decrease upwards in both Al (IV) and A-site occupancy in amphiboles of the

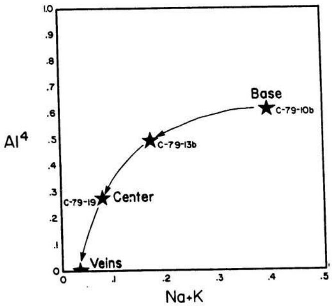

Figure 45. Composition of amphiboles in the Rainy Lake Intrusive Complex plotted in terms of atoms of tetrahedrally coordinated aluminum versus atoms of sodium and potassium.

Rainy Lake system is suggested by the limited data of Figure 45.

While Helz did not investigate subsolidus amphibole-H_2O partitioning, the similar trends found in amphiboles during this study suggest that subsolidus temperatures decreased steadily upwards in the intrusion during their formation. However, as there is little or no experimental work on the crystal chemistry and partitioning of various elements into actinolites this conclusion should be regarded with caution.

Major and trace element chemistry

Results of whole rock analyses of samples from the intrusion are presented in Tables 7a and 7b. The concentrations are shown graphically versus stratigraphic height in Figures 46a, b, c, and d.

For the most part the chemical variations show a strong correlation with mineralogy. Note that the two samples of albitite veins (C-79-21, C-79-26) have very low abundances of P_2O_5, total Fe, MgO, Ba, Rb, and Sr compared to other parts of the pluton. Also, those samples have the highest concentrations of sodium found in the intrusion. Further note that the highest sample from the intrusion, collected from the upper border phase, is generally much closer in composition to the lower monzodiorite than the upper syenitic parts of the intrusion.

Rare earth elements

Rare earth element (REE) concentrations of seventeen rocks from the Rainy Lake Intrusive Complex are presented in Table 8. All samples exhibit the light REE enrichment patterns and high overall abundances typical of the Labine Group.

Ce, Eu, and Yb are plotted versus stratigraphic height in Figure 47. The important features to note on the plots are that Ce

TABLE 7A: Major and trace element analyses, Rainy Lake Intrusive Complex.

Sample No.	C-79-11	C-79-12	C-79-13b	C-79-14	C-79-15	C-79-16	C-79-17	C-79-18	C-79-19	C-79-20
SiO_2	55.0	53.6	53.6	50.8	54.2	55.5	54.8	55.9	58.3	60.8
TiO_2	0.66	0.51	0.63	0.72	0.94	0.92	1.03	0.73	0.86	0.83
Al_2O_3	19.7	20.6	20.5	18.9	19.2	18.7	18.6	17.8	17.0	16.9
Fe_2O_3**	6.02	5.98	6.04	7.75	7.68	6.75	6.54	7.04	5.38	5.25
MnO	0.29	0.10	0.25	0.22	0.37	0.18	0.28	0.15	0.14	0.06
MgO	2.26	2.24	2.25	2.54	2.58	2.48	2.62	2.18	2.18	1.77
CaO	4.29	5.49	5.24	5.14	5.17	5.49	5.01	3.65	3.68	3.16
Na_2O	3.89	4.18	3.51	3.21	3.68	4.64	4.48	4.14	6.26	7.38
K_2O	4.73	3.51	3.89	3.72	3.72	3.60	4.25	4.69	2.92	2.56
P_2O_5	0.26	0.26	0.27	0.55	0.51	0.51	0.57	0.42	0.48	0.35
LOI	2.66	2.81	2.57	2.81	2.23	1.72	1.82	2.17	1.50	0.90
Total	99.76	99.28	98.75	98.36	100.28	100.55	100.00	98.87	98.71	99.96
Nb	8	3	4	8	4	9	6	14	13	13
Zr	129	64	87	89	83	107	126	165	160	180
Y	25	15	18	24	24	34	35	31	41	36
Sr	521	652	560	572	524	509	498	286	227	189
U	2	0	2	0	1	4	1	0	2	1
Rb	153	112	126	117	120	92	111	109	50	42
Th	10	9	6	1	8	2	10	1	11	11
Pb	13	5	10	21	24	1	22	10	7	21
Ga	20	19	19	21	16	22	15	22	20	20
Zn	275	77	83	170	304	115	306	108	102	43
Cu	8	4	38	38	4	0	0	0	0	6
Ni	13	22	21	9	17	8	16	1	3	6
Cr	18	22	14	10	0	4	0	0	0	0
V	131	104	145	212	193	155	168	148	130	109
Ba	1028	935	904	1158	1614	984	1160	1423	819	849

**Total Fe as Fe_2O_3. Oxides in weight percent; trace elements in parts per million.

TABLE 7B: Major and trace element analyses, Rainy Lake Intrusive Complex.

Sample No.	C-79-21	C-79-22	C-79-23	C-79-24	C-79-25	C-79-26	C-79-27	H-79-16	Terra Mag
SiO_2	66.1	61.4	61.1	61.3	64.0	66.0	57.9	---	10.9
TiO_2	0.92	0.73	0.76	0.86	0.63	0.59	0.65	---	0.08
Al_2O_3	17.6	16.7	16.1	16.5	14.8	15.3	17.5	---	0.24
Fe_2O_3**	1.53	4.80	5.33	6.35	4.95	2.06	6.03	---	73.3
MnO	0.05	0.06	0.10	0.08	0.12	0.04	0.18	---	0.07
MgO	0.51	1.88	1.66	1.82	1.31	0.49	2.79	---	2.01
CaO	0.88	2.48	2.22	2.13	2.22	2.49	3.99	---	5.41
Na_2O	9.41	7.82	5.80	5.95	7.72	8.88	6.01	---	0.04
K_2O	0.72	1.28	3.14	3.24	0.64	0.38	2.27	---	0.05
P_2O_5	0.03	0.44	0.44	0.51	0.46	0.02	0.32	---	2.90
LOI	1.37	1.19	2.12	1.64	1.78	2.56	2.68	---	-1.34
Total	99.27	98.78	98.77	100.38	98.63	98.81	100.32	---	93.66
Nb	19	17	14	16	20	19	11	7	17
Zr	247	208	213	199	271	260	150	143	21
Y	25	38	38	43	58	23	30	27	153
Sr	48	136	157	144	72	60	290	391	13
U	1	1	4	3	2	9	3	4	11
Rb	14	44	86	83	4	8	106	349	10
Th	0	13	12	8	11	12	10	12	11
Pb	5	6	15	23	4	15	10	17	7
Ga	23	19	21	20	22	21	18	12	5
Zn	49	44	53	62	58	126	125	139	177
Cu	2	0	17	16	0	25	0	4	0
Ni	0	1	4	5	4	3	26	55	67
Cr	0	0	0	0	0	0	58	131	3
V	24	58	90	85	117	44	151	183	1243
Ba	112	479	1002	869	74	87	687	1153	8
								La	740
								Ce	1152

**Total Fe as Fe_2O_3. Oxides in weight percent; trace elements in parts/million.

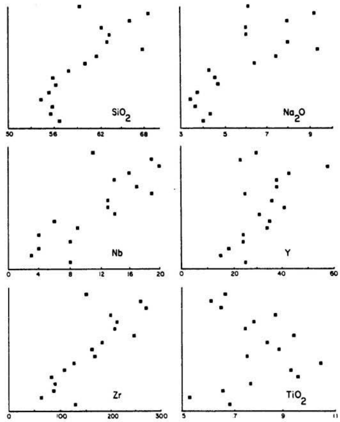

Figure 46a. Variations of SiO_2, Nb, Zr, Na_2O, Y and TiO_2 plotted with respect to height in the Rainy Lake Intrusive Complex. Oxides in weight percent; trace elements in ppm. Vertical scale is approximately 1.5 km.

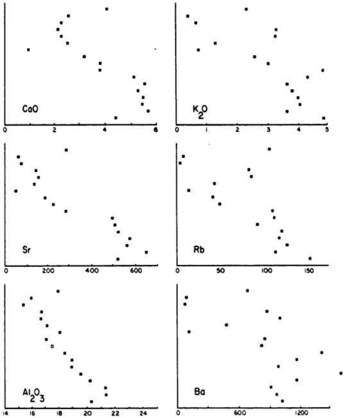

Figure 46b. Variations of CaO, Sr, Al_2O_3, K_2O, Rb and Ba plotted with respect to height in the Rainy Lake Intrusive Complex. Oxides in weight percent; trace elements in ppm. Vertical scale is approximately 1.5 km.

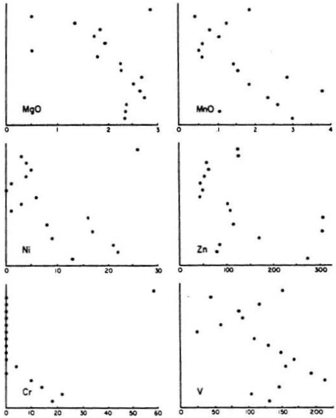

Figure 46c. Variations of MgO, Ni, Cr, MnO, Zn, and V plotted with respect to height in the Rainy Lake Intrusive Complex. Oxides in weight percent; trace elements in ppm. Vertical scale is approximately 1.5 km.

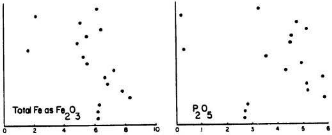

Figure 46d. Variations in weight percent Fe_2O_3 and P_2O_5 plotted with respect to height in the Rainy Lake Intrusive Complex. Vertical scale is approximately 1.5 km.

TABLE 8: Rare earth element analyses, Rainy Lake Intrusive Complex.

Sample No.	C-79-11	C-79-12	C-79-13b	C-79-15	C-79-16	C-79-17	C-79-18	C-79-19	C-79-20
La	20.86	21.94	24.10	22.09	25.87	40.56	23.38	26.55	18.97
Ce	44.99	46.95	52.11	44.14	53.75	80.57	50.72	50.72	44.80
Pr	5.49	5.11	6.43	---	7.41	10.27	7.41	7.07	6.12
Nd	22.97	21.30	23.55	28.52	31.82	44.43	30.70	30.88	27.44
Sm	3.80	3.85	3.99	5.46	6.54	9.39	6.92	6.15	6.38
Eu	0.84	0.99	1.29	1.69	1.28	1.33	0.99	0.96	1.33
Gd	3.54	2.51	2.92	4.77	5.13	6.46	5.07	4.92	4.45
Dy	---	2.14	3.46	3.72	4.02	5.80	4.81	5.38	5.63
Er	1.82	1.47	1.33	2.21	2.63	2.09	2.63	2.60	2.69
Yb	1.49	1.20	1.69	2.19	3.28	2.34	3.27	2.10	2.65

Sample No.	C-79-21	C-79-22	C-79-23	C-79-24	C-79-25	C-79-26	C-79-27	H-79-16
La	---	---	20.65	---	107.81	19.72	28.63	31.75
Ce	15.61	47.62	47.45	47.52	234.18	37.09	63.59	65.50
Pr	2.07	6.49	---	7.17	24.89	4.13	7.50	7.57
Nd	7.76	28.61	28.00	28.57	94.60	18.81	30.33	31.63
Sm	1.67	5.82	6.47	5.59	13.78	4.27	5.54	6.32
Eu	0.27	1.08	1.42	1.02	1.30	1.06	1.25	1.32
Gd	1.36	5.02	5.40	5.42	7.47	3.45	4.03	4.77
Dy	1.92	5.55	5.09	4.33	7.14	3.03	4.27	4.90
Er	1.58	2.62	2.44	2.54	3.05	1.55	1.68	2.12
Yb	1.98	3.34	2.49	2.67	3.21	---	2.23	2.06

All values in parts/million.

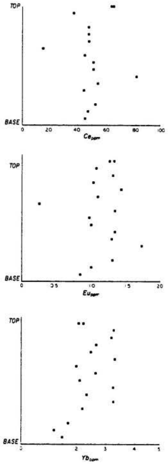

Figure 47. Selected rare earth elements plotted versus height in the Rainy Lake Intrusive Complex.

concentrations are nearly constant regardless of stratigraphic height; Eu concentrations increase upwards in the lowermost parts of the monzodiorite but otherwise remain constant throughout most of the body; and Yb concentrations show a slight increase upwards.

Strontium isotopes

The results of strontium isotopic analyses of samples from the intrusion are presented in Table 9. Model ages, calculated using an initial $^{87}Sr/^{86}Sr$ isotopic ratio of 0.7025, are plotted versus stratigraphic height in Figure 48. The data clearly indicate that Rb-Sr systematics in the upper half of the pluton have been severely disturbed and that the system has not remained closed with respect to Rb and/or Sr. Therefore, the rocks cannot be dated by the Rb-Sr method (Faure, 1977).

Water content and magma temperature

Plagioclase was the liquidus phase in the Rainy Lake magma and it can be inferred from arguments presented in conjunction with lavas of the Camsell River Formation that the Rainy Lake magma contained 2 percent or less H_2O. By similar reasoning to that used for the Balachey Intrusive Complex, the depth of emplacement is considered to be 3 or 4 km.

Once the pressure and water content of an andesitic magma are known it is easy to estimate the liquidus temperature of the magma by using published experimental data. With 2 percent water at less than 5 kb the liquidus temperature for andesitic magmas is slightly less than 1100°C (Green, 1972; Eggler and Burnham, 1973).

Most of the crystallization of an andesitic magma takes place over a short temperature interval 50 to 100° below the liquidus

TABLE 9: Strontium isotopic analyses, Rainy Lake Intrusive Complex.

Sample No.	ppm Rb	ppm Sr	Rb/Sr	$^{87}Rb/^{86}Sr$	$^{87}Sr/^{86}Sr$
H-79-16	347	388	.89589	2.60±.01	.7690±.0001
C-79-27	104	288	.36237	1.051±.005	.7296±.0001
C-79-26	58	68	.85351	2.47±.01	.7131±.0004
C-79-24	82	150	.54718	1.730±.008	1.671±.001
C-79-23	86	165	.52267	1.518±.008	.7450±.0001
C-79-22	42	138	.30794	.891±.004	.7154±.0001
C-79-21	15	54	.26961	.780±.004	.7129±.0002
C-79-20	43	202	.21413	.630±.003	.88489±.00009
C-79-17	111	495	.22481	.651±.003	.7197±.0001
C-79-16	92	522	.17585	.549±.003	1.509±.006
C-79-15	120	516	.23172	.671±.003	.72047±.00007
C-79-14	113	579	.19464	.563±.003	.7185±.0001
C-79-12	110	642	.17125	.496±.002	.7171±.0003
C-79-11	150	530	.28309	.820±.004	.7245±.0001
R1-3	193	424	.45415	1.318±.007	.7363±.0001
R1-4	79	554	.14291	.413±.002	.71355±.00009
RL-12	84	560	.14926	.432±.002	.71454±.00004
RL-14	94	449	.20994	.608±.003	.7190±.0001

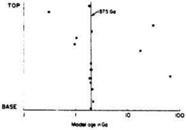

Figure 48. Calculated model ages using an initial ratio of 0.7025 for selected samples of the Rainy Lake Intrusive Complex plotted versus height in the intrusion. Note that x axis is logarithmic. Vertical scale is about 1.5 km.

(Marsh, 1981). As the Rainy Lake magma was about one-third crystalline when intruded, it can be inferred that the temperature of the magma was about 1000°C when emplaced.

Alteration

The Rainy Lake Intrusive Complex has a similar alteration halo to that of the Balachey Intrusive Complex but the zones are not as well-defined and have been modified by the emplacement of younger intrusions. There do, however, appear to be larger bodies of magnetite-apatite-actinolite (Figure 49) above the roof of the Rainy Lake Intrusive Complex than occur around the Balachey.

The bodies of magnetite-apatite-actinolite led Badham and Morton (1976) to speculate that an iron phosphate liquid separated from the intrusive as an immiscible liquid. This appears unlikely for the following reasons:

1. Many veins contain only amphibole and/or apatite. Magnetite can be absent. Thus there is often more silica than iron in the veins.
2. Amphiboles typically grow orthogonal to the vein walls, a texture more suggestive of deposition from hydrothermal fluids than a magmatic melt.
3. The veins are often zoned with margins of amphibole and magnetite and cores of apatite-a texture incompatible with their derivation from a single iron phosphate melt.
4. Granular magnetite-apatite-actinolite often replaces individual beds of sedimentary rock (Figures 50 and 51) and selectively replaces matrices of ash-flow tuffs of the Camsell River Formation.

Figure 49. Body of granular magnetite-apatite-actinolite above roof of Rainy Lake Intrusive Complex.

Figure 50. Granular magnetite-apatite-actinolite replacing sedimentary rocks of the Arden Formation.

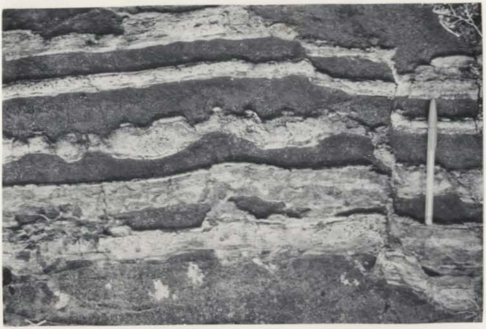

Figure 51. Granular magnetite-apatite-actinolite replacing alternate beds of sedimentary rock above roof of Rainy Lake Intrusion.

5. The composition of amphiboles in the veins suggests low temperature crystallization not the temperatures of over 1000°C that are needed to maintain an iron-phosphate melt (C. Thompson, personal communication, 1981).
6. Apatite coats fractures in the upper syenite which indicates that it was solid enough to fracture when the apatite crystallized.
7. It does not explain the intense albitization of the upper part of the intrusion, its chemistry, nor its Rb-Sr systematics.
8. Lastly, an iron-phosphate liquid will sink, due to greater density, in a silicate liquid (Daly, 1915) and therefore magnetite-apatite-actinolite bodies separated from a silicate liquid by immiscibility should occur at the bottom of the intrusion, not at the top, as is the case in the Rainy Lake Intrusive Complex.

All of the above data are, however, compatible with a hydrothermal origin.

Interpretation

The Rainy Lake Intrusive Complex, like the Balachey Pluton, appears compositionally related to the Camsell River Formation. The pluton did not rise as close to the surface as the Balachey but its effect on the country rocks was similar.

When first intruded, the pluton was probably a relatively homogeneous body of andesitic magma containing 30-35 percent large andesine phenocrysts. Magma adjacent to the walls was rapidly chilled to form the porphyritic border phase. As the plagioclase crystals occurring in the lower monzodiorite are nearly the same size as those of the upper and lower border phases there was not much plagioclase growth after emplacement. The major difference between the two zones is that the lower monzodiorite contains 60-65 percent plagioclase phenocrysts while the border phases contain only 30-35 percent. Apparently some mechanism mechanically concentrated plagioclase phenocrysts in the lower part of the intrusion.

While it is not possible to reliably predict the viscosity of the Rainy Lake magma, experimental work and subsequent thermal modeling suggest that when a body of magma the size, composition, temperature, and water content of the Rainy Lake is intruded, it will naturally convect (Shaw, 1965; Bartlett, 1969; Murase and McBirney, 1973; McBirney and Noyes, 1979). Therefore, the Rainy Lake melt probably began to convect shortly after intrusion. Since convective rates are many orders of magnitude greater than crystal settling rates calculated by using Stokes Law (Rice, 1980) it is unlikely that the plagioclase crystals settled slowly to the bottom. Instead, a more attractive possibility is that the crystals were carried downward by convection currents and deposited near the base.

The upper parts of the intrusion as seen today do not reflect the original composition of the differentiated magma. Calculations by Tirrul (1976) and the author of this report clearly demonstrate the inability of plagioclase and amphibole-clinopyroxene fractionation to yield liquids of the composition found in the upper parts of the Rainy Lake from any reasonable original bulk composition. Furthermore, REE data is incompatible with a simple fractionation model. Instead, it is suggested that the upper part of the intrusion is a metasomatic rock generated by hydrothermal convection, and/or retrograde boiling.

While retrograde boiling may have generated the fractures in the roof of the intrusion (see Burnham, 1979; Burnham and Ohmoto, 1980) which are now filled with magnetite-apatite-actinolite and may have even altered the upper part of the body, the water to rock ratio would not, in all likelihood, have been large enough to pervasively alter the entire pluton and its wall rocks to their present state. The only mechanism capable of doing so appears to be cooling by hydrothermal convection. By this mechanism vast quantities of meteoric water circulate through the cooling intrusion and heat is transferred outward into the country rocks (Taylor, 1979; Parmentier and Schedl, 1981). Furthermore, virtually identical alteration types are seen in the country rocks around the Balachey Pluton and it would be difficult to argue that this alteration is anything but hydrothermal.

Therefore, one might make the argument, based on similarities with the Balachey Pluton that the upper syenite, composed mostly of albite, is equivalent to the inner albite zone of the Balachey halo and that the magnetite-apatite-actinolite zone is represented by the fracture coatings of apatite in the syenite, the veins of magnetite-apatite-actinolite in the border phase, and the larger bodies of magnetite-apatite-actinolite above its roof. Similarly, the large sulphide zones which host the polymetallic ore veins of Terra Mine, located on Arden Peninsula, could be the pyrite-chalcopyrite halo.

The iron, phosphorous, and magnesium of the magnetite-apatite-actinolite bodies could have been derived from the albitite veins, which are depleted in those elements relative to the rest of the syenite. Volumetrically there was enough iron, magnesium, and phosphorous lost from the veins to easily produce the volume of those elements present in the magnetite-apatite-actinolite bodies. It is hypothesized that the veins were the main fluid pathways during hydrothermal alteration.

It is not known whether or not the intrusion was completely solid when the alteration took place but the sharp contact of the syenite with the upper border phase and the large differences in alteration between them suggest that alteration commenced prior to complete crystallization of the magma. The tremendous increase in sodium in the upper half of the intrusion relative to the lower half requires a source for that element other than the pluton or the country rocks because neither is depleted in sodium. NaCl-rich brines may have remained as intergranular fluids in marine sandstones of the Conjuror Bay Formation, present just beneath the intrusion.

Elsewhere in the world, Bookstrom (1977) interpreted magnetite-actinolite deposits at El Romeral, Chile as products of hydrothermal alteration while Fiske and others (1963) attributed magnetite-apatite-actinolite bodies above the roof of the Tatoosh pluton to volatile streaming. The bodies at Great Bear Lake are similar to magnetite-apatite-actinolite deposits at Kiruna, Sweden (Geijer and Ödman, 1974) and in the St. Francois Mountains, Missouri (Snyder, 1969). Both the Rainy Lake Intrusive Complex and Balachey Pluton have many features in common with the Tatoosh and other epizonal plutons described in the literature (Table 10). The alteration is somewhat akin to that of porphyry copper systems (Lowell and Guilbert, 1974; Gustafson and Hunt, 1975; Lanier and others, 1975) but the haloes of both Balachey and Rainy Lake intrusions are appreciably larger than those systems. Plutons like the Rainy Lake or Balachey may be the type of subvolcanic plutons ultimately responsible for the heavy pyritization of surficial rocks of arc volcanoes (see Taylor, 1959).

TABLE 10: Comparison of epizonal plutons (modified after Schweickert, 1976).

	Cloudy Pass batholith*	Tatoosh pluton[2]	China Garden pluton[3]	Rainy Lake intrusive[4]	Balachey intrusive[4]
Chief rock type:	grano-diorite	grano-diorite	quartz monzonite	monzo-diorite	quartz monzonite
Euhedral plagioclase:	common	common	common	common	common
Interstitial quartz and K-feldspar:	yes	yes	yes	yes	yes
Plagioclase replaced by late feldspar and quartz:	yes	?	yes	yes	yes
Rocks altered:	yes	yes	yes	yes	yes
Chilled borders:	yes	yes	yes	yes	yes
Porphyritic facies:	yes	yes	yes	yes	yes

*Crter (1969); [2]Fiske and others (1963); [3]Schweickert (1976); [4]This report

White Eagle Tuff

The White Eagle Tuff is a densely welded ash-flow sheet and associated breccias named for its exposures near White Eagle Falls along the Camsell River between Clut Lake and Balachey Lake. It generally lies unconformably on the Camsell River Formation, but on the mainland south of Conjuror Bay it lies on Moose Bay Tuff. Northeast from Clut Lake to northeastern Balachey Lake the tuff is overlain by a distinctive brick red rhyodacite ash-flow tuff which is strongly eutaxitic or by clastics of the Uranium Point Formation. It is overlain by Animal Andesite north of Balachey Lake, while in the southeast Conjuror Bay area and east of Clut Lake the tuff is found beneath younger ash-flow tuffs.

Distribution and thickness

The White Eagle Tuff is exposed almost continuously in a 2 to 4 km wide north-south trending belt from Grouard Lake nearly to Conjuror Bay (Map 1), a distance of about 20 km. There the tuff is exposed in a series of open northwest-southeast trending folds with axes that plunge shallowly northwestward such that the base of the tuff is exposed only in the southeast, on Clut Island and on the eastern isthmus between Clut and Grouard Lake. Throughout the entire belt there is nowhere exposed a complete section, which makes accurate measurement of its thickness impossible. However, continuous sections greater than 1.5 km thick are exposed in fold limbs.

All along the southwest margin of this belt the tuff interfingers with and grades into the coarse sedimentary breccia which unconformably overlies the Balachey Pluton. This breccia is here termed the mesobreccia member of the White Eagle Tuff.

The tuff is also well-exposed south and west of Animal Lake. About 30–40 m of nearly flat-lying tuff occur south of the lake but the top of the unit is not exposed. To the west of the lake White Eagle Tuff is a maximum of 350 m thick.

Exposures of the tuff are also found on islands in eastern Conjuror Bay and on the mainland south of the bay. At those localities the tuff is nowhere thicker than 200 m but sections are not complete.

General lithology

The White Eagle Tuff is a composite ash-flow sheet, composed of densely welded and devitrified andesitic to dacitic ash-flows (Table 11). Partially welded tuff is present only at the top and bottom of the unit in the thinner preserved sections west of Balachey Lake.

Exposures at the southeast end of Clut Lake contain altered and fractured blocks of Camsell River Formation up to 1 km in diameter and a few blocks of Balachey Lake Intrusive ranging up to 100 m across. Often large blocks with brecciated margins have many smaller fragments of the same rock type around them. In a crude way the size of the blocks becomes larger in stratigraphically higher sections of the tuff. Where blocks are numerous the tuff contains abundant xenocrysts of green amphibole similar to green amphiboles filling vesicles in Camsell River andesite flows.

Elsewhere the tuff varies in lithic content but is typically lithic-rich with lithics generally making up 10–20 percent of the rock. In a few areas lithic fragments of foliated granitoids occur and were probably derived from the Hottah Terrane.

Phenocryst abundance and size in the White Eagle Tuff were not studied in detail but total phenocryst content typically ranges

TABLE 11: Major and trace element analyses, White Eagle Tuff.

Sample No.	H-79-199	P-79-71	P-79-73a	P-80-60	H-79-180	P-80-58	P-80-59	P-79-102	H-79-198	J-80-4
SiO_2	60.8	62.5	64.9	64.8	62.2	64.0	63.2	63.4	62.6	63.7
TiO_2	0.43	0.58	0.43	0.45	0.40	0.34	0.53	0.60	0.40	0.55
Al_2O_3	15.0	15.8	14.4	15.3	15.5	15.6	15.7	14.7	14.8	15.9
Fe_2O_3	5.42	5.23	3.47	4.68	5.31	4.85	5.52	5.75	5.55	5.38
MnO	0.13	0.12	0.15	0.10	0.07	0.16	0.17	0.10	0.14	0.10
MgO	2.19	1.89	1.66	1.91	2.09	1.92	2.18	2.87	2.51	2.33
CaO	3.13	3.32	2.89	3.13	1.86	3.39	4.08	2.20	3.20	3.65
Na_2O	3.19	3.64	3.02	3.49	4.26	3.41	3.39	3.43	3.20	3.20
K_2O	3.96	3.81	3.84	3.99	3.20	4.19	3.63	3.90	2.69	3.80
P_2O_5	0.12	0.21	0.11	0.12	0.11	0.19	0.12	0.21	0.09	0.17
LOI	4.44	2.61	3.92	1.66	3.61	1.63	1.80	2.57	3.43	1.17
Total	98.81	99.71	98.79	99.83	98.61	99.68	100.32	99.73	98.61	99.95
Nb	9	12	10	11	9	11	11	10	9	10
Zr	132	141	155	141	122	140	132	166	111	145
Y	26	26	20	24	17	26	32	21	22	30
Sr	273	398	281	326	151	348	364	233	245	376
U	8	5	4	3	1	5	5	5	3	3
Rb	140	139	137	130	80	154	133	133	96	148
Th	8	19	21	14	8	13	11	14	10	12
Pb	28	19	19	32	3	41	37	12	25	31
Ga		18	19	21	17			25	19	23
Zn	135	100	129	106	54	238	141	170	270	111
Cu	32	6	11	25	14	9	28	15	18	0
Ni		4	24	5				28	10	4
Cr	13	7	21	10	7	3	0	75	19	7
V	106	98	57	77	77	86	318	144	93	84
La	39	52	42	40	21	32		54	35	39
Ce	64	51	68	70	62	60		91	49	63
Ba	719	785	1051	781	972	808	683	922	827	795

**Total Fe as Fe_2O_3. Oxides in weight percent;trace elements in parts/million.

from 25-35 percent of the rock (Figure 52). The phenocrysts in the rock are broken crystals of plagioclase, hornblende, biotite, and quartz, along with subhedral to euhedral microphenocrysts of magnetite. In general the phenocrysts are less than 3 mm in diameter but a few are as large as 5 mm.

In structurally deeper levels of exposure the tuff is richer in quartz while quartz is generally very sparse, if present at all, in the upper parts.

Pumice, typically highly flattened, is present in nearly all exposures but in some thick sections is partially obscured by welding, devitrification, and/or post-depositional alteration. West of Balachey Lake and in the Conjuror Bay area black fiammé 10-15 cm in diameter and 1 cm thick are very conspicuous.

Petrography

Thin section examination of the White Eagle Tuff shows it to mostly contain broken crystals of plagioclase up to 3 mm long, now ubiquitously replaced by carbonate and epidote in a massive groundmass of finely intergrown quartz, feldspars, and alteration minerals that typically mask original textures. However, in a few specimens, collected high in the sheet, well-preserved vitroclastic textures were seen. Ragged plates of biotite (to 1 mm) completely altered to epidote, chlorite, and opaque oxides make up no more than 5 percent of the bulk. Amphibole, as large as 3.5 mm, makes up another 1 or 2 percent of the total and it too is typically altered to assemblages of epidote and carbonate. There are typically a few small (0.5 mm) quartz chips present but they only make up more than 1 percent of the bulk in the stratigraphically lowest parts of the tuff. Opaque iron-titanium oxides

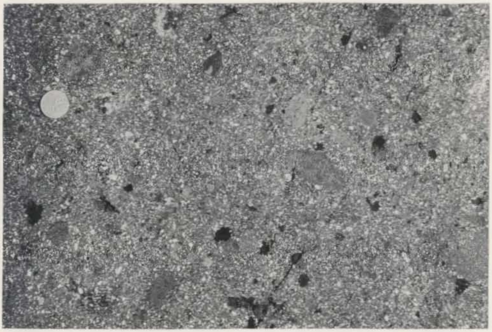

Figure 52. Crystal, lithic-rich tuff typical of intra-cauldron facies White Eagle Tuff.

most commonly occur as tiny grains in altered biotite but are also present as anhedral microphenocrysts less than 1 mm across.

Interpretation

The abrupt pinch-out of tremendously thick sections of the tuff, coupled with the zones of megabreccia indicate that most exposures of the White Eagle Tuff represent intracauldron facies tuff. The thin simple cooling units exposed south and west of Animal Lake and in the Conjuror Bay area are not propylitized, contain abundant pumice, and have unwelded, or poorly-welded bases. Therefore, they are most easily and logically interpreted as remnants of the outflow sheet. The name, Clut cauldron, is proposed for the cauldron because it is so well exposed near Clut Lake.

The gargantuan blocks of Camsell River Formation and Balachey Pluton that occur in the tuff south of Clut Lake probably represent material which spalled from the steep cauldron walls during collapse of the cauldron. This, along with the order of magnitude thickness difference between the intracauldron and outflow facies tuff, clearly demonstrates that subsidence occurred simultaneously with ash-flow eruptions. The crude inverse grading of blocks may indicate that relief on the scarp increased with time. This suggests that ash-flow volcanism was not able to keep pace with subsidence.

Mesobreccia member

The informal term mesobreccia member is here applied to the thick local assemblage of breccias along the northeastern margin of the Balachey Pluton (Map 1). The mesobreccia member interfingers with the ash-flow tuff and in many places is gradational with it. In the field the units were mapped on the basis of matrix type. That is, if the matrix was muddy or silty it was mapped as mesobreccia but if tuffaceous it was assigned to the ash-flow tuff. Typical relationships between the two units are illustrated in Figure 53. From there diagrams it can be seen that the mesobreccia occurs as northeastward thinning wedges. The base of the breccia is not exposed but presumably it rests on Camsell River Formation as does the ash-flow tuff. The breccia is overlain by the Uranium Point Formation. The unconformity (see section on Balachey Pluton contacts) with the Balachey Pluton is nearly always vertical but locally is roughly horizontal such that the contact is step-like in cross-section.

The mesobreccia is generally an unsorted mixture of clasts (1 cm-2 m in diameter) and matrix, in places clast supported and in others matrix supported (Figures 54 and 55). The breccia is poorly-bedded and typically massive but in places there are graded beds and discrete zones which contain only pebbles of Balachey Pluton. Dip of these units are less than 15° to the northeast.

The clast population varies considerably from place to place. Generally exposures closer to the Balachey Pluton contain a higher proportion of Balachey Pluton clasts than do those farther from the contact. Other common clast types are altered fragments of Camsell River Formation, pebbles of magnetite and sulphides, and cobbles of a distinctive quartz-plagioclase porphyry.

Clast shapes span the entire range from rectangular to spheroid and both extremes are commonly found adjacent to one another in the same breccia tongues. Some Balachey clasts are nearly perfect quadrilaterals suggesting that they are still bounded by original joint surfaces.

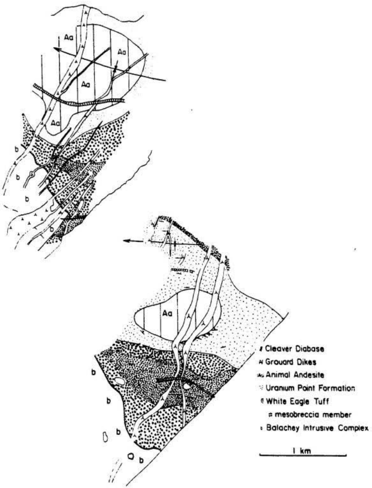

Figure 53. Sketch maps illustrating relations between White Eagle Tuff and mesobreccia member. See Map 1 for locations.

Figure 54. Detail of mesobreccia member of White Eagle Tuff showing angular fragments of Balachey Intrusive Complex.

Figure 55. Rounded and angular clasts of Balachey Intrusive Complex in muddy matrix, mesobreccia member, White Eagle Tuff.

Interpretation

The occurrence of the mesobreccia member as northeastward thinning wedges coupled with the nearly ubiquitous clasts of Balachey Pluton which become more common towards the intrusion indicate that the unnamed breccia was derived from the southwest. The interfingering relationships of the breccia with the White Eagle Tuff indicate that deposition of the breccia went on contemporaneously with eruption and deposition of the tuff.

As mentioned in an earlier section (Balachey Pluton) the unconformity between the breccia and the Balachey Pluton is presently a nearly vertical buttress facing northeast. When the shallow northeastward dips of the breccia are returned to a horizontal position the unconformity still dips steeply to the northeast indicating that the contact remained as a steep scarp during deposition of both the breccia and the White Eagle Tuff.

The above relations are interpreted to indicate that the mesobreccia represents material shed from the southwest wall of Clut cauldron during collapse of the central block of the cauldron. Similar deposits have been described in Tertiary cauldrons by several workers (Lipman, 1976; Ratté and Steven, 1967; Lambert, 1972).

Uranium Point Formation

This is a unit dominantly composed of interbedded sandstone, siltstone, mudstone, and pyroclastic rocks which conformably overlie both the mesobreccia and intracauldron facies White Eagle Tuff. It is overlain by Animal Andesite. The lower contact of the formation is defined as the first sandstone or siltstone bed above the White Eagle Tuff or mesobreccia member while the upper contact is placed at the base of the first lava flow.

The Uranium Point Formation outcrops north of the Balachey Pluton (Maps 1 and 2) and is a maximum of 50 m thick. It is not present outside Clut cauldron.

Beds of sandstone-siltstone range in thickness up to 1 m and are composed of angular to subangular volcanic debris. They are generally planar bedded but locally ripple drift and low angle cross-lamination were seen. Siltstones and sandstones are often draped with laminations of purplish mudstone. The mudstone-sandstone ratio varies from dominantly sandstone to dominantly mudstone. Convolutions are common where there is abundant mudstone. Beds of mudstone range from paper-thin laminations to 15 mm thick and are typically continuous on an outcrop scale.

Some of the sandstones are pebbly with a wide variety of volcanic clasts, typically subrounded to angular. Angular chips and flat-pebbles of carbonate are common in some beds (Figure 56). In two outcrops pebbly conglomerate is found but outcrops were not sufficient to determine the bed geometry.

Commonly interbedded with the clastic units, especially in the northwest, are ashstones and devitrified crystal and lapilli tuffs. These beds are laterally continuous and average about 15 cm thick. While most are probably of airfall origin some are crossbedded and rippled indicating that they were reworked. At the northwest end of Balachey Lake the top of the unit contains ash-flow tuff with well-developed eutaxitic structure. The tuff is a simple cooling unit that weathers orange-red. It is about 30 metres thick. The upper portion of the tuff is extremely lithic-rich and contains about 50 percent aphanitic volcanic rock chips.

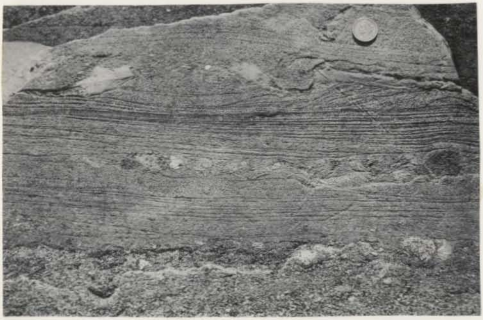

Figure 56. Crossbedded and ripple-laminated volcanogenic sandstone holding angular carbonate fragments, Uranium Point Formation.

Two common features of the finer units, both clastic and pyroclastic, are the occurrence of syn-sedimentary normal faults (Figure 57) and slump folds (Figure 58). Measurements of both features indicate that slumping was toward the southwest, that is, toward the wall of Clut cauldron (see Figure 60).

Bouldery and cobbly clastic dikes up to 1 m wide and commonly carrying clasts of Balachey Pluton occur locally. They have a sandy to muddy matrix.

Interpretation

The abundance of fine clastic detritus coupled with the general lack of current structures suggests that Uranium Point Formation was deposited in relatively quiet water. The stratigraphic position of the unit above and below subaerial units and its local distribution makes a marine origin unlikely. Thus, a lacustrine environment is favoured for the deposition of the formation.

The presence of the unit only inside Clut cauldron suggests that lake(s) developed in the topographic depression remaining after collapse of the cauldron. Periodic volcanic eruptions from unknown sources occasionally deposited pyroclastic units within the lake.

The occurrence of the southwest directed slumping and syn-sedimentary normal faulting suggests that the central part of the cauldron was uplifted during or shortly after deposition of the Uranium Point Formation. This uplift or resurgence is thought to be related to the emplacement of the Calder Quartz Monzonite more or less in the central parts of Clut cauldron.

Figure 57. Synsedimentary normal faults in interbedded sandstone and mudstone of Uranium Point Formation.

Figure 58. Slump fold in alternating mudstone-ashstone, Uranium Point Formation.

Calder Quartz Monzonite

Hornblende-biotite quartz monzonite and minor monzogranite is exposed in a 100 km^2 wedge-shaped area extending west from the Calder River to Ghosty Lake and south at least as far as Grouard Lake. It is here named Calder Quartz Monzonite after its exposures west of the Calder River.

The southwestern contact of the body is intrusive and roughly parallels the southwestern margin of Clut cauldron at a distance of about 8 km. The original extent of the pluton to the north-northeast is unknown as it was intruded by the Hooker Megacrystic Granite.

Seriate quartz monzonite is characteristic of the unit (Figure 59). Subhedral tablets of plagioclase (to 5 mm) are surrounded by potassium feldspar, quartz and ferromagnesium minerals. Commonly the plagioclases form glomeroporphyritic clots containing from 3 to 6 crystals. Biotite is always more common than hornblende with the combined total ranging from 8 to 15 percent of the rock. Both often form clots.

Xenoliths of volcanic rocks are generally sparse but where they do occur they are typically less than 0.5 m across and strongly altered. Compositionally it is very similar to the White Eagle Tuff and if one compares the whole rock analyses of the Calder Quartz Monzonite (Table 12) to those of the White Eagle Tuff (Table 11) one will see a strong similarity in overall composition.

Interpretation

The compositional similarity of the Calder Quartz Monzonite to the White Eagle Tuff and the fact that the southwest contact of the pluton parallels the margin of Clut cauldron suggest that it may be a

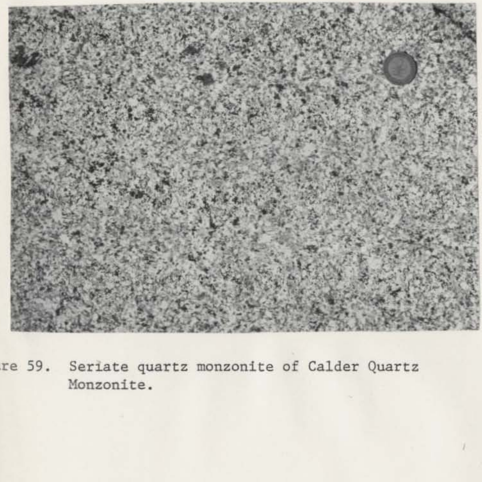

Figure 59. Seriate quartz monzonite of Calder Quartz Monzonite.

TABLE 12: Major and trace element content of Calder Quartz Monzonite

Sample No.	K-80-39	H-80-59	P-80-37	H-80-19
SiO_2	65.4	64.0	64.4	64.0
TiO_2	0.62	0.64	0.68	0.72
Al_2O_3	15.2	15.4	15.7	15.7
Fe_2O_3**	3.90	4.22	4.41	4.63
MnO	0.07	0.18	0.07	0.08
MgO	1.91	2.36	2.35	2.80
CaO	3.53	3.24	3.94	2.87
Na_2O	3.11	3.22	3.22	2.99
K_2O	4.28	4.22	4.10	4.10
P_2O_5	0.11	0.11	0.11	0.15
LOI	1.08	1.89	1.06	1.99
Total	99.21	99.48	100.04	100.03
Nb	13	13	15	13
Zr	165	179	186	199
Y	35	33	34	42
Sr	313	308	348	325
U	nd	8	1	3
Rb	158	175	184	163
Th	17	20	12	18
Pb	19	42	27	12
Ga				
Zn	55	198	60	72
Cu	12	27	26	nd
Ni				
Cr	28	22	18	35
V	65	335	332	69
La	57			50
Ce	79	37	33	84
Ba	779	1042	863	871

**Total Fe as Fe_2O_3

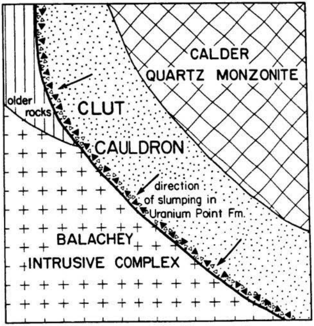

Figure 60. Palinspastic reconstruction of southwestern Clut cauldron showing relationship of Calder Quartz Monzonite to cauldron margin.

subcauldron pluton. The emplacement of the pluton might then be responsible for the doming or resurgence of the central part of the cauldron suggested by the direction of stumping in the Uranium Point Formation as shown in Figure 60.

Animal Andesite

Animal Andesite is an accumulation of pargasitic and augite porphyritic andesite (Table 13) lava flows, breccia and tuff which occur in the cores of two broad synclines north of the Balachey Pluton (Map 1). The formation overlies the Uranium Point Formation and is overlain by the "younger ash-flow tuffs." It is named for exposures north of Animal Lake.

Lavas of the formation are easily separated from those of the Camsell River Formation by their stratigraphic position and their lesser degree of alteration. They are also less plagioclase porphyritic, sometimes nearly aphyric, and have fewer amygdules than andesites of the Camsell River Formation. In the field, amphibole, clinopyroxene and plagioclase phenocrysts are commonly visible. Large quartz and potassium feldspar xenocrysts are also characteristic of some of the lavas.

The lower contact of the formation is often well-exposed and sedimentary rocks of the Uranium Point Formation are baked and altered. Sometimes the sedimentary rocks are caught up in the basal few metres of the lowest flow in the pile.

In general lava flows of Animal Andesite are massive with minor columnar joints, although one flow-banded lava was found (Figure 61). Platy-jointed bases are common in most flows but some flows have auto-brecciated margins. The flows are shades of dark-gray and reddish-purple on fresh surfaces and a light brown or gray on the weathered surfaces.

TABLE 13: Major and trace element analyses of lava flows, Animal Andesite.

Sample No.	H-80-91	H-80-81	H-80-108	H-80-89	H-80-85	P-79-138	H-80-93	P-79-104	P-79-139	P-79-95
SiO_2	58.0	56.5	56.6	53.9	57.4	58.6	53.6	60.1	60.3	52.8
TiO_2	0.91	0.72	0.71	0.87	0.74	0.72	0.74	0.59	0.63	0.83
Al_2O_3	16.2	15.1	15.2	14.7	15.6	15.9	13.6	15.3	15.6	14.9
Fe_2O_3**	6.57	6.63	6.92	7.57	7.09	6.47	8.15	5.71	4.86	7.71
MnO	0.12	0.12	0.09	0.17	0.22	0.11	0.18	0.08	0.14	0.18
MgO	3.58	4.56	4.17	6.32	4.96	3.09	8.38	3.30	3.04	5.66
CaO	4.68	4.51	3.88	6.37	5.04	4.95	7.08	2.05	4.49	5.08
Na_2O	3.13	3.27	3.45	2.00	2.31	2.67	1.97	3.42	3.15	3.94
K_2O	3.68	3.48	3.14	4.08	4.92	3.63	2.65	4.86	3.79	2.66
P_2O_5	0.20	0.19	0.23	0.26	0.28	0.16	0.18	0.18	0.19	0.22
LOI	2.09	4.58	5.20	2.33	1.80	3.64	3.29	3.12	2.59	5.49
Total	99.16	99.66	99.59	98.57	100.36	99.94	99.82	98.71	98.78	99.47
Nb	11	10	10	10	10	14	9	12	14	10
Zr	179	185	167	157	167	174	134	189	179	163
Y	24	32	26	26	26	29	19	28	26	21
Sr	587	343	351	579	602	406	442	329	466	523
U	0	2	0	8	3	0	9	5	3	3
Rb	99	117	99	109	152	119	77	167	147	77
Th	7	7	12	12	12	11	6	18	12	10
Pb	45	19	11	21	82	19	17	16	18	15
Ga	21	21	18	19	23	23		22	20	22
Zn	130	117	90	129	189	125	130	135	119	198
Cu	11	0	0	191	33	6	41	0	0	16
Ni	23	37	32	89	40	16		12	12	54
Cr	57	110	81	226	76	22	48	60	32	170
V	138	144	142	170	139	111	160	111	96	157
La	69	65	79	74	72	53	49	57	57	36
Ce	84	79	99	87	82	74	85	71	65	71
Ba	1217	1172	935	1372	1529	880	1025	1305	951	1022

**Total Fe as Fe_2O_3. Oxides in weight percent; trace elements in parts/million.

Figure 61. Flow banding in Animal Andesite lava flow.

Due north of Balachey Lake the lava flows are intercalated with andesitic breccias and tuff. Beds are generally massive to poorly-graded. Block and bombs within them are often oxidized to a purplish-red colour and are scoriaceous. An oval shaped pipe of intrusive andesite, which may represent a feeder for the pyroclastic units and/or lava flows, is exposed in this area. The entire assemblage probably constitutes a small, composite cone created by Strombolian eruptions and quiet effusions of less gas charged lava.

Petrography

Lavas of the Animal Andesite are aphanitic to porphyritic dark rocks containing variable proportions of plagioclase, clinopyroxene, and amphibole. A summary of the modal composition of various lavas is given in Table 14.

Every flow is altered to some degree. Some are relatively fresh with only incipient alteration of feldspar phenocrysts. Others are strongly propylitized with complete saussuritization of plagioclase and replacement of amphiboles and/or pyroxenes by carbonate and chlorite. In those rocks original groundmass textures are partially or completely destroyed by the formation of anhedra of feldspar and quartz.

In less altered samples phenocrysts are commonly set in either an orthophyric or pilotaxitic matrix. A few flows are microdiktytaxitic while others are intersertal.

Plagioclase phenocrysts, up to 5 mm long, are commonly zoned with cores ranging from andesine to medium labradorite (An_{55}-An_{61}) and rims of oligoclase (An_{15}-An_{25}). In many of the altered flows plagioclase may be completely albitized or have albite rims. Several flows contain poorly terminated plagioclase phenocrysts with tiny inclusions

TABLE 14: Modal analyses of lava flows, Animal Andesite.

Sample No.	%groundmass	%pyroxene	%plagioclase	%amphibole	%opaques	%quartz xenocrysts
H-80-91	94	5	---	---	1	---
H-80-96	69	22	1	---	8	---
P-79-164	56	28	---	12	4	---
P-79-104	56	9	30	---	5	---
P-79-107	75	3	21	---	1	---
P-79-105	66	10	20	---	4	---
P-79-142	68	---	24	5	3	---
J-80-75	78	11	9	1	1	---
J-80-76	89	6	1	---	2	2
P-79-109	67	9	19	---	5	---
P-79-82	82	1	12	3	2	---
H-80-90	89	6	2	2	1	1
H-80-89	76	20	1	---	2	2
H-80-92	89	4	5	1	1	---
H-80-93	79	15	2	2	1	1
H-80-86	81	12	---	5	2	---
H-80-88	70	21	5	3	1	1
P-79-72	67	---	23	8	2	---
P-79-95	80	---	6	12	2	1

Modes based on 1000points/thin section. Figures rounded to nearest percent.

of chlorite, clinopyroxene, and quartz, perhaps after glass. In some of the phenocrysts inclusions are so numerous that the phenocrysts have a skeletal appearance. In many rocks distinction between phenocrysts and groundmass microlites is arbitrary because crystals intermediate in size are also present.

Pyroxene forms stubby prisms as long as 7 mm and anhedral grains or subhedral prisms in the groundmass. The phenocrysts are calcic clinopyroxene, mostly augite (Figure 62). They are dark green to black in hand specimen. Round and irregular-shaped crystal clots of subhedral-anhedral augite are a common constituent. The largest one observed was irregular in shape and 8 mm in diameter. Similar clots have been described in calc-alkaline andesites by Stewart (1975) and by Garcia and Jacobson (1979).

Strongly resorbed quartz xenocrysts, up to 5 mm, are common in lavas north of Balachey Lake. The xenocrysts are typically armoured by coronas of augite microphenocrysts (Figure 63). The microphenocrysts are often arranged so that their long axis is orthogonal to the surface of the xenocryst. Nests of slender apatite needles are a common accessory in the coronas. Coronas of clinopyroxene are commonly found around quartz xenocrysts in various regions of the world in both extrusive and intrusive rocks (Muir, 1953; Kuno, 1950; Doe and others, 1969; Sato, 1975).

Prisms of amphibole (less than 3 mm) are typically pargasitic (Figure 64) and nearly always display some type of reaction relationship (Figure 65). Some are completely pseudomorphed by opacite and are highly corroded. In others there is a thin rind of pyroxenes, plagioclase, and opaque oxides. In one flow there are opacitic rims around resorbed pargasite phenocrysts which indicates that the amphiboles were out of equilibrium with the melt prior to eruption. Opacitic amphiboles

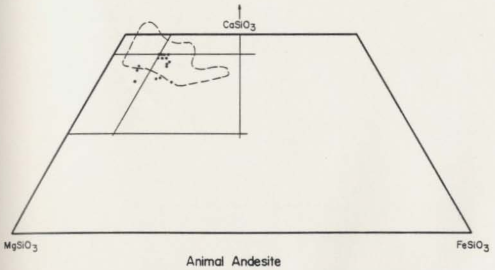

Figure 62. Clinopyroxene compositions of Animal Andesite. Field of clinopyroxenes from high-K andesites after Gill (1981).

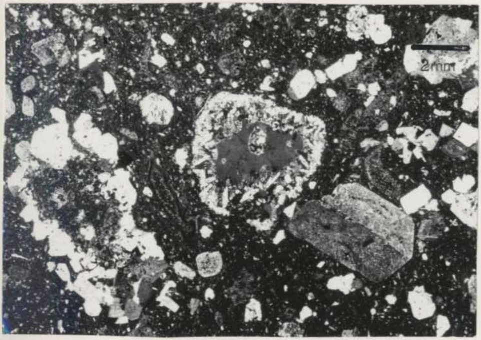

Figure 63. Clinopyroxene armoured quartz xenocryst (centre), altered K-spar xenocryst, and clinopyroxene clots, Animal Andesite.

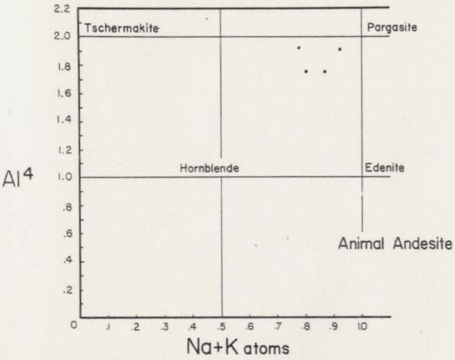

Figure 64. Composition of amphiboles in Animal Andesite expressed in terms of atoms of tetrahedrally-coordinated aluminum versus atoms of sodium and potassium (A-site occupancy).

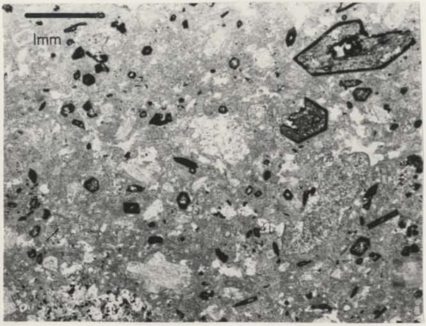

Figure 65. Photomicrograph of amphibole porphyritic andesite flow. Note opacitic rims.

are especially common in calc-alkaline volcanic rocks and are usually attributed to a drastic reduction in water pressure during, or just prior to, eruption (Kuno, 1950; Stewart, 1975; Garcia and Jacobson, 1979).

Interpretation

The local accumulations of blocks and bombs, thick sections of lavas, and lack of intercalated sedimentary rocks are characteristic of near-source areas of andesitic stratocones. Animal Andesite is preserved both inside and outside Clut cauldron which may indicate that vents were located in both areas or perhaps that there was little relief on the cauldron margin during eruption of the andesites.

The most siliceous samples of Animal Andesite have similar silica contents to the least siliceous samples of White Eagle Tuff yet the lavas have higher concentrations of Rb, La, Ce, Zr, and Ba. Therefore, the two units do not appear to have been genetically related by mixing, crystal fractionation of observed phases, or assimilation of quartz and potassium feldspar because none of those mechanisms can increase Rb, La, Ce, Zr and Ba downward in a magma chamber and maintain the same silica value. Soret diffusion, as advocated by Hildreth (1981), could reproduce the chemical variation for most of the elements but not for Rb or SiO_2, both of which appear to be concentrated upwards by that mechanism. Therefore, magma erupted as Animal Andesite was probably a different batch than that which erupted the White Eagle Tuff.

"Younger Ash-Flow Tuffs"

The youngest stratigraphic unit of the area is a compositionally diverse sequence of apparent simple cooling units of ash-flow tuff and minor intercalated sedimentary rocks here informally termed the "younger ash-flow tuffs." They range in composition from andesite to rhyolite but the more siliceous compositions dominate (Tables 15a and b). The younger ash-flow tuffs appear to rest on White Eagle Tuff everywhere except for a small area on the mainland east of Conjuror Bay where they overlie Animal Andesite. Nowhere in the map area was the top of this unit found.

Distribution and thickness

Extensive erosion and folding have left only a fragmentary record of the distribution of the younger ash-flow tuffs; they outcrop in just two regions of the map area: on islands in Conjuror Bay and east of Clut Lake (Map 1). The two areas were not studied in enough detail to correlate individual cooling units between them but overall lithologies and stratigraphic position above the White Eagle Tuff are generally similar.

In the Conjuror Bay area the thickness of the unit is perhaps 1.5 km but faulting and lack of continuous exposure due to the water of Conjuror Bay make exact thickness estimates unreliable. The thickness of the pile east of Clut Lake is even greater, perhaps 2 km, but there much of the pile is not very eutaxitic and therefore structural control is lacking.

Lithologic description

The younger ash-flow tuffs are an assemblage of cooling units whose individual thicknesses are on the order of 100-250 m. Cooling units were distinguished in the field on the basis of sedimentary intercalations and unwelded zones.

Many of the ash-flow units of the younger ash-flow tuff generally contain modal potassium feldspar which helps to distinguish them from White Eagle Tuff which generally does not contain modal

TABLE 15A: Major and trace element analyses of the "younger ash-flow tuffs", Conjuror Bay section.

Sample No.	H-79-137	H-79-138	H-79-129
SiO_2	72.3	72.1	67.5
TiO_2	0.22	0.31	0.29
Al_2O_3	12.2	12.5	13.7
Fe_2O_3	3.49	3.88	3.91
MnO	0.09	0.11	0.22
MgO	0.76	1.11	2.26
CaO	0.60	0.20	0.93
Na_2O	2.41	1.68	3.02
K_2O	5.91	6.34	4.83
P_2O_5	0.04	0.02	nd
LOI	1.66	2.22	2.38
Total	99.69	100.47	99.04
Nb	21	22	17
Zr	298	340	151
Y	64	64	34
Sr	96	40	176
U	5	6	5
Rb	230	194	183
Th	24	24	24
Pb	6	0	7
Ga		16	20
Zn	98	98	277
Cu	15	7	19
Ni		3	11
Cr	nd	nd	16
V	239	11	63
La		63	42
Ce	89	130	71
Ba	1009	1040	851

**Total Fe as Fe_2O_3.

TABLE 15B: Major and trace element analyses of "younger ash-flow tuffs", Clut Lake area.

Sample No.	H-80-38	H-80-39	H-80-40	H-80-41	H-80-42	H-80-44	H-80-45	H-80-46
SiO_2	66.9	66.5	69.0	56.1	68.0	67.1	67.7	74.0
TiO_2	0.42	0.40	0.35	0.55	0.29	0.44	0.34	0.14
Al_2O_3	16.0	15.6	15.9	18.9	16.1	16.8	16.2	13.3
Fe_2O_3**	2.95	3.85	1.89	2.98	2.43	3.13	2.63	1.73
MnO	0.06	0.06	0.07	0.27	0.11	0.04	0.05	0.02
MgO	1.04	0.62	0.53	1.17	0.63	0.63	0.59	0.34
CaO	2.33	1.71	1.35	5.29	1.81	2.47	1.16	0.63
Na_2O	2.40	3.45	4.04	5.63	3.26	3.57	3.17	2.81
K_2O	4.98	5.47	5.50	4.39	5.38	5.18	6.08	5.68
P_2O_5	0.14	0.07	0.06	0.07	0.09	0.06	0.09	0.02
LOI	1.14	1.13	1.46	4.77	1.36	0.88	1.25	0.90
Total	98.36	98.86	100.15	100.12	99.46	100.30	99.26	99.59
Nb	16	16	19	19	17	15	19	17
Zr	230	228	251	248	210	281	329	188
Y	46	46	49	43	39	38	39	40
Sr	200	183	126	194	165	239	198	86
U	15	10	6	18	10	8	5	9
Rb	214	226	219	186	241	195	229	241
Th	29	21	27	34	29	21	26	33
Pb	35	26	24	27	30	38	37	37
Ga	19	20		19			21	
Zn	68	49	85	108	72	49	60	43
Cu	17	10	15	8	13	20	9	19
Ni	2	2		1			0	
Cr	0	0		0			0	
V	33	39	279	33	24	280	10	177
La	57	50		66	53		81	
Ce	101	83	50	94	96	48	144	53
Ba	945	1160	959	825	1181	1283	2077	736

**Total Fe as Fe_2O_3. Oxides in weight percent; trace elements in parts/million.

potassium feldspar. Space does not permit a detailed description of every cooling unit present in the "younger ash-flow tuffs." Therefore, only three of the cooling units, and their intercalated sedimentary rocks, located in the Conjuror Bay area will be discussed here.

The lowest cooling unit in the Conjuror Bay area is a rhyolitic tuff which has a basal bouldery zone at least 20 m thick. Boulders in this part of the tuff, range up to 3 or 4 m in diameter and are closely packed in a tuffaceous matrix (Figure 66). In a recent paper Walker and others (1981) have attributed basal bouldery zones of ash-flows to differential settling during flow.

The basal zone grades up into a zone 10-15 m thick which contains large recumbent flow folds (Figure 67). The folds are similar to the secondary flow folds of Chapin and Lowell (1979) which they interpret to have originated when ash-flow tuff crept downslope towards a valley axis from oversteepened valley walls. Above the flow-folded zone, and gradational with it, the tuff is brick-red and contains abundant flattened pumice fragments often with a faint lineation. Those parts of the cooling unit above the flow-folded zone display well developed columnar jointing. This jointing is especially evident in upper parts of the tuff where it weathers crumbly due to poor welding.

In general, the tuff is lithic-rich with angular chips and pebbles of a wide variety of rock types locally making up to 10 percent of the rock except in the aforementioned basal zone where lithics are more abundant than tuffaceous material.

The top of this tuff is poorly exposed but appears to be covered by a metre of laminated rhyolitic ashstone, which may represent airfall material related to the eruption which produced the youngest ash-flow in the cooling unit.

Figure 66. Large block in basal lag of ash-flow tuff, younger ash-flow tuffs, Conjuror Bay.

Figure 67. Secondary flow folds above basal lag breccia, younger ash-flow tuffs, Conjuror Bay.

One-half kilometre west, this horizon is represented by slightly cobbly, planar-bedded, lithic arkose with fine partings, minor rippled tops, and occasional mudcracks. Beds are generally 5 cm to 1 m thick. Ripple crests indicate that these sandstones were derived from either the north or the south and the angularity of nearly all grains suggests that provenance was local.

Overlying the thin sedimentary interval is another cooling unit of rhyolitic ash flow tuff. This tuff also has a bouldery base but fragments (less than 0.5 m) are not nearly as large as those of the lower cooling unit.

Above the unwelded bouldery base the tuff is incipiently welded and is crystal poor. It weathers light gray. Lapilli, most of which are pumice constitutes 10 to 20 percent of the unit and pebble-size lithic fragments make up another 10 percent.

Within 10 m upsection the tuff becomes densely welded and weathers brick-red with well-developed columnar jointing. Crystal fragments increase in abundance upsection.

The top of this tuff is marked by another epiclastic interval. At least one large (15 m) intensely fractured block of rhyolitic to dacitic ashstone and crystal tuffs intercalated with hematitic red mudstone beds 10 to 30 cm thick occurs in this interval. Locally there are minor conglomerates and devitrified ashstone beds. The conglomerates are clast supported and contain subrounded to rounded boulders and cobbles of andesite, white chert, and rhyolite in fragmental matrix of angular sand grains.

One hundred metres to the west are spectacular outcrops of densely welded ash-flow tuff. This tuff is very eutaxitic with flattened pumice to 50 cm (Figure 68). Up section black fiammé become

Figure 68. Eutaxitic foliation in cooling unit 3.

Figure 69. Densely welded ash-flow tuff showing dark black fiammé.

conspicuous (Figure 69) and lithophysael cavities of vapour phase origin are found beneath lithic fragments. Phenocrysts in this tuff are plagioclase, quartz, potassium feldspar, chloritized biotite and altered pyroxene. The tuff was folded prior to eruption and deposition of the next highest cooling unit in the section. However, due to limited outcrop, structural relations are unclear and this unit may be a large block.

The above sequence is unconformably overlain by the basal unwelded zone of the next cooling unit in the sequence. Although the tuff is generally phenocryst poor at the base, quartz appears as the dominant phenocryst in the field about 20 m above the lower contact. It is conspicuous for only a few tens of metres. Biotite appears in hand specimen midway through the cooling unit.

The tuff is strongly eutaxitic except near the base and the top of the cooling unit. Lithic fragments made up to 15 percent of the bulk.

Petrography

All of the original glass in the "younger ash-flow tuffs" has been devitrified to cryptofelsite yet vitroclastic textures are remarkably well preserved (Figure 70). Every ash flow of the unit is porphyritic. Modal analyses of several units are presented in Table 16. Only the lowest cooling unit in the Conjuror Bay section which is mineralogically typical of the "younger ash-flow tuffs" will be described here. The unit contains phenocrysts of quartz, orthoclase, plagioclase, and altered pyroxene in a reddish oxidized matrix crowded with devitrified shards, many of which are bent around phenocrysts giving the rock a pronounced fluidal banding. Nearly all shards are rimmed by opaques. Approximately 5 percent of the tuff is made up of shattered, cracked

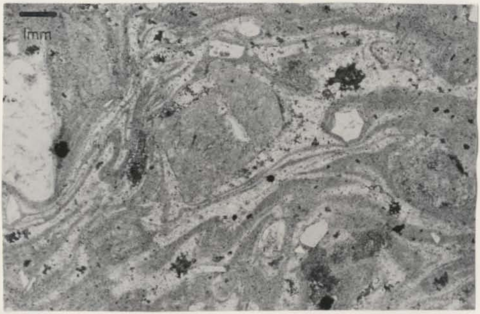

Figure 70. Photomicrograph of densely welded ash-flow tuff showing well preserved vitroclastic texture.

TABLE 16: Modal analyses of "younger ash-flow tuffs".

Sample No.	%plagioclase	%quartz	%K-spar	%pyroxene	amph. %biotite	%opaque	%groundmass
H-79-182	9	19	9	4	—	<1	60
H-79-143	14	5	4	--	11	<1	67
P-79-129	21	7	—	3	4	<1	67
H-79-136	4	4	5	--	<1	<<1	86
H-79-137	7	11	8	1	—	<<1	72
H-79-138	2	5	10	2	—	<1	80

and embayed bipyramidal euhedra of quartz, some of which reach 5 mm across. Tabular phenocrysts of orthoclase, measuring to 3 mm are cracked, corroded and make up about 10 percent by volume. Broken and twinned tabular plagioclase from minute specks to chips measuring 4 mm, constitute 5 percent of the bulk and contain tiny red euhedra of hematite. Relict pyroxenes (less than 2 mm) make up less than 1 percent of the rock. All are replaced by chlorite and opaque oxides.

In the middle part of the cooling unit quartz is slightly more abundant and orthoclase phenocryst fragments are larger (4 mm). The matrix is completely recrystallized to microfelsite dusted with hematite.

Altered mafic minerals increase in number upwards in the tuff and reach 4 percent in the stratigraphically highest thin section examined. The percentage of small crystal chips increases to about 30 percent of the bulk.

Interpretation

The "younger ash-flow tuffs" are all simple cooling units of medium thickness. Therefore, they are likely remnants of outflow facies tuff. The tuffs appear to fill topographic depressions, probably stream valleys, as evidenced by the intercalated sandstone and conglomerate. Most cooling units are mineralogically-zoned and therefore probably erupted from compositionally-zoned magma chambers but the chemical variations within single cooling units were not studied. The sources for the tuffs are unknown and probably lay outside the map area.

"KQP" Porphyry

This is a porphyritic intrusion comprising potassium feldspar, quartz, and plagioclase phenocrysts in a pinkish aphanitic matrix. It is a sill-like body that intrudes the base of the Moose Bay Tuff from

Black Bear Lake to Conjuror Bay. The sill is also present on islands in Conjuror Bay where it intrudes the "younger ash-flow tuffs." There, the body follows the topographic margin of Mule Bay cauldron. The porphyry itself is intruded by the tonalite-diorite suite and is therefore older.

On islands in Conjuror Bay the intrusion contains abundant xenoliths of Bloom Basalt. Most of the basalt blocks are intensely brecciated and altered.

Examination of thin sections of the porphyry show it to contain rounded and embayed quartz phenocrysts (5 mm), chloritized biotite (1 mm), euhedral to subhedral, sericitized plagioclase, and euhedral-subhedral microperthite in a granophyric groundmass of quartz and alkali feldspar. Both the plagioclase and mircoperthite tend to form glomeroporphyritic clots up to 6 mm in diameter.

Interpretation

The granophyric groundmass of the intrusion indicates that it was emplaced relatively near the surface. The intrusion follows the topographic margin of Mule Bay cauldron and might be considered a ring pluton genetically related to the Moose Bay Tuff. However, it is clearly younger than even the Clut cauldron and therefore not likely related to the older Mule Bay cauldron. This indicates that extreme caution must be exercised when interpreting ring dikes or plutons to be related to even a spatially related cauldron for here is a case where the only relation between the two appears to be that the cauldron provided a zone of weakness for a much younger intrusion.

Quartz Diorite

These intrusive bodies are ovoid to laccolith-shaped quartz diorites generally less than 4 km in diameter. They occur south of the Balachey Pluton (Map 1). If all members of the suite are the same age then their emplacement must be later than the younger ash-flow tuffs because one member of the suite intrudes the potassium feldspar-quartz-plagioclase porphyry (Map 1) which itself cuts the younger ash-flow tuffs. As the quartz diorites are intruded by the north-south porphyry dike swarm they must predate the late biotite granites and thus are not part of the hornblende tonalite suite (G4) of Hoffman and McGlynn (1977).

Plagioclase Porphyry

Intruding the diorite above the roof of the Rainy Lake Intrusive Complex is a pink to flesh coloured plagioclase porphyry that is exposed in cross section. It is roughly oval in shape with semi-concordant roof and floor. Contacts with all country rocks are razor sharp.

This unit was mapped by Badham (1972) as an extrusive but contact relations, such as local apophyses which cut and metamorphose the country rocks, clearly indicate its intrusive nature (Map 1). Furthermore, country rocks, including the diorites are often brecciated adjacent to the contacts.

The body is texturally homogeneous. It consists throughout of albitized plagioclase euhedra 1-3 mm in length and irregular mafic clots, now altered to assemblages of chlorite, epidote, sphene, opaques, and carbonate, sitting in a fine-grained mosaic of equigranular albite, orthoclase, and quartz.

Both the map pattern (Map 1) and evidence at individual outcrops indicate that the porphyry postdates the diorite bodies. Since, as argued earlier, the diorites postdate the Rainy Lake Intrusive Complex, then the porphyry must also postdate the emplacement of the Rainy Lake Extrusive Complex.

Grouard Dikes

North-south trending porphyritic dikes occur throughout the map area and are here termed the Grouard dikes after exposures at the north end of Grouard Lake. They postdate folding and cut all rock types except Cleaver Diabase and syenogranite plutons.

The dikes vary in width from 1 m to many tens of metres and are often continuous along strike for several kilometres. Variable amounts of plagioclase, hornblende, biotite, quartz, and potassium feldspar phenocrysts in a pink to brick-red aphanitic matrix characterize the dikes. Some contain all five phases while others contain only two or three. In some the margins are plagioclase-hornblende porphyritic while the more interior portions contain all five phases.

In some specimens euhedral bipyramids of quartz (5 mm) constitute 10-15 percent of the rock while in others they are rounded and embayed by resorption. Plagioclase (to 10 percent), often completely sericitized, forms subhedral to euhedral crystals up to 5 mm across. Microperthitic alkali feldspars (<2 cm) are subhedral-euhedral but are often broken. Prisms of hornblende (<2 mm) are occasionally fresh but more typically are altered to assemblages of sphene, chlorites, epidote, carbonate, and opaque oxides. Biotite, occurring as subhedral flakes up to 2 mm across, is partly or wholly altered to chlorite. In a few dikes, phenocrysts of magnetite occur as anhedral grains less than 1 mm

TABLE 17: Major and trace element analyses of diorites.

Sample No.	H-79-60	H-79-202	P-79-171
SiO_2	59.1	55.9	58.1
TiO_2	0.60	0.96	0.51
Al_2O_3	16.6	17.2	17.1
Fe_2O_3**	7.53	5.06	7.61
MnO	0.41	0.33	0.42
MgO	2.61	3.93	3.40
CaO	4.60	6.62	1.86
Na_2O	2.64	4.94	4.14
K_2O	2.53	2.49	2.99
P_2O_5	0.27	0.26	0.21
LOI	2.74	2.12	2.98
Total	99.63	99.81	99.32
Nb	4	8	5
Zr	110	139	136
Y	20	28	18
Sr	438	271	296
U	2	nd	3
Rb	93	97	95
Th	nd	7	4
Pb	14	173	7
Ga		24	20
Zn	251	402	375
Cu	12	48	9
Ni		3	4
Cr	nd	9	nd
V	98	155	104
La	20	32	30
Ce	45	27	62
Ba	1098	864	1247

**Total Fe as Fe_2O_3.

in diameter. The groundmass is typically cryptocrystalline felsite which sometimes displays a mottled texture.

Available chemical analyses (Table 18) indicate that the dikes contain between 65 and 70 percent SiO_2. With respect to other chemical components they appear little different from many other rocks of the belt.

North-South Trending Mafic Dikes

These fine-grained dikes occur mainly west of Smallwood Lake north and south of Rainy Lake. They trend nearly north-south and post-date the intrusion of the Grouard dikes. Their age relation relative to the Cleaver dikes is unknown but they are considerably more altered than those dikes and therefore probably older. While these dikes are mostly less than 3 or 4 metres across and not especially numerous they are mentioned here because one of them cuts mineralized veins at Norex mine, located between Smallwood and Rainy Lakes. This is an important relationship because this dike is not of the same age as diabase on Arden Peninsula and because the vein it cuts contains Ni-Co arsenides on both sides of the dike yet is silver-bearing on only one side.

Hooker Megacrystic Granite

Hornblende-biotite-alkali feldspar megacrystic syenogranite which postdates folding in the area, underlies nearly 200 km^2 in the northeastern corner of the White Eagle Falls 1:50,000 sheet. It is here named Hooker Megacrystic Granite after its exposures at Hooker Lake, which lies out of the map area to the north.

The contacts with wall rocks are always sharp. Adjacent to the contact there is commonly a border phase several metres wide consisting of patches of quartz-potassium feldspar porphyry, aplite,

TABLE 18: Major and trace element analyses, Grouard Dikes

Sample No.	P-79-140	P-79-23	H-79-197
SiO_2	65.6	68.5	70.8
TiO_2	0.53	0.32	0.22
Al_2O_3	14.6	14.4	12.5
Fe_2O_3**	3.53	2.79	3.54
MnO	0.07	0.05	0.08
MgO	1.85	0.98	0.41
CaO	3.07	1.56	1.15
Na_2O	3.55	3.63	3.16
K_2O	4.00	4.35	5.39
P_2O_5	0.04	0.09	0.12
LOI	2.47	2.69	1.71
Total	99.31	99.36	99.08
Nb	13	13	22
Zr	174	168	319
Y	28	22	49
Sr	301	97	102
U	7	9	8
Rb	163	159	179
Th	23	26	21
Pb	21	12	33
Ga			21
Zn	84	62	96
Cu	24	25	70
Ni	0	0	0
Cr	30	9	0
V	57	37	7
La	52	56	60
Ce	88	104	82
Ba	847	851	1237

**Total Fe as Fe_2O_3. Oxides in weight percent; trace elements in parts/million.

pegmatite, and graphic granite. Calder Quartz Monzonite appears little-altered at the contact but is intruded by aplite dikes. Other rock types, such as White Eagle Tuff and Animal Andesite are visibly altered within 3 or 4 metres of the contact and tend to weather a pinkish colour, probably due to albitization. The dip of the contact is variable. In places it dips gently away from the pluton at about 30° while in others it is nearly vertical. Locally the contact is horizontal and Hooker overlies Calder Quartz Monzonite.

The presence of potassium feldspar megacrysts up to 5 cm long is distinctive. They constitute from as little as 5, to as much as 40 percent of the rock. Quartz (15-20 percent) commonly occurs as irregular blobs and clots 8-10 mm across. Anhedral flakes of biotite also tend to form clots (<10 mm) and make up 8-16 percent of the bulk. Subhedral plagioclase to 10 mm is heavily seriticized and subhedral.

Locally near the margins of the intrusion prismatic green amphibole to 7 mm predominates over biotite. A pecular feature of the amphiboles is the occurrence of lenticular zones of quartz parallel to longitudinal cleavage traces. Chlorite and opaque oxides have a similar occurrence but do not occur together with the quartz. In places with abundant amphibole granophyric intergrowths of quartz and microcline make up to 5 percent of the rock. Locally the amphibole is intimately intergrown with the granophyre which occasionally has finely disseminated hematite along the boundaries between the feldspar and quartz.

Interpretation

The Hooker Megacrystic Granite, like other syenogranite plutons of the Great Bear Magmatic Zone (Hoffman and McGlynn, 1976) postdates folding in the area. As many of the folds elsewhere in the zone have steep, nearly vertical, limbs the crust was significantly shortened by this event. Consequently, it was also thickened. Such an event could well have thickened the crust enough so that its base was partially melted. This could have given rise to the Hooker megacrystic granite and the other G-3 plutons of the Great Bear Magmatic Zone. The possibility that the G-3 plutons were merely slow rising bodies related to the rest of the Great Bear Magmatic Zone is effectively ruled out by the magmatic gap of 10 to 20 million years (S. Bowring, personal communication, 1982) between most of the Great Bear magmatism and the emplacement of the G-3 plutons. Crustal thickening by folding is, at present, the only mechanism known which could have generated the G-3 plutons.

Other Plutons

Only brief mention will be made regarding other granitoid plutons of the area.

Richardson (G-3): Mainly coarse-grained biotite-hornblende monzogranite characterized by centimetre-size clots of quartz and locally by megacrysts of potassium feldspar.

Unnamed syenogranites (G-3): Typically coarse-grained biotite syenogranite with only minor hornblende.

Yen (G-2): This pluton is a composite body of medium-grained hornblende-biotite and biotite-hornblende granodiorite, quartz monzonite, and monzogranite. It generally contains 20-25 percent ferromagnesium minerals, often forming clots.

Tla (G-3): This intrusive is also composite. It comprises medium-grained hornblende-biotite monzogranite and quartz monzonite often with fine-grained patches containing potassium feldspar megacrysts. In general ferromagnesium minerals are much smaller than those in the Yen.

Transcurrent Faults

Numerous northeast-southwest trending transcurrent faults, typical of those found throughout the Great Bear Magmatic Zone and the rest of the Circum-Slave Province area, postdate all previously discussed rocks. The faults are nearly always vertical and are reasonably straight for long distances (Map 1). They are commonly linked to one another by east-west trending faults which have much smaller separations. It is the east-west faults that host the economic ore veins of the area.

The fault zones themselves are nearly always filled with quartz veins and stockwork, some of which are 50 m wide. Brecciation and annealing relationships of the quartz in the stockworks indicate that most faults had several periods of movement (see Furnival, 1935). Wall rocks adjacent to the fault zones are intensely altered to distances up to 150 metres away from the fault zones.

It may have been this hydrothermal alteration that played havoc with the Rb-Sr systematics of the area (Appendix 3) as much smaller veins and faults, possibly related to the transcurrent faults, are present in nearly every outcrop. As the transcurrent fault system occurs throughout Wopmay Orogen and Athapuscow Aulacogen it is interesting to speculate even further and suggest that such a process has operated over a much wider area because Rb-Sr systematics from rocks in both areas have been disturbed. Nearly all rocks analyzed from Wopmay Orogen and Athapuscow Aulacogen yield points which form reasonably good linear arrays whose regression lines have slopes about 100 my younger than U-Pb zircon ages (Baadsgaard and others, 1973; Goff and others, 1982; Easton, personal communication, 1982; Van Schmus and Bowring, 1980; personal communication) implying large-scale, low-grade alteration over huge areas.

Cleaver Diabase

An east-west swarm of diabase dikes which postdate transcurrent faulting was mapped by Hildebrand (1982) in the Echo Bay area (Map 3). Hoffman (1982) termed them Cleaver Diabase. Similar diabase dikes with similar trends also occur in the Camsell River area and are much more numerous there than in the Echo Bay belt. They are considered to also be of the same suite and so the name Cleaver Diabase is also used.

The dikes are variably altered; none are fresh. They have an ophitic to subophitic texture with 35 to 40 percent subhedral to anhedral augite, typically partially altered to mixtures of green amphibole, chlorites, opaque oxides, and plagioclase. Plagioclase phenocrysts are typically euhedral laths of labradorite which may make up as much as 50 percent of the bulk. The remainder of the rock is interstitial material comprising alteration products such as epidote, carbonate and sphene, and primary material (granophyre, magnetite). Many of the dikes contain euhedral cubes of pyrite.

Gunbarrel Gabbro

This intrusion is a large sheet-like body which slices through all rocks of the area including Cleaver Diabase. It is exposed from the mouth of the Camsell River to the north end of Yen Lake (Map 1). Badham (1972) mapped this unit as an esker, perhaps due to its sinuous appearance on air photographs, but the coarsely crystalline mosaic of pyroxene and plagioclase can hardly be mistaken for unconsolidated sediment in outcrop.

TABLE 19: Major and trace element analyses, Hooker Megacrystic Granite.

Sample No.	H-80-58	P-80-36	P-80-38	J-80-12	J-80-14
SiO_2	65.9	73.7	71.7	74.9	72.3
TiO_2	0.57	0.34	0.14	0.28	0.20
Al_2O_3	13.6	12.7	13.0	12.5	13.1
Fe_2O_3**	5.90	2.21	2.95	2.40	2.71
MnO	0.44	0.03	0.07	0.04	0.06
MgO	1.39	0.35	0.88	0.32	0.72
CaO	1.31	1.34	0.28	1.23	0.40
Na_2O	2.52	2.61	2.37	2.72	2.43
K_2O	5.10	5.63	6.08	4.86	5.45
P_2O_5	0.14	0.08	0.07	0.12	0.12
LOI	1.45	0.92	1.40	0.64	1.14
Total	98.32	99.61	98.94	100.01	98.63
Nb	27	22	18	29	30
Zr	340	211	236	203	278
Y	77	74	68	83	80
Sr	134	84	69	47	63
U	8	14	7	13	13
Rb	211	307	277	428	289
Th	30	43	51	75	45
Pb	64	41	21	43	22
Ga	19			19	18
Zn	311	43	53	30	50
Cu	5	11	14	0	0
Ni	2			0	0
Cr	0	0	0	0	0
V	40	11	18	6	13
La	82	123	153	86	130
Ce	142	208	254	147	186
Ba	1448	518	660	180	473

**Total Fe as Fe_2O_3. Oxides in weight percent; trace elements in parts/million.

Figure 71. Hooker Megacrystic Granite.

The gabbro is a coarsely crystalline rock with well-developed ophitic texture comprising 50-60 percent labradorite to andesine phenocrysts and 35-40 percent subhedral to anhedral augite. Anhedral grains of opaque iron-titanium oxides constitute another 3 to 5 percent of the rock. Interstitial material comprises feldspar, granophyre and opaques.

SUMMARY OF GEOLOGIC HISTORY

Mature, crossbedded quartz arenite, 30 metres thick, was deposited unconformably on the Hottah Terrane. As subsidence continued, finer-grained sediments accumulated below wave base and periodic eruptions of pyroclastic ejecta, from unknown sources, deposited lapilli tuff into the basin.

Later, perhaps during a period of extension, large volumes of pillow basalt, associated breccias and aquagene tuff were erupted and accumulated to thicknesses exceeding 2 kilometres. Subsidence kept pace with volcanism and in places patch reefs developed where piles of basalt built up close to sea level. These rocks were intruded by porphyritic sills and dikes of a siliceous nature, and still later by a swarm of gabbro and diabase sheets.

A period of uplift ensued and subaerial ash-flow eruptions of rhyolite led to collapse of Mule Bay cauldron, in which 2 km of tuff ponded (Figure 72a). The topographically low-standing core of the cauldron then became the locus for fluvial and lacustrine sedimentation as streams drained nearby highlands (72b). Silicic volcanism, perhaps erupted from the same magma body responsible for the earlier ash-flows, continued and rhyolite flows and ashstone are now found intercalated with the sedimentary rocks.

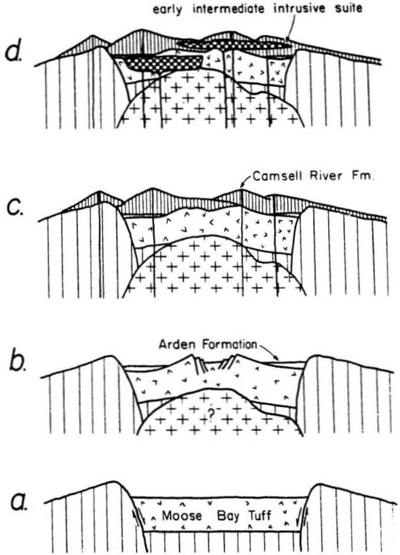

Figure 72. Cartoon illustrating evolution of the LaBine Group in the map area.

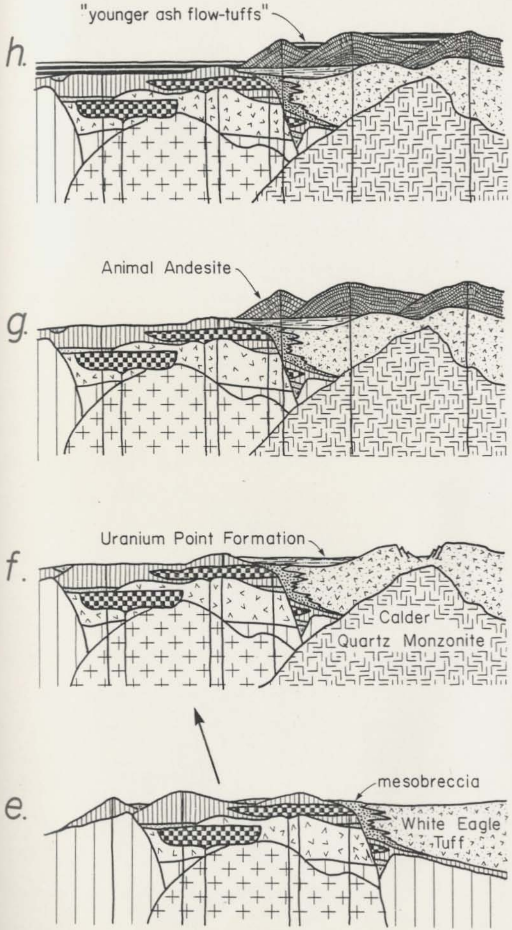
"younger ash flow-tuffs"
h.
Animal Andesite
g.
Uranium Point Formation
f.
Calder
Quartz Monzonite
mesobreccia
e.
White Eagle
Tuff

Shortly thereafter, at least one large stratovolcano of augite-plagioclase porphyritic andesite developed near the cauldron and large amounts of andesite spilled into the depression (72c). The large compositional gap between the ash-flow tuff and the andesite suggest that the two were not erupted from the same magma chamber. Instead, they are two magma batches.

Distinctive quartz monzonite-monzodiorite sheet-like plutons, similar to the magma bodies likely to have fed the andesitic eruptions, were emplaced at shallow levels into the andesite pile (Figure 72d). They intensely altered themselves and their wall rocks as they cooled, mainly by hydrothermal convection.

Younger ash-flow eruptions of crystal-rich dacite caused collapse of Clut cauldron, which was accompanied by landsliding and avalanching of the steep cauldron walls. This resulted in coarse breccias of andesite and intrusive debris which intertongue with the propylitized intracauldron facies tuff adjacent to the walls (Figure 72e).

Clut cauldron also became the site for fluvio-lacustrine sedimentation (Figure 72f) after ash-flow eruptions had ceased but periodic pyroclastic eruptions from unknown sources deposited material into the shallow lakes. Emplacement of a large quartz monzonite pluton into the central part of the cauldron probably caused resurgence of the central block (Figure 72f). During this uplift unconsolidated lacustrine sediments slumped away from the domed core toward the cauldron margins.

Volcanoes of augite and pargasite-bearing andesite developed after collapse (Figure 72g). The timing of this volcanism relative to resurgence of Clut cauldron is unknown. They could have been erupted from a deeper level of the same magma chamber as the White Eagle tuff or Calder quartz monzonite but this is not likely as they are richer in elements likely to be concentrated towards the roof of a magma chamber.

Shortly after andesitic eruptions ceased, compositionally varied ash-flows were erupted from unknown sources and filled topographic depressions (Figure 72h). Next, varied high-level intrusions, ranging from small ovoid bodies of diorite and plagioclase porphyry to pseudo-ring dikes were emplaced into the volcanic piles.

There was a pause in igneous activity and the entire belt was folded about northwest-southeast trending axes. This folding resulted in severe crustal shortening and probably thickened the crust so that its base was partially melted and as a consequence large bodies of granitic melt rose nearly to the surface. Just prior to their final emplacement, during a period of east-west extension swarms of siliceous porphyry dikes were intruded.

After solidification of the dikes and the granite plutons the area was subjected to east-west compressional stresses which resulted in brittle fracturing at high structural levels. The end result was the myriad of northeast-southwest trending transcurrent faults that cut the entire Great Bear Magmatic Zone. The fault zones acted as conduits for hydrothermal fluids, and rocks within and adjacent to the faults were intensely altered.

Much younger events include intrusion of east-west trending diabase dikes and large sheets of gabbro.

CHEMISTRY

Volcanic rock petrochemistry is highly complicated by post-eruptive processes which modify the original magmatic composition. These processes include devitrification, deuteric processes, vapour phase transport and crystallization, fumarolic alteration, and hydration through interaction with ground water (Smith, 1960; Keith and Muffler, 1978; Lipman, 1965). Contact metamorphism and hydrothermal systems, related to contemporaneous or later events, may further modify earlier alteration making it difficult to determine the original magmatic composition.

Nevertheless, the general agreement between the classification based on phenocryst proportions and the bulk rock chemistry suggests that in most rocks there have been only minor changes in SiO_2 contents during alteration. In general, the LaBine Group is of intermediate composition with most SiO_2 values clustering between 55 and 72 percent (Figure 73), a chemical characteristic of calc-alkaline volcanic rocks (Green, 1980). Alkali and alkaline-earth variations indicate that these elements were extremely mobile during alteration and cannot be used for classifications although the suite shows no Fe enrichment trend on an AMF diagram (Figure 74).

Titanium, while certainly mobile to some degree under appropriate conditions, may be less mobile than most other elements (Pearce and Cann, 1973). TiO_2 values for all rocks analyzed are less than 1.0 percent. Intermediate rocks with low TiO_2 (<1.75 percent) dominate Tertiary-Recent volcanic provinces classified as orogenic (i.e. volcanic arcs) by Ewart and LeMaitre (1980). Green (1980) believed that typical TiO_2 values for island arc and continental arc rock series are less than 1.2 percent.

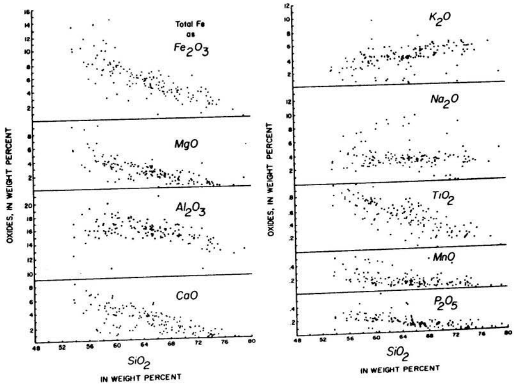

Figure 73. Variation diagrams for all analyzed rocks from LaBine Group and plutonic rocks of the entire study area except the Rainy Lake Intrusive Complex.

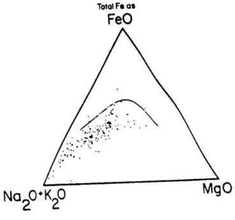

Figure 74. AFM diagram for all analyzed rocks from the study area except the Rainy Lake Intrusive Complex. Calc-alkaline-Tholeiitic dividing line from Irvine and Barangar (1971).

Furthermore, calc-alkaline extrusive rocks of continental arcs such as the Taupo Zone of New Zealand (Ewart and others, 1977; Cole, 1978, 1979), the Andes (for example: Kussmaul and others, 1977; Deruelle, 1978), Papua (MacKenzie, 1976) and the Pontid arc (Egin and others, 1979) nearly always have TiO_2 less than 1.0 percent.

Rare earth element (REE) analyses of rocks from the LaBine Group exhibit light REE enrichment patterns and the high overall abundances typical of high-K continental volcanic arcs such as the Chilean Andes (Thorpe and others, 1976, 1979), the Taupo Zone (Ewart and others, 1977; Cole, 1979), and Sardinia (Dupuy and others, 1979).

INTERPRETATION

Although alkali and alkaline earth metals were mobile during hydrothermal alteration, the original phenocryst mineralogy (quartz, potassium feldspar, biotite, hornblende, augite, and plagioclase) coupled with SiO_2, TiO_2, and REE values indicate that the LaBine volcanic field is a high-K, calc-alkaline belt of mainly intermediate composition rocks that fall within the broad class of orogenic volcanic rocks (Ewart and LeMaitre, 1980). In detail, they are chemically similar to continental arcs related to subduction such as the Andes. Furthermore, microprobe analyses show that calcic clinopyroxenes and amphiboles found in LaBine Group andesites are similar to those occurring in younger high-K, calc-alkaline andesites (Jakes and White, 1972; Ujike and Onuki, 1976; Ujike, 1977; Gill, 1981). Similarly, pyroxene clots and opacitic amphiboles found in Animal Andesite are also commonly observed in calc-alkaline andesites (see Garcia and Jacobson, 1979).

In overall stratigraphy, mode of eruption, and mineralogy the LaBine Group resembles Cenozoic volcanic fields of the western United

States such as the San Juan volcanic field (Steven and Lipman, 1976), the Datil-Mogollon volcanic field (Elston and others, 1976), and the Elkhorn Mountain volcanic field (Klepper and others, 1971). Cogent arguments have been made by several authors that the calc-alkaline volcanic rocks in those fields were related to oblique, low-angle subduction of the Farallon plate beneath the North American continent during the Eocene-Oligocene (Lipman and others, 1971, 1972; Elston, 1976; Coney and Reynolds, 1977; Lipman, 1980).

Although genetic details of volcanic arc magmatism are still controversial, there seems little doubt that arc magmatism is a multistage product of lithospheric subduction (Marsh, 1979). I see no compelling reason to invoke an ad hoc model to explain the origin of LaBine Group volcanic rocks as they have readily identifiable Cenozoic analogs. Therefore, I conclude that the LaBine Group represents a remnant of an early Proterozoic continental volcanic arc and that subduction, which may be the principal driving mechanism of plate tectonics (Forsyth and Uyeda, 1975; Richter, 1977; Chapple and Tullis, 1977), was occurring at least by about 1.9 Ga ago.

TECTONIC MODEL

The tectonic model presented here is similar to that presented by Hoffman (1980a) but some refinements and modifications have been made in light of new geochronological and field data. The model is shown schematically in Figure 75.

In this model the Hottah Terrane is considered to be allochthonous with respect to the Slave Craton and to be the remnant of a microcontinent or arc which collided with the Slave Craton over a westward-dipping Benioff zone (Figure 75a). The collision resulted in

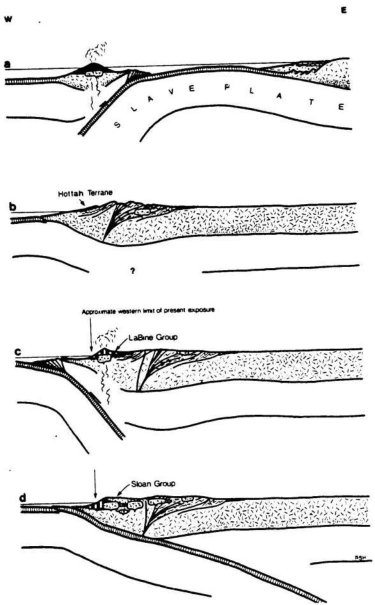

Figure 75. Proposed tectonic model for the origin of the LaBine Group and related rocks. See text for explanation.

accretion and deformation of the microcontinent and deformation of the western edge of the Slave Craton with its westward-facing passive margin sequence (Figure 75b).

Continent-microcontinent or continent-arc collisions are by no means rare in the geologic record. Excellent examples of more recent continent-small plate collisions are present along the northwestern edge of the Australian continent where the edge of the Australian-New Guinea shelf is presently colliding with the Banda arc (Von der Borch, 1979). During the Miocene, an early Tertiary arc was accreted to the continent at New Guinea (Hamilton, 1979). Other examples of continent-microcontinent collision occur in the Eastern European Alpine System (Burchfiel, 1980) where several collisions are believed to have occurred from mid-Cretaceous to the Recent. In the northern Canadian Cordillera Tempelman-Kluit (1979) interpreted geologic relations in terms of a Late Jurassic-early Cretaceous continent-microcontinent collision.

In Wopmay Orogen the age of the collision is interpreted to have occurred between about 1.92 and 1.89 Ga. Metamorphic isograds, which postdate the major pulse of thrusting in the deformed passive margin sequence (Hoffman and others, 1980), are related to mesozonal S-type plutons (St-Onge and Carmichael, 1979) whose mean age is 1.89 ± 0.1 Ga[1] (Van Schmus and Bowring, 1980). Deformation of the Hottah Terrane must postdate a deformed pluton found at Hottah Lake dated at 1.92 ± 0.01 Ga (Van Schmus and Bowring, 1980). If deformation in both belts was related to the same event, as postulated here, then the age of deformation is bracketed between 1.92 ± 0.01 Ga and 1.89 ± 0.01 Ga.

---

[1]Age determinations by Van Schmus and Bowring are U-Pb zircon ages.

The LaBine Group, which rests unconformably on the Hottah Terrane and lacks its penetrative fabric, must be younger than the microcontinent-continent collision. If the LaBine Group is a volcanic arc related to subduction, then it must have developed over an eastwardly-dipping subduction zone, as the ocean east of the microcontinent had already closed. This interpretation requires that following collision subduction changed from westward-dipping on the east side of the microcontinent to eastward-dipping on the west side (Figure 75c).

Many examples of continent-arc or microcontinent collisions appear to have involved a reversal of subduction direction following collision. Hamilton (1979) presented evidence for incipient subduction reversal north of the island of Alor, as a result of collision between the Banda Arc and the Australian Continent. He also suggested that reversal of subduction direction occurred after arc-continent collision at New Guinea. The Miocene collision of the Apulian fragment with Euro-Russian continental crust was along a southward-dipping subduction zone while present day subduction under the Hellenic Arc is northward (Burchfiel, 1980). In the northern Canadian Cordilleran example of continent-microcontinent collision subduction is also believed to have stepped outward of the accreted terrane and reversed direction (Tempelman-Kluit, 1979).

Independent support for an eastward-dipping subduction zone following collision in Wopmay orogen occurs in the East Arm Thrust Belt, located 300 km southeast of Port Radium (Figure 1). There a group of calc-alkaline laccoliths, strikingly similar in composition, alteration and metalliferous deposits to the Mystery Island Intrusive Suite, are distributed axially over the length of the aulacogen, which trends normal to the Wopmay continental margin. The laccoliths exhibit compositional changes ranging from diorite in the west to quartz monzonite in the east (Hoffman and others, 1977). Badham (1978) considered this to be an oversimplification but stated that both potassium feldspar and biotite content in the laccoliths increased eastward.

The compositional trend in these laccoliths is similar to those of magmatic arcs (Moore, 1959, 1961; Ninkovitch and Hays, 1972; Kistler, 1974; Dickinson, 1975)--a similarity first pointed out by Hoffman and others (1977) who suggested that the intrusions might be a result of subduction.

The laccoliths postdate westerly-derived orogenic molasse presumably produced during collision and have an apparent age of 1.86 Ga ± .02 Ga (Van Schmus and Bowring, personal communication)--the same age or slightly younger than the LaBine Group. Thus, they support the concept of an eastward-dipping subduction zone that postdated the microcontinent-continent collision.

At the present time magmatism occurs above Benioff zones where they are about 100-200 km below the surface (see for example: Isacks and Barazangi, 1977). If this was also the case during the early Proterozoic then the Benioff zone postulated to have generated the laccoliths must have been fairly shallow, for they occur up to 250 km from the trench believed to have existed west of the accreted microcontinent.

A shallow Benioff zone might explain the conspicuous absence of similar magmatism in the Slave craton which should have resulted if a lithospheric slab was being subducted in an eastward direction. Perhaps the dip of the slab was so shallow that there was no asthenospheric wedge above the Benioff zone except under the aulacogen, where it presumably had upwelled during the initial rifting which created the Wopmay continental margin. The possibility that the presence of asthenospheric mantle above a Benioff zone is necessary for arc magmatism to occur has been proposed by Lipman (1980) and Dewey (1980). They both believed that extincti-n of magmatic activity in the Peruvian Andes is related to extreme flattening of the Benioff zone such that there is no asthenospheric mantle wedge present above it.

If this hypothesis is correct then why was there magmatism of the LaBine Group? I suggest that it may have been for one of three reasons: (1) possibly the subducting lithospheric slab was segmented, in much the same manner as modern slabs (Carr and others, 1979; Isacks and Barazangi, 1977) so that the segment dipping under the aulacogen was dipping at a shallower angle than the segment descending beneath the LaBine region, or; (2) if LaBine volcanism is slightly older than the laccoliths in the aulacogen, the dip of the downgoing slab could have decreased with time or; (3) the presence of thin lithosphere in the suture zone, which the LaBine Group likely buries.

ORIGIN OF LABINE GROUP MAGMATISM

The mineralogy, styles of volcanism, and petrochemistry of the LaBine Group are so similar to modern and Tertiary orogenic rocks that they are likely to have originated in a similar manner. As outlined by Green (1980) there are four basic models for the generation of orogenic magmas.

(1) Deep fractionation of low SiO_2 amphibole from mantle derived mafic magma (Green and Ringwood, 1968; Cawthorn and O'Hara, 1973; Hollaway and Burnham, 1972; Allen and Boettcher, 1978).

(2) Melting of mantle peridotite by infusion of slab-derived water at depths of 60-100 km. Melts produced in this fashion then reach the composition of basaltic andesite by olivine fractionation (Nicholls and Ringwood, 1973).

(3) Partial melting of subducted oceanic crust at depths of 100-200 km to produce (a) basaltic andesite (Greenwood and Ringwood, 1968; Marsh and Carmichael, 1974; Marsh, 1979a, b), or (b) silica enriched magmas which migrate upwards and melt mantle peridotite (Ringwood, 1974, 1975; Nicholls, 1974).

(4) Melting of continental crust by influx of H_2O or by under-plating with mafic magmas (Pichler and Zeil, 1972).

Furthermore, during their ascent through the crust, magmas generated by any of the above mechanisms can be further modified by fractionation (Carr and others, 1981), mixing (Eichelberger, 1975; Anderson, 1976) or assimilation (Myers and Marsh, 1981).

In models (1) and (2), water, presumably derived from the subducted oceanic slab, rises into the mantle where it lowers the solidus of peridotite enough for partial melting to ensue. The major objection to this idea is that high contents of H_2O (10-20 percent) are necessary to get andesitic liquids from mantle peridotite (Wyllie and others, 1976) and the dominance of plagioclase as a liquidus phase in andesites of the LaBine Group suggests that they had low water contents (Ewart, 1976; Marsh, 1976; Gill, 1981; Green, 1972). Low water contents have been reported for many orogenic andesites (Eggler, 1972; Eggler and Burnham, 1973; Garcia and Jacobson, 1979; Sekine and others, 1979; Marsh, 1976). Furthermore, based on experimental work by Shaw (1974) there is some doubt whether water could diffuse quickly enough to generate arc magmas in the mantle wedge within the necessary time frame

(Marsh, 1976, 1979).

Even if andesites could be primary peridotite melts, possibility (1) is unlikely to have been responsible for generating LaBine Group andesites because REE data from the LaBine Group is incompatible with amphibole fractionation. Partition coefficients for HREE are 0.3-0.4 (Schnetzler and Philipots, 1970) and therefore amphibole fractionation would increase HREE abundance in the remaining melt. One characteristic of LaBine Group andesites is their consistent contents of HREE at about ten times chrondrite (Figure 7 7). Rocks of the LaBine Group do not show the concave upward pattern characteristic of amphibole fractionation. Likewise, the moderate contents (10-50 ppm) of nickel in LaBine Group rocks rules out model 2 because fractionation of olivine will severely deplete the remaining liquid in nickel (Duke, 1976).

Model 4 could yield many of the magmas found in continental volcanic arcs, such as the LaBine Group, but the occurrence of arcs on oceanic crust (i.e., Aleutians, Marianas, etc.) indicates that magmas derived from continental crust are not the primary magmas of arc volcanism. Also, the temperatures necessary to derive andesitic melts with about 2 percent water from the lower crust (30-50 km depth) are on the order of 1100°C (Wyllie and others, 1976). Thus in order to generate low H_2O andesitic melts from the lower crust there must be addition of magma from below or else the crust must be substantially thickened by shortening.

Yet there can be little doubt that batholiths are generated in continental crust, for in volcanic arcs built on oceanic crust there are small intrusions of tonalite, trondhjemite, and plagiogranite but no batholiths comparable to those of western North and South America

(Waters, 1948; Bateman, 1981). In this regard the Kurile-Kamchatka and Aleutian-Alaskan Peninsula arcs are particularly instructive because both pass longitudinally from oceanic to continental crust. Where developed on oceanic crust they are very narrow (<10 km) and comprise mostly stratovolcanoes of basaltic andesite with only subordinate volumes of more siliceous rocks. Yet as soon as continental crust is encountered the arcs widen to about 100 km, volcanism becomes much richer in silica and incompatible elements, voluminous pyroclastic materials are erupted in the form of ash-flows, and large composite batholiths are emplaced into the volcanic suprastructure. These are fundamental differences which clearly indicate that continental crust is involved in the generation of batholiths and their related eruptive products. A similar conclusion is reached from consideration of isotopic data from continental arcs (Zartman, 1974; Carter and others, 1978; Tilton and Barreiro, 1980; DePaolo, 1981b; James, 1981), as well as experimental phase petrology (Wyllie and others, 1976; Wyllie, 1977). Furthermore, REE data from the LaBine Group suggests that the magmas were never in equilibrium with more than a percent or two garnet (Figure 76). As garnet is almost certainly present in quartz eclogite (Green and Ringwood, 1968; Stern and Wyllie, 1978; Sekine and others, 1981), rocks of the LaBine Group were not likely to have been derived directly from the subducted slab.

Thus, somewhat of a paradox emerges: magmas of the continental crust are not the primary magmas of arcs yet continental arcs are generated in the crust. The paradox can be easily resolved if slab-generated melts rise into or beneath continental crust and cause widespread partial melting of crustal material. This mechanism is similar to that recently proposed by Hildreth (1981), McCourt (1980) and DePaolo (1981) and

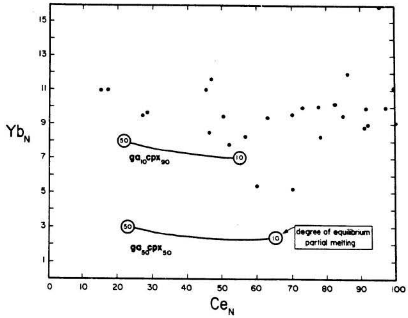

Figure 76. Chondrite normalized Ce versus Yb plot for analyzed samples from the LaBine Group. Partial melting models of mixtures of garnet and clinopyroxene are from Thorpe and others (1979).

earlier by Pichler and Zeil (1972), Ewart and othera (1977).

If rocks of the LaBine Group were generated in the crust then it is fundamental to the understanding of their petrogenesis whether the ash-flow tuffs, plutons, and andesites are related to one another by crystal fractionation, variable degrees of partial melting in the source region, or different degrees of mixing and/or assimilation. All analyzed rocks of the LaBine Group, as well as younger granitoid rocks, form smooth variation trends of the major elements which might suggest that they are genetically related. However, field and chronological arguments suggest that it is highly unlikely that the rock suites are related to one another by simple crystal fractionation. For example, there is at least a 15 million year time gap between LaBine Group volcanism and the emplacement of the younger syenogranite plutons (Bowring, personal communication, 1982). Furthermore, the similar abundances and fractionation trends for the REE indicate that the ash-flow tuffs of the LaBine Group were not derived from andesitic melts similar to those erupted as lavas occurring in the Camsell River, Animal, and Echo Bay andesites by any type of crystal fractionation (Figure 77). This does not mean that crystal fractionation was not an important process, for the compositional zoning found in several major ash-flow tuff sheets suggests that within individual magma chambers it may have occurred, but merely that it is not possible to derive all ash-flow tuffs of the belt from one magma type by crystal fractionation.

Assimilation of upper crustal rocks provides a simple mechanism for enriching magmas in incompatible elements such as K, Rb, U, and Th. The role of this mechanism is difficult to evaluate for the following reasons: (1) little is known of the chemical and isotopic characteristics of the basement to the group; (2) rubidium-strontium isotopic

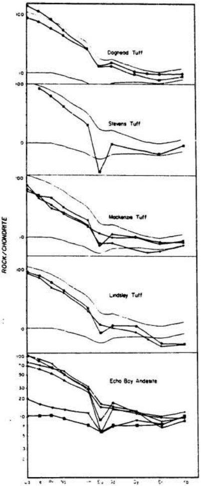

Figure 77. REE analyses normalized to chondrite for some stratigraphic units of the LaBine Group in their relative stratigraphic positions. Lines on plots of ash-flow tuffs indicate field of Echo Bay Andesite.

systematics of rocks of the group have been severely disturbed; and (3) assimilation can produce trends parallel to differentiation trends. However, Animal Andesite is the only rock type of the LaBine Group for which evidence of high-level contamination is found.

Therefore, I conclude that most rocks of the LaBine Group and associated plutons were probably generated by partial fusion of lower crustal material and possibly mixing of those melts with slab-derived basaltic andesite.

While it appears likely that continental crust is involved in the generation of batholiths in general, and specifically the LaBine Group and associated plutons, there are major uncertainties which preclude accurate modeling of the melting and/or mixing processes that take place during their creation. For example, we know from the work of many (Moorbath, 1975; Pride and Muecke, 1980, 1981; Green and others, 1972; Bridgewater and others, 1978; Weaver and others, 1978; Sighinolfi, 1971; O'Nions and Pankhurst, 1978) that old lower continental crust is depleted in U, K, Rb, and Th, some of the elements in which continental arc volcanism is typically enriched, but we know virtually nothing about the composition of juvenile lower continental crust. Furthermore, even if the composition and nature of the lower crust were known, partition coefficients are not known with enough accuracy to quantitatively evaluate partial melting and mixing models. Among the unknowns, most of which are known to affect partitioning of elements, are the effects of changing mineral composition, varying bulk composition (see Hildreth, 1981), effects of oxygen fugacity, pressure and temperature changes, volatile complexing, presence or absence of trace minerals, phase petrology effects, and zone-refining effects on wall rocks (Shaw, 1977; DePaolo, 1981a).

Overall, the entire body of geological and geochemical evidence clearly suggests that the Great Bear Magmatic Zone is a continental arc. This brief section will attempt to demonstrate, by ruling out other possibilities, that a magmatic arc is the most reasonable interpretation of the available data. Other possible tectonic environments for volcanic belts fall into 2 basic classes: (1) rift-type (eg. Afar region of Ethiopia or Basin and Range region of the southwestern U.S.) or (2) collisional (i.e. Tibetan Plateau of China).

(1) A rift-type environment is unsatisfactory because rift volcanism is typically bimodal (basalt-high silica rhyolite) while the Great Bear Magmatic Zone is clearly compositionally continuous from low silica andesite to rhyolite with intermediate compositions predominating (for a complete and illuminating discussion of rift-type volcanism see Easton, 1982).

(2) Continental collision might be able to generate rocks with similar compositions to those of the Great Bear Magmatic Zone, by crustal fusion related to collisional thickening of the crust. However, such belts (i.e. Tibetan Plateau) are topographically high-standing features and therefore it is unlikely that the huge volumes of high-level plutonic and volcanic rocks characteristic of the Great Bear Magmatic Zone would be preserved in the geologic record if they were generated by continental collision.

DISCUSSION

The preservation of stratovolcanoes and other high-level volcanic rocks in the LaBine Group, and in the Great Bear Magmatic Zone as a whole, suggest that the region was subsiding during volcanism for otherwise the normally high-standing volcanoes would have been quickly eroded. The hypothesis that the Great Bear Volcano-Plutonic Belt was a region of subsidence during volcanism was first put forth by Hoffman and McGlynn (1977) who argued that the belt subsided in response to bending of a strike-slip fault.

Volcanic arcs often contain basins of various kinds. For example, grabens presently being filled with volcanics and related sediments are well-developed in the Cascades (Fyfe and McBirney, 1975), Nicaragua (McBirney, 1969), Ecuador (Williams and McBirney, 1979), and New Zealand (Ewart and others, 1977; Cole, 1979; Reyners, 1980). The Central American arc contains other types of basins besides grabens. In Honduras, "intermontane tectonic troughs" developed during and after eruption of andesitic to basaltic lavas and breccias of the early Tertiary Matagalpa Formation, and many Miocene ash-flow sheets filled those, as well as other, broad, shallow basins (Williams and McBirney, 1969). Williams and McBirney (1969) also described a series of north-south trending, <u>en echelon</u> basins such as the Sula basin, and the huge Comayagua Valley of Honduras. Furthermore, many individual Central American volcanoes, such as those found in Gautemala (Williams and others, 1964), are located within sags or depressions.

However, the volcanism and structure of the entire Great Bear Magmatic Belt displays remarkable similarities to another type of depression found in several continental volcanic arcs. This class of depressions is much larger than the average wrench basin and is exemplified by the Eocene-Miocene Longitudinal Depression of Chile (Zeil, 1980; Levi and Aguirre, 1981) and the coastal lowlands of eastern Hokkaido, Japan (Oide, 1968). These depressions, which lie at elevations close to sea level, are about 100 km across, several hundreds of kilometres long, and appear to serve as loci for voluminous pyroclastic eruptions and cauldrons.

These depressions are not grabens in the classical sense, for while there is often evidence for block faulting, there is little, if any, for the listric normal faulting and concomitant rotation of crustal blocks that seem to characterize continental rifts (i.e., western Basin and Range Province, Wright and Troxel, 1973; Anderson, 1971; Afar, Morton and Black, 1975). Instead their regional structure is that of a huge syncline where sections of volcanic and sedimentary rocks tens of thousands of metres thick are exposed. In the Longitudinal Depression of Chile, these sections comprise series of overlapping lenses (Levi and Aguirre, 1981).

By comparison, the Great Bear Magmatic Zone is startling in its similarities. For example, the overall pre-folding structure is crudely synclinal; tens of thousands of metres of section occur in series of overlapping lenses (Hoffman and McGlynn, 1976); and cataclysmic eruptions of ash-flow tuff dominated the volcanism.

Another example of this class of depressions may be the "graben-synclines" of Kamchatka, in which cauldrons and ash-flow tuffs are concentrated (Erlich, 1968). Yet another may be the Nicaraguan Depression (Weyl, 1980), which also contains numerous cauldrons (Carr and others, 1981).

If these basins do indeed form a distinct class of basins formed in continental arcs, and they did not originate by extension, to what do they owe their origin? I suggest that the mechanism may be crustal sagging, or downwarping, due mostly to loss of material out of the immediate vicinity by airfall associated with the voluminous ash-flow tuff eruptions.

Consider that the volume of ash-flow tuff present in the synclines is on the order of tens of thousands, perhaps even hundreds of thousands, of cubic kilometres, for the average centre may erupt somewhere between 50 and 500 km^3 of material and each basin contains many such centres. Consider also that during ash-flow eruptions as much as half the erupted volume occurs as fine vitric ash which rises to great heights as a turbulent cloud and ultimately is widely dispersed by high-level wind (Sparks and Walker, 1977; Lipman, 1975; Flood and others, 1980; Walker, 1972; Fisher, 1966b; Izett, 1981; Walter, 1981). Therefore depending on the relative volume of material added to the crust from below, there could be a net loss of crustal material from the area of the surface volcanism, itself leading to subsidence.

The crust may also sink if its overall density is increased either by adding denser material, or by removing more siliceous material. If one accepts earlier arguments that it is mafic magma that migrates upwards and fuses continental crust then it is necessary to know whether or not the mafic magma can generate an equivalent volume of more siliceous magma. Calculations by Marsh (unpublished manuscript, 1981), suggest that under most conditions basalt emplaced into the lower crust does contain enough energy to generate an equivalent volume of siliceous magma.

If the volumes of material added to the crust were much larger than those created in the crust by the infusion then the crust would be thickened and thus tend to rise isostatically because basalt is less dense than mantle periodotite. The fact that the synclinal basins under consideration here are topographically low-standing features located close to sea-level, and remain so for many millions of years afterwards indicates that the crust was not thickened by underplating. Thus, in order for the area to remain at more or less the same elevation with respect to sea level the following equality must apply:

$$(\text{density})_{\text{bas and}}(V)_{\text{bas and}} = (\text{density})_{\text{vit ash}}(V)_{\text{vit ash}}$$

where $V_{\text{bas and}}$ and $V_{\text{vit ash}}$ equal the volume of basaltic andesite added to the crust and the volume of vitric ash erupted out of the immediate area, respectively. Approximate values for the density of basaltic andesite are about 2.5 g/cm^3 in the temperature range of 1200-1400°C while those for rhyolitic melts at 800°C are about 2.3 g/cm^3 (Murase and McBirney, 1973). The density difference between the two is only about 8 percent and therefore the two volumes must be approximately equal.

The lower crust will, in all likelihood, become denser as the basaltic andesite crystallizes to mafic granulite--a rock denser than partial melts generated by the influx of basaltic andesite. However, the upper and middle crust may become less dense as a result of the migration and crystallization of less dense magmas generated in the deep crust. Without knowing the composition of the crustal column it is impossible to quantitatively evaluate these effects. Nevertheless, the mass of material added to the crust must still approximate the mass of material lost if the region is to remain in isostatic equilibrium.

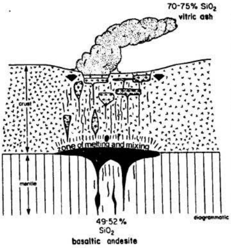

Figure 78. Cartoon illustrating a model for the origin of synclinal basins in continental volcanic arcs. Note that material is constantly being removed from the lower crust and brought to the surface. Because new, slab-derived basaltic andesite, roughly equivalent to the mass of vitric ash leaving the region, is added to the crust, the area is one of subsidence, yet the entire crustal column is able to maintain crude isostatic equilibrium. This process tends to reorganize the continental crust.

By looking at the volumes of magma erupted and intruded in modern oceanic island arcs it is possible to approximate the amount of magma arriving at the base of the crust in continental arcs. Estimates for this volume range between 1 and 10 km^3 per million years per km of arc (Marsh, 1979).

The volume of magma erupted in a typical continental arc has to be approximated. We are only interested in the volume of pyroclastic material erupted because lava flows and intrusions do not generate vitric ash. Smith (1979) has shown that there is a crude linear relationship between ash-flow volume and caldera area. For example, a volume of erupted material equal to 500 km^3 will have originated from a caldera nearly 30 km in diameter.

Because there does not appear to be a characteristic spacing of cauldrons in continental arcs it is necessary to assume a spacing for the purposes of calculation. For the sake of simplicity, calderas with diameters of 30 km are spaced with their centres 30 km apart. This is thought to be a reasonable assumption considering that some areas will have no cauldrons while in others cauldrons will overlap.

The frequency of cauldron formation is assumed to be 1 per million years based on their frequency of occurrence in the Datil-Mogollon volcanic field of New Mexico (Bowring, personal communication, 1982). If the above approximations are correct then about 17 km^3 of pyroclastic material are erupted per km every million years of which about half will be erupted as fine vitric ash and be removed from the area. Thus the estimate for the volume of vitric ash erupted is about 8.5 $km^3\ my^{-1}\ km^{-1}$, a volume comparable to those estimated for eruption and intrusion in island arcs.

This can be further tested, without the assumptions of caldera diameter and spacing used above, by examination of the pyroclastic eruption rates in well-mapped volcanic fields such as the San Juan volcanic field, southwestern Colorado. There Steven and Lipman (1976) estimate that about 9000 km^3 of pyroclastic material was erupted between 30 my and 22 my ago. That is equivalent to a rate of about 1100 km^3 per million years. As the San Juan volcanic field is approximately 100 km by 100 km this equals 11 km^3 per km of length. Therefore 5.5 km^3 of vitric ash were erupted out of the region for every km per million years. This approximation is also well within the estimated range of eruption and intrusion in island arcs developed on oceanic crust.

Francis and Rundle (1976) estimated the volume of ash-flow tuff present in a 115 km long section of the central Andes to be 1.5×10^3 km^3 and arrived at a rate of production per 1 km length of 1.3 cubic kilometres per million years. Although they were aware that ash-flows may lose 50 percent of their material by high-level atmospheric transport, their calculations were based only on the volume of tuff preserved. Thus, the rate at which vitric ash was erupted and removed from the area was probably also about 1.3 km^3 per million years per kilometre of length--again a volume of similar magnitude to those suggested for island arc magmatism.

All of the above estimates are consistent and of the same magnitude as estimates for intrusion and extrusion rates in arcs built on oceanic crust. This suggests that the model presented here for the origin of the synclinal basins and the volcanics which fill them is plausible.

The above calculations can also be used to place constraints on the origin of magmatism in continental volcanic arcs. For example, since the volume of magma erupted and intruded in oceanic arcs is roughly equal to, or less than, the volume of magma erupted or intruded in continental arcs it is not possible for continental arc magmatism to be derived from the mafic magmas by any type of differentiation for perhaps 10 volumes of mafic magma are needed to generate 2 volumes of granodiorite. This argument and the consistent lack of batholiths where there is no continental crust virtually demand that they be the product of continental crust.

Yet ever since it was recognized that parts of the continental crust are enriched in radiogenic ^{87}Sr relative to the upper mantle (Faure and Hurley, 1963) some geologists have argued that batholiths of continental arcs with low initial $^{87}Sr/^{86}Sr$ were mantle derived. They dc this even though low initial Sr ratios do not by themselves indicate a direct mantle origin. For example, it is widely known, but perhaps not widely enough, that there are several ways other than directly from the mantle from which to derive rocks with low initial Sr ratios:

1. juvenile continental crust ultimately derived from the mantle;
2. rocks with low Rb-Sr ratios such as depleted granulites (Tarney and Windley, 1977);
3. mixtures of crustal and mantle material;
4. lower continental crust that has isotopically re-equilibrated, perhaps with the aid of a fluid phase, with the large mantle reservoir (Armstrong, 1968; Collerson and Fryer, 1978; Bell, 1981).

Therefore, in light of the above arguments, I find it difficult to accept recent claims, based mainly on strontium isotopic data, that batholiths of continental arcs and their consanguinous volcanic rocks are generated directly in the mantle (Brown and Hennessy, 1978; Atherton and others, 1979; Thorpe and others, 1979; Cobbing and Dennis, 1982). In support of this conclusion, the Holocene Edgecumbe volcanic field, S.E. Alaska displays an excellent example of hybrid melts generated by the influx of mantle-derived basalt into sialic crust; partial melting of that crust, and subsequently mixing to produce rhyodacite, andesite, and dacite--all with initial $^{87}Sr/^{86}Sr$ ratios less than .7048 (Myers and Marsh, 1981).

By using Sm-Nd isotopes in conjunction with Rb-Sr isotopes one can apparently rule out the possibility that batholiths of continental arcs are derived from old continental crust with low Rb-Sr ratios (see DePaolo, 1981) but they do not rule out possibilities (1), (3), and (4) as sources. Even the much-heralded Lu-Hf isotopic system apparently cannot rule out possibilities (1) and (3) if the juvenile crust is less than 150 my old (Patchett and others, 1981).

CONCLUSIONS

In conclusion, work to date in the western part of the Great Bear Magmatic Belt suggests the following:

(1) Sheet-like quartz monzonite and monzodiorite plutons with wide alteration haloes are intimately associated with andesitic stratovolcanoes while more siliceous dome-shaped quartz monzonite and granodiorite plutons are associated with voluminous ash-flow tuff eruptions and cauldrons. Ring complexes were not seen although cauldrons are common.

(2) I-type batholiths and associated calc-alkaline to shoshonitic volcanic rocks are poorly understood, multistage products of subduction-related slab-melting and subsequent partial fusion of lower continental crust.

(3) Subduction, which is the main driving force for plate tectonics, has been active since at least the early Proterozoic.

(4) The LaBine Group developed over an east-dipping subduction zone which developed after accretion of the Hottah Terrane to the west side of the Slave Plate.

REFERENCES CITED

Allen, J.C. and Boettcher, A.L.
1978: Amphiboles in andesite and basalt: II, Stability as a function of P-T-fH_2-fO_2; American Mineralogist, v. 63, p. 1074-1087.

Anderson, R.E.
1971: Thin skin distension in Tertiary rocks of southeastern Nevada; Geological Society of America Bulletin, v. 82, p. 43-58.

Anderson, A.T.
1976: Magma mixing: Petrological process and volcanological tool; Journal of Volcanology and Geothermal Research, v. 1, p. 3-33.

Armstrong, R.L.
1968: A model for the evolution of strontium and lead isotopes in a dynamic earth; Reviews of Geophysics, v. 6, p. 175-199.

Atherton, M.P., McCourt, W.J., Sanderson, L.M. and Taylor, W.P.
1979: The geochemical character of the segmented Peruvian Coastal Batholiths and associated volcanics; in The Origin of Coastal Batholiths: Geochemical Evidence, Atherton, M.P. and Tarney, J., eds., Shiva Publishing Ltd., Orpington, p. 45-64.

Baadsgaard, H., Morton, R.D. and Olade, M.A.D.
1973: Rb-Sr isotopic age for the Precambrian lavas of the Seton Formation, East Arm of Great Slave Lake, Northwest Territories; Canadian Journal of Earth Sciences, v. 10, p. 1579-1582.

Badham, J.P.N.
1972: The Camsell River-Conjuror Bay area, Great Bear Lake, N.W.T.; Canadian Journal of Earth Sciences, v. 9, p. 1460-1468.

1973a: Calcalkaline volcanism and plutonism from the Great Bear Batholith, N.W.T.; Canadian Journal of Earth Sciences, v. 10, p. 1319-1328.

1973b: Volcanogenesis, orogenesis and metallogenesis, Camsell River, N.W.T.; unpublished Ph.D. thesis, University of Alberta, Edmonton, 334 p.

1975: Mineralogy, paragenesis and origin of the Ag-Ni, Co arsenide mineralization, Camsell River, N.W.T., Canada; Mineralium Deposita, v. 10, p. 153-175.

1978: Magnetite-apatite-amphibole-uranium and silver-arsenide mineralization in lower Proterozoic igneous rocks, East Arm, Great Slave Lake, Canada; Economic Geology, v. 73, p. 1474-1491.

Badham, J.P.N. and Morton, R.D.
1976: Magnetite-apatite intrusions and calc-alkaline magmatism, Camsell River, N.W.T.; Canadian Journal of Earth Sciences, v. 13, p. 348-354.

Badham, J.P.N., Robinson, B.W., and Morton, R.D.
1972: Geology and genesis of Great Bear Lake silver deposits; 24th International Geological Congress, Montreal, Section 4, p. 541-547.

Bailey, R.A.
1976: Volcanism, structure, and geochronology of Long Valley Caldera, Mono County, California; Journal of Geophysical Research, v. 81, no. 5, p. 725-744.

Bailey, R.A. and Koeppen, R.P.
1977: Preliminary geologic map of Long Valley Caldera, Mono County, California; United States Geological Survey, Open File 77-468 (2 sheets).

Bartlett, R.W.
1969: Magma Convection, temperature distribution, and differentiation; American Journal of Science, v. 267, p. 1067-1082.

Bateman, P.C.
1981: Geologic and geophysical constraints on models for the origin of the Sierra Nevada batholith, California; in The Geotectonic Development of California, W.G. Ernst, ed., Prentice-Hall, Englewood Cliffs, New Jersey, p. 71-86.

Beach, A.
1979: Pressure solution as a metamorphic process in deformed terrigenous sedimentary rocks; Lithos, v. 12, p. 51-58.

Bell, J.M.
1901: Report of the Topography and Geology of Great Bear Lake and of a chain of lakes and streams thence to Great Slave Lake; Geological Survey of Canada, Annual Report 1901, p. 5c-35c.

Bell, K.
1981: Continental crust compromise; Nature, v. 291, p. 189-190.

Bookstrom, A.A.
1977: The magnetite deposits of El Romeral, Chile; Economic Geology, v. 72, p. 1104-1130.

Bridgewater, D., Collerson, K.D. and Myers, J.S.
1978: The development of the Archean Gneiss Complex of the North Atlantic region; in Evolution of the Earth's crust, D.H. Tarling, ed., Academic Press, p. 19-69.

Brown, G.C. and Hennessy, J.
1978: The initiation and thermal diversity of granite magmatism; Philosophical Transactions of the Royal Society of London, v. 288, p. 631-643.

Burchfiel, B.C.
1980: Eastern European Alpine system and the Carpathian orocline as an example of collision tectonics; Tectonophysics, v. 63, p. 31-61.

Burnham, C.W.
1979: Magmas and hydrothermal fluids; in Geochemistry of Hydrothermal Ore Deposits, H.L. Barnes, ed., Wiley-Interscience, New York, p. 71-136.

Burnham, C.W. and Ohmoto, H.
1980: Late processes of felsic magmatism; in Ishihara, S. and Takenovchi, S., eds., Granite Magmatism and Related Mineralization, The Society of Mining Geologists of Japan, Mining Geology Special Issue, No. 8, p. 1-11.

Bussell, M.A., Pitcher, W.S. and Wilson, P.A.
1976: Ring complexes of the Peruvian Coastal Batholith: a long-standing subvolcanic regime; Canadian Journal of Earth Science, v. 13, p. 1020-1030.

Byers, F.M., Carr, W.J., Orkild, P.O., Quinlivan, W.D., and Sargent, K.A.
1976: Volcanic suites and related cauldrons of Timber Mountain-Oasis Valley caldera complex, southern Nevada; United States Geological Survey, Professional Paper 919, 70 p.

Campbell, D.D.
1955: Geology of the pitchblende deposits of Port Radium, Great Bear Lake, N.W.T.; unpublished Ph.D. thesis, California Institute of Technology, Pasadena, 323 p.

1957: Port Radium Mine; in Structural Geology of Canadian Ore Deposits; Canadian Institute of Mining and Metallurgy, p. 177-189.

Carr, M.J., Mayfield, D.G., and Walker, J.A.
1981: Relation of lava compositions to volcano size and structure in El Salvador; Journal of Volcanology and Geothermal Research, v. 10, p. 35-48.

Carr, M.J., Rose, W.I., and Mayfield, D.G.
1979: Potassium content of lavas and depth to the seismic zone in Central America; Journal of Volcanology and Geothermal Research, v. 5, p. 387-401.

Carter, S.R., Evensen, N.M., Hamilton, P.J. and O'Nions, R.K.
1978: Neodymium and strontium isotope evidence for crustal contamination of continental volcanics; Science, v. 202, p. 743-747.

Cater, F.W.
1969: The Cloudy Pass Epizonal Batholith and Associated Subvolcanic Rocks; Geological Society of America Special Paper 116, 54 p.

Cawthorn, R.G. and O'Hara, M.J.
1976: Amphibole fractionation in calc-alkaline magma genesis; American Journal of Science, v. 276, p. 309-329.

Chapin, C.E. and Lowell, G.R.
1979: Primary and secondary flow structures in ash-flow tuffs of the Gribbles Run paleovalley, central Colorado; in Ash-Flow Tuffs, Chapin, C.E. and Elston, W.E., eds., Geological Society of America Special Paper 180, p. 137-154.

Chapple, W.M. and Tullis, T.E.
1977: Evaluation of the forces that drive the plates; Journal of Geophysical Research, v. 82, p. 1967-1984.

Cobbing, E.J. and Dennis, J.G.
1982: Discussion on the origin of granites; Journal of the Geological Society of London, v. 139, p. 103-105.

Cole, J.W.
1978: Andesites of the Tongariro Volcanic Centre, North Island, New Zealand; Journal of Volcanology and Geothermal Research, v. 3, p. 121-153.

1979: Structure, petrology, and genesis of Cenozoic volcanism, Taupo Volcanic Zone, New Zealand - a review; New Zealand Journal of Geology and Geophysics, v. 22, p. 637-657.

Cole, J.W. and Lewis, K.B.
1981: Evolution of the Taupo-Hikurangi subduction system; Tectonophysics, v. 72, p. 1-21.

Collerson, K.D. and Fryer, B.J.
1978: The role of fluids in the formation and subsequent development of early continental crust; Contributions to Mineralogy and Petrology, v. 67, p. 151-167.

Coney, P.J. and Reynolds, S.J.
1977: Cordilleran Benioff zones; Nature, v. 270, p. 403-406.

Daly, R.A.
1915: Origin of the Iron Ores at Kiruna; Vetenskapliga Och Praktiska Undersokningar I Lappland, Geology 5, 31 p.

1933: Igneous Rocks and the Depths of the Earth; McGraw-Hill, New York, 598 p.

de Albuquerque, C.A.R.
1974: Geochemistry of actinolitic hornblendes from tonalitic rocks, Northern Portugal; Geochimica et Cosmochimica Acta, v. 38, p. 787-803.

De Paolo, D.J.
1981a: Trace element and isotopic effects of combined wallrock assimilation and fractional crystallization; Earth and Planetary Science Letters, v. 53, p. 189-162.

1981b: A neodymium and strontium isotopic study of the Mesozoic calc-alkaline granite batholiths of the Sierra Nevada and Peninsular Ranges, California; Journal of Geophysical Research, v. 86, no. B11, p. 10470-10488.

Deruelle, B.
1978: Calc-alkaline and shoshonitic lavas from five Andea volcanoes (between latitudes 21°45' and 24°30'S) and the distribution of Plio-Quaternary volcanism of the south-central and southern Andes; Journal of Volcanology and Geothermal Research, v. 3, p. 281-298.

Dewey, J.F.
1980: Episodicity, sequence, and style at convergent plate boundaries; in The Continental Crust and its Mineral Deposits, D.W. Strangway, ed., Geological Association of Canada, Special Paper 20, p. 553-573.

Dickinson, W.R.
1975: Potash-depth (k-h) relations in continental margin and intraoceanic magmatic arcs; Geology, v. 3, p. 53-56.

Doe, B.R., Lipman, P.W., Hedge, C.E. and Kurasawa, H.
1969: Primitive and contaminated basalts from the southern Rocky Mountains, U.S.A.; Contributions to Mineralogy and Petrology, v. 21, p. 142-156.

Duke, J.M.
1976: Distribution of the period four transition elements among olivine, calcic clinopyroxene and mafic silicate liquid: experimental results; Journal of Petrology, v. 17, p. 499-521.

Dupuy, C., Dostal, J., and Coulon, C.
1979: Geochemistry and origin of andesitic rocks from north-western Sardinia; Journal of Volcanology and Geothermal Research, v. 6, p. 375-389.

Easton, R.M.
1982: Tectonic significance of the Akaitcho Group, Wopmay Orogen, N.W.T., Unpublished Ph.D. dissertation, Memorial University of Newfoundland, St. John's, Newfoundland, 395 p.

Eggler, D.H.
1972: Amphibole stability in H_2O-undersaturated calc-alkaline melts; Earth and Planetary Science Letters, v. 15, p. 28-34.

Eggler, D.H. and Burnham, C.W.
1973: Crystallization and fractionation trends in the system andesite-H_2O- CO_2-O_2 at pressures to 10 kb; Geological Society of America Bulletin, v. 84, p. 2517-2532.

Egin, D., Hirst, D.M., and Phillips, R.
1979: The petrology and geochemistry of volcanic rocks from the northern Harsit River area, Pontid Volcanic Province, Northeastern Turkey; Journal of Volcanology and Geothermal Research, v. 6, p. 105-123.

Eichelberger, J.C.
1975: Origin of andesite and dacite: Evidence of mixing at Glass Mountain in California and at other circum-Pacific volcanoes; Geological Society of America Bulletin, v. 86, p. 1381-1391.

Elston, W.E.
1976: Tectonic significance of mid-Tertiary volcanism in the Basin and Range Province: a critical review with special reference to New Mexico; in Cenozoic Volcanism in Southwestern New Mexico, W.E. Elston and S.A. Northrop, ed., New Mexico Geological Society, Special Publication No. 5, p. 93-102.

Elston, W.E., Rhodes, R.C., Coney, P.J., and Deal, E.G.
1976: Progress report on the Mogollon Plateau volcanic field, No. 3, Surface expression of a pluton; in Cenozoic Volcanism in Southwestern New Mexico, W.E. Elston and S.A. Northrop, ed., New Mexico Geological Society Special Publication No. 5, p. 3-28.

Erlich, E.N.
1968: Recent movements and quaternary volcanic activity within the Kamchatka Territory; Pacific Geology, v. 1, p. 23-39.

Ernst, W.G.
1968: Amphiboles; Springer-Verlag, New York, 125 p.

Ewart, A.
1976: A petrological study of the younger Tongan andesites and dacites, and the olivine tholeiites to Niva Fo'ou Island, S.W. Pacific; Contributions to Mineralogy and Petrology, v. 58, p. 1-21.

Ewart, A. and LeMaitre, R.W.
1980: Some regional compositional differences within Tertiary-Recent orogenic magmas; Chemical Geology, v. 30, p. 257-283.

Ewart, A., Brothers, R.N., and Mateau, A.
1977: An outline of the geology and geochemistry and the possible petrogenetic evolution of the volcanic rocks of the Tonga-Kermadec- New Zealand Island Arc; Journal of Volcanology and Geothermal Research, v. 2, p. 205-250.

Faure, G.
1977: Principles of Isotope Geology; John-Wiley, New York, 464 p.

Faure, G. and Hurley, P.M.
1963: The isotopic composition of strontium in oceanic and continental basalt: Application to the origin of igneous rocks; Journal of Petrology, v. 4, p. 31-50.

Feniak, M.
1947: The geology of Dowdell Peninsula, Great Bear Lake, Northwest Territories; Geological Survey of Canada, Central Technical File 86E/16-1.

1952: MacAlpine Channel, Great Bear Lake, Northwest Territories; Geological Survey of Canada, Map 1011a (with descriptive notes).

Fisher, R.V.
1966a: Rocks composed of volcanic fragments and their classification; Earth Science Reviews, v. 1, p. 287-298.

1966b: Mechanism of deposition from pyroclastic flows; American Journal of Science, v. 264, p. 350-363.

Fiske, R.S., Hopson, C.A. and Waters, A.C.
1963: Geology of Mount Rainer National Park, Washington; United States Geological Survey Professional Paper 444, 93 p.

Flood, R.H., Shaw, S.E. and Chappell, B.W.
1980: Mineralogical and chemical matching of plutonic and associated volcanic units, New England Batholith, Australia; Chemical Geology, v. 29, p. 163-170.

Forsyth, D. and Uyeda, S.
1975: On the relative importance of the driving forces of plate motion; Geophysical Journal of the Royal Astronomical Society, v. 43, p. 163-200.

Fortier, Y.O.
1948: Geology of Glacier Lake areas, Great Bear Lake, Northwest Territories; Geological Survey of Canada, Central Technical File 86E/16-1.

Francis, P.W., Baker, M.C.W. and Halls, C.
1981: The Kari Kari caldera, Bolivia, and the Cerro Rico stock; Journal of Volcanology and Geothermal Research, v. 10, p. 113-124.

Francis, P.W. and Rundle, C.C.
1976: Rates of production of the main magma types in the central Andes; Geological Survey of America Bulletin, v. 87, p. 474-480.

Fraser, J.A., Hoffman, P.F., Irving, T.N. and Mursky, G.
1972: The Bear Province; in Variations in Tectonic Styles in Canada, Price, R.A. and Douglas, R.J.W., eds., Geological Association of Canada Special Paper 11, p. 454-503.

Freund, R.
1970: Rotation of strike-slip faults in Sistan, southeast Iran; Journal of Geology, v. 78, p. 188-200.

1974: Kinematics of transform and transcurrent faults; Tectonophysics, v. 21, p. 93-134.

Fryer, B.J.
1977: Rare earth evidence in iron formations for changing Precambrian oxidation states; Geochimica et Cosmochimica, v. 41, p. 361-367.

Furnival, G.M.
1935: The large quartz veins of Great Bear Lake, Canada; Economic Geology, v. 30, p. 843-850.

1939: Geology of the area north of Contact Lake, N.W.T.; American Journal of Science, v. 237, p. 478-489.

Fyfe, W.S. and McBirney, A.R.
1975: Subduction and the structure of andesitic volcanic belts; American Journal of Science, v. 275-A, p. 285-297.

Garcia, M.O. and Jacobson, S.S.
1979: Crystal clots, amphibole fractionation and the evolution of calc-alkaline magmas; Contributions to Mineralogy and Petrology, v. 69, p. 319-327.

Geijer, P. and Odman, O.H.
1974: The emplacement of the Kiruna iron ores and related deposits; Sveriges Geologie Undersokning, Serial C, no. 700, 48 p.

Ghandi, S.S.
1978: Geological observations and exploration guides to uranium in the Bear and Slave structural provinces and the Nonacho Basin, District of Mackenzie; in Report of Activities, Part B, Geological Survey of Canada Paper 78-1B, p. 141-150.

Gill, J.B.
1981: Orogenic andesites and plate tectonics, Springer-Verlag, New York, 390 p.

Gilluly, J.
1948: Origin of Granite; Geological Society of America Memoir 28, 139 p.

Goff, S.P., Baadsgaard, H., Muehlenbachs, K., and Scarfe, C.M.
1982: Rb-Sr isochron ages, magmatic $^{87}Sr/^{86}Sr$ initial ratios and oxygen isotope geochemistry of the Proterozoic lava flows and intrusions of the East Arm of Great Slave Lake, Northwest Territories, Canada; Canadian Journal of Earth Sciences, v. 19, p. 343-356.

Green, T.H.
1972: Crystallization of calc-alkaline andesite under controlled high-pressure hydrous conditions; Contributions to Mineralogy and Petrology. v. 34, p. 150-166.

1980: Island arc and continent-building magmatism - a review of petrogenic models based on experimental petrology and geochemistry; Tectonophysics, v. 63, p. 367-385.

Green, T.H., Brunfelt, A.O. and Heier, K.S.
1972: Rare-earth element distribution and K/Rb ratios in granulites, mangerites and anorthosites, Lofoten-Vesteraalen, Norway; Geochimica et Cosmochimica Acta, v. 36, p. 241-257.

Green, T.H., and Ringwood, A.E.
1968: Genesis of the Calc-Alkaline Igneous Rock Suite; Contributions to Mineralogy and Petrology, v. 18, p.105-162.

Guilbert, J.M. and Lowell, J.D.
1974: Variations in zoning patterns in porphyry ore deposits; Canadian Mining and Metallurgical Bulletin, v. 67, p. 1-11.

Gustafson, L.B. and Hunt, J.P.
1975: The porphyry copper deposit at El Salvador, Chile: Economic Geology, v. 70, p. 857-912.

Hamilton, D.L., Burnham, C.W. and Osborn, E.F.
1964: The solubility of water and effects of oxygen fugacity and water content on crystallization in mafic magmas; Journal of Petrology, v. 5, p. 21-39.

Hamilton, W.
1979: Tectonics of the Indonesian Region; United States Geological Survey, Professional Paper 1078, p. 230-270.

Hamilton, W. and Myers, W.B.
1967: The nature of batholiths; United States Geological Survey, Professional Paper 554-C, p. C1-C30.

Helz, R.T.
1973: Phase relations of basalts in their melting range at P_{H_2O}= 5 kb as a function of oxygen fugacity; Journal of Petrology, v. 14, p. 249-302.

1979: Alkali exchange between hornblende and melt: a temperature-sensitive reaction; American Mineralogist, v. 64, p. 953-965.

Hildebrand, R.S.
1981: Early Proterozoic LaBine Group of Wopmay Orogen: Remnant of a continental volcanic arc developed during oblique convergence; in Proterozoic Basins of Canada, F.H.A. Campbell, ed., Geological Survey of Canada, Paper 81-10, p. 133-156.

Hildreth, W.

1981: Gradients in silicic magma chambers: implications for lithospheric magmatism; Journal of Geophysical Research, v. 86, no. B11, p. 10153-10192.

Hoffman, P.F.

1972: Cross-section of the Coronation Geosyncline (Aphebian), Tree River to Great Bear Lake, District of Mackenzie (86 J, K, O, P); in Report of Activities, April to October, 1971, Geological Survey of Canada, Paper 72-1, Part A, p. 119-125.

1973: Evolution of an early Proterozoic continental margin: the Coronation geosyncline and associated aulacogens of the northwestern Canadian Shield; Philosophical Transactions of the Royal Society of London, A, v. 273, p. 547-581.

1976: Environmental diversity of middle Precambrian stromatolites; in Stromatolites, M.R. Walter, ed., Elsevier, New York, p. 599-611.

1978: Geology of the Sloan River map-area (86K), District of Mackenzie; Geological Survey of Canada, Open File Map 535.

Hoffman, P.F.

1980a: Wopmay Orogen: A Wilson Cycle of early Proterozoic age in the northwest of the Canadian Shield; in The Continental Crust and Its Mineral Deposits; D.W. Strangway, ed., Geological Association of Canada, Special Paper 20, p. 523-549.

1980b: Conjugate transcurrent faults in north-central Wopmay Orogen (early Proterozoic) and their dipslip reactivation during post- orogenic extension, Hepburn Lake map-area (86J), District of Mackenzie; in Current Research, Part A, Geological Survey of Canada, Paper 80-1A, p. 183-185.

1982: Geology of the Sloan River map area (86K); Geological Survey of Canada, Open File Map.

Hoffman, P.F. and McGlynn, J.C.

1977: Great Bear Batholith: A volcano-plutonic depression; in Volcanic Regimes in Canada, W.R.A. Baragar, L.C. Coleman and J.M. Hall, eds., Geological Association of Canada, Special Paper 16, p. 170-192.

Hoffman, P.F., Bell, I.R., Hildebrand, R.S. and Thorstad, L.

1977: Geology of the Athapuscow Aulacogen, east arm of Great Slave Lake, District of Mackenzie; in Report of Activities, Part A, Geological Survey of Canada, Paper 17-1A, p. 117-129.

Hoffman, P.F., Bell, I.R., Hildebrand, R.S. and Thorstad, L.
1977: Geology of the Athapuscow Aulacogen, east arm of Great Slave Lake, District of Mackenzie; in Report of Activities, Part A, Geological Survey of Canada, Paper 17-1A, p. 117-129.

Hoffman, P.F., Bell, I.R. and Tirrul, R.
1976: Sloan River map-area (86K), Great Bear Lake District of Mackenzie; in Report of Activities, Part A, Geological Survey of Canada, Paper 76-1A, p. 353-358.

Hoffman, P.F. and St-Onge, M.R.
1981: Contemporaneous thrusting and conjugate transcurrent faulting during the second collision in Wopmay Orogen: Implications for the subsurface structure of post-orogenic outliers; in Current Research, Part A, Geological Survey of Canada, Paper 81-1A, p. 251-257.

Hoffman, P.F., St-Onge, M.R., Easton, R.M., Grotzinger, J. and Schulze, D.L.
1980: Syntectonic plutonism in north-central Wopmay Orogen (early Proterozoic), Hepburn Lake Map Area, District of Mackenzie; in Current Research, Part A, Geological Survey of Canada, Paper 80-1A, p. 171-177.

Hoffman, P.F., Bowring, S.A., Easton, R.M., Hildebrand, R.S., St-Onge, M. and Van Schmus, R.
in press: Continental collisions and magmatic arcs of Wopmay Orogen: A Review of the evidence; in Proterozoic Tectonic Regimes, L. Medaris, ed., Geological Society of America Special Paper.

Hollaway, J.R. and Burnham, C.W.
1972: Melting relations of basalt with equilibrium water pressure less than total pressure; Journal of Petrology, v. 13, p. 1-29.

Irvine, T.N. and Baragar, W.R.A.
1971: A Guide to the chemical classification of the common volcanic rocks; Canadian Journal of Earth Sciences, v. 8, p. 523-548.

Isacks, B.L. and Barazangi, M.
1977: Geometry of Benioff zones: Lateral segmentation and downwards bending of the subducted lithosphere; in Island Arcs, Deep Sea Trenches and Back-Arc Basins; M. Talwani and W.C. Pitman, ed., American Geophysical Union, p. 99-114.

Izett, G.A.
1981: Volcanic ash beds: recorders of upper Cenozoic silicic pyroclastic volcanism in the western United States; Journal of Geophysical Research, v. 86, no. B11, p. 10200-10222.

Irvine, T.N. and Baragar, W.R.A.
1971: A Guide to the chemical classification of the common volcanic rocks; Canadian Journal of Earth Sciences, v. 8, p. 523-548.

Isacks, B.L. and Barazangi, M.
1977: Geometry of Benioff zones: Lateral segmentation and downwards bending of the subducted lithosphere; in Island Arcs, Deep Sea Trenches and Back-Arc Basins; M. Talwani and W.C. Pitman, ed., American Geophysical Union, p. 99-114.

Izett, G.A.
1981: Volcanic ash beds: recorders of upper Cenozoic silicic pyroclastic volcanism in the western United States; Journal of Geophysical Research, v. 86, no. B11, p. 10200-10222.

Irvine, T.N. and Baragar, W.R.A.
1971: A Guide to the chemical classification of the common volcanic rocks; Canadian Journal of Earth Sciences, v. 8, p. 523-548.

Jakes, P. and White, A.J.R.
1972: Hornblendes from calc-alkaline volcanic rocks of island arcs and continental margins; American Mineralogist, v. 57, p. 887-902.

James, D.E.
1981: The combined use of oxygen and radiogenic isotopes as indicators of crustal contamination; Annual Review of Earth and Planetary Sciences, v. 9, p. 311-344.

Joliffe, A.W. and Bateman, J.D.
1944: Map of Eldorado map-area; Geological Survey of Canada, Central Technical File 86E/16-1.

Jory, L.T.
1964: Mineralogical and isotopic relations in the Port Radium pitchblende deposit, Great Bear Lake, Canada; unpublished Ph.D. thesis, Calilfornia Institute of Technology, Pasadena, 275 p.

Katsui, Y.
1955: Geology and petrology of the volcano Mashu, Hokkaido, Japan; Journal of the Geological Society of Japan, v. 61, p. 481-495.

Katsui, Y., Ando, S. and Inaba, K.
1975: Formation and magmatic evolution of Mashu volcano, east Hokkaido, Japan; Journal of the Faculty of Science, Hokkaido University, Serial IV, v. 16, p. 533-552.

Keith, T.E.C. and Muffler, L.J.P.
1978: Minerals produced during cooling and hydrothermal alteration of ash flow tuff from Yellowstone Drill Hole Y-5; Journal of Volcanology and Geothermal Research, v. 3, p. 373-402.

Kidd, D.F.
1932: A pitchblende-silver deposit, Great Bear Lake, Canada; Economic Geology, v. 27, p. 145.

1933: Great Bear Lake area, Northwest Territories; Geological Survey of Canada, Summer Report 1932, Part C, p. 1-36.

1936: Rae to Great Bear Lake, Mackenzie District, N.W.T.; Geological Survey of Canada, Memoir 187.

Kistler, R.W.
1974: Phanerozoic Batholiths in Western North America; Annual Review of Earth and Planetary Sciences, v. 2, p. 403-418.

Klepper, M.R., Robinson, G.D., and Smedes, H.W.
1971: On the nature of the Boulder batholith; Geological Society of America Bulletin, v. 82, p. 1563-1580.

Kuno, H.
1950: Petrology of Hakone volcano and the adjacent areas, Japan; Geological Society of America Bulletin, v. 61, p. 957-1020.

Kushiro, I.
1972: Effect of water on the composition of magmas formed at high pressures; Journal of Petrology, v. 13, p. 311-334.

Kussmaul, S., Hormann, P.K., Ploskonka, E., and Subieta, T.
1977: Volcanism and structure of southwestern Bolivia; Journal of Volcanology and Geothermal Research, v. 2, p. 73-111.

Lambert, I.B. and Wyllie, P.J.
1972: Melting of gabbro (quartz eclogite) with excess water to 35 kilobars, with geological applications; Journal of Geology, v. 80, p. 693-708.

Lambert, M.B.
1972: The Bennett Lake Cauldron Subsidence Complex, British Columbia and Yukon Territory; Geological Survey of Canada Bulletin 227, 213 p.

Lanier, G., Folsom, R.B. and Cone, S.
1975: Alteration of equigranular quartz monzonite, Bingham Mining District, Utah; in Guidebook to the Bingham Mining District, Bray, R.E. and Wilson, J.C., eds., Bingham Canyon, Utah, p. 73-97.

Leake, B.E.
1978: Nomenclature of amphiboles; American Mineralogist, v. 63, p. 1023-1052.

Levi, B. and Aguirre, L.
1981: Ensialic spreading-subsidence in the Mesozoic and Paleogene of Central Chile; Journal of the Geological Society of London, v. 138, p. 75-81.

Lipman, P.W.
1965: Chemical comparison of glassy and crystalline volcanic rocks; United States Geological Survey, Bulletin 1201-D, p. D1-D24.

1975: Evolution of the Platoro Caldera Complex and Related Volcanic Rocks, Southeastern San Juan Mountains, Colorado; United States Geological Survey Professional Paper 852, 128 p.

1976: Caldera-collapse breccias in the western San Juan Mountains, Colorado; Geological Society of American Bulletin, v. 87, p. 1397-1410.

1980: Cenozoic volcanism in the Western United States: Implications for continental tectonics; in Continental Tectonics, B.C. Burchfiel et al., ed., National Academy of Sciences Studies in Geophysics, Washington, D.C., p. 161-174.

Lipman, P.W., Boethke, P. and Taylor, H.
1981: Penrose Conference report: Silicic volcanism; Geology, v. 9, p. 94-96.

Lipman, P.W., Prostka, H.J., and Christiansen, R.L.
1971: Evolving subduction zones in the western United States, as interpreted from igneous rocks; Science, v. 148, p. 821-825.

1972: Cenozoic volcanism and plate-tectonic evolution of the western United States: 1. Early and middle Cenozoic; Philosophic Transactions of the Royal Society of London, v. 271.

Lord, C.S. and Parsons, W.H.
1947: The Camsell River map area; Geological Survey of Canada, Map 1014A.

Mackenzie, D.E.
1976: Nature and origin of Late Cainozoic volcanoes in western Papua, New Guinea; in Volcanism in Australasia, R.W. Johnson, ed., Elsevier, Amsterdam, p. 221-238.

Marsh, B.D.
1976: Some Aleutian andesites: Their nature and source; Journal of Geology, v. 84, p. 27-45.

1979: Island-arc volcanism; American Scientist, v. 67, p. 161-172.

Marsh, B.D.
1981: On the crystallinity, probability of occurrence, and rheology of lava and magma; Contributions to Mineralogy and Petrology, v. 78, p. 85-98.

Mechanics and energetics of magma formation and ascension; unpublished manuscript.

Marsh, B.D. and Carmichael, I.S.E.
1974: Benioff zone magmatism; Journal of Geophysical Research, v. 79, p. 1196-1206.

Matumoto, T.
1943: Four gigantic calderas in Kyushu; Japanese Journal of Geology and Geography, v. 19, p. 36-37.

McBirney, A.R. and Noyes
1979: Crystallization and layering of the Skaergaard intrusion; Journal of Petrology, v. 20, p. 487-554.

McCourt, W.J.
1981: The geochemistry and petrography of the coastal batholiths of Peru, Lima segment; Journal of the Geological Society of London, v. 138, p. 407-420.

McGlynn, J.C.
1974: Geology of the Calder River Map Area (86F), District of Mackenzie; in Report of Activities, Part A, Geological Survey of Canada Paper 74-1A, p. 383-385.

1975: Geology of the Calder River Map Area (86F), District of Mackenzie, in Report of Activities, Part A, Geological Survey of Canada Paper 75-1A, p. 339-341.

1976: Geology of the Calder River (86F) and Leith Peninsula (86E) map areas, District of Mackenzie; in Report of Activities, part A, Geological Survey of Canada Paper 76-1A, p. 359-361.

Moore, J.G.
1959: The quartz diorite boundary line in the western United States; Journal of Geology, v. 67, p. 198-210.

Moore, J.G., Grontz, A., and Blake, M.C., Jr.
1961: The quartz diorite line in northwestern North America; United States Geological Survey, Professional Paper 424C, p. C87-C90.

Myers, J.D. and Marsh, B.D.
1981: Geology and petrogenesis of the Edgecumbe volcanic field, S.E. Alaska: The interaction of basalt and sialic crust; Contributions to Mineralogy and Petrology, v. 77, p. 272-287.

Moorbath, S.
1975: Evolution of Precambrian crust from strontium isotopic evidence; Nature, v. 254, p. 395-398.

Muir, I.D.
1953: Quartzite xenoliths from the Balluchulish Granodiorite; Geological Magazine, v. 90, p. 409-428.

Murase, T. and McBirney, A.R.
1973: Properties of some common igneous rocks and their melts at high temperatures; Geological Society of America Bulletin, v. 84, p. 3563-3592.

Mursky, G.
1973: Geology of the Port Radium map-area, District of Mackenzie; Geological Survey of Canada, Memoir 374, 40 p.

Mysen, B.O., Kushiro, I., Nicholls, I.A. and Ringwood, A.E.
1974: A possible mantle origin for andesitic magmas: discussion of a paper by Nicholls and Ringwood; Earth and Planetary Science Letters, v. 21, p. 221-229.

Nakamura, K. and Uyeda, S.
1980: Stress gradient in arc-back arc regions and plate subduction; Journal of Geophysical Research, v. 85, no. B11, p. 6419-6428.

Nicholls, I.A.
1974: Liquids in equilibrium with perioditic mineral assemblages at high water pressures; Contributions to Mineralogy and Petrology, v. 45, p. 289-316.

Nicholls, I.A. and Ringwood, A.E.
1973: Effect of water on olivine stability in tholeiites and the production of silica-saturated magmas in the island-arc environment; Journal of Geology, v. 81, p. 285-300.

Ninkovitch, D. and Hays, J.D.
1972: Mediterranean island arcs and origin of high potash volcanoes; Earth and Planetary Science Letters, v. 16, p. 331-345.

Oide, K.
1968: Geotectonic conditions for the formation of the Krakatau-type calderas in Japan; Pacific Geology, v. 1, p. 119-135.

O'Nions, R.K. and Pankhurst, R.J.
1978: Early Archean rocks and geochemical evolution of the Earth's crust; Earth and Planetary Science Letters, v. 38, p. 211-236.

Padgham, W.A., Shegelski, R.J., Murphy, J.D. and Jefferson, C.W.
1974: Geology, White Eagle Falls (86F/12), District of Mackenzie, N.W.T.; Department of Indian Affairs and Northern Development Open File 199.

Papike, J.J., Cameron, K.L. and Baldwin, K.
1974: Amphiboles and pyroxenes: characterization of other than quadrilateral components and estimates of ferric iron from microprobe data; Geological Society of America, Abstracts with Programs, v. 6, no. 7, p. 1053-1054.

Parmentier, E.M. and Schedl, A.
1981: Thermal aureoles of igneous intrusions: some possible indications of hydrothermal convective cooling; The Journal of Geology, v. 89, p. 1-22.

Patchett, P.J., Kouva, O., Hedge, C.E. and Tatsumoto, M.
1981: Evolution of continental crust and mantle heterogeneity-evidence from Hf isotopes; Contributions to Mineralogy and Petrology, v. 78, p. 279-297.

Pearce, J.A. and Cann, J.R.
1973: Tectonic setting of basic volcanic rocks determined using trace element analyses; Earth and Planetary Science Letters, v. 19, p. 290-300.

Pichler, H. and Zeil, W.
1972: The Cenozoic rhyolite-andesite associations of the Chilean Andes; Bulletin Volcanologique, v. 35, p. 424-452.

Pitcher, W.S. and Berger, A.R.
1972: The Geology of Donegal: A study of Granite Emplacement and Unroofing; Wiley-Interscience, New York, 435 p.

Pride, C. and Muecke, G.K.
1980: Rare earth element geochemistry of the Scourian Complex, N.W. Scotland - Evidence for the granite-granulite link; Contributions to Mineralogy and Petrology, v. 73, p. 403-412.

1981: Rare earth element distributions among coexisting granulite facies minerals, Scourian Complex, N.W. Scotland; Contributions to Mineralogy and Petrology, v. 76, p. 463-471.

Ratté, J.C. and Steven, T.A.
1967: Ash-flows and Related Volcanic Rocks Associated with the Creede Caldera, San Juan Mountains, Colorado; United States Geological Survey Professional Paper 524-H, 58 p.

Reyners, M.
1980: A microearthquake study of the plate boundary, North Island, New Zealand; Geophysical Journal of the Royal Astronomical Society, v. 63, p. 1-22.

Rice, A.
1981: Convective Fractionation: A mechanism to provide cryptic zoning (macrosegregration), layering, crescumulates, banded tuffs, and explosive volcanism in igneous processes; Journal of Geophysical Research, v. 86, no. B1, p. 405-417.

Richter, F.M.
1977: On the driving mechanism of plate tectonics; Tectonophysics, v. 38, p. 61-88.

Riley, C.
1935: The granite porphyries of Great Bear Lake, Northwest Territories, Canada; Journal of Geology, v. 43, p. 497-523.

Ringwood, A.R.
1974: The petrological evolution of island arc systems; Journal of the Geological Society of London, v. 130, p. 183-204.

Ringwood, A.E.
1975: Composition and Petrology of the Earth's Mantle; McGraw-Hill, New York, N.Y., 618 p.

Sekine, T., Katsura, T. and Aramaki, S.
1979: Water saturated phase relations of some andesites with application to the estimation of the initial temperature and water pressure at the time of eruption; Geochimica et Cosmochimica Acta, v. 43, p. 1367-1376.

Sekine, T., Wyllie, P.J. and Baker, D.R.
1981: Phase relationships at 30 K bar for quartz eclogite composition in $CaO-MgO-Al_2O_3-SiO_2-H_2O$ with implications for subduction zone magmas; American Mineralogist, v. 66, p. 938-950.

Shaw, D.M.
1977: Trace element behavior during anatexis; <u>in</u> Magma Genesis; Dick, H.J.B., ed., State of Oregon Department of Geology and Mineral Industries, Bulletin 96, p. 189-214.

Shaw, H.R.
1965: Comments on viscosity, crystal settling, and convection in granitic magmas; American Journal of Science, v. 263, p. 120-152.

1972: Viscosities of magmatic silicate liquids: an empirical method of prediction; American Journal of Science, v. 272, p. 870-893.

1974: Diffusion of H_2O in granitic liquids: Part I. Experimental data; Part II. Mass transfer in magma chambers; <u>in</u> Geochemical transport and kinetics, Hoffman, A.W., Giletti, B.J., Yoder, H.S., and Yund, R.A., eds., Carnegie Institute of Washington, Publication 634, p. 139-170.

Shegelski, R.J.
1973: Geology and mineralogy of the Terra silver mine, Camsell River, N.W.T.; unpublished M.Sc. thesis, University of Toronto, Toronto, 169 p.

Shegelski, R.S. and Murphy, J.D.
1973: Geology of the Camsell River silver district, Great Bear Lake area; Department of Indian Affairs and Northern Development Open File Map 135.

Shegelski, R.J. and Scott, S.D.
1975: Geology and mineralogy of the silver-uranium-arsenide veins of the Camsell River District, Great Bear Lake, N.W.T.; Geological Society of America Abstracts with Programs, v. 7, no. 6, p. 857-858.

Sighinolfi, G.P.
1971: Investigations into deep crustal levels: fractionation effects and geochemical trends related to high-grade metamorphism; Geochimica et Cosmochimica Acta, v. 34, p. 1005-1021.

Smedes, H.W. and Prostka, H.J.
1972: Stratigraphic Framework of the Absaroka Volcanic Supergroup in the Yellowstone National Park Region; United States Geological Survey, Professional Paper 729-C, 33 p.

Smith, R.L.
1960a: Ash-flows; Geological Society of America Bulletin, v. 71, p. 795-842.

1960b: Zones and zonal variations in welded ash flows: United States welded ash-flows; United States Geological Survey, Professional Paper 354F, p. F149-F159.

1979: Ash-flow magmatism; in Ash-flow Tuffs, C.E. Chapin and W.E. Elston, ed.; Geological Society of America, Special Paper 180, p. 5-27.

Smith, R.L. and Bailey, R.A.
1968: Resurgent cauldrons; Geological Society of America, Memoir 116, p. 613-662.

Smith, R.L., Bailey, R.A., and Ross, C.S.
1970: Geologic map of the Jemez Mountains, New Mexico; United States Geological Survey Map I-571 (reprinted 1976).

Snyder, F.G.
1969: Precambrian iron deposits in Missouri; Economic Geology Monograph 4, p. 231-238.

Sparks, R.S.J. and Walker, G.P.L.
1977: The significance of vitric-enriched air-fall ashes associated with crystal-enriched ignimbrites; Journal of Volcanology and Geothermal Research, v. 2, p. 329-341.

Stern, C.R. and Wyllie, P.J.
1978: Phase compositions through crystallization intervals in basalt-andesite-H_2O at 30 Kbar with implications for subduction zone magmas; American Mineralogist, v. 63, p. 641-663.

Steven, T.A. and Lipman, P.W.
1973: Geological Map of the Spar City Quadrangle; United States Geological Survey Map GQ-1052.

1976: Calderas of the San Juan volcanic field, southwestern Colorado; United States Geological Survey, Professional Paper 958, 35 p.

Steven, T.A. and Ratté, J.C.
1965: Geology and structural control of ore deposition in the Creede District, San Juan Mountains, Colorado; United States Geological Survey, Professional Paper 487, 90 p.

1973: Geological Map of the Creede Quadrangle; United States Geological Survey, Map GQ-1053.

Stewart, D.C.
1975: Crystal clots in calc-alkaline andesites as breakdown products of high-Al amphiboles; Contributions to Mineralogy and Petrology, v. 53, p. 195-204.

Streckeisen, A.L.
1967: Classification and nomenclature of igneous rocks; Nves Jahrhuch Mineralogishe Moh, v. 107, p. 144-150.

1973: Plutonic Rocks. Classification and nomenclature recommended by the IUGS Subcommission on the Systematics of Igneous Rocks; Geotimes, October 1973, p. 26-30.

Tarney, J. and Windley, B.F.
1977: Chemistry, thermal gradients and evolution of the lower continental crust; Journal of the Geological Society of London, v. 134, p. 153-172.

Taylor, G.A.
1959: Notes on Savo volcano, 1959; The Geological Survey of the British Solomon Islands, Geological Record 1959-62, p. 168-173.

Taylor, H.P., Jr.
1979: Oxygen and hydrogen isotope relationships in hydrothermal mineral deposits; in Geochemistry of Hydrothermal Ore Deposits, H.L. Barnes, ed.; Wiley-Interscience, New York, p. 236-277.

Taylor, R.P.
1981: Isotope geology of the Bakircay porphyry copper prospects, northern Turkey; Mineralium Deposita, v. 16, p. 375-390.

Taylor, S.R. and Gorton, M.P.
1977: Geochemical application of spark source mass spectography - III. Element sensitivity, precision, and accuracy; Geochimica et Cosmochimica Acta, v. 41, p. 1375-1380.

Templeman-Kluit, D.J.
1979: Transported cataclasite, ophiolite and granodiorite in Yukon: evidence of arc-continent collision; Geological Survey of Canada, Paper 79-14, 27 p.

Thorpe, R.
1974: Lead isotope evidence on the genesis of the silver-arsenide vein deposits of the Cobalt and Great Bear Lake areas, Canada; Economic Geology, v. 69, p. 777-791.

Thorpe, R.S. and Francis, P.W.
1979: Petrogenetic relationships of volcanic and intrusive rocks of the Andes; in Origin of Granite Batholiths: Geochemical Evidence, Atherton, M.P. and Tarney, J., eds., Shiva Publishing Ltd., Orpington, p. 65-75.

Thorpe, R.S., Potts, P.J., and Francis, P.W.
1976: Rare earth data and petrogenesis of andesite from the North Chilean Andes; Contributions to Mineralogy and Petrology, v. 54, p. 65-78.

Thorpe, R.S., Francis, P.W. and Moorbath, S.
1979: Rare earth and strontium isotope evidence concerning the petrogenesis of North Chilean ignimbrites; Earth and Planetary Science Letters, v. 42, p. 359-367.

Thurber, J.B.
1946: Glacier Bay-Cameron Bay area, Great Bear Lake, N.W.T.; Geological Survey of Canada, Central Technical File 86E/16-1.

Tilton, G.R. and Barreiro, B.A.
1980: Origin of lead in Andean calc-alkaline lavas; southern Peru; Science, v. 210, p. 1245-1247.

Tirrul, R.
1976: The Geology of the Rainy Lake Igneous Complex, District of Mackenzie, Northwest Territories; unpublished B.Sc. thesis, Queen's University, Kingston, Ontario, 115 p.

Ujike, O.
1977: Chemical compositions of amphibole phenocrysts in calc-alkaline volcanic rocks: A compilation of 95 analyses; Journal of the Japanese Association of Petroleum and Economic Geologists, v. 72, p. 85-93.

Ujike, O. and Onuki, H.
1976: Phenocrystic hornblendes from Tertiary andesites and dacites, Kagawa Prefecture, Japan; Journal of the Japanese Association of Petroleum and Economic Geologists, v. 71, p. 389-399.

Van Bemmelen, R.W.
1949: The Geology of Indonesia, Martinus Nijhoff, The Hague, 732 p.

Van Schmus, W.R. and Bowring, S.A.
1980: Chronology of igneous events in the Wopmay Orogeny, Northwest Territories, Canada; Geological Society of America, Abstracts with Programs, v. 12, no. 7, p. 540.

Verstappen, H. Th.
1973: A geomorphological reconnaissance of Sumatra and adjacent islands (Indonesia); Wolters-Noordhoff, Groningen, The Netherlands, 182 p.

Violette, B.
1979: Precambrian Geology of the Hottah Lake area, District of Mackenzie, N.W.T.; unpublished B.Sc. thesis, University of Ottawa.

Von der Borch, C.C.
1979: Continent-island arc collision in the Banda Arc; Tectonophysics, v. 54, p. 169-193.

Walker, G.P.L.
1972: Crystal concentration in ignimbrites; Contributions to Mineralogy and Petrology, v. 36, p. 135-146.

1981: Generation and dispersal of fine ash and dust by volcanic eruptions; Journal of Volcanology and Geothermal Research, v. 11, p. 81-92.

Walker, G.P.L., Self, S. and Froggatt, P.C.
1981: The ground layer of the Taupo ignimbrite: A striking example of sedimentation from a pyroclastic flow; Journal of Volcanology and Geothermal Research, v. 10, p. 1-11.

Waters, A.C.
1948: Discussion; in Origin of Granite, J. Gilluly, ed., The Geological Society of America Memoir 28, p. 104-108.

Weaver, B.L., Tarney, J., Windley, B.F., Sugavanam, E.B. and Venkato-Rao, V.
1978: Madras granulites: geochemistry and P-T conditions of crystallization; in Archean Geochemistry, Windley, B.F. and Naqvi, S.M., eds., Elsevier, Amsterdam, p. 177-204.

Weyl, R.
1980: Geology of Central America; Gebruder Borntraeger, Berlin, 371 p.

Williams, H. and McBirney, A.R.
1969: Volcanic history of Honduras; University of California Publications in Geological Sciences, v. 85, p. 1-101.

1979: Volcanology: Freeman, Cooper and Co., San Francisco, 397 p.

Williams, H., McBirney, A.R., and Dengo, G.
1964: Geological reconnaissance of southeastern Guatemala; University of California Publications in Geological Sciences, v. 50, p. 1-62.

Wilson, A.
1979: Petrology and Geochemistry of the Upper Hottah Lake Sequence, Hottah Lake, District of Mackenzie, Northwest Territories; unpublished B.Sc. thesis, McMaster University, Hamilton, Ontario.

Withers, R.L.
1979: Mineral Deposits of the Northrim Mine and a Brief Enquiry into the Genesis of Veins of the (Ag, Bi, Ni, Co, As) Type; unpublished M.Sc. thesis, University of Alberta, Edmonton, Alberta, 271 p.

Wright, L.A. and Troxel, B.W.
1973: Shallow-fault interpretation of Basin and Range structure, southwestern Great Basin; in Gravity and Tectonics, DeJong, K.A. and Scholten, R., eds., John Wiley, New York, p. 397-407.

Wyllie, P.J.
1977: Crustal anatexis: an experimental review; Tectonophysics, v. 43, p. 41-71.

1977: From crucibles through subduction to batholiths; in Energetics of Geological Processes, Saxena, S.K. and Bhattacharji, S., eds., Springer-Verlag, New York, p. 289-433.

Wyllie, P.J., Huang, W., Stern, C.R. and Maaloe, S.
1976: Granitic magmas: possible and impossible sources, water contents, and crystallization sequences; Canadian Journal of Earth Sciences, v. 13, p. 1007-1019.

Zartman, R.E.
1974: Lead isotopic provinces in the Cordillera of the western United States and their geologic significance; Economic Geology, v. 69, p. 792-805.

Zeil, W.
1979: The Andes: A Geological Review; Gebruder Borntraeger, Berlin, 260 p.

APPENDICES

Appendix 1

Analyses of rocks from the Echo Bay belt

	Echo Bay Formation										
Sample no.	H-77-53b	H-77-140	H-77-53	H-78-350	H-78-352	H-77-15	H-77-50	H-77-51	H-77-80	H-77-95	H-77-96
SiO_2	54.0	63.7	54.9	56.1	60.2	61.0	58.0	57.7	55.3	56.5	58.6
TiO_2	0.44	0.40	0.65	0.60	0.48	0.47	0.66	0.71	0.68	0.75	0.77
Al_2O_3	14.2	16.4	16.6	17.7	16.2	16.4	14.7	17.5	14.8	18.3	17.4
Fe_2O_3**	10.7	3.57	10.3	7.06	4.82	6.11	7.40	6.00	10.4	8.46	6.03
MnO	0.43	0.16	0.32	0.14	0.17	0.07	0.26	0.17	0.44	0.18	0.16
MgO	3.40	1.95	4.03	3.27	2.06	1.21	4.74	2.67	3.65	1.97	1.82
CaO	2.93	1.53	1.54	4.21	2.96	1.80	4.09	3.58	1.17	1.94	4.86
Na_2O	3.71	1.75	3.89	2.19	3.68	3.83	2.20	2.86	3.55	3.41	3.58
K_2O	2.37	5.26	3.63	4.55	4.52	5.36	4.13	5.17	3.91	5.41	3.91
P_2O_5	0.26	0.09	0.27	0.21	0.15	0.14	0.15	0.25	0.07	0.25	0.28
LOI	5.81	4.98	2.46	2.51	3.24	3.36	2.72	2.85	3.36	8.46	6.03
Total	98.21	99.79	98.59	98.54	98.46	99.75	99.05	99.46	97.28	99.02	99.76
Nb	14	20	10	11	15	17	11	10	10	11	11
Zr	137	233	149	160	166	213	166	162	162	160	163
Y	45	32	18	28	29	30	29	27	24	29	25
Sr	62	107	129	293	308	216	305	555	64	151	553
U	3	5	2	3	5	6	4	3	1	0	0
Rb	43	210	119	170	170	183	125	124	89	159	126
Th	15	22	15	20	20	22	19	15	14	11	1
Pb	18	5	9	16	12	16	16	6	9	16	21
Ga	11	16	12	16	13	14	13	18	12	22	21
Zn	136	62	211	118	327	48	260	94	340	232	144
Cu	24	0	0	0	4	0	0	57	33	35	49
Ni	7	16	21	24	21	16	50	20	20	7	11
Cr	250	3	88	37	28	10	197	17	54	13	15
V	112	33	173	124	111	65	147	107	182	110	110
Ba	511	870	1028	870	1172	1198	880	1624	1499	1539	1150
La	-	-	-	-	-	23.53	33.74	-	-	-	-
Ce	-	-	13.67	-	-	53.39	70.03	59.45	8.54	-	-
Pr	-	-	1.67	-	-	5.73	7.79	7.61	1.27	-	-
Nd	-	-	8.07	-	-	24.29	30.35	28.96	5.65	-	-
Sm	-	-	2.28	-	-	4.12	5.48	6.25	1.39	-	-
Eu	-	-	0.41	-	-	0.73	0.64	1.20	0.42	-	-
Gd	-	-	1.83	-	-	3.34	4.50	3.94	1.91	-	-
Dy	-	-	2.87	-	-	3.57	3.82	4.14	-	-	-
Er	-	-	1.65	-	-	2.02	2.13	1.81	1.58	-	-
Yb	-	-	2.27	-	-	1.77	2.50	2.11	2.28	-	-

**Total Fe as Fe_2O_3

Appendix 1 (cont.)

Analyses of rocks from the Echo Bay belt

	Doghead Tuff						Lindsley Tuff			
Sample no:	H-78-665	H-78-377	H-78-376	H-78-651	H-78-663	H-78-375	H-78-563	H-78-354	H-78-355	H-78-356
SiO_2	59.4	59.9	61.8	56.7	60.3	60.8	66.4	64.0	62.5	62.3
TiO_2	0.55	0.51	0.46	0.51	0.36	0.51	0.20	0.49	0.36	0.36
Al_2O_3	14.5	14.2	13.5	15.2	13.8	14.9	12.8	15.1	16.0	15.6
Fe_2O_3**	5.56	4.58	4.00	5.78	4.09	6.03	3.26	5.60	6.15	6.30
MnO	0.12	0.23	0.11	0.12	0.27	0.11	0.92	0.20	0.09	0.13
MgO	3.01	3.35	2.11	3.51	2.79	2.96	1.97	1.59	2.35	3.02
CaO	3.20	3.11	4.71	3.34	4.95	3.85	2.34	2.04	4.53	2.01
Na_2O	3.12	2.03	2.93	2.93	1.76	2.91	0.52	2.66	2.67	3.60
K_2O	4.25	5.09	3.63	3.98	3.78	3.82	5.21	4.93	3.05	2.30
P_2O_5	-	-	0.09	0.13	0.15	0.14	0.06	-	0.11	0.08
LOI	5.30	5.86	5.68	5.19	6.73	3.74	6.30	2.64	1.49	3.42
Total	99.01	98.86	99.62	99.49	98.98	99.77	99.98	99.25	99.30	99.15
Nb	10	12	11	11	11	9	11	15	9	8
Zr	179	169	154	163	163	163	120	161	115	112
Y	23	29	26	27	26	26	22	28	23	25
Sr	265	83	118	310	121	219	28	160	279	280
U	3	5	6	5	3	5	5	5	3	3
Rb	157	175	156	142	162	155	177	227	123	126
Th	20	25	24	21	21	21	17	24	12	12
Pb	26	12	17	19	19	25	7	12	12	34
Ga	18	16	11	15	10	14	12	12	16	12
Zn	287	102	108	246	186	214	26	222	55	185
Cu	0	106	86	0	5	68	0	0	15	0
Ni	30	34	25	27	30	34	14	22	18	14
Cr	51	46	41	37	46	48	4	23	15	19
V	104	112	102	109	104	118	48	85	90	101
Ba	1068	672	541	995	890	761	543	628	580	510
La	27.46	38.32	43.60	-	34.55	-	-	-	26.15	23.39
Ce	59.85	79.00	82.43	-	74.62	72.66	-	-	57.13	48.74
Pr	6.81	8.29	9.57	-	8.50	9.71	-	-	5.53	5.84
Nd	25.95	30.63	31.85	-	29.43	30.22	-	-	23.68	21.86
Sm	4.78	5.15	4.93	-	4.64	5.85	-	-	3.69	4.16
Eu	0.41	0.96	0.82	-	0.46	0.97	-	-	0.85	0.60
Gd	4.12	3.69	3.43	-	3.64	3.59	-	-	2.66	2.92
Dy	3.52	3.44	2.93	-	4.51	4.41	-	-	2.84	3.64
Er	2.39	2.11	1.66	-	1.54	1.74	-	-	1.08	1.22
Yb	-	2.08	1.89	-	1.93	-	-	-	1.09	1.13

**Total Fe as Fe_2O_3

Appendix 1 (cont.)

Analyses of rocks from the Echo Bay belt

	--Western Channel	Tuff-----		-------Stevens Tuff---------			early intermediate ----intrusive suite--------			Hogarth pluton
Sample no.	H-78-572	H-78-421	H-78-624	H-78-398	H-78-564	H-78-399	H-77-170	H-77-124	H-77-52	H-78-351
SiO_2	63.4	70.0	71.5	65.2	65.9	64.6	64.0	53.7	59.3	62.7
TiO_2	0.22	0.23	0.18	tr	0.14	0.16	0.35	0.73	0.58	0.30
Al_2O_3	14.2	14.5	13.3	14.1	14.1	14.6	14.0	15.6	14.2	14.6
Fe_2O_3**	5.04	3.08	1.82	4.16	3.98	3.64	6.03	6.00	7.08	3.19
MnO	0.12	0.04	0.07	0.20	0.61	0.15	0.08	0.26	0.17	0.08
MgO	1.64	0.52	0.57	1.09	2.28	1.29	1.76	3.42	3.63	1.88
CaO	2.34	0.87	1.05	2.89	1.80	2.32	1.17	4.42	4.83	3.08
Na_2O	2.72	3.44	2.80	2.00	0.53	2.51	1.18	5.43	2.56	3.33
K_2O	4.75	5.09	5.48	4.39	6.00	4.04	7.07	2.55	4.19	3.90
P_2O_5	na	0.05	na	0.04	0.08	0.06	0.12	0.17	na	0.06
LOI	4.25	1.74	2.68	4.58	5.30	4.49	2.98	4.34	2.34	3.98
Total	98.68	99.56	99.45	98.65	99.12	99.16				
Nb	13	13	17	13	14	14	20	9	13	12
Zr	167	173	150	135	135	143	237	132	166	138
Y	26	24	22	21	23	23	18	27	29	27
Sr	81	135	127	89	35	132	125	185	299	208
U	4	6	8	4	6	5	8	1	4	5
Rb	157	215	209	176	206	156	281	92	162	139
Th	16	27	28	22	22	21	41	10	18	22
Pb	8	21	23	6	8	7	12	21	22	6
Ga	16	14	12	13	16	16	12	17	12	14
Zn	35	125	86	67	25	92	60	275	192	84
Cu	nd	nd	nd	3	nd	4	24	nd	10	nd
Ni	22	10	11	10	17	12	24	17	41	19
Cr	27	2	nd	nd	2	2	23	84	122	22
V	82	39	19	41	44	42	80	195	124	66
La(xrf)	45	80	45	43	47	42	13	29	33	47
Ce(xrf)	69	116	76	59	81	58	40	47	63	75
Ba	854	875	811	394	812	577	1332	714	896	537
La	31.36	54.46	35.92	35.41	-	-	10.07	15.09	33.66	42.75
Ce	60.89	105.70	66.80	63.01	68.79	-	22.11	36.45	73.98	81.08
Pr	7.37	10.48	6.45	6.87	7.40	-	2.69	4.51	8.98	8.55
Nd	24.72	34.66	23.15	21.95	25.52	-	11.27	19.71	30.32	30.00
Sm	4.02	4.51	4.19	4.14	4.01	-	2.19	4.41	5.37	4.87
Eu	0.87	0.15	0.45	0.00	0.23	-	0.14	1.20	0.43	0.74
Gd	3.23	2.58	2.38	2.26	2.57	-	2.19	3.53	3.47	3.60
Dy	3.81	2.62	2.58	3.42	3.55	-	2.23	4.59	4.05	3.65
Er	1.83	1.47	1.13	1.45	1.43	-	1.38	1.97	1.43	2.02
Yb	1.99	2.08	2.12	2.09	1.98	-	1.97	2.30	1.83	2.33

**Total Fe asFe_2O_3

Appendix 1 (cont.)

Analyses of rocks from the Echo Bay belt

	Cornwall Tuff					Rocher Rouge Tuff			
Sample no.	H-78-512	H-78-675	H-78-513	H-78-676	H-78-677	H-78-626	H-78-430	H-78-573	H-78-427
SiO_2	69.2	69.0	66.9	65.5	65.3	60.7	64.0	64.4	67.0
TiO_2	0.20	0.15	0.13	0.24	tr	0.43	0.56	0.13	0.42
Al_2O_3	13.9	14.1	13.5	14.8	9.07	16.4	16.1	14.2	14.2
Fe_2O_3**	5.90	3.54	2.65	4.80	3.82	5.59	4.23	3.82	3.54
MnO	0.09	0.13	0.35	0.16	0.74	0.15	0.13	0.13	0.06
MgO	0.84	1.55	1.76	1.47	3.09	1.95	1.77	0.95	1.22
CaO	0.45	1.06	1.67	0.90	5.11	3.08	1.90	2.61	1.61
Na_2O	0.10	0.10	0.52	1.80	0.10	2.53	3.47	2.56	2.82
K_2O	6.03	5.75	6.00	5.62	2.48	4.50	5.56	5.29	5.81
P_2O_5	0.10	0.07	0.09	0.05	0.04	0.13	0.09	0.13	0.09
LOI	3.18	4.53	5.23	3.64	10.41	4.70	2.18	4.11	1.65
Total	99.99	99.98	98.80	98.76	100.16	100.24	99.99	98.33	98.42
Nb	13	14	13	14	8	13	16	15	15
Zr	162	162	159	169	89	182	166	138	171
Y	21	20	22	20	32	33	38	26	39
Sr	17	18	36	23	8	219	286	126	364
U	6	5	6	6	3	3	6	5	5
Rb	245	206	232	208	122	130	210	196	194
Th	29	28	25	28	20	16	31	24	30
Pb	11	17	13	10	7	22	30	8	49
Ga	11	16	16	15	9	17	14	16	14
Zn	79	166	36	96	48	212	221	48	86
Cu	24	112	39	-	89	14	-	-	7
Ni	17	16	24	14	9	19	23	19	21
Cr	3	-	4	2	-	4	11	1	15
V	31	29	34	41	11	71	57	43	59
Ba	1073	902	728	1097	113	1402	824	887	831

**Total Fe as Fe_2O_3

APPENDIX 2: Strontium isotopic analyses, LaBine Group and associated plutons.

Sample No.		ppm Rb	ppm Sr	Rb/Sr	$^{87}Rb/^{86}Sr$	$^{87}Sr/^{86}Sr$
H-77-53	(Lcm)	114	124	.92408	2.675 ± .009	.76987 ± .0003
H-77-53b	(Lcm)	42	58	.72393	2.09 ± .01	.75609 ± .00045
H-77-15	(Lcm)	180	212	.84773	2.454 ± .009	.76463 ± .00008
H-78-399	(Lst)	159	134	1.1887	3.44 ± .01	.78861 ± .00041
H-78-676	(Lct)	206	24	8.5625	24.8 ± .3	1.3388 ± .00039
H-78-355	(Llt)	125	281	.44539	1.289 ± .005	.73748 ± .00005
H-78-181	(Lmt)	164	33	4.9849	14.4 ± .1	1.0082 ± .00028
H-79-199	(Lwt)	136	275	.49492	1.433 ± .005	.72713 ± .0011
P-79-129	(Ly)	183	181	1.0166	2.94 ± .01	.77964 ± .00016
H-79-138	(Ly)	188	52	3.5905	10.39 ± .08	.96217 ± .00058
H-80-93	(Laa)	73	434	.16743	.484 ± .002	.71577 ± .00009
H-80-89	(Laa)	105	565	.18513	.536 ± .004	.71336 ± .00067
H-80-7	(Lcl)	107	422	.25284	.732 ± .006	.72146 ± .00006
P-79-97	(Lcl)	125	287	.43322	1.254 ± .005	.73505 ± .00005
J-79-93	(Bic)	180	1[illegible]	1.28[illegible]	3.73 ± .01	.79894 ± .00036
J-79-62	(Bic)	155	266	.58232	1.686 ± .009	.74865 ± .00056
J-79-66	(Bic)	132	218	.60444	1.750 ± .006	.74713 ± .00017
H-79-40	(Bic)	137	282	.48424	1.402 ± .004	.73907 ± .00014
H-80-24	(Bic)	148	266	.55879	1.618 ± .006	.74642 ± .00014
P-80-37	(Cqm)	179	347	.51581	1.49 ± .01	.74373 ± .00006

APPENDIX 3: Major and trace element analyses, Camsell River-Conjuror Bay area.

Sample No:	P-79-180(r)	P-79-119(Lwx)	P-79-153(Lmls)	P-79-56(r)	P-79-150(r)	H-80-104(g)
SiO_2	75.0	82.9	67.9	71.7	71.7	49.3
TiO_2	0.07	0.06	0.40	tr	0.13	2.20
Al_2O_3	13.3	9.28	13.8	13.8	14.2	11.8
Fe_2O_3	0.74	0.57	4.57	1.79	1.38	18.82
MnO	0.06	0.06	0.13	0.14	0.04	0.36
MgO	0.32	0.84	2.53	0.56	0.61	4.08
CaO	0.73	0.06	2.51	0.49	0.80	7.98
Na_2O	3.26	tr	2.16	3.10	4.56	2.78
K_2O	4.07	5.26	2.78	4.80	4.15	1.20
P_2O_5	tr	0.01	0.09	0.06	tr	0.22
LOI	1.48	1.34	1.99	1.77	1.86	1.71
Total	99.07	99.06	98.86	98.21	99.43	100.45
Nb	13	7	10	15	12	9
Zr	47	54	144	90	117	144
Y	22	22	35	36	24	57
Sr	32	35	153	58	63	128
U	0	4	9	5	0	1
Rb	151	149	156	152	101	35
Th	2	8	12	16	12	3
Pb	5	7	9	2	0	10
Zn	20	48	103	19	10	196
Cu	16	0	0	17	17	28
Cr	0	0	35	0	0	0
V	2	0	142	1	11	526
La	17	17	51	25	49	53
Ce	29	14	63	75	90	75
Ba	342	1016	968	903	1063	345

**Total Fe as Fe_2O_3. Oxides in weight percent; trace elements in parts/million.

APPENDIX 3 (cont.): Major and trace element analyses, Camsell River-Conjuror Bay area.

Sample No.	P-80-121(Hd)	P-80-96(s)	J-80-94(2Y)	P-80-119(Hd)	P-80-63(2Y)	J-80-114(3T)	J-80-124(Hd)
SiO_2	69.5	71.9	65.5	68.3	64.5	70.1	64.0
TiO_2	0.45	0.15	0.55	0.53	0.65	0.29	0.72
Al_2O_3	13.4	13.7	14.4	14.6	14.3	14.0	15.2
Fe_2O_3**	4.20	2.18	4.37	3.86	4.99	2.29	5.75
MnO	0.07	0.17	0.06	0.10	0.11	0.05	0.23
MgO	0.58	0.75	1.76	1.56	2.42	0.74	2.96
CaO	1.70	0.57	3.30	1.85	2.60	1.71	3.33
Na_2O	2.79	3.23	2.96	3.23	2.70	3.47	2.58
K_2O	5.51	4.87	4.41	4.32	4.52	4.62	4.00
P_2O_5	0.08	0.03	0.10	0.11	0.09	tr	0.11
LOI	0.98	1.54	1.40	1.10	1.85	1.44	1.77
Total	99.27	99.09	98.80	99.56	98.73	98.71	100.65
Nb	25	11	11	13	16	17	11
Zr	289	78	147	177	180	156	157
Y	91	19	27	44	38	32	29
Sr	86	104	214	240	224	188	309
U	10	5	3	9	4	7	2
Rb	299	188	196	155	199	236	151
Th	54	13	15	21	24	30	13
Pb	32	17	22	13	34	29	14
Zn	66	56	48	59	75	46	106
Cu	15	20	16	22	17	12	19
Cr	0	0	0	0	18	3	38
V	256	157	268	269	84	22	108
La					45	56	61
Ce	117		16	26	69	82	105
Ba	520	714	518	736	717	711	1045

**Total Fe as Fe_2O_3. Oxides in weight percent; trace elements in parts/million.

APPENDIX 4

Clinopyroxene H-79-131

	NA	MG	AL	SI	K	CA	TI	CR	MN	FE	NI	TOTAL
BG	1.07	2.05	3.62	4.28	.64	1.69	2.86	10.15	1.79	2.78	2.14	
C1	.25	7.77	.16	25.43	.03	17.34	.12	-.07	.07	6.84	.05	
BC	.34	12.88	.31	54.40	.03	24.26	.20	.00	.09	8.79	.07	
AC	.38	13.30	.31	52.35	.03	24.13	.19	.00	.10	8.98	.07	99.86
FM	.027	.746	.013	1.973	.001	.974	.004	.000	.002	.282	.002	4.024

	NA	MG	AL	SI	K	CA	TI	CR	MN	FE	NI	TOTAL
BG	.29	1.53	3.62	3.64	.70	.94	3.29	6.13	1.41	2.35	2.54	
C1	.54	7.83	.21	25.96	.01	17.09	.06	.03	.04	6.46	.02	
BC	.73	12.98	.40	55.53	.01	23.91	.10	.04	.05	8.31	.03	
AC	.81	13.38	.40	53.41	.01	23.81	.10	.04	.05	8.49	.03	100.54
FM	.058	.742	.017	1.988	.003	.949	.002	.001	.001	.264	.000	4.022

	NA	MG	AL	SI	K	CA	TI	CR	MN	FE	NI	TOTAL
BG	.64	.77	4.30	5.14	.77	.94	3.42	7.16	1.73	1.92	3.04	
C1	.57	8.08	.21	25.41	.02	17.58	.09	.00	.10	6.39	.00	
BC	.77	13.39	.40	54.37	.02	24.59	.14	.00	.13	8.22	.00	
AC	.86	13.81	.41	52.41	.02	24.47	.14	.00	.13	8.40	.00	100.65
FM	.061	.769	.017	1.958	.000	.979	.003	.000	.003	.262	.000	4.051

	NA	MG	AL	SI	K	CA	TI	CR	MN	FE	NI	TOTAL
BG	.39	1.75	3.59	5.00	.71	1.10	2.82	5.77	2.07	2.03	2.71	
C1	.56	7.70	.18	25.35	.05	17.68	.07	.04	.05	7.18	.00	
BC	.75	12.76	.33	54.22	.05	24.73	.12	.05	.06	9.24	.00	
AC	.85	13.26	.33	52.28	.05	24.59	.11	.05	.07	9.43	.09	101.02
FM	.061	.739	.014	1.956	.002	.985	.002	.001	.001	.294	.000	4.055

	NA	MG	AL	SI	K	CA	TI	CR	MN	FE	NI	TOTAL
BG	.48	2.84	4.51	3.88	.48	1.41	3.91	7.45	1.73	2.80	2.08	
C1	.37	8.47	.16	26.18	.04	16.59	.05	.00	.15	5.69	.04	
BC	.49	14.05	.30	56.00	.07	23.21	.09	.00	.20	7.32	.04	
AC	.54	14.32	.30	53.86	.07	23.16	.09	.00	.20	7.48	.05	100.07
FM	.038	.792	.013	1.998	.003	.920	.002	.000	.005	.232	.001	4.003

Clinopyroxene P-79-97

	NA	MG	AL	SI	K	CA	TI	CR	MN	FE	NI	TOTAL
BG	.86	3.09	5.32	3.38	3.79	5.48	11.07	22.77	1.59	1.59	2.84	
C1	.21	8.45	1.50	23.88	-.01	12.90	.31	-.01	.28	10.11	.03	
BC	.28	13.35	1.89	51.98	.00	15.05	.51	.00	.36	13.00	.03	
AC	.33	14.09	1.95	50.33	.00	17.91	.50	.00	.36	13.20	.04	98.71
FM	.023	.804	.087	1.927	.000	.734	.013	.000	.011	.422	.000	4.023

	NA	MG	AL	SI	K	CA	TI	CR	MN	FE	NI	TOTAL
BG	.59	.71	2.84	5.34	2.77	4.30	12.88	18.77	1.41	1.98	2.70	
C1	.20	6.21	.97	24.08	.01	13.27	.26	.03	.24	9.48	.01	
BC	.27	13.62	1.84	51.52	.01	18.56	.43	.04	.30	12.20	.01	
AC	.31	14.29	1.88	50.65	.01	18.45	.43	.04	.31	12.40	.01	96.77
FM	.022	.812	.083	1.931	.000	.753	.011	.001	.010	.395	.000	4.017

	NA	MG	AL	SI	K	CA	TI	CR	MN	FE	NI	TOTAL
BG	.73	1.91	3.77	5.11	2.65	5.30	11.99	21.45	1.36	2.12	3.22	
C1	.21	8.07	1.05	23.85	.00	13.15	.30	.00	.27	9.77	-.02	
BC	.29	13.38	1.98	51.02	.00	18.40	.49	.00	.33	12.85	.00	
AC	.34	14.11	2.03	50.26	.00	18.27	.48	.00	.35	13.05	.00	98.89
FM	.024	.802	.090	1.920	.000	.746	.013	.000	.011	.417	.000	4.025

	NA	MG	AL	SI	K	CA	TI	CR	MN	FE	NI	TOTAL
BG	.34	2.62	4.14	3.98	3.45	5.66	15.41	20.01	2.13	2.38	3.58	
C1	.22	8.04	1.00	23.54	.00	13.12	.31	.01	.27	10.21	-.02	
BC	.30	13.32	1.89	50.35	.00	15.35	.52	.01	.35	13.23	.00	
AC	.35	14.10	1.95	49.66	.00	18.21	.50	.01	.35	13.44	.09	98.57
FM	.024	.809	.088	1.912	.000	.750	.013	.000	.011	.433	.000	4.040

	NA	MG	AL	SI	K	CA	TI	CR	MN	FE	NI	TOTAL
BG	.79	3.09	4.22	5.74	2.84	5.78	10.92	20.74	1.77	1.98	1.98	
C1	.22	7.57	1.14	23.93	.00	13.16	.34	.05	.26	10.15	.04	
BC	.29	13.05	2.15	51.18	.00	18.42	.56	.08	.33	13.08	.05	
AC	.34	13.80	2.20	50.43	.00	18.27	.54	.03	.34	13.26	.05	99.32
FM	.024	.782	.098	1.920	.000	.743	.014	.002	.010	.422	.001	4.019

	NA	MG	AL	SI	K	CA	TI	CR	MN	FE	NI	TOTAL
BG	.43	1.83	3.98	4.41	3.33	4.29	12.19	21.67	1.75	2.39	2.95	
C1	.21	8.26	.92	24.94	.00	13.25	.30	.01	.21	9.24	.00	
BC	.29	13.69	1.73	53.36	.00	18.53	.51	.01	.27	11.88	.00	
AC	.33	14.31	1.77	52.29	.02	18.43	.49	.01	.28	12.09	.00	100.00
FM	.023	.799	.077	1.958	.000	.743	.013	.000	.009	.378	.000	3.997

Clinopyroxene H-80-93

	NA	MG	AL	SI	K	CA	TI	CR	MN	FE	NI	TOTAL
BG	.39	1.66	3.48	4.98	2.85	4.81	11.04	17.30	1.32	2.38	2.16	
C1	.18	10.23	1.65	24.72	.00	14.72	.33	.27	.11	4.79	.04	
BC	.24	16.96	3.11	52.89	.00	20.59	.55	.40	.14	6.15	.05	
AC	.26	16.98	3.14	51.91	.00	20.57	.54	.41	.14	6.30	.05	100.32
Fm	.018	.920	.135	1.950	.000	.807	.014	.012	.004	.192	.001	4.008

	NA	MG	AL	SI	K	CA	TI	CR	MN	FE	NI	TOTAL
BG	.85	2.62	3.26	7.37	2.78	3.72	11.08	18.61	1.47	2.98	2.19	
C1	.17	10.70	.61	25.87	.00	14.68	.18	.10	.11	4.93	.03	
BC	.22	17.75	1.15	55.34	.00	20.53	.30	.14	.14	6.34	.04	
AC	.24	17.75	1.17	53.92	.00	20.53	.30	.14	.14	6.50	.04	100.73
Fm	.017	.962	.049	1.961	.000	.799	.007	.003	.004	.197	.001	4.000

	NA	MG	AL	SI	K	CA	TI	CR	MN	FE	NI	TOTAL
BG	.40	2.60	2.67	5.34	3.46	5.38	11.50	18.84	1.41	1.59	2.51	
C1	.23	9.64	1.79	24.79	.00	14.55	.41	.01	.11	5.84	.05	
BC	.31	15.99	3.39	53.04	.00	20.35	.68	.02	.13	7.51	.07	
AC	.34	16.16	3.42	52.11	.00	20.31	.67	.02	.14	[illegible]	.07	100.40
Fm	.025	.880	.146	1.985	.000	.794	.018	.000	.003	.233	.002	4.006

Clinopyroxene H-80-90

	NA	MG	AL	SI	K	CA	TI	CR	MN	FE	NI	TOTAL
BG	.14	1.71	3.87	5.31	.59	.90	2.57	5.99	1.45	1.63	3.02	
C1	.24	9.45	1.67	24.96	-.01	14.93	.32	.11	.10	4.98	-.02	
BC	.32	15.67	3.16	53.40	.00	20.89	.53	.15	.13	6.41	.00	
AC	.35	15.74	3.17	52.20	.00	20.86	.52	.16	.13	6.56	.00	99.68
FM	.023	.864	.137	1.923	.000	.823	.014	.004	.003	.201	.000	3.992

	NA	MG	AL	SI	K	CA	TI	CR	MN	FE	NI	TOTAL
BG	.20	2.93	5.63	5.52	.41	1.12	3.23	5.38	1.46	1.02	2.66	
C1	.25	9.07	1.77	24.39	.05	15.31	.32	.10	.08	5.16	.02	
BC	.34	15.04	3.34	52.18	.05	21.42	.53	.14	.11	6.64	.03	
AC	.36	15.16	3.34	51.03	.05	21.37	.52	.14	.11	6.79	.03	98.91
FM	.026	.843	.146	1.905	.002	.854	.014	.003	.003	.211	.000	4.009

	NA	MG	AL	SI	K	CA	TI	CR	MN	FE	NI	TOTAL
BG	.20	3.67	3.41	5.11	.23	.90	3.38	5.41	2.02	1.63	2.89	
C1	.20	9.30	1.78	23.53	.05	15.93	.21	.12	.10	5.25	.00	
BC	.27	15.42	3.36	50.33	.06	22.28	.34	.18	.13	6.75	.00	
AC	.29	15.57	3.38	49.38	.06	22.21	.34	.18	.13	6.90	.00	98.46
FM	.021	.877	.149	1.867	.002	.899	.009	.004	.003	.217	.000	4.049

	NA	MG	AL	SI	K	CA	TI	CR	MN	FE	NI	TOTAL
BG	.54	1.22	2.45	5.31	.91	1.12	2.47	5.66	1.18	3.88	2.76	
C1	.20	9.26	1.85	23.98	-.02	15.71	.37	.12	.14	5.10	.00	
BC	.27	15.36	3.49	51.30	.00	21.98	.61	.17	.18	6.55	.00	
AC	.30	15.48	3.51	50.28	.00	21.91	.60	.18	.19	6.71	.00	99.15
FM	.021	.862	.153	1.879	.000	.877	.016	.004	.005	.209	.000	4.027

	NA	MG	AL	SI	K	CA	TI	CR	MN	FE	NI	TOTAL
BG	.78	2.69	4.41	4.49	1.02	1.34	3.07	6.61	2.34	3.18	2.20	
C1	.16	9.14	2.05	24.29	-.03	14.64	.38	.07	.04	5.36	.02	
BC	.22	15.16	3.87	51.95	.00	20.48	.63	.10	.04	6.39	.02	
AC	.24	15.27	3.88	50.96	.00	20.45	.62	.10	.04	7.05	.03	98.63
FM	.016	.849	.169	1.903	.000	.817	.016	.002	.001	.219	.000	3.992

Clinopyroxene H-80-90

	NA	MG	AL	SI	K	CA	TI	CR	MN	FE	NI	TOTAL
BG	.44	1.91	3.90	5.53	.68	1.12	2.53	6.09	1.83	2.07	2.84	
C1	.07	9.27	1.51	24.46	.00	16.30	.41	.05	.12	5.05	-.02	
BC	.09	15.37	2.86	52.34	.00	22.80	.68	.07	.15	6.49	.00	
AC	.10	15.47	2.86	51.05	.00	22.73	.67	.08	.16	6.64	.00	99.77
FM	.006	.856	.125	1.896	.000	.904	.018	.002	.004	.206	.000	4.018

	NA	MG	AL	SI	K	CA	TI	CR	MN	FE	NI	TOTAL
BG	.45	3.64	3.52	4.86	1.41	1.55	3.23	5.98	1.66	1.82	2.63	
C1	.19	9.80	1.28	24.79	-.07	16.20	.25	.01	.05	4.76	.04	
BC	.26	16.25	2.41	53.03	.00	22.66	.41	.02	.07	6.13	.05	
AC	.28	16.30	2.43	51.73	.00	22.62	.41	.02	.07	6.27	.05	100.18
FM	.019	.896	.105	1.909	.000	.895	.011	.000	.002	.192	.001	4.030

	NA	MG	AL	SI	K	CA	TI	CR	MN	FE	NI	TOTAL
BG	.34	1.94	2.98	4.45	.61	1.34	2.61	5.81	1.41	1.62	3.91	
C1	.14	9.39	1.36	24.09	.03	16.15	.37	.09	.16	4.58	-.09	
BC	.18	15.57	2.57	51.53	.03	22.60	.62	.14	.20	5.89	.00	
AC	.20	15.64	2.59	50.25	.03	22.54	.61	.14	.20	6.03	.00	98.22
FM	.013	.878	.114	1.895	.001	.911	.017	.003	.005	.189	.000	4.025

	NA	MG	AL	SI	K	CA	TI	CR	MN	FE	NI	TOTAL
BG	.15	2.66	3.32	3.83	.60	1.33	2.70	5.70	1.80	2.02	2.62	
C1	.13	9.13	1.44	24.47	.02	15.25	.29	.23	.11	4.54	.04	
BC	.18	15.13	2.72	52.34	.02	21.34	.47	.34	.13	5.83	.05	
AC	.19	15.18	2.73	50.98	.02	21.31	.47	.35	.14	5.97	.05	97.38
FM	.013	.854	.121	1.925	.000	.862	.013	.010	.003	.188	.001	3.991

	NA	MG	AL	SI	K	CA	TI	CR	MN	FE	NI	TOTAL
SD	.04	.28	.09	.25	.04	.53	.07	.10	.04	.22	.06	
C1	.13	9.34	1.41	24.45	.00	15.83	.32	.12	.11	4.69	.00	
BC	.17	15.49	2.66	52.31	.00	22.14	.53	.18	.13	6.04	.00	
AC	.18	15.55	2.66	50.99	.00	22.10	.52	.18	.14	6.18	.00	98.50
FM	.013	.869	.118	1.911	.000	.886	.014	.004	.003	.193	.000	4.011

Clinopyroxene H-80-90

	NA	MG	AL	SI	K	CA	TI	CR	MN	FE	NI	TOTAL
;	.37	1.54	3.37	5.02	.71	1.16	2.65	6.65	1.63	2.51	2.95	
I	.26	8.98	2.18	23.50	.01	15.64	.41	.02	.17	5.80	.00	
:	.34	14.89	4.13	50.26	.01	21.88	.68	.03	.22	7.46	.00	
:	.38	15.13	4.15	49.48	.01	21.80	.67	.04	.23	7.63	.00	99.50
1	.027	.844	.182	1.853	.000	.875	.019	.000	.006	.238	.000	4.045

	NA	MG	AL	SI	K	CA	TI	CR	MN	FE	NI	TOTAL
G	.20	1.49	3.88	3.65	1.29	1.11	3.03	6.45	1.53	2.23	2.52	
.1	.12	9.13	2.21	23.66	-.05	15.11	.36	.06	.09	5.64	.01	
:C	.16	15.13	4.17	50.61	.00	21.14	.61	.08	.11	7.25	.01	
C	.18	15.29	4.19	49.80	.00	21.08	.59	.09	.11	7.42	.01	98.76
M	.012	.854	.185	1.868	.000	.846	.016	.002	.003	.232	.000	4.017

	NA	MG	AL	SI	K	CA	TI	CR	MN	FE	NI	TOTAL
IG	.30	1.94	2.91	5.67	.20	.89	3.16	5.70	1.68	2.02	2.42	
:1	.22	9.33	1.88	23.88	.05	15.08	.41	.11	.12	5.25	.06	
IC	.29	15.47	3.55	51.09	.05	21.09	.69	.16	.16	6.76	.08	
IC	.32	15.62	3.58	50.17	.05	21.04	.68	.17	.16	6.91	.08	98.78
M	.023	.872	.157	1.881	.002	.845	.019	.004	.004	.215	.002	4.024

	NA	MG	AL	SI	K	CA	TI	CR	MN	FE	NI	TOTAL
SD	.11	4.02	4.54	2.83	.32	.96	.13	.05	.04	1.77	.03	
C1	.16	7.39	4.07	22.46	.15	15.64	.34	.06	.11	6.27	.03	
BC	.21	12.25	7.68	48.06	.18	21.88	.57	.09	.14	8.06	.03	
AC	.24	12.50	7.62	47.68	.18	21.78	.55	.09	.14	8.23	.04	99.05
FM	.016	.701	.337	1.798	.007	.879	.015	.002	.004	.259	.000	4.020

	NA	MG	AL	SI	K	CA	TI	CR	MN	FE	NI	TOTAL
G	.20	2.27	4.18	5.58	.82	.95	2.89	6.33	1.91	1.99	3.21	
:1	.40	9.96	1.72	25.13	.00	15.39	.15	.31	.05	3.17	.00	
C	.54	16.51	3.25	53.76	.00	21.54	.25	.45	.06	4.07	.00	
C	.57	16.32	3.24	52.40	.00	21.56	.24	.48	.07	4.18	.00	99.06
M	.040	.894	.140	1.929	.000	.850	.006	.013	.001	.128	.000	4.001

	NA	MG	AL	SI	K	CA	TI	CR	MN	FE	NI	TOTAL
G	.41	1.23	3.67	5.54	.39	.86	2.52	5.75	2.02	3.23	3.03	
1	.09	9.33	1.76	24.64	.04	15.11	.42	.09	.07	5.14	-.03	
C	.12	15.47	3.33	52.70	.05	21.13	.70	.14	.08	6.61	.00	
C	.13	15.55	3.34	51.54	.04	21.09	.69	.14	.09	6.76	.00	99.37
M	.008	.858	.146	1.911	.001	.837	.018	.003	.002	.208	.000	3.993

Clinopyroxena H-80-92

NA	MG	AL	SI	K	CA	TI	CR	MN	FE	NI	TOTAL
.66	1.90	2.60	3.37	3.14	4.80	11.58	21.23	1.72	2.27	2.94	
.19	9.52	2.15	24.03	.01	14.75	.38	.16	.13	6.1[illegible]	-.02	
.25	15.78	4.06	51.40	.01	20.64	.63	.23	.16	7.84	.00	
.27	15.99	4.10	50.71	.01	20.57	.61	.24	.17	8.01	.00	100.69
.019	.878	.177	1.867	.000	.812	.016	.095	.004	.246	.000	4.027

NA	MG	AL	SI	K	CA	TI	CR	MN	FE	NI	TOTAL
.19	2.60	3.89	4.16	1.98	6.76	12.47	18.85	1.31	2.17	2.51	
.34	11.77	.92	26.11	.01	13.62	.14	.46	.11	3.03	.02	
.46	19.51	1.74	55.84	.01	19.05	.23	.67	.14	4.66	.02	
.48	19.23	1.77	54.63	.01	19.09	.22	.70	.14	4.78	.02	101.09
.033	1.028	.073	1.960	.000	.733	.005	.019	.004	.143	.000	3.999

NA	MG	AL	SI	K	CA	TI	CR	MN	FE	NI	TOTAL
.79	2.36	4.50	5.15	3.38	6.33	11.40	20.01	1.48	2.77	2.43	
.20	11.12	1.23	25.96	.09	14.66	.20	.55	.07	3.51	.05	
.27	18.44	2.32	55.54	.09	20.54	.33	.80	.08	4.51	.07	
.28	18.21	2.34	54.23	.00	20.57	.32	.83	.09	4.63	.07	101.56
.019	.972	.098	1.942	.000	.789	.008	.023	.002	.137	.002	3.991

NA	MG	AL	SI	K	CA	TI	CR	MN	FE	NI	TOTAL
1.05	1.42	3.32	3.16	2.58	4.58	11.20	19.59	1.23	1.43	2.69	
.20	11.16	1.16	25.21	.01	14.40	.16	.64	.06	3.32	.03	
.26	18.50	2.20	56.07	.01	20.27	.27	.93	.07	4.27	.04	
.27	18.23	2.21	54.68	.01	20.[illegible]	.26	.98	.07	4.39	.04	101.43
.019	.971	.092	1.955	.000	.777	.006	.027	.002	.131	.001	3.980

NA	MG	AL	SI	K	CA	TI	CR	MN	FE	NI	TOTAL
.34	3.09	3.80	4.35	2.93	3.70	13.74	21.51	1.49	1.76	2.26	
.13	11.02	1.14	25.66	.01	14.73	.16	.59	.06	3.01	.09	
.17	18.26	2.14	54.89	.01	20.61	- .27	.87	.07	3.87	.11	
.18	17.96	2.16	53.49	.01	20.65	.26	.90	.07	3.97	.12	99.78
.012	.974	.092	1.947	.000	.805	.006	.025	.002	.121	.003	3.987

NA	MG	AL	SI	K	CA	TI	CR	MN	FE	NI	TOTAL
.43	1.66	5.20	3.96	2.[illegible]	[illegible]	10.16	21.41	1.36	1.[illegible]	2.63	
.28	10.95	1.16	25.54	.01	14.22	.16	.61	.09	3.42	.05	
.38	18.15	2.19	54.63	.01	19.89	.27	.88	.11	4.40	.06	
.40	17.94	2.21	53.35	.01	19.92	.26	.92	.11	4.52	.06	99.70
.020	.975	.094	1.947	.000	.773	.006	.025	.003	.137	.001	3.9[illegible]

Amphibole P-79-82

	NA	MG	AL	SI	K	CA	TI	CR	MN	FE	NI	TOTAL
BG	.20	1.91	4.29	3.58	3.98	5.26	12.55	22.31	1.54	2.38	2.59	
CI	1.52	8.79	5.74	19.29	.91	8.05	1.98	-.01	.09	8.61	.04	
BC	2.04	14.57	10.85	41.27	1.09	11.26	3.31	.00	.11	11.07	.04	
AC	2.29	15.21	11.14	42.73	1.07	11.20	3.19	.00	.11	11.23	.05	98.22
FM	.646	3.315	1.919	6.253	.197	1.756	.348	.000	.013	1.374	.004	15.829

	NA	MG	AL	SI	K	CA	TI	CR	MN	FE	NI	TOTAL
BG	.63	2.20	3.31	4.90	3.10	5.06	11.31	21.70	1.93	2.37	2.10	
CI	1.70	8.98	6.56	18.70	.85	8.00	1.77	.01	.03	8.29	.05	
BC	2.29	14.84	12.40	40.01	1.02	11.20	2.74	.02	.04	10.66	.06	
AC	2.53	15.48	12.73	41.74	1.00	11.15	2.84	.02	.04	10.82	.07	98.42
FM	.715	3.368	2.169	5.992	.184	1.744	.308	.000	.004	1.319	.004	15.927

	NA	MG	AL	SI	K	CA	TI	CR	MN	FE	NI	TOTAL
BG	1.00	2.40	3.59	4.33	3.00	5.95	8.66	19.46	1.51	2.00	2.80	
CI	1.34	6.64	6.48	13.68	.91*	7.97	1.77	.04	.09	9.03	.00	
BC	1.80	14.32	12.25	39.75	1.10	11.15	2.95	.05	.11	11.62	.00	
AC	2.02	14.96	12.56	41.63	1.08	11.09	2.84	.05	.11	11.77	.00	98.11
FM	.573	3.273	2.173	6.115	.198	1.742	.310	.004	.013	1.444	.000	15.846

	NA	MG	AL	SI	K	CA	TI	CR	MN	FE	NI	TOTAL
BG	.20	2.86	2.14	4.38	1.98	7.67	14.24	26.32	1.59	2.78	2.80	
CI	1.57	8.80	5.62	19.54	.73	[illegible]	1.76	-.04	.12	8.50	.00	
BC	2.11	14.56	11.00	41.79	1.12	11.34	3.28	.00	.16	10.94	.00	
AC	2.35	15.21	11.28	43.23	1.09	11.29	3.16	.00	.16	11.09	.00	98.[illegible]
FM	.660	3.269	1.930	6.275	.200	1.755	.345	.000	.017	1.346	.000	15.815

	NA	MG	AL	SI	K	CA	TI	CR	MN	FE	NI	TOTAL
BG	.39	2.36	2.62	4.18	1.98	5.48	14.98	21.27	1.33	3.18	3.25	
CI	1.20	5.97	5.78	15.76	.45	9.00	2.02	.00	.13	8.62	-.04	
BC	2.15	14.50	10.92	40.35	1.14	11.19	3.38	.03	.15	11.09	.00	
AC	2.41	15.48	11.24	42.07	1.11	11.13	3.25	.00	.16	11.25	.00	98.[illegible]
FM	.656	3.389	1.944	6.133	.207	1.750	.357	.000	.017	1.379	.000	15.913

Amphibole P-79-95

NA	MG	AL	SI	K	CA	TI	CR	MN	FE	NI	TOTAL
.50	1.59	3.47	4.83	3.00	5.32	11.97	20.23	1.50	2.37	2.73	
1.38	8.72	6.18	19.33	.93	8.01	1.79	-.01	.13	8.89	.01	
1.85	14.45	11.67	41.36	1.12	11.21	2.98	.00	.17	11.44	.01	
2.07	15.09	11.96	42.91	1.09	11.16	2.87	.00	.17	11.59	.01	98.93
.584	3.267	2.047	6.235	.200	1.735	.311	.000	.017	1.407	.000	15.803

NA	MG	AL	SI	K	CA	TI	CR	MN	FE	NI	TOTAL
.59	1.42	2.38	4.18	1.98	5.48	14.01	20.17	1.57	1.79	2.51	
1.22	8.61	6.12	19.40	.87	7.97	1.71	.00	.07	8.47	.05	
1.64	14.28	11.56	41.50	1.04	11.15	2.85	.00	.08	10.90	.07	
1.83	14.83	11.81	42.98	1.02	11.11	2.76	.00	.08	11.05	.07	97.56
.521	3.239	2.039	6.303	.189	1.742	.301	.000	.008	1.355	.008	15.705

NA	MG	AL	SI	K	CA	TI	CR	MN	FE	NI	TOTAL
.39	1.19	4.77	6.57	3.58	5.26	14.30	23.10	1.73	.99	1.98	
1.48	8.28	6.13	19.39	.92	7.91	1.79	-.01	.08	8.68	.04	
1.99	13.72	11.57	41.49	1.11	11.07	2.99	.00	.11	11.16	.05	
2.23	14.34	11.82	42.95	1.09	11.02	2.89	.00	.11	11.32	.05	97.81
.632	3.134	2.040	6.302	.202	1.730	.314	.000	.013	1.386	.004	15.757

NA	MG	AL	SI	K	CA	TI	CR	MN	FE	NI	TOTAL
.20	2.38	3.81	2.98	3.18	5.70	11.65	19.08	2.46	1.79	3.07	
1.61	8.53	6.11	18.73	.86	7.93	1.74	.02	.04	9.09	-.01	
2.17	14.14	11.55	40.06	1.03	11.10	2.90	.02	.05	11.70	.00	
2.44	14.84	11.88	41.68	1.01	11.04	2.79	.02	.05	11.86	.00	97.59
.698	3.266	2.069	6.160	.187	1.748	.308	.000	.004	1.461	.000	15.900

NA	MG	AL	SI	K	CA	TI	CR	MN	FE	NI	TOTAL
.80	2.62	3.34	6.16	2.38	3.72	11.55	21.70	1.77	2.98	2.38	
1.52	8.49	6.20	19.13	.83	8.10	1.76	-.01	.11	8.93	.03	
2.04	14.08	11.71	40.93	1.00	11.33	2.93	.00	.13	11.48	.04	
2.29	14.74	12.00	42.50	.97	11.28	2.83	.00	.14	11.64	.04	98.42
.648	3.210	2.069	6.215	.180	1.764	.309	.000	.013	1.420	.004	15.833

Amphibole C-79-10b

	NA	MG	AL	SI	K	CA	TI	CR	MN	FE	NI	TOTAL
G	.34	1.88	3.37	5.82	.71	1.13	3.16	6.30	1.78	2.09	2.80	
C1	.65	9.62	1.49	25.25	.29	8.03	.30	.00	.07	10.30	-.01	
C	.88	15.95	2.81	54.02	.35	11.23	.51	.00	.09	13.25	.00	
C	1.00	16.65	2.91	53.85	.34	11.22	.49	.00	.09	13.45	.00	100.00
M	.273	3.500	.480	7.602	.058	1.694	.049	.000	.008	1.586	.000	15.251

	NA	MG	AL	SI	K	CA	TI	CR	MN	FE	NI	TOTAL
G	.41	1.48	3.54	4.13	.65	1.59	3.24	7.51	1.69	2.27	3.09	
1	.67	9.11	2.16	24.49	.56	8.46	.32	-.04	.15	11.24	.00	
C	.90	15.10	4.09	52.39	.68	11.83	.53	.00	.19	14.46	.00	
C	1.03	15.91	4.23	52.54	.66	11.80	.52	.00	.19	14.66	.00	101.54
M	.280	3.334	.697	7.387	.115	1.774	.053	.000	.021	1.721	.000	15.383

	NA	MG	AL	SI	K	CA	TI	CR	MN	FE	NI	TOTAL
G	.41	1.98	4.20	4.54	.19	1.36	3.02	5.45	1.11	3.30	1.23	
C1	.50	9.32	1.61	24.83	.52	8.37	.39	.01	.10	11.55	.09	
C	.67	15.45	3.03	53.12	.63	11.71	.65	.02	.13	14.85	.12	
C	.77	16.31	3.15	53.12	.61	11.68	.63	.02	.13	15.05	.13	101.59
M	.206	3.418	.520	7.472	.107	1.758	.066	.000	.012	1.771	.012	15.343

	NA	MG	AL	SI	K	CA	TI	CR	MN	FE	NI	TOTAL
D	.09	.21	.30	.31	.13	.19	.05	.02	.03	.59	.06	
1	.58	9.34	1.71	24.85	.47	8.30	.35	-.01	.10	11.16	.04	
C	.78	15.48	3.24	53.16	.57	11.62	.59	.00	.13	14.35	.05	
C	.89	16.29	3.36	53.16	.56	11.59	.57	.00	.13	14.55	.05	101.15
M	.244	3.417	.553	7.482	.099	1.748	.058	.000	.012	1.710	.004	15.326

Amphibole C-79-13b

	NA	MG	AL	SI	K	CA	TI	CR	MN	FE	NI	TOTAL
BG	.34	1.75	3.96	5.15	.91	1.30	2.96	7.36	1.73	2.55	2.45	
C1	.16	4.16	1.25	24.09	.29	9.59	.13	.02	.24	18.55	.06	
BC	.21	6.89	2.37	51.52	.34	13.41	.21	.03	.31	23.86	.07	
AC	.27	7.83	2.45	51.02	.33	13.21	.20	.03	.31	23.94	.08	99.68
FM	.075	1.746	.431	7.649	.062	2.120	.022	.000	.040	3.000	.009	15.151

	NA	MG	AL	SI	K	CA	TI	CR	MN	FE	NI	TOTAL
BG	.38	2.44	3.84	5.09	.45	.44	3.12	7.48	2.27	2.84	2.88	
C1	.24	3.34	2.95	20.24	.41	12.25	4.63	.00	.15	11.91	.01	
BC	.32	5.53	5.58	43.30	.49	17.14	7.72	.00	.19	15.32	.01	
AC	.40	6.11	5.59	42.74	.47	16.76	7.42	.00	.19	15.46	.01	95.15
FM	.119	1.420	1.026	6.672	.091	2.804	.871	.000	.022	2.016	.000	15.042

	NA	MG	AL	SI	K	CA	TI	CR	MN	FE	NI	TOTAL
G	1.49	2.92	3.17	4.07	.73	1.56	3.12	6.95	1.62	3.87	2.64	
1	.42	5.20	1.71	23.86	.70	7.20	.10	.00	.25	16.04	.05	
C	.56	8.61	3.24	51.04	.84	10.07	.17	.00	.32	20.63	.06	
C	.70	9.57	3.34	50.82	.82	9.98	.16	.00	.32	20.75	.07	96.52
M	.205	2.163	.596	7.708	.156	1.620	.018	.000	.040	2.630	.004	15.139

	NA	MG	AL	SI	K	CA	TI	CR	MN	FE	NI	TOTAL
G	.16	1.95	3.41	4.27	.81	.44	3.91	7.63	2.19	1.83	3.53	
1	.09	4.75	1.66	24.13	.20	7.93	.00	-.01	.21	17.05	-.03	
C	.11	7.88	3.13	51.63	.24	11.09	.00	.00	.28	21.94	.00	
C	.14	8.80	3.23	51.28	.23	10.96	.00	.00	.28	22.05	.00	96.96
M	.040	1.979	.572	7.752	.044	1.775	.000	.000	.035	2.787	.000	14.984

	NA	MG	AL	SI	K	CA	TI	CR	MN	FE	NI	TOTAL
	.14	.72	.64	1.71	.21	2.03	2.04	.02	.04	2.52	.04	
	.20	4.44	1.85	23.29	.36	8.98	.97	.00	.21	16.12	.01	
	.26	7.36	3.49	49.82	.43	12.56	1.61	.00	.27	20.73	.01	
	.32	8.22	3.58	49.41	.42	12.39	1.54	.00	.27	20.86	.01	97.02
	.093	1.860	.638	7.512	.080	2.016	.174	.000	.031	2.649	.000	15.053

Amphibole C-79-19

	NA	MG	AL	SI	K	CA	TI	CR	MN	FE	NI	TOTAL
BG	.68	2.13	3.51	5.52	.64	1.16	2.88	6.98	1.77	2.01	2.96	
C1	.27	6.97	1.88	24.21	.10	9.25	.07	-.05	.25	14.09	-.02	
BC	.36	11.56	3.55	51.79	.12	12.95	.11	.00	.32	18.12	.00	
AC	.43	12.54	3.66	51.68	.12	12.84	.11	.00	.33	18.30	.00	100.00
FM	.031	.707	.163	1.954	.005	.520	.002	.000	.010	.578	.000	3.970

	NA	MG	AL	SI	K	CA	TI	CR	MN	FE	NI	TOTAL
BG	.47	2.00	3.43	5.86	.88	1.16	3.00	6.56	1.80	2.89	3.20	
C1	.13	5.90	.81	24.95	.08	9.87	.04	.02	.17	15.92	.00	
BC	.18	9.78	1.53	53.38	.09	13.81	.06	.02	.21	20.48	.00	
AC	.21	10.81	1.58	52.70	.09	13.66	.06	.02	.22	20.64	.00	99.99
FM	.060	2.362	.271	7.728	.013	2.147	.004	.000	.025	2.530	.000	15.140

	NA	MG	AL	SI	K	CA	TI	CR	MN	FE	NI	TOTAL
BG	.41	1.71	4.13	5.73	.61	.67	3.20	5.92	1.72	2.66	2.86	
C1	.21	5.75	1.04	24.65	.06	10.84	.14	.03	.16	15.66	.00	
BC	.29	9.53	1.97	52.73	.07	15.16	.23	.04	.20	20.14	.00	
AC	.36	10.54	2.03	52.08	.07	14.98	.21	.04	.20	20.31	.00	100.82
FM	.098	2.291	.347	7.599	.013	2.342	.021	.004	.021	2.475	.000	15.209

	NA	MG	AL	SI	K	CA	TI	CR	MN	FE	NI	TOTAL
BG	.78	1.96	3.40	5.93	.67	1.12	2.91	6.78	2.05	1.84	2.96	
C1	.16	5.62	1.11	24.19	.07	10.46	.09	.02	.11	16.74	-.02	
BC	.22	9.31	2.09	51.74	.09	14.63	.16	.03	.13	21.54	.00	
AC	.28	10.38	2.16	51.29	.09	14.45	.15	.03	.14	21.68	.00	100.64
FM	.078	2.277	.372	7.554	.013	2.277	.013	.000	.013	2.666	.000	15.262

	NA	MG	AL	SI	K	CA	TI	CR	MN	FE	NI	TOTAL
BG	.24	1.98	4.66	4.74	.58	1.05	3.14	5.84	2.64	2.47	2.41	
C1	.20	7.12	1.21	25.44	.07	9.47	.01	.02	.13	13.11	.05	
BC	.27	11.80	2.28	54.42	.08	13.25	.01	.03	.16	16.87	.07	
AC	.32	12.70	2.34	53.77	.08	13.16	.01	.04	.17	17.06	.07	99.72
FM	.089	2.726	.394	7.754	.013	2.031	.000	.000	.017	2.057	.000	15.087

Amphibole in Magnetite-Apatite-Actinolite Vein

	NA	MG	AL	SI	K	CA	TI	CR	MN	FE	NI	TOTAL
BG	.27	1.77	4.05	4.84	.79	.71	3.20	6.73	1.69	1.93	2.34	
C1	.05	9.36	.17	25.96	.01	8.83	.01	.01	.16	10.01	.04	
BC	.07	15.51	.32	55.54	.01	12.35	.02	.02	.20	12.88	.04	
AC	.08	16.14	.32	54.57	.01	12.33	.02	.02	.21	13.09	.05	96.83
FM	.021	3.495	.055	7.923	.000	1.918	.000	.000	.021	1.590	.004	15.027

	NA	MG	AL	SI	K	CA	TI	CR	MN	FE	NI	TOTAL
BG	.15	.98	3.80	4.95	1.32	.68	2.94	6.13	1.05	3.92	2.61	
C1	.07	4.24	.34	24.62	-.03	8.59	.03	.07	.60	18.80	.05	
BC	.09	7.03	.63	52.66	.00	12.02	.05	.09	.77	24.18	.06	
AC	.12	8.03	.66	51.88	.00	11.84	.05	.09	.77	24.24	.06	97.72
FM	.032	1.900	.121	8.255	.000	2.017	.004	.009	.103	3.222	.004	15.667

APPENDIX 5a

Major element analyses were performed by standard atomic absorption techniques. One half of one gram of rock powder was dissolved in a solution of 5 ml HF, 50 ml H_3BO_3, and 145 ml H_2O and was heated on a steam bath.

Precision:

Oxide	Range	No of samples	Mean	Std. Dev.
SiO_2	76.0-76.6	8	76.4	.2976
TiO_2	0.12-0.22	8	0.17	.0366
Al_2O_3	11.8-11.9	8	11.9	.0463
Fe_2O_3**	1.06-1.13	8	1.08	.0301
MnO	0.01-0.01	8	0.01	.0000
MgO	0.24-0.28	8	0.26	.0167
CaO	0.40-0.50	8	0.45	.0354
Na_2O	2.67-2.75	8	2.71	.0324
K_2O	4.22-4.34	8	4.28	.0351
SiO_2	62.2-63.1	8	62.7	.2973
TiO_2	0.20-0.40	8	0.31	.0674
Al_2O_3	14.4-14.8	8	14.6	.1458
Fe_2O_3	4.49-4.80	8	4.68	.1178
MnO	0.10-0.10	8	0.10	.0000
MgO	2.32-2.40	8	2.37	.0301
CaO	3.72-3.86	8	3.78	.0483
Na_2O	2.15-2.19	8	2.18	.0160
K_2O	4.10-4.28	8	4.15	.0632

Accuracy:

Oxide	Pub. Val.	No of Analyses	Mean	Std. Dev.
		GSP-1		
SiO_2	67.27	7	68.65	0.60
TiO_2	0.65	7	0.60	0.08
Al_2O_3	15.18	7	14.77	0.22
Fe_2O_3**	4.26	8	4.22	0.07
CaO	2.06	8	1.94	0.07
MgO	0.98	7	0.96	0.03
Na_2O	2.77	8	2.74	0.06
K_2O	5.50	6	5.44	0.12
MnO	0.04	8	0.04	0.01
		AGV-1		
SiO_2	58.97	3	59.63	0.90
TiO_2	1.06	3	1.08	0.11
Al_2O_3	17.01	4	17.13	0.23
Fe_2O_3**	6.73	4	6.70	0.33
CaO	4.94	4	4.78	0.16
MgO	1.53	4	1.47	0.07
Na_2O	4.26	4	4.06	0.12
K_2O	2.86	3	2.88	0.10
MnO	0.10	4	0.10	0.00

Published values from Abbey, 1970

APPENDIX 5b

For trace elements, pellets comprising 10 g of rock powder and 1.4-1.5 g of phenol formaldehyde were pressed to 50 MPa and analyzed on a Phillips 1450 X-ray flouresence spectrometer. International standards were used for calibration purposes. Estimates of analytical uncertainty are 3-5 percent or 1 ppm, whichever is the larger (Easton, 1982). Easton (1982) has shown that the effects of sample inhomogeneity, contamination, or variation in outcrop are within the analytical uncertainty of the method.

For REE, calibration of the XRF was by using international standards and spec pure samples of the REE. Estimated analytical uncertainty is ± 10 percent. Easton (1982) has compared the XRF thin film method with Intrumental Neutron Activation Analysis and has demonstrated that any variation is within analytical uncertainty. Precision, or repeatability, of the XRF method is also well within the analytical uncertainty.

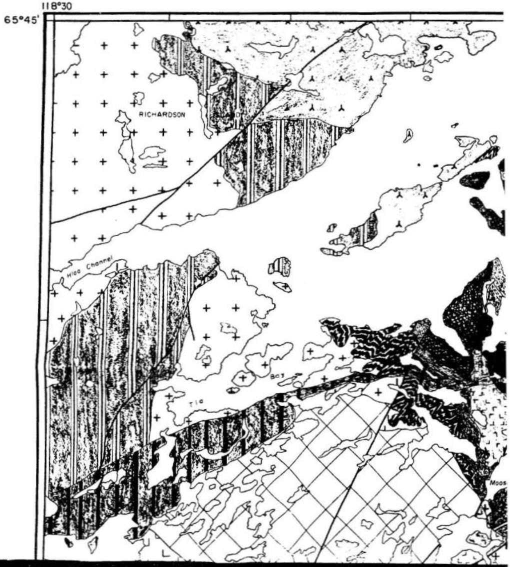
118°30
65°45'
RICHARDSON
Hloo Channel
Bay
Tla
Moos

118°
Bloo
Island
Cobalt Island
Animal
Lake
Mule
Bay
Moose Bay
Balachey

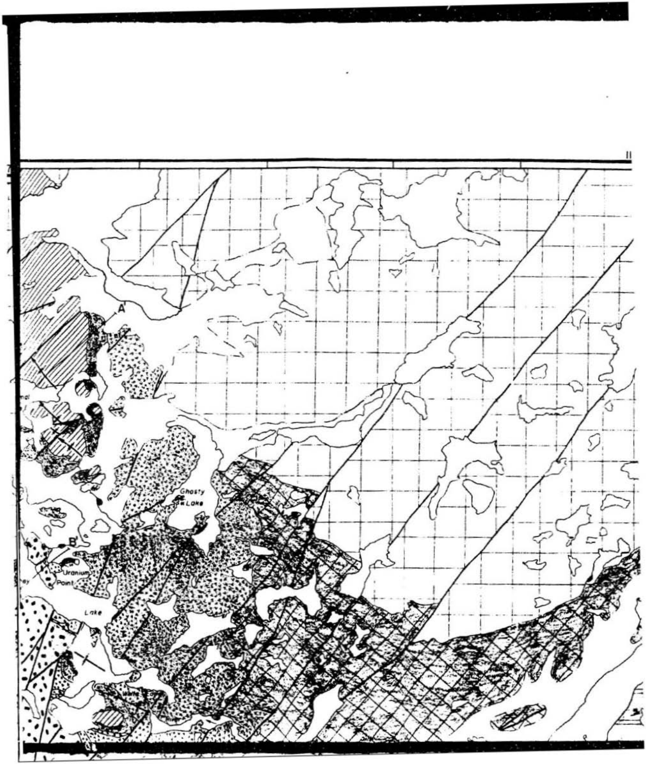

A'
Ghosty
Lake
B'
Uranium
Point
Lake

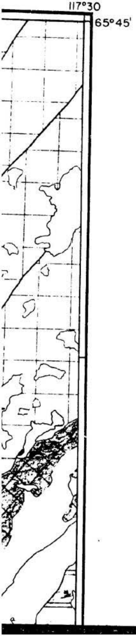
117°30
65°45'

NATIONAL TOPOGRAPHIC SYSTEM 1:50,000

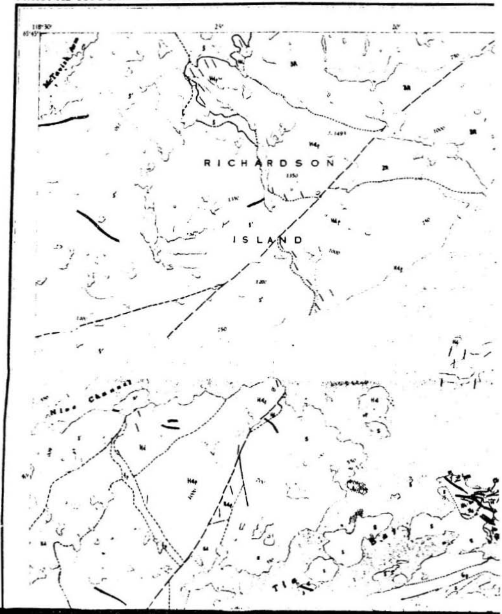

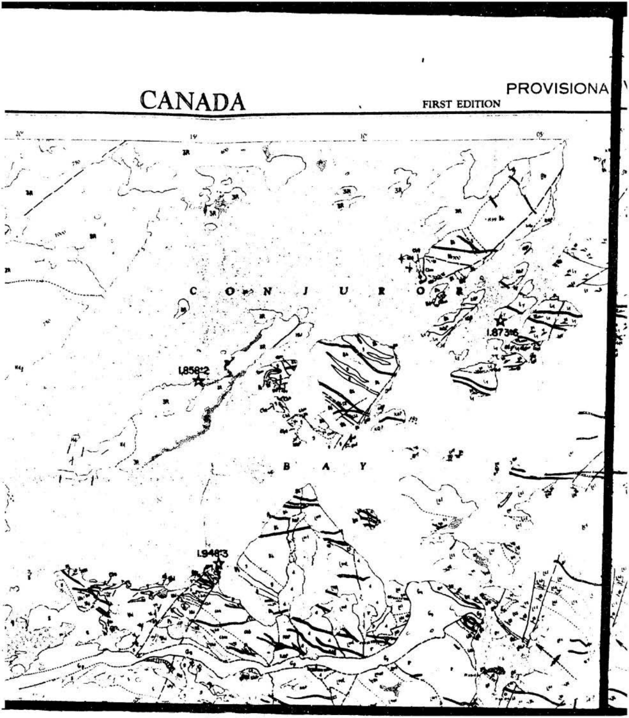
CANADA
FIRST EDITION
PROVISIONA
C O N J U R O R
B A Y
1,858±2
1,873±6
1,948±3

VISIONAL MAP

SHEET 86 E/9

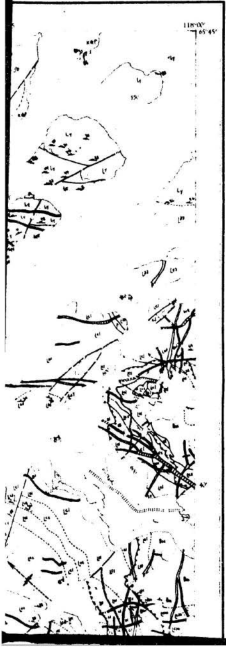

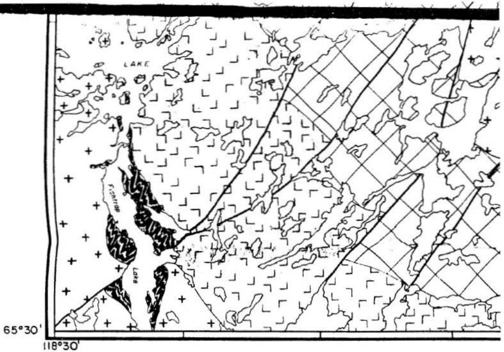

? Gunbarrel Gabbro

GREAT BEAR MAGMATIC

McTav

unnamed granites

Hooker Granite

Richardson Granite'

Tla Granite

Yen Pluton

plagioclase porphyry

quartz diorite

cambrian

hebian

ABINE GROUP

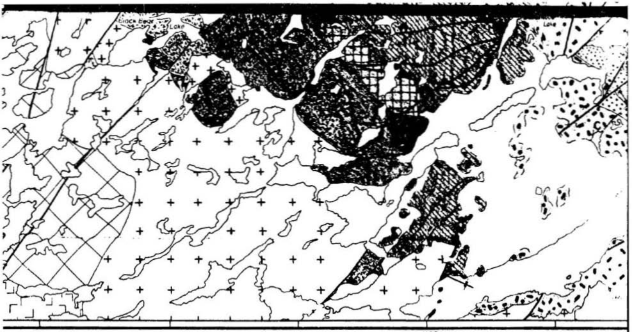

GEOLOGICAL MAP

of the

CAMSELL RIVER-CONJUROR AREA

R MAGMATIC BELT

McTavish Supergroup

ABINE GROUP

- "younger ash-flow tuffs"[4]
- Animal Andesite
- Uranium Point Formation
- White Eagle Tuff
  - mesobreccia member
- Camsell River Formation
- Arden Formation
- Moose Bay Tuff

Clut Cauldron Complex

Mule Bay Cauldron Complex

A

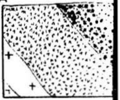


CLUT
ISLAND
CLUT
LAKE
GROUARD LAKE


0 1 2 3 4kilometres

ROR BAY

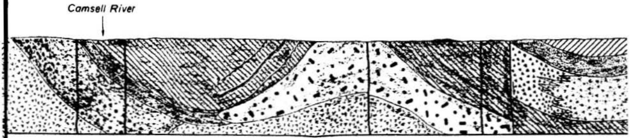
Camsell River

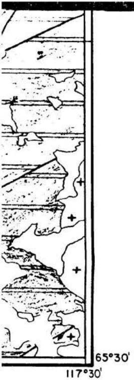
65°30'
117°30'

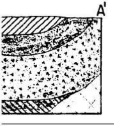
A'

Produced and printed by the SURVEYS AND MAPPING BRANCH, DEPARTMENT OF MINES AND TECHNICAL SURVEYS, [illegible] 1950 and 1954

The nomenclature on this map has not been submitted to the Canadian Board on Geographical Names and may be subject to revision

REFERENCE

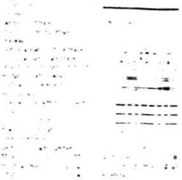

MAP I

the Canadian
ision

RAINY LAKE

DISTRICT OF MACKENZIE

NORTHWEST TERRITORIES

SCALE 1:50 000

REFERENCE

R.S. HILDEBRAND

1982

preliminary map

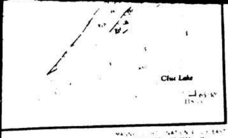

86 E 9

Appendix

MAP I

CAN

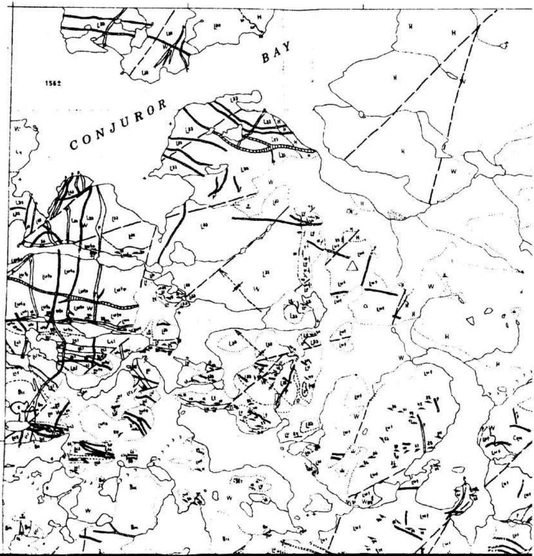

CANADA

EDITIO

EDITION 1   86 F/12

Military users,
refer to this map
Reference de la ca
pour usage milita

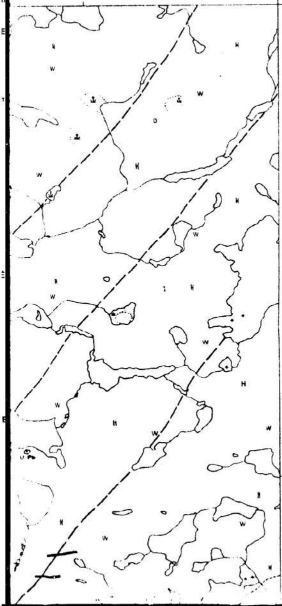

LEGEND - LÉGENDE

ROADS AND RELATED FEATURES	ROUTES ET OUVRAGES CONNEXI
HARD SURFACE ALL WEATHER	SURFACE PAVEE TOUTES SAISONS
LOOSE SURFACE	GRAVIER
CART TRACK WINTER ROAD	CHEMIN DE TERRE D HIVER
TRAIL CUT LINE PORTAGE	SENTIER PERCEE PORTAGE
BUILT-UP AREA	AGGLOMERATION
RAILWAY SIDING STATION STOP	CHEMIN DE FER VOIE D'EVITEMENT GARE ARRÊ
BRIDGE	PONT
SEAPLANE BASE ANCHORAGE	HYDROAÉROPORT MOUILLAGE
LANDMARK FEATURES	**POINTS DE REPÈRE**
HOUSE BARN	MAISON GRANGE
CHURCH SCHOOL	ÉGLISE ÉCOLE
POST OFFICE	BUREAU DE POSTE
HISTORICAL SITE	LIEU HISTORIQUE
TOWERS FIRE RADIO	TOURS FEU RADIO
WELL OIL GAS	PUITS PETROLE GAZ
TANK OIL GASOLINE WATER	RÉSERVOIR PÉTROLE ESSENCE EAU
TELEPHONE LINE	LIGNE TÉLÉPHONIQUE
POWER TRANSMISSION LINE	LIGNE DE TRANSPORT D ENERGIE
MINE	MINE
CUTTING EMBANKMENT	DÉBLAI REMBLAI
GRAVEL PIT	GRAVIÈRE
BOUNDARIES AND SURVEY CONTROL	**FRONTIÈRES ET POINTS DE RÉFI**
INTERNATIONAL PROVINCIAL, BOUNDARY MONUMENT	INTERNATIONALE PROVINCIALE, BORNE FRONTIÈRE
COUNTY DISTRICT	COMTÉ DISTRICT
TOWNSHIP PARISH SURVEYED UNSURVEYED	CANTON PAROISSE ARPENTÉE NON ARPENTÉE
TOWNSHIP DLS SURVEYED UNSURVEYED	TOWNSHIP ATC ARPENTEE NON ARPENTEE
SECTION CORNERS	COINS DE SECTION
MUNICIPALITY	MUNICIPALITÉ
INDIAN RESERVE PARK ETC	RESERVE INDIENNE PARC ETC
HORIZONTAL SURVEY POINT	REPÈRE PLANIMÉTRIQUE
BENCH MARK WITH ELEVATION	REPÈRE DE NIVELLEMENT AVEC COTE
SPOT ELEVATION PRECISE LAND WATER	POINT COTE PRECIS SUR TERRE SUR L EAU
DRAINAGE AND RELATED FEATURES	**DRAINAGE ET OUVRAGES CONN**
STREAM SHORELINE INDEFINITE	COURS D EAU RIVE IMPRÉCISE
DIRECTION OF FLOW	DIRECTION DU COURANT
LAKE INTERMITTENT LAKE	LAC LAC INTERMITTENT
FLOODED LAND	TERRAIN INONDÉ
MARSH SWAMP (WOODED)	MARAIS MARÉCAGE (BOISÉ)
DRY RIVER BED WITH CHANNELS	LIT DE COURS D EAU TARI AVEC CHENAUX
SAND ABOVE IN WATER	SABLE AU DESSUS DANS L EAU
STRING BOG	MARÉCAGE EN ENFILADE
TUNDRA PONDS POLYGONS	TOUNDRA ETANGS SOLS POLYGONAUX
RAPIDS FALLS RAPIDS	RAPIDES CHUTES RAPIDES
FORESHORE FLATS	ESTRANS
ROCK	ROCHE
DAM	BARRAGE
WHARF	QUAI
DITCH	FOSSE
RELIEF FEATURES	**RELIEF**

users.
his map as
e de la carte
ze militaire

SERIES	A701	SERIE
MAP	86 F/12	CARTE
EDITION	1 MCE	EDITION

ONNEXES

12

ARE ARRÊT

P

GP

DE RÉFÉRENCES

UNSURVEYED

ENTÉE

E BM 965

R L EAU 397 720

CONNEXES

W

NAUX

SB

AUX TP PG

EF

DAM

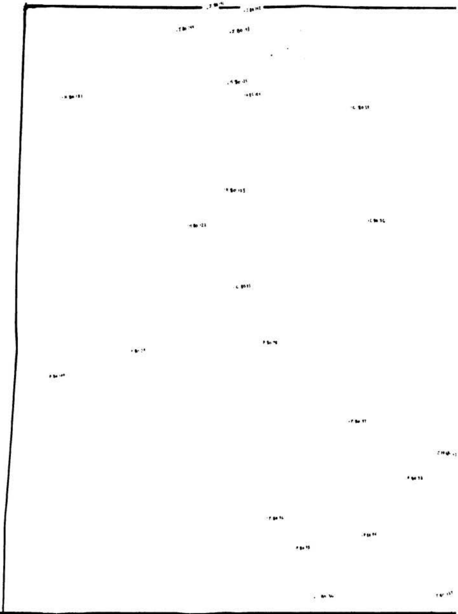

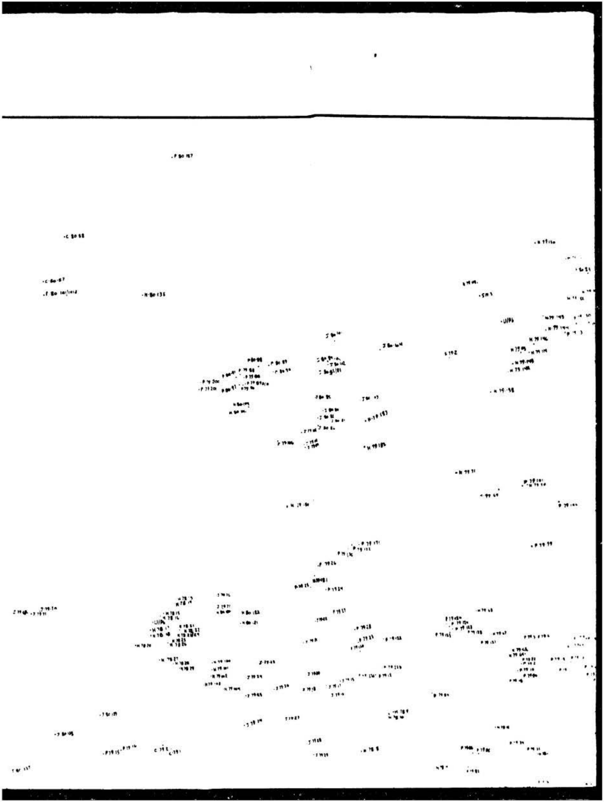

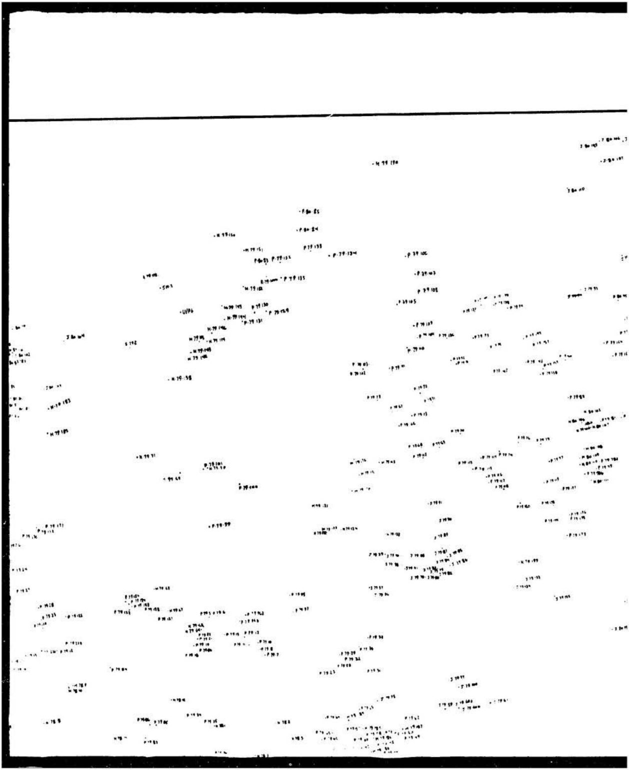

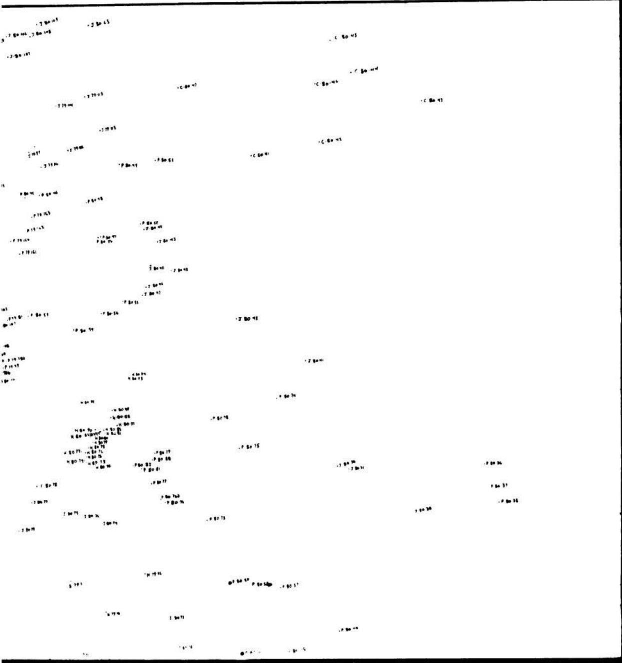

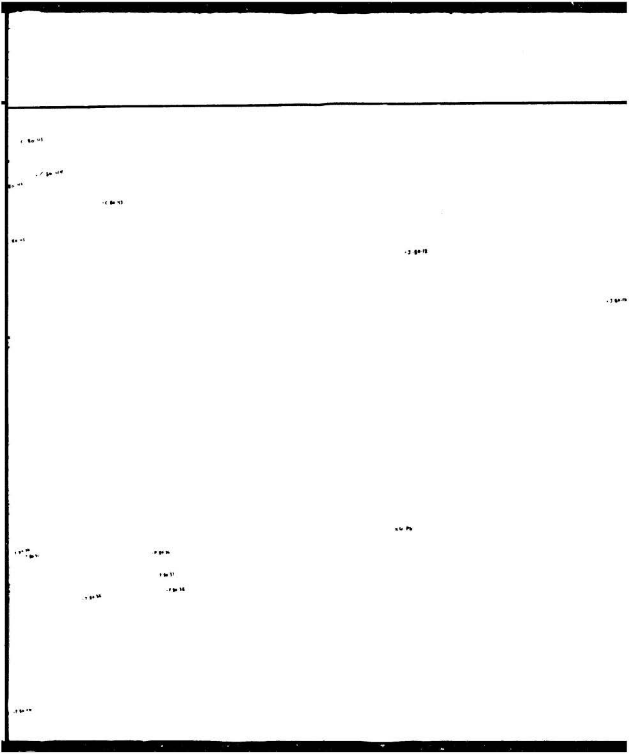

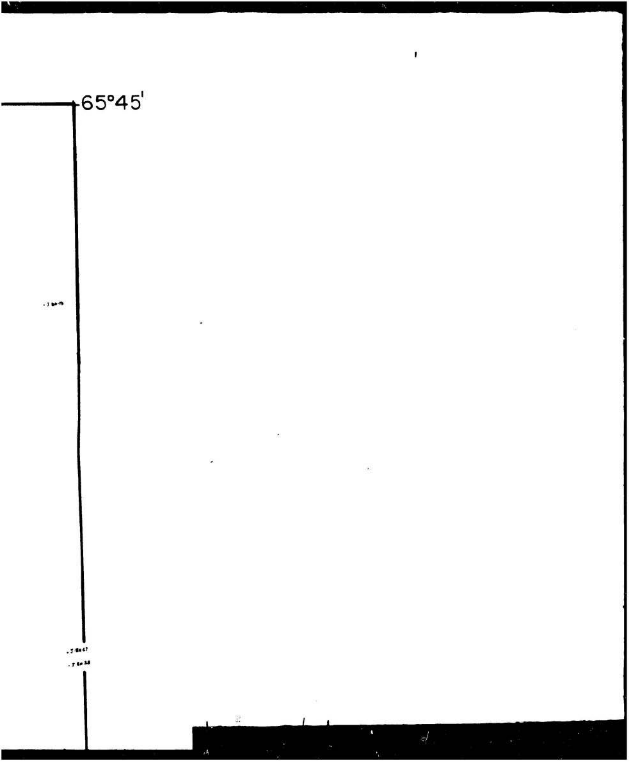
65°45'


BALACHEY
LAKE
1868±8
CAMSELL
156±
180±
LAKE
T

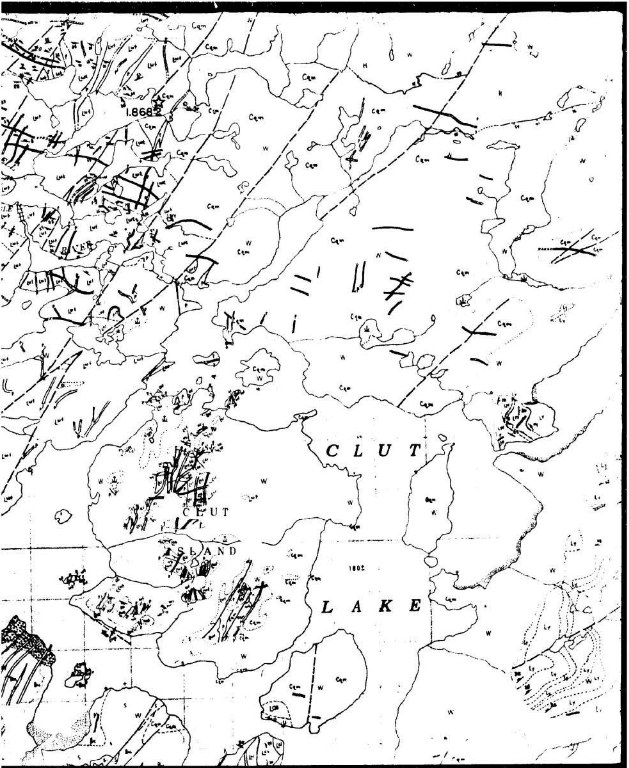

1.8682
RIVER
CLUT
CLUT
ISLAND
LAKE

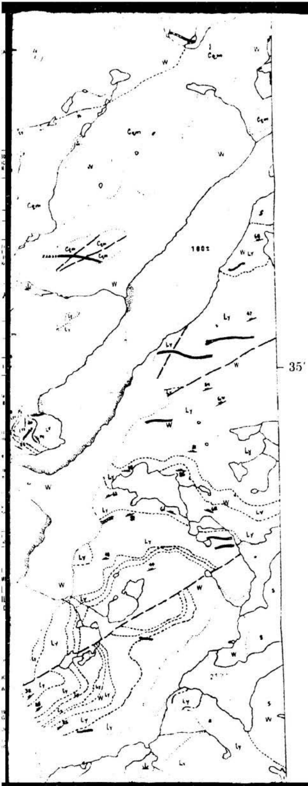

CONTOUR	
APPROXIMATE CONTOURS	COURBES DE NIVEAU APPROXIMATIVES
DEPRESSION CONTOUR	COURBE DE CUVETTE
SPOT ELEVATION APPROXIMATE LAND WATER	POINT COTE APPROXIMATIF SUR TERRE SUR L
ESKER	ESKER
PINGO	PINGO
SAND SAND DUNES	SABLE DUNES
PALSA BOG	PALSE
WOODED AREA	RÉGION BOISÉE
CLEARED AREA	RÉGION DÉBOISÉE

PHOTOGRAPHY PHOTOGRAPHIE

COMPILATION		RESTITUTION
31 A 14355 8 54 36	56 A 14350 8 54 62	23 A 14401 8 54 18

REVISION REVISION

GRID ZONE DESIGNATION DÉSIGNATION DE LA ZONE DU QUADRILLAGE	100 000 M ... IDENTI...
11W	

EASTING Read number on grid line immediately to left of point

LONGITUDE EST Noter le chiffre de ... du quadrillage immédiatement à ... du repère

NORTHING Read number on grid line immediately below point

LATITUDE NORD Noter le chiffre de ... du quadrillage immédiatement ... du repère

ONE THOUSAND
UNIVERSAL TRANSVERSE
ZONE 1
QUADRILLAGE DE M
UNIVERSEL TRANSVERSE

86 E/16	86 F/13	86 F/14
86 E/9	**86 F/12**	86 F/11
86 E/8	86 F/5	86 F/6

The 1976 MAGNETIC BEARING ... EAST of GRID NORTH

ANNUAL CHANGE DECREASI...

GRID NORTH is 0 41 ... for centre of map

Le REPÈRE MAGNÉTIQUE en ... EST du NORD DU QUADRILLA...

VARIATION ANNUELLE DÉCR...

NORD DU QUADRILLAGE est ... NORD GÉOGRAPHIQUE au ce...

SUR L'EAU

SAND

PB

W

C

000 M SQUARE IDENTIFICATION
IDENTIFICATION DU CARRÉ
DE 100 000 M

MC

ig grid line

ttre de la ligne
tement à gauche

97

are from

ernes du carré
pere en direction est

5

975

grid line

hiffre de la ligne
tement en dessous

98

are from

4

984

975984

ISAND METRE
VERSE MERCATOR GRID
ONE 11
DE MILLE MÈTRES
SVERSE DE MERCATOR

EARING is 39.33 (703 mils)

REASING 9.1

mils) WEST OF TRUE NORTH

UE en 1976 est à 39.33 (703 mils)
DRILLAGE

DÉCROISSANTE 9.1

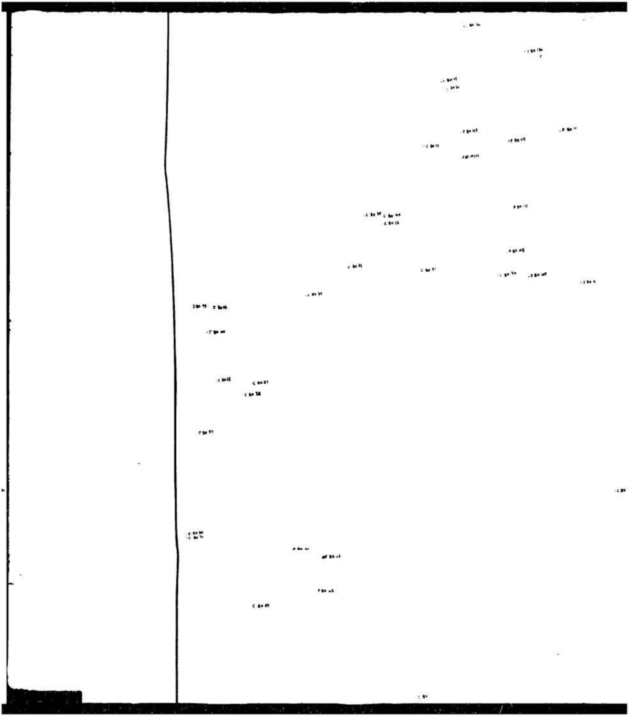

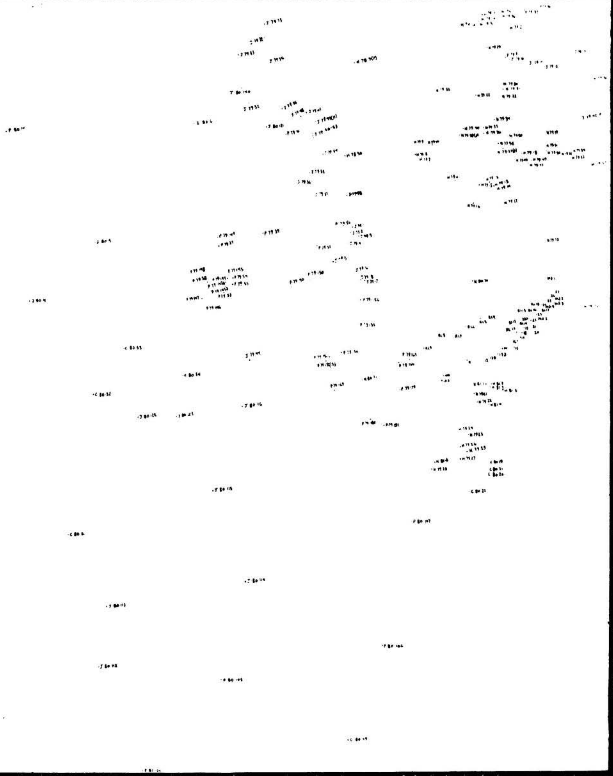

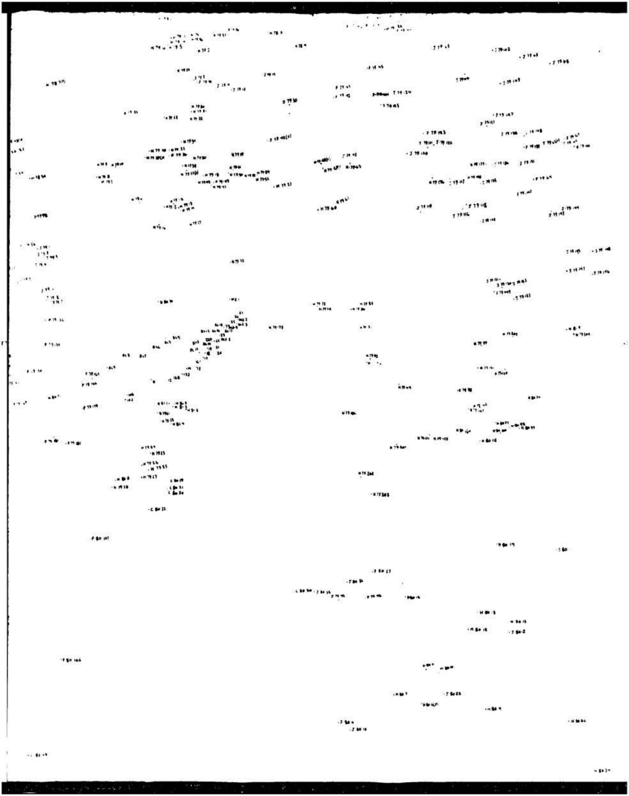

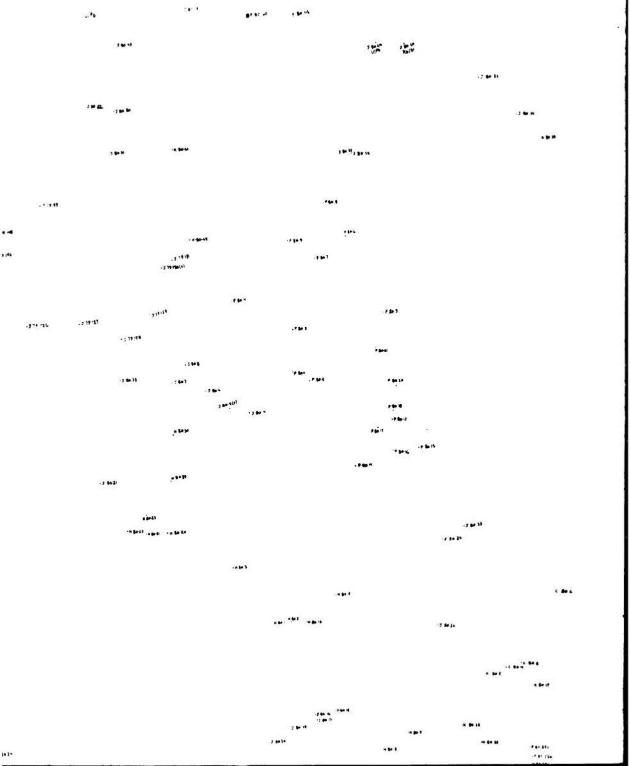

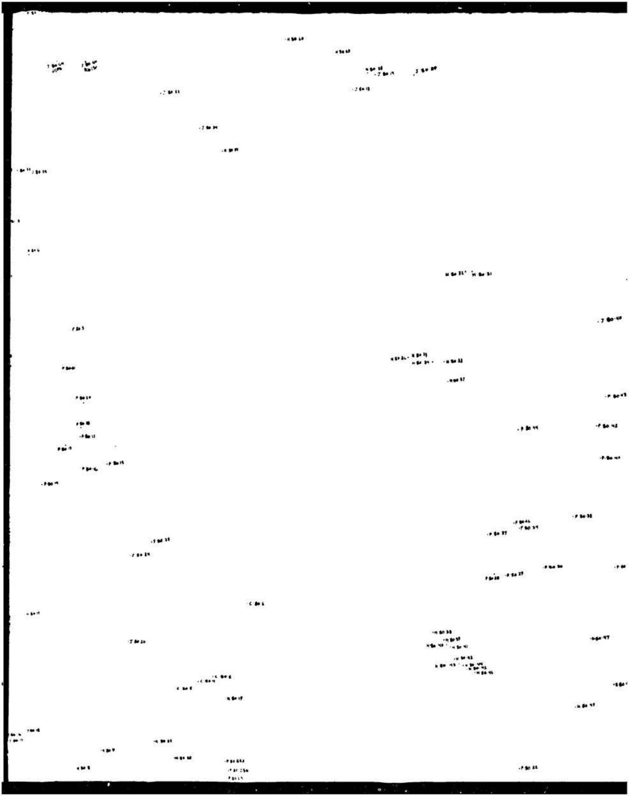

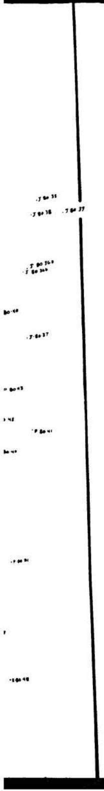

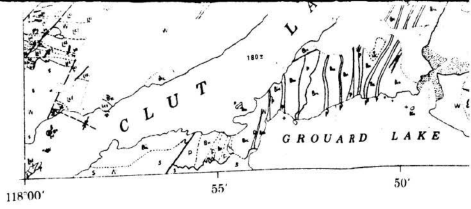

ELEVATIONS IN METRES ABOVE MEANSEA LEVEL

CONTOUR INTERVAL .... 10 METRES

NORTH AMERICAN DATUM

TRANSVERSE MERCATOR PROJECTION

MAP 2

preliminary map

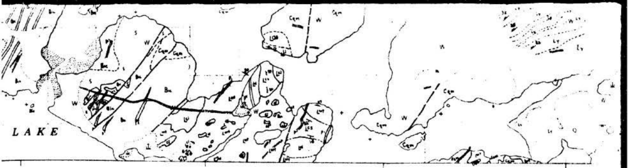

50' 45' 40' 35'

WHITE EAGLE FALLS

DISTRICT OF MACKENZIE

NORTHWEST TERRITORIES

EL
S

Scale 1:50,000 Échelle

Miles 1 0 2 3 Miles
Metres 1000 0 1000 2000 3000 4000 Metres
Yards 1000 0 1000 2000 3000 4000 Verges

ÉLÉVATIONS EN MÈTRES AU-DESSUS DU NIVEAU MOYEN DE LA MER

ÉQUIDISTANCE DES COURBES .... 10 MÈTRES

SYSTÈME DE RÉFÉRENCE GÉODÉSIQUE NORD AMÉRICAIN 1927

PROJECTION TRANSVERSE DE MERCATOR

R.S. HILDEBRAND

1982

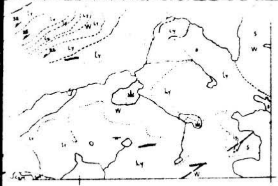

86 E/9 | 86 F/12 | 86 F/11

86 E/8 | 86 F/5 | 86 F/6

LE REPÈRE MAGNÉTIQUE en 1976 EST du NORD DU QUADRILLAGE

VARIATION ANNUELLE DE CROISS

NORD DU QUADRILLAGE est 0.41 NORD GÉOGRAPHIQUE au centre

CONVERSION SCALE FOR ELEVATIONS
ÉCHELLE DE CONVERSION DES ÉLÉVATIONS

S DU NIVEAU MOYEN DE LA MER

S 10 MÈTRES

QUE NORD AMÉRICAIN 1927

DE MERCATOR

ÉTABLIE PAR LA DIRECTION DES LEVÉS ET DE LA CARTOGRAPHIE, MINISTÈRE DE L'ÉNERGIE, DES MINES ET DES RESSOURCES, OTTAWA ... 1974

LES CARTES SONT EN VENTE AU BUREAU DES CARTES DU CANADA, MINISTÈRE DE L'ÉNERGIE, DES MINES ET DES RESSOURCES, OTTAWA, OU CHEZ LE VENDEUR LE PLUS PRÈS

AND

QUADRILLAGE

Metres

Pieds

86 F/12

EDITION 1

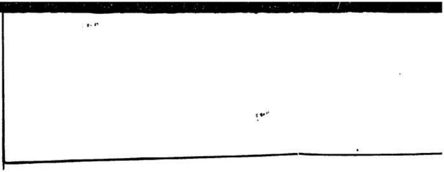

118°30

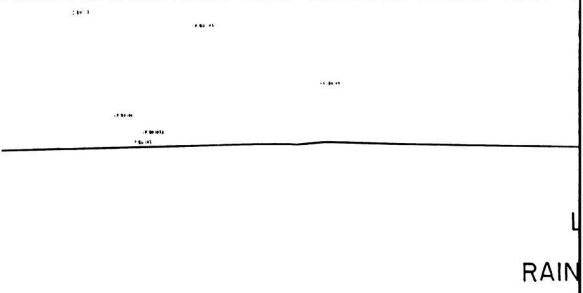
L
RAIN

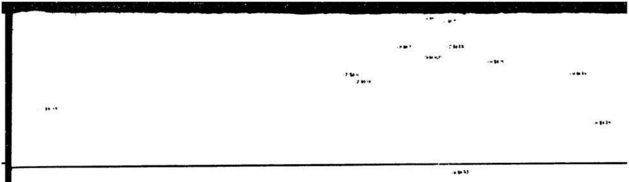

LOCATION OF SAMPLES

RAINY LAKE and WHITE EAGLE

1:50,000 SHEETS

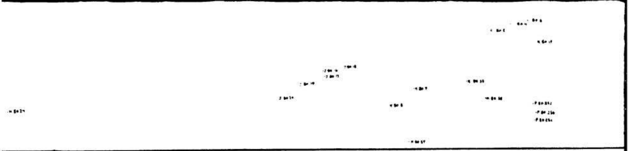

LE FALLS

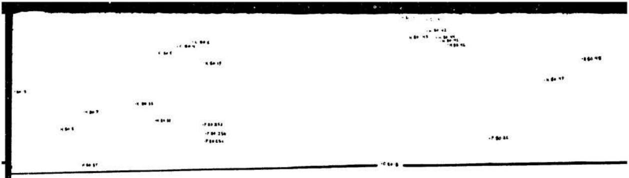

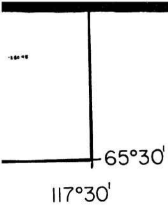
65°30'
117°30'

LEGEND

MIDDLE PROTEROZOIC

d — *Diabase and gabbro; near-vertical north-south and east-west trending dykes, and nearly flat lying sheets*

HORNBY BAY GROUP

HB2 — *Coarse grained quartz sandstone and volcanic-lithic sandstone, gritstone and conglomerate; trough and planar cross-bedding; white to light pink*

HB1 — *Medium- to fine-grained quartz sandstone and volcanic-lithic sandstone; ripple marked and crossbedded; minor mudstone, siltstone and conglomerate; rusty red*

EARLY PROTEROZOIC

GREAT BEAR BATHOLITH (G1m - G3)

G3dg, G3dk G3gk, G3a G3ga — *Coarse grained biotite-hornblende (chlorite-epidote) syenogranite (k) and monzogranite (a) and granodiorite (g)*[1]: G3d, *Dowdell pluton;* G3g, *Gilleran pluton*

G2t, G2h, G2r — *Medium grained hornblende-biotite (epidote-chlorite) granodiorite (g) and monzogranite:* G2t, *Torrie pluton;* G2h, *Hogarth pluton (may predate Sloan Group);* G2r, *Rogers pluton*

Gm — *Fine- to medium-grained leucocratic monzonite or quartz monzonite near Cameron Bay; age uncertain*

Gd — *Fine grained altered diorite at Sparkplug Lake; age uncertain*

G1m — *MYSTERY ISLAND INTRUSIVE SUITE: medium grained diorite, quartz monzonite, quartz syenite and granodiorite; semiconcordant sheets; wide alteration haloes, comprising an inner bleached and albitized zone, a central zone of actinolite-apatite-magnetite pods, breccias, veins and replacement, and an outer zone of chalcopyrite and pyrite gossan; important polymetallic ore veins occur within the alteration haloes, at least one intrusion of this suite is demonstrably contemporaneous with LaBine Group volcanism*

McTAVISH VOLCANIC FIELD (Lp - Sm)

SLOAN GROUP (Sd - Sm)

Sm — *MULLIGAN PORPHYRY: intrusive plagioclase-quartz porphyry; forms sills near the LaBine Group - Sloan Group contact*

Sd — *DOMEX FORMATION: dacite and rhyodacite ash flow tuff sheets, mostly crystal-rich, massive to eutaxitic; glomeroporphyritic (potassium feldspar) zone near the base*

LABINE GROUP (Lp - Lrp)

Lrp — *Intrusive rhyolite porphyry; biotite-quartz porphyry south of Elizabeth Lake, on Achook Island and Rocher Rouge Island; plagioclase-potassium feldspar-quartz porphyry on Cornwall Island*

Ldp — *Intrusive dacite porphyry; hornblende-plagioclase porphyry on Doghead Peninsula and south of Achook Island*

Lf — *FENIAK FORMATION: water-laid crystal tuff and devitrified ashstone; thin ash flow tuff sheets; minor epiclastic sediments, mostly fine grained; includes the following members:*

Ldf — *Dacite flow on Achook Island and Cornwall Island, plagioclase porphyritic; flow-banded basal zone, highly altered*

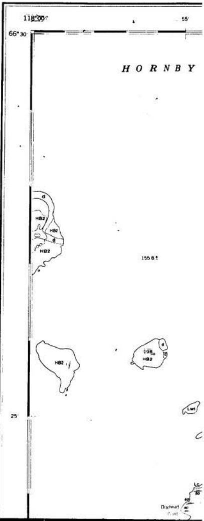

ykes,
and
ipple
rusty
ionzo-
in
mon-
oup);
non-
ition
e of
f an
eins
non-
sills
stel-
near
s, on
uartz
nin-
l ash
s the
por-

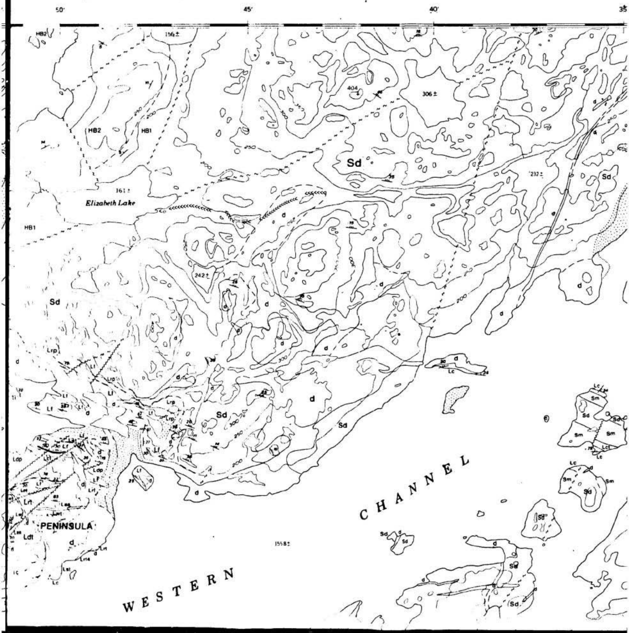

50'
45'
40'
35'
HB2
HB1
156±
404
306±
Sd
161±
Elizabeth Lake
232±
242±
d
Lrp
Lf
Lc
Sm
Ldp
Lrt
Ldt
PENINSULA
1558±
WESTERN
CHANNEL

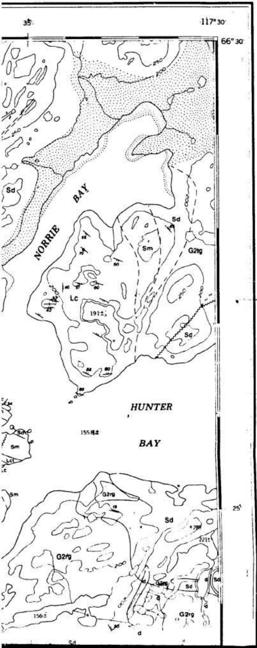
35'
117°30'
66°30'
NORRIE BAY
Sd
Sm
G2rg
Lc
HUNTER
BAY
Sd
G2rg
25'

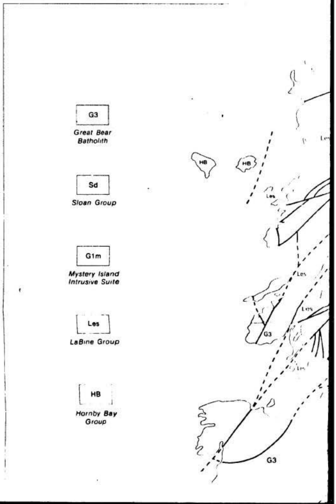
G3
Great Bear Batholith
Sd
Sloan Group
G1m
Mystery Island Intrusive Suite
Les
LaBine Group
HB
Hornby Bay Group
HB
G3

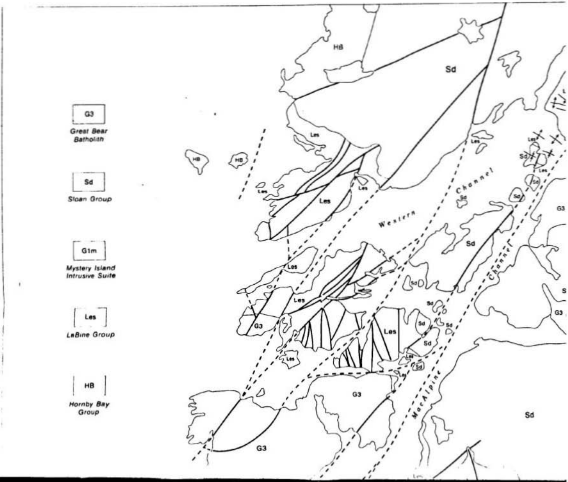

G3
Great Bear Batholith
Sd
Sloan Group
G1m
Mystery Island Intrusive Suite
Les
LaBine Group
HB
Hornby Bay Group
HB
Sd
Les
Western
Channel
MacAlpine
Channel
G3
Sd
Les

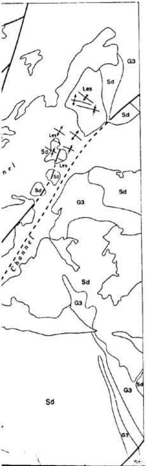
G3
Sd
Les
Sd
Les
Sd
Les
Sd
nel
Sd
Sd
G3
Channel
Sd
G3
Sd
G3
Sd
G3

Lt ... following members.

Ldf — Dacite flow on Achook Island and Cornwall Island; plagioclase porphyritic; flow-banded basal zone; highly altered

Lct — CORNWALL TUFF: ash flow tuff sheet containing 5-15 per cent crystals of plagioclase, quartz, hornblende and potassium feldspar; nonwelded to moderately welded; propylitized intracauldron facies on Achook Island, Cornwall Island and Stevens Island; outflow facies interbedded with water-laid pyroclastic and epiclastic rocks on Doghead Peninsula; conspicuous 4 m thick stromatolitic dolomite bed on Doghead Peninsula and Achook Island

Lc — CAMERON BAY FORMATION: planar and crossbedded, volcanic-lithic and feldspathic sandstone and gritstone; ripple-laminated siltstone and mudstone with mud cracks; hematitic polymictic conglomerate of mainly volcano-plutonic provenance, locally with 90 per cent orthoquartzite clasts; thin beds and erosional remnants of devitrified ashstone; local talus and explosion breccias near volcanic flow-domes; ash-flow tuff units not designated as informal members (Lt); cauldron-collapse breccias interfingered with ash flow tuff members; includes the following members:

Lrf4 — Rhyolite flow on Achook Island; steeply dipping foliation; highly altered

Lrt — ROCHER ROUGE TUFF: ash flow tuff sheet on Doghead Peninsula containing up to 20 per cent crystals of plagioclase and hornblende; very densely welded; abundant lithic fragments near the base

Laa — ACHOOK ANDESITE: flows and explosion breccias of amygdaloidal, aphanitic to porphyritic andesite; dominant phenocrysts are plagioclase and hornblende; intercalated with several ash flow tuff members; more amygdaloidal and less porphyritic than andesite in the Echo Bay Formation

Lwt — WESTERN CHANNEL TUFF: ash flow tuff sheet containing less than 5 per cent crystals of plagioclase, potassium feldspar, biotite and quartz; moderately to densely welded; red to flesh-coloured

Ldt — DOGHEAD TUFF: ash flow tuff sheet containing up to 35 per cent crystals of plagioclase, hornblende and biotite; densely welded; strongly flattened pumice fragments up to 50 cm in diameter near the base on Doghead Peninsula, and both basal and upper pumice-rich zones on Achook Island; brick-red to green; exclusively intracauldron facies

Lrf3 — Rhyolite flow on Stevens Island; flow banded; small, sparse phenocrysts of quartz

Lst — STEVENS TUFF: ash flow tuff sheet characterized by abundant, coarse, partly resorbed phenocrysts of quartz; basal agglutinated ash beds; distinctive quartz-porphyritic lithic fragments locally constitute 30 per cent of the unit on Cornwall Island, Achook Island and Doghead Peninsula; moderately to densely welded

Lrf2 — Rhyolite flow in Lindsley Bay; pink aphanitic flow containing sparse minute phenocrysts of quartz

Lmt — MACKENZIE TUFF: composite ash flow tuff sheet containing less than 10 per cent crystals of plagioclase, quartz and potassium feldspar; red to grey; abundant accretionary lapilli near the top on MacKenzie Island; much interbedded sandstone on Vance Peninsula

Llt — LINDSLEY TUFF: ash flow tuff sheet containing up to 25 per cent crystals, zoned from mostly quartz near the base to mostly plagioclase near the top; red; moderately to densely welded; probably intracauldron facies on Achook Island, Stevens Island and MacKenzie Island

Lrf1 — Rhyolite flow on MacKenzie Island; aphanitic; flow banded and flow folded; abundant silica-lined cavities

Lt — Unnamed tuff

McTAVISH A

(GREAT BEAR LA

WESTE
Dughead Point
TAVISH ARM
EAT BEAR LAKE)
ROCHER ROUGE ISLAND
ACHOOK ISLAND
CORNWALL ISLAND
HOGARTH ISLAND
MacALPINE
1558±
396+
375
334+


WES
BOADWAY
ISLAND
CHANNEL
DOMEX
BAY
CORNWALL
ISLAND
ISLAND
MacALPINE
Mulligan
Lake
Hook
165±
1558±
364
346
251±
216±
175±
264
G2h
Sd
Sm
Lct
Ldf
Laa
Lc
Lrp
Lsl
d

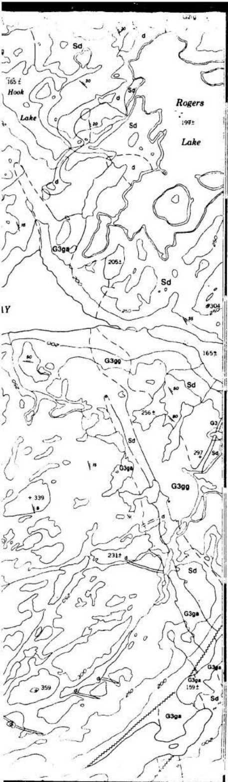

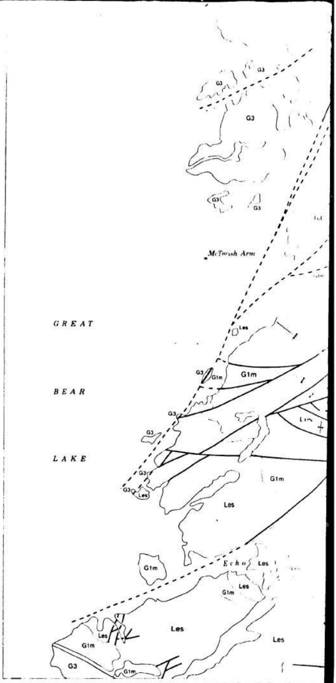

TECTONIC MAP OF ECHO BAY

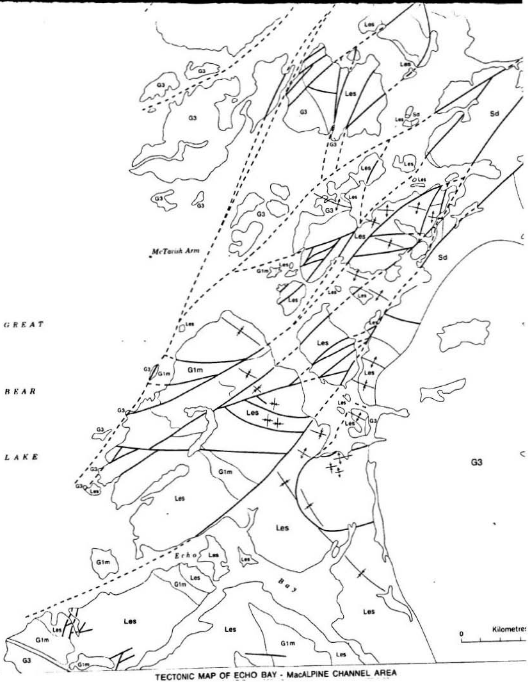

TECTONIC MAP OF ECHO BAY - MacALPINE CHANNEL AREA

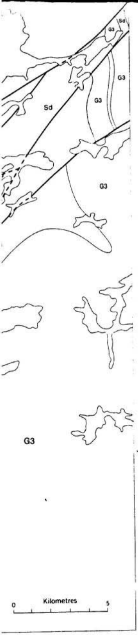

Sd
G3
Sd
G3
G3
G3
G3
G3
0
Kilometres
5

ECHO BAY FORMATION (Lem- Lef)

Lef — *SPARKPLUG LAKE MEMBER: porphyritic andesite flows and breccia distinguished only by their stratigraphic position above the MacKenzie Tuff; includes a small cone and vent complex south of Lindsley Bay (Lef')*

Les — *SURPRISE LAKE MEMBER: porphyritic (hornblende-augite-plagioclase) andesite flows and breccia; many flows trachytic; some flows oxidized to a brick-red colour; includes thin sedimentary interbeds (Les') and minor laharic breccia*

Lec — *COBALT PORPHYRY MEMBER: intrusive hornblende-plagioclase porphyry and microdiorite*

Lem — *MILE LAKE MEMBER: porphyritic andesite flows interbedded with volcanogenic sandstone and conglomerate, and andesitic lapilli tuff and ashstone*

Lp — *PORT RADIUM FORMATION: thin bedded, fine grained sandstone and siltstone with at least two carbonate interbeds less than 1 m thick; all exposures lie within alteration haloes of the Mystery Island Intrusive Suite*

([1]Plutonic rocks names follow recommendations of Streckeisen, 1976)

Geological boundary (defined, approximate) ....

Bedding, tops known (inclined) ....

Bedding, tops unknown (inclined, vertical) ....

Flow banding (inclined, vertical) ....

Eutaxitic foliation ....

Fault (defined, approximate) ....

Geological compilation and interpretation by R.S. Hildebrand, 1980. LaBine Group mapped by R.S. Hildebrand, 1977-1979, assisted by K.S. Pelletier, 1978-79. Sloan Group and G3 plutons from Geological Survey of Canada Open File 535 by P.F. Hoffman, 1978. East-west diabase dykes in the Sloan Group from Geological Survey of Canada Map 1011A by M. Feniak. G.M. Ross (Carleton University) generously provided unpublished information on the Hornby Bay Group. Echo Bay Mines Limited gave permission to publish the inset map of LaBine Point.
The field work was supported by the Department of Indian and Northern Affairs. The generous co-operation of Dr. W.A. Padgham and his staff is gratefully acknowledged.

Geological cartography by P. Corrigan, Geological Survey of Canada

Any revisions or additional geological information known to the user would be welcomed by the Geological Survey of Canada

Base map cartography, with selected contouring at 50 metre intervals, by the Geological Survey of Canada from maps published at the same scale by the Surveys and Mapping Branch in 1977

Copies of the topographical editions of this map may be obtained from the Canada Map Office, Department of Energy, Mines and Resources, Ottawa, K1A 0E9

Approximate magnetic declination 1981, 37°17.8' East, decreasing 16.9' annually

Elevations in metres above mean sea level

WORKMAN
ISLAND
STEVENS
ISLAND
VANCE
PENINSULA
McTAVISH ARM
(GREAT BEAR LAKE)
LINDSLEY
MACKENZIE

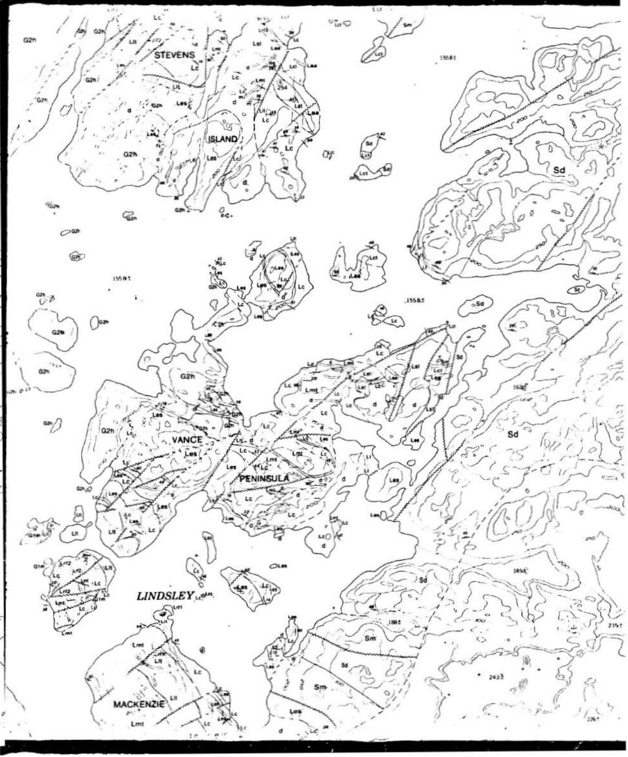

STEVENS
ISLAND
VANCE
PENINSULA
LINDSLEY
MACKENZIE

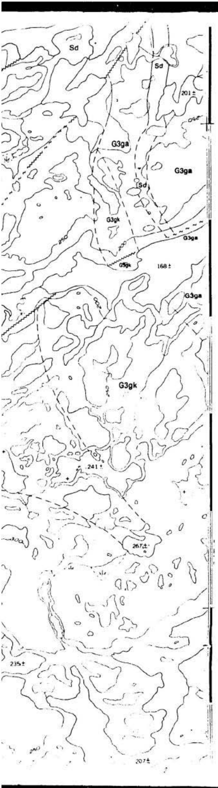

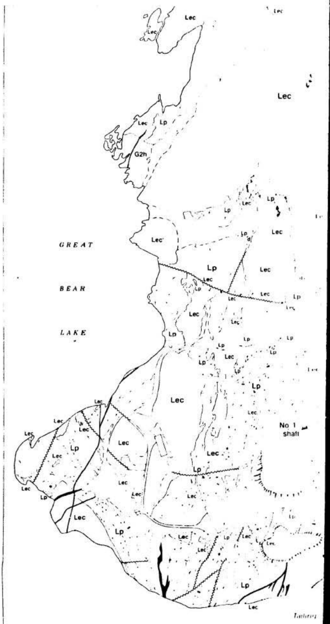

COBALT PORPHYRY (Lec-Lec')

d Diabase

Lec Hornblende-plagioclase porphyry

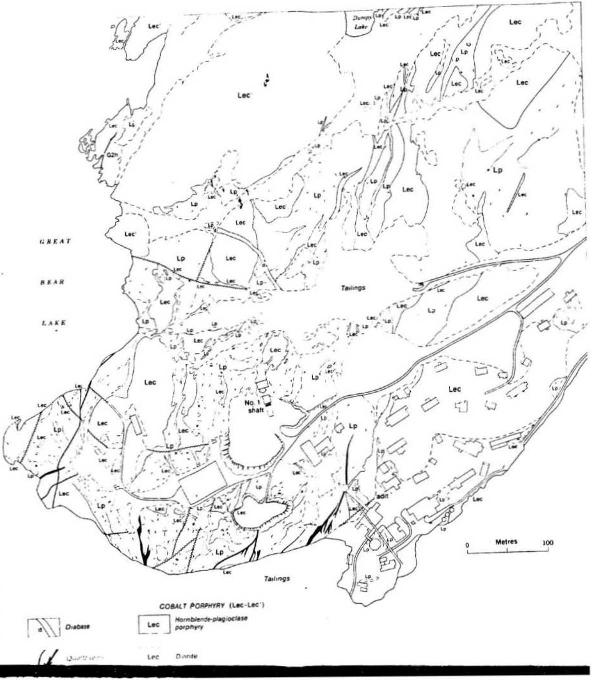

Dumps Lake
GREAT
BEAR
LAKE
Tailings
No. 1 shaft
adit
Tailings
Metres
0
100
COBALT PORPHYRY (Lec-Lec')
Diabase
Lec
Hornblende-plagioclase porphyry
Lec
Diorite

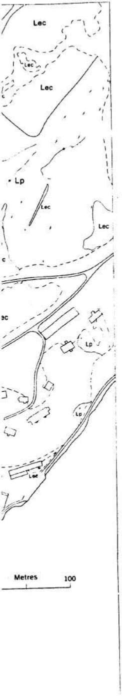
Lec
Lec
Lec
Lp
Lec
Lec
Lp
Lp
Metres
100

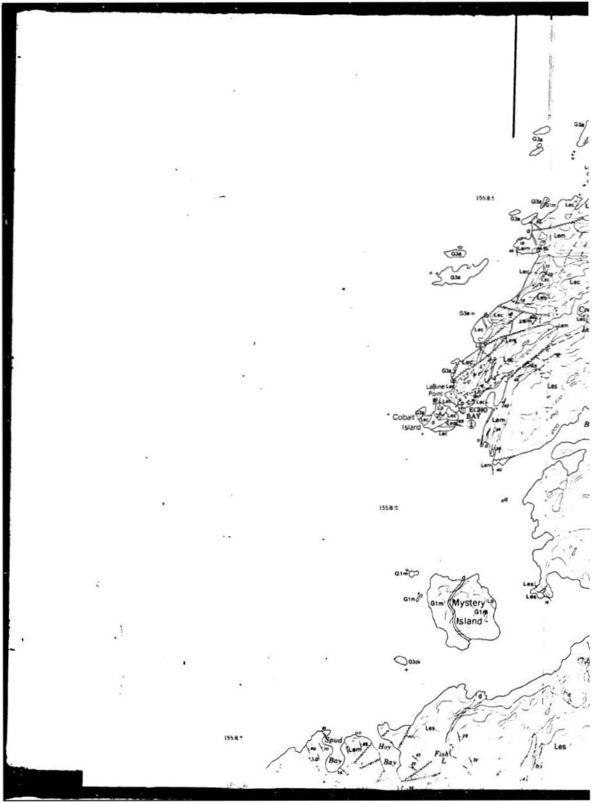

1558±
G3a
G1m
Lec
Lem
Les
LaBine Point
Cobalt Island
ECHO BAY
1558±
Mystery Island
G1m
Lp
G3dk
1558±
Spud Bay
Hoy Bay
Fish L
Les


MACKENZIE
ISLAND
BAY
Sparkplug Lake
Put Lake
Wop Lake
Glacier Lake
Airfield
Cleaver L
Towers
Tanks
Teapot Lake
Glacier
Servant Lake
Cameron Bay
Gossan Island
ECHO
ARM
BAY
Surprise L.

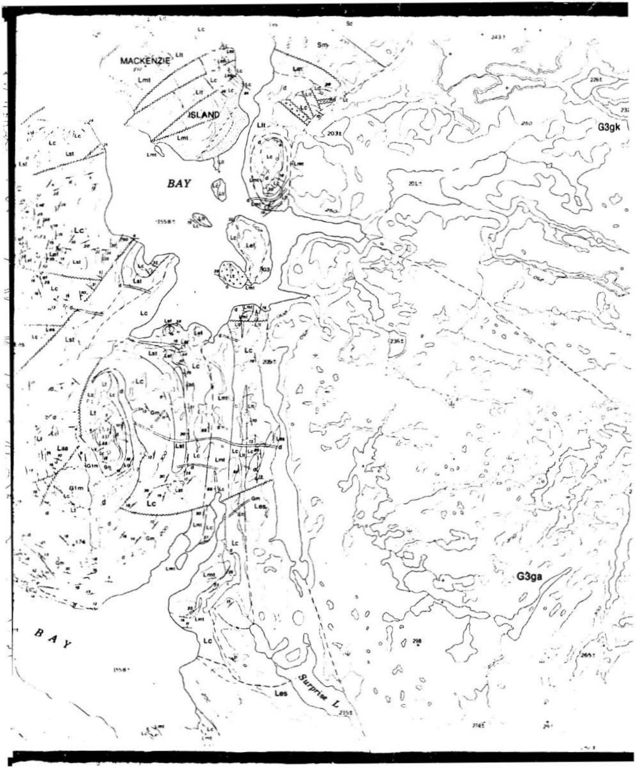

MACKENZIE
ISLAND
BAY
BAY
Surprise L
G3gk
G3ga
Lc
Lmt
Llt
Lst
Les
Laa
Gm
G1m
Sm
203±
201±
205±
236±
298
265±
215±

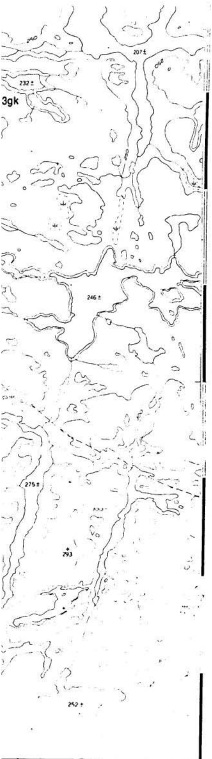

d	*Diabase*
(symbol)	*Quartz veins*
G2h	*Hogarth Pluton*

COBALT PORPHYRY (Lec-Lec)

Lec	*Hornblende-plagioclase porphyry*
Lec'	*Diorite*
Lp	*PORT RADIUM FORMATION* *Sedimentary rocks*

GEOLOGY OF LABINE POI

GEOLOGICAL SURVEY OF CANADA

MAP 15

GEOLO

ECHO BAY - MacALPI

DISTRICT OF

Scale 1:50

Kilometres 1 0

Miles 1 0

Universal Transverse M

Tailings

COBALT PORPHYRY (Lec-Lec')

d	Diabase	Lec	Hornblende-plagioclase porphyry
	Quartz veins	Lec'	Diorite
G2h	Hogarth Pluton	Lp	PORT RADIUM FORMATION: Sedimentary rocks

GEOLOGY OF LABINE POINT (see map for location)

GEOLOGICAL SURVEY OF CANADA — COMMISSION GÉOLOGIQUE DU CANADA

DEPARTMENT OF ENERGY, MINES AND RESOURCES
MINISTÈRE DE L'ÉNERGIE DES MINES ET DES RESSOURCES

MAP 1546A

GEOLOGY

ECHO BAY - MacALPINE CHANNEL AREA

DISTRICT OF MACKENZIE

Scale 1:50,000

Kilometres 1 0 1 2 3 4 Kilometres

Miles 1 0 1 2 Miles

Universal Transverse Mercator Projection

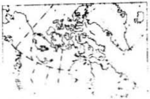

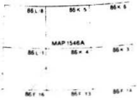

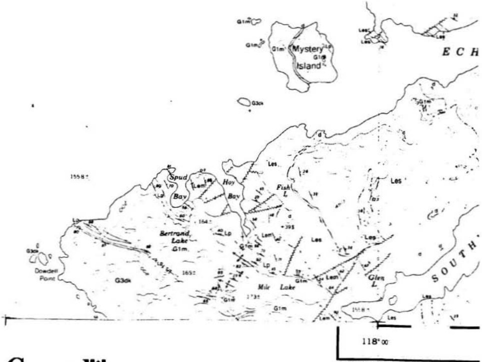

Canada

Copies of this map may be obtained
from the Geological Survey of Canada
601 Booth Street, Ottawa, Ontario K1A 0E8
3303 33rd Street N.W., Calgary, Alberta T2L 2A7

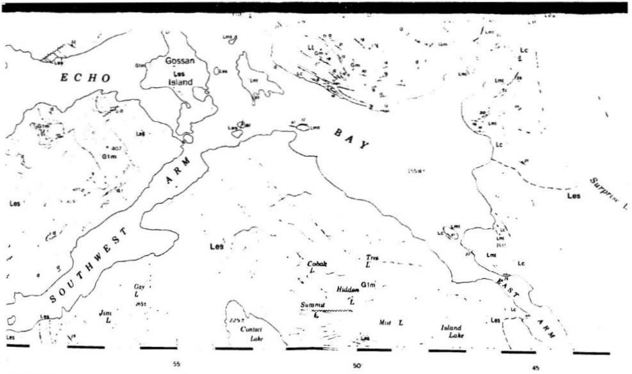

is be obtained
Survey of Canada
awa, Ontario K1A 0E8
W., Calgary, Alberta T2L 2A7

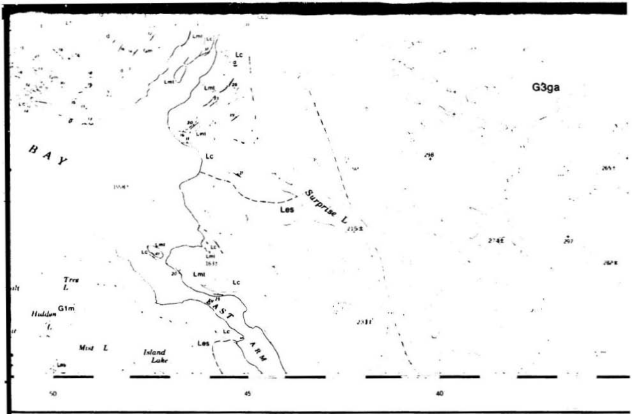

G3ga
BAY
Lc
Lmt
Surprise L
Les
Tree L
G1m
Hulden L
Mist L
Island Lake
EAST ARM
298
50
45
40

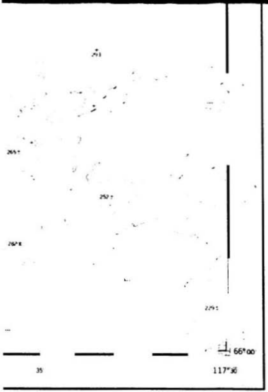

Printed by the Surveys and Mapping Branch

Scale 1

Kilometres 1 0 1

Miles 1 0

Universal Transverse Mer

INDEX MAP

UNEDITED

Scale 1:50,000

Kilometres 1 0 1 2 3 4 Kilometres

Miles 1 0 1 2 Miles

Universal Transverse Mercator Projection

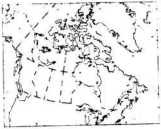

INDEX MAP

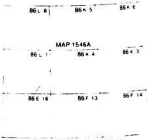

NATIONAL TOPOGRAPHIC SYSTEM REFERENCE

66°00

30

Branch 196?

UNEDITED COPY

LEGEND TO ACCOMPANY RAINY LAKE AND WHITE I

Gg	Gunbarrel Gabbro, coarse-grained g
	Cleaver Diabase, northwest-southea altered.
S	unnamed syenogranite plutons, most biotite syenogranite, minor ite; medium-grained biotite
3R	Richardson Granite, coarse-grained ite and syenogranite; often cally contains 20% large qu
3T	Tla Granite, medium to coarse-grai often k-spar porphyritic.
H	Hooker Megacrystic Granite, k-spar ite, hornblende-bearing nea
Hb	hornblende porphyritic dikes, typi east-west but occassionally
BQ	biotite-quartz porphyry, age unkno
r	granite porphyry, mostly quartz an microphenocrysts in a pink
r'	potassium feldspar porphyry
fp	fine-grained, k-spar porphyritic m unknown.
p	Grouard Dikes, mostly north-south iable amounts of plagioclase and potassium feldspar phenc coloured matrix. Locally hol
Pp	plagioclase porphyry
d	diorite and tonalite, mostly fine-g ovoid-shaped bodies.
KQP	potassium feldspar-quartz-plagiocla ic margin of Mule Bay cauldr
2Y	Yen Intrusive Suite, medium-grained monzonite($2Y_1$); medium-grain diorite($2Y_2$); medium-grained granite($2Y_3$); all members of magnesium minerals(up to 25%

WHITE EAGLE FALLS GEOLOGICAL MAPS

rained gabbro
-southeast trending diabase dikes,

ns, mostly coarse-grained hornblende-
e, minor hornblende-biotite monzogran-
biotite granite(S').
-grained biotite-hornblende monzogran-
e; often k-spar porphyritic, and typi-
large quartz blebs.
rse-grained hornblende-biotite granite,
ritic.
, k-spar megacrystic biotite syenogran-
ring near margins.
es, typically metre-wide and trending
ionally north-south trending.
ge unknown.
uartz and biotite phenocrysts and
a pink aphanitic matrix.

ritic monzonite and monzogranite, age

-south trending dikes containing var-
gioclase, hornblende, quartz, biotite,
ar phenocrysts in a flesh to brick-red
ally holocrystalline.

y fine-grained, plagioclase porphyritic

lagioclase porphyry, intrudes topograph-
y cauldron.
-grained biotite-hornblende quartz
um-grained biotite-hornblende grano-
-grained biotite-hornblende monzo-
mbers of the suite are rich in ferro-
to 25%).

LABINE GROUP:

Ly "younger ash-flow tuffs", simple
containing 10-40% phenocry
rocks(Lys).

Laa Animal Andesite, Lavas and brecci
oxene bearing andesite. Ma
xenocrysts of quartz and/o
centre occurs north of Bal

Cqm Calder Quartz Monzonite, hornblen
minor monzogranite. It is
pluton predates Animal And
related to Clut cauldron a

Lt unnamed ash-flow tuff, typically

Lu Uranium Point Formation, mudstone
stone, ash-flow tuff, crys

Lw White Eagle Tuff, mostly crystal-
flow tuff. Dominant phenoc
and plagioclase. Contains
Phenocryst content up to 3
intensely propylitized; ou
and vitric tuff at base of
Lwm mesobreccia member, b
interfingers with int
Tuff; contains angula
sive Complex, sulphic
ioclase-quartz porphy

------------ U N C O N F O R M

Bic Balachey Intrusive Complex, mediu
monzonite and monzodiorite

R Rainy Lake Intrusive Complex, hor
monzonite(Rm), syenite(Rs)
(Rd). Both the Rainy Lake
have undergone intense sub
and have wide alteration h

A augite intrusions, augite porphyr
Camsell River Formation.

Q quartz porphyry, found only east

simple cooling units of ash-flow tuff
phenocrysts. Intercalated sedimentary

d breccias of amphibole and/or clinopyr-
site. Many flows contain conspicuous
tz and/or k-spar. A possible eruptive
h of Balachey Lake.
hornblende-bioite quartz monzonite,
. It is not known whether or not this
imal Andesite but it is thought to be
uldron and therefore included here.
pically very lithic rich.
mudstone, siltstone, sandstone, ash-
ff, crystal tuff, minor conglomerate.
crystal-lithic and lithic-crystal ash
t phenocrysts are biotite, amphibole,
ontains minor quartz in basal zones.
up to 35%. Intracauldron facies(Lwt)
ized; outflow facies(Lwto); crystal
base of outflow sheet(Lwx);
ember, breccia and conglomerate which
with intracauldron facies White Eagle
s angular fragments of Balachey Intru-
, sulphides, altered andesite, and plag-
z porphyry.
R M I T Y ----------------------
x, medium-grained hornblende quartz
zodiorite
lex, hornblende monzodiorite(Rmd),
nite(Rs), porphyritic border monzonite
iny Lake and Balachey Intrusive Complexes
tense subsolidus hydrothermal alteration
ration haloes.
e porphyritic bodies intrusive into the
mation.
nly east of Rainy Lake, intensely altered.

Lc	Camsell River Formation, lava flow	
	conglomerate and laharic br	
	(Lce), sandstone, ashstone,	
	erate(Lcs), monzonite(Lcm),	
	ity of the Camsell River Fo	
La	Arden Formation, interbedded rhyol	
	breccia(Lab), rebrecciated	
	(Lac), mudstone(Lam), lithi	
Lm	Moose Bay Tuff, upper member: lihi	
	(Lmt)	
	esit	
	lower member: sand	
	ande	
	tuff	
	sand	

--------------U N C O N F O R M I

g	gabbro and diabase sheets, sometim	
	cm-size plagioclase phenoc	
Ps	porphyritic dikes and sills, plagi	
Bb	Bloom Basalt, dominantly pillow la	
	interpillow sedimentary ro	
	dolomite(Bd).	
Cb	Conjuror Bay Formation, upper memb	
	lower memb	

--------------U N C O N F O R M I

Hg	gabbro, diabase, clinopyroxenite,	
Hd	quartz diorite and quartz monzonit	
	porphyritic phases(Hdp).	
Hhl	Holly Lake metamorphic suite, meta	
	tary and volcanic rocks.	

☆U-Pb ages obtained from zircons are prelim
ed by S. A. Bowring and R. Van Schmus, 198

strike and dip of bedding st
strike and dip of tectonic foliation

flows(Lcl),ash-flow tuff(Lca),
lc breccia(Lcc), explosion breccia
tone, lapilli tuff, minor conglom-
.cm), diorite(Lcd). The vast major-
er Formation is andesitic.
rhyolitic ashstone-dolomite(Lad),
ated breccia(Lab'), conglomerate
lithic arkose and conglomerate(Las).
lihic-rich rhyolite ash-flow tuff
(Lmt), andesitic tuff(Lmat), and-
esite flows(Lmaf), sandstone(Lms).
sandstone(Lmls), breccia(Lmlb),
andesite flows(Lmla), mudstone(Lmlm),
tuff(Lmlt), conglomerate with minor
sandstone and mudstone(Lmlc).
M I T Y-------------------------
metimes containing conspicuous
henocrysts.
plagioclase-quartz-k-spar porphyritic.
ow lavas, minor aquagene tuff, and
ry rocks, stromatolitic and oolitic

member: sandstone, ashstone, silt-
stone, chert, lapilli tuff,
conglomerate and breccia(Cbm).
member: crossbedded quartz arenite,
minor vein quartz pebble con-
glomerate(Cba).
M I T Y-------------------------
ite, variably deformed.
zonite, typically foliated, k-spar
dp).
metamorphosed and deformed sedimen-
cks.

---

reliminary and were graciously provid-
, 1982.

strike and dip of eutaxitic foliation
tion